INFLUENCES OF SYSTEM IMPERFECTIONS ON THE PERFORMANCE OF CAM-FOLLOWER SYSTEMS

By

HO-RYONG KIM, B.Eng., M.Eng.

A Thesis

Submitted to the School of Graduate Studies

in Partial Fulfilment of the Requirements

for the Degree

Doctor of Philosophy

McMaster University

January 1982

INFLUENCES OF SYSTEM IMPERFECTIONS

ON THE

PERFORMANCE OF CAM-FOLLOWER SYSTEMS

DOCTOR OF PHILOSOPHY (1982) McMASTER UNIVERSITY

(Mechanical Engineering) Hamilton, Ontario

TITLE : Influences of System Imperfections on the Performance of Cam-Follower Systems

AUTHOR : Ho-Ryong Kim, B.Eng. (Yon Sei University, Seoul, Korea)

M.Eng. (McMaster University)

SUPERVISOR : Professor W. R. Newcombe

NUMBER OF PAGES : xii ; 244

ABSTRACT

The cam-follower mechanism is a most important machine element used to control the complicated motion of machine parts, and the accuracy of the motions and subsequent machine performance depends on the cam-follower output. Imperfections in the system affect this output, and an investigation of all possible effects is carried out here through the analytical and simulation means developed.

The imperfections considered here include all factors that cause a design to deviate from the theoretical model. These factors have generally been neglected in the past because of their complexity. They are classified in the following three categories :

1. Geometrical Imperfections
   a) Machining or manufacturing errors : Tolerances
   b) Backlashes or clearances
2. Kinematic Imperfections
   a) Non-constant angular velocity of cam
   b) Impossibility of a perfectly manufactured cam profile
   c) Asymmetry between rise and return period
3. Dynamic Imperfections
   a) Inertial mass
   b) Flexibility of system elements
   c) Energy dissipation

The performance of the system is indicated by its responses, such as time responses (displacements, velocities and accelerations) and inertial responses (contact forces or stresses, torques and inertia forces).

To investigate the effects of the imperfections, the mechanism of a translating roller follower-cam system driven by a motor through a rigid coupling is simulated on a digital computer dynamically and stochastically. The dynamic simulation, which will produce the effects of the kinematic and dynamic imperfections, is accomplished on the basis of an eleven degree of freedom model which was carefully devised to include all possible properties or factors concerning the real system behavior, such as flexibility of cam shaft, non-constant angular velocity of the cam due to torsional vibration, jump phenomenon caused by inertia force, preloading of the retaining spring, cantilever effects of follower due to pressure angle, nonlinear damping, and the exact contact condition between cam and roller follower. In the model, an analytical method to calculate the spring constant of the interface between cam and follower is introduced by using Hertzian deflection characteristics. To analyse the effects of geometric imperfections which involve random characteristics, the ground and finished cam profile is modelled stochastically by generating normally distributed random numbers and applying a cubic polynomial spline function to obtain the cam profile.

Thus, the compounded effects of tolerances and flexibility in the system can be investigated.

The motion equations derived from the dynamic model and stochastic model consist of simultaneous nonlinear differential equations in which the factors having a random nature are implicitly included. To solve the motion equations the refined Runge-Kutta algorithm is utilized so that the computing accuracy can be controlled.

The PDP-11/34 minicomputer and its graphic peripheral devices are exploited by the overlay technique. Intermediate results are transferred to subsidiary memory while renewing the previously executed memory, so as to diminish the processing cost of the dynamic and stochastic simulation program as well as to compensate for the insufficient main memory.

Finally, the results of the simulation are analyzed and compared with the work of other researchers, in which the effect of an imperfect profile has usually been neglected.

ACKNOWLEDGEMENTS

The sincerest appreciation is expressed to my supervisor, Professor W. R. Newcombe, for his continuous encouragement, invaluable advice and expert guidance, without which this work would not have been possible.

The constructive criticism and valuable suggestions, of Dr. J. Tlusty, Dr. B. Latto and Dr. R. M. Korol as members of the supervisory committee throughout the course of this work are also sincerely appreciated.

Financial support from the Department of Mechanical Engineering, McMaster University, and the National Research Council of Canada is gratefully acknowledged.

Finally, special thanks go to my wife, Hwa-Sook, for her expert typing, limitless patience and encouragement during this thesis work.

TABLE OF CONTENTS

NOMENCLATURE

C_{cc}	:	viscous damping coefficient of cam shaft bearing and air friction by cam
C_f	:	friction damping coefficient of follower guide i.e. slide bearing
C_{f1}	:	structural damping coefficient of the follower part between load and follower guide
C_{mb}	:	viscous damping coefficient of motor bearing
C_{s1}	:	structural damping coefficient of shaft between motor and coupling
C_{s2}	:	structural damping coefficient of shaft between coupling and cam
F_p	:	preload by return spring
F_c	:	contact force between cam and roller
I_c	:	polar moment of inertia of cam
I_{cp}	:	polar moment of inertia of coupling
I_m	:	polar moment of motor armature
K_f	:	stiffness of follower part between sliding bearing and load
K_{hc}	:	horizontal effective spring constant of cantilever portion of follower
K_{hs}	:	horizontal effective spring constant of cam shaft due to the deformation of cam shaft bearing with some effect of shaft bending

K_{rb} : spring constant of roller bearing and its shaft

K_{rs} : stiffness of return spring

K_{s1} : stiffness of shaft between motor and coupling

K_{s2} : stiffness of shaft between coupling and cam

K_{vc} : vertical effective spring constant of cantilever portion of follower

K_{vs} : horizontal effective spring constant of cam shaft due to the deformation of cam shaft bearing with some effect of shaft bending

M_{cs} : mass of cam and its shaft

M_f : mass of follower part between load and slide bearing

M_{fc} : effective mass of cantilever portion of follower and 1/3 of return spring mass

M_l : mass of load

M_r : mass of roller

T_i : input torque to motor armature

T_o : output torque to cam

x, x_1, x_2, x_3 : horizontal displacement of contact point between cam and roller, cam, roller, and cantilever portion of follower respectively

$\dot{x}, \dot{x}_1, \dot{x}_2, \dot{x}_3$: velocity of x, x_1, x_2, and x_3 respectively

$\ddot{x}, \ddot{x}_1, \ddot{x}_2, \ddot{x}_3$: acceleration of x, x_1, x_2, and x_3 respectively

$y, y_1, y_2, y_3, y_4, y_5$: vertical displacement of contact point between cam and roller, cam, roller, cantilever portion of follower, follower part between load and slide bearing, and load respectively

$\dot{y}, \dot{y}_1, \dot{y}_2, \dot{y}_3, \dot{y}_4, \dot{y}_5$: velocity of y, y_1, y_2, y_3, y_4, and y_5 respectively

$\ddot{y}, \ddot{y}_1, \ddot{y}_2, \ddot{y}_3, \ddot{y}_4, \ddot{y}_5$: acceleration of y, y_1, y_2, y_3, y_4 and y_5 respectively

δ_{rs} : spring length to be compressed during assembly

$\theta_m, \theta_{cp}, \theta_c$: angular displacement of motor armature, coupling and cam respectively

$\dot{\theta}_m, \dot{\theta}_{cp}, \dot{\theta}_c$: angular velocity of θ_m, θ_{cp}, and θ_c respectively

$\ddot{\theta}_m, \ddot{\theta}_{cp}, \ddot{\theta}_c$: angular acceleration of θ_m, θ_{cp}, and θ_c respectively

ϕ : pressure angle

CHAPTER I

INTRODUCTION

I.1. Background

Modern machines perform many complicated tasks, and a serious demand is placed on their components to move with precision in a prescribed mode at high speed. The cam-follower mechanism, which falls in the general class of direct contact mechanisms, is a very versatile mechanical device and is capable of producing almost any specified motion requirement under high or low speed operation. Therefore, it is generally specified in the design of modern machines such as automatic production machines, indexing machines, computer peripheral devices, valve gears of internal combustion engines, printing machines, and automatic machine tools.

The overall performance of a machine is significantly affected by the accuracy or performance of the prime mechanism which controls the major motion of the machine. As an indispensable mechanism for versatile motion control, the cam-follower system has naturally been studied for several decades, and, in accordance with a recent demand for increasing the efficiency of machine performance under high speed operation, more accurate and more adaptable information is required in practice for predicting the actual performance of this system.

I.2. Overview of Previous Work

About a half century ago, the cam-follower system was studied only from a kinematic point of view, in which the characteristics of cam motion curves were a major topic, with the objective of minimizing the nominal acceleration to reduce dynamic loading. Consequently, the parabolic or constant acceleration curve, which has the lowest possible theoretical maximum acceleration, was the most commonly used curve.

As machine speeds increased, problems involving vibration of the follower, chattering, and noisy operation arose, thereby significantly affecting the performance of the system. Since then, several investigations have been carried out to examine and attempt to improve the kinematic and dynamic behavior of a cam-follower mechanism. In the following, they are abstracted in chronological order.

Testing a series of self-adjusting valve mechanisms, Dudley [1] found that the resonant vibration (surging) of a retaining spring, which has been blamed for the distorted motion of valves, affects the valve motion much less than the flexibility of the mechanism whose rigidity has been assumed perfect. However, stiffening of the valve linkage adds weight and requires increased force from the valve springs. He proposed, as a better approach, a new cam profile program - the polynomial curve, which produces less vibration with a flexible linkage.

Based on experimental results from a turret indexing mechanism operated by cams having parabolic, harmonic and straight line profiles,

Gagne [2] made the following suggestions for high speed cam design:

1. Reduce backlash to prevent chattering.
2. Acceleration should not be abrupt.
3. Inertial forces should be balanced against the change in spring load.
4. Slight profile error can be serious.
5. Preloaded oversize antifriction bearings can solve the backlash problem.

Mitchell [3] showed experimentally the dynamic advantage of the cycloidal curve over the parabolic and harmonic motion curves. The latter two had been in popular use because the parabolic curve has the lowest overall theoretical acceleration among the three curves, and the harmonic produces the smallest pressure angle, whereas the cycloidal had not showed any special advantage. In his experiment, the cycloidal was observed to have the lowest rate of acceleration, causing much less noise, vibration and fatigue failure.

Neklutine [4] proposed a method for computing curves and choosing a curve which gives minimum vibration. The dimensionless maximum acceleration and velocity coefficients, and the ratio of static stress and vibrational stress, were used for the criteria.

Using a dynamic model with one degree of freedom, Barkan [5] calculated the motion of an automobile engine valve through a flexible linkage, taking friction forces as damping. He particularly studied the forces produced by the resonant vibration of a retaining spring. No

consideration was given to the contact condition, the effects of the motion curve characteristics, and the roughness of the cam profile. The angular velocity of the cam was assumed constant.

Stoddart [6] devised the polydyne cam, elaborationg the polynomial equation presented by Dudley [1] and combining it with the dynamics of a follower system. This approach originated because of the faulty operation of high speed, highly flexible systems, attributed to the difference between cam command and follower mass response. Only elasticity in the linkage was considered to be responsible for the difference.

Kloomok and Muffley [7] suggested how to select and blend profile curves by using a quarter or half cycle of each curve, and how to minimize inertia forces for high speed operation. They illustrated a method of synthesizing profiles by blending profile curves properly.

Johnson [8] introduced a finite difference method to cam design as a numerical procedure by which:

1. Velocity and acceleration can be calculated directly from a given cam.
2. The effect of machining tolerances on velocity and acceleration can be predicted.
3. Cam profile can be numerically adjusted according to the condition specified in the cam design.

In his book [9], Rothbart included the basic principles and

information related to cam design, dynamics and accuracy, and proposed a simple criterion for determining the allowable tolerance of each motion curve with respect to a straight line.

By applying the previously introduced finite difference method to profile error analysis, Johnson [10] presented a method to analyse the influence of dimensional variations upon velocity and acceleration. He classified the profile errors (Fig. I.1) into a displacement error (t) and a cam angle error (e), attempting to obtain the deterministic values of deviations on velocity and acceleration due to the errors.

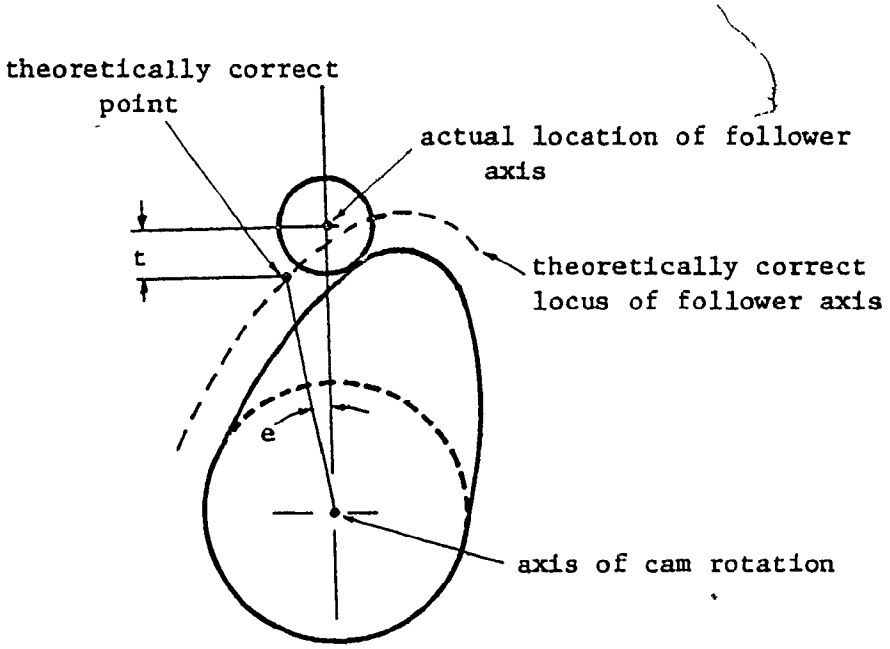

Fig. I.1. Cam Profile Errors in [10].

In order to reduce the maximum acceleration, Kloomok and Muffley [11] suggested the 9th order polynomial curve, which has 10 constants which can be calculated by a curve fitting method. The usefulness of computers in calculating the relatively large numbers of constant values was emphasized.

Mercer and Holowenko [12] analysed the residual vibrational stress characteristics of a cam contour based on a one degree of freedom model (Fig. I.2) in which the following were assumed:

1. Cam contour is perfect.
2. The cam drives the follower positively (no jumping).
3. Cam speed is constant.
4. Damping is neglected.
5. A knife edge follower is used.

As a result of their analysis, they pointed out that:

1. Neither acceleration nor jerk alone controls vibratory stresses.
2. Blending of acceleration curves so as to avoid discontinuities in the jerk curve is not sufficient to produce a general reduction of the residual stress.
3. Constructing acceleration diagrams so as to elude high order Fourier components does not guarantee outstanding dynamic characteristics.

Taking a two degree of freedom model (Fig. I.3) as an example, and applying the finite difference method to solve the applicable

differential equations, Johnson [13] discussed how to analyse a mechanism having more than two degrees of freedom.

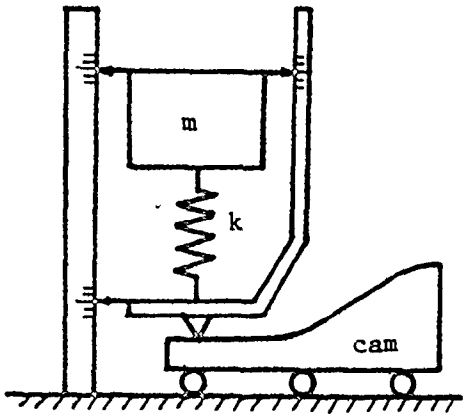

Fig. I.2. One Degree of Freedom Dynamic Model used in [12].

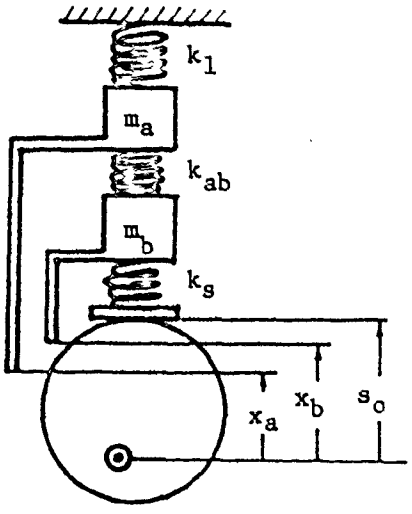

Fig. I.3. Two Degree of Freedom Dynamic Model used in [13].

Based on a model with one degree of freedom and no damping (Fig. I.4), Okcuoglu [14] applied the polydyne cam design method in [6] to the cam mechanism of a differential lever system, which should generate a 7th order polynomial according to the calculated profile of the polydyne cam.

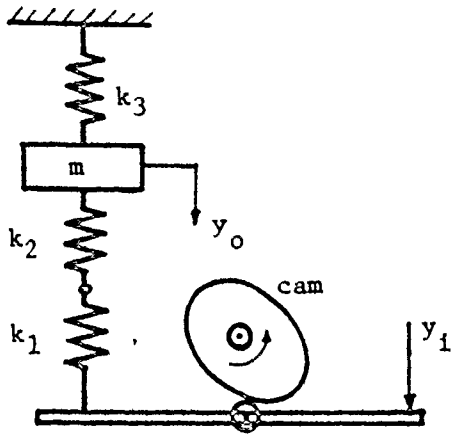

Fig. I.4. One Degree of Freedom Dynamic Model used in [14].

On the problem of how to remove discontinuities in the acceleration curve, in order to avoid transient disturbances while reducing the peak value of acceleration, Weber [15] proposed the use of a Fourier sine series of cycloidal curves, along with a generalized filter theory which provides a practically smooth curve fitting between two points, taking their boundary conditions into consideration. After expressing a desired output in terms of actual displacement perturbations, an indefinite input function and the output function are related together

by the filter theory to define the input function.

Hebeler [16] used a one degree of freedom model shown in Fig. I.5. to analyse the response of a dwell-rise-dwell system driven by a cycloidal motion cam. In his analysis, the response was obtained in terms of the ratio of cam rise time to the period of natural vibration of the linkage. The simplest motion equation obtained was solved by the Laplace transformation method, neglecting damping, retaining spring (jump phenomenon) and cam speed.

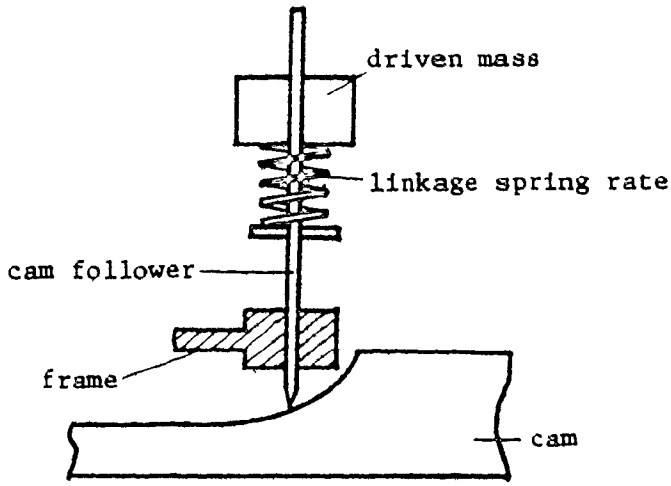

Fig. I.5. One Degree of Freedom Dynamic Model used in [16].

Sarring [17] criticized the assumption that cam angular velocity remains constant, by showing that in the actual mechanism the angular velocity varies and induces instantaneous

torque changes (galloping). To reduce the galloping, he suggested the idea of compensating the torque by counter-balancing the mechanism (Fig.I.6), while presenting a hypothetical torque compensated system (Fig. I.7). The basic idea is that the compensating torque is determined so as to cancel the original torque.

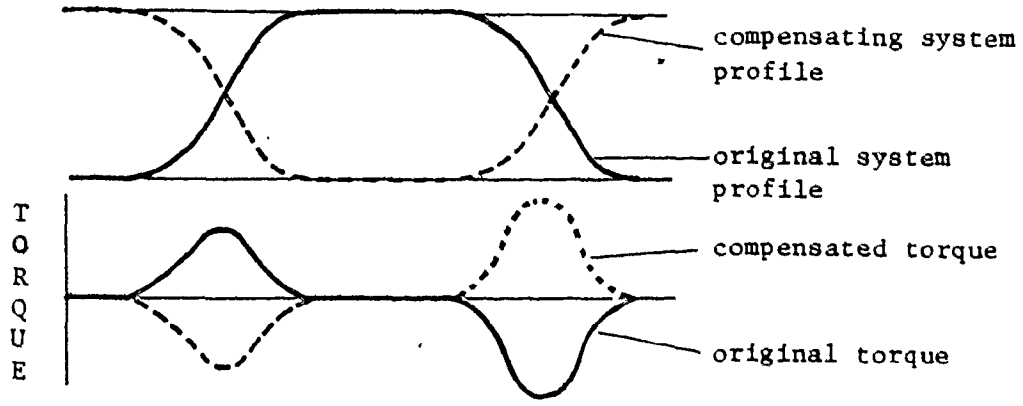

Fig. I.6. Torque Compensation of Mechanism by Counter-balancing suggested in [17].

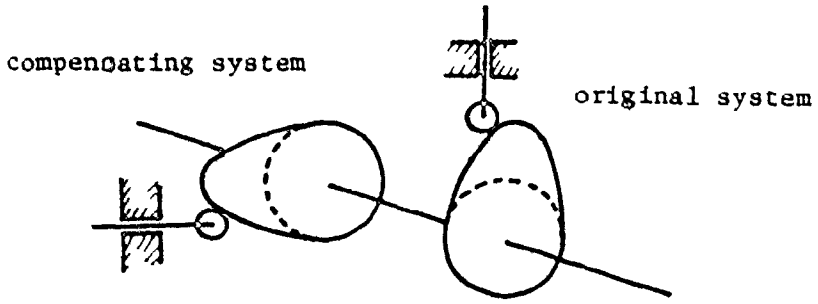

Fig. I.7. A Hypothetical Torque Compensated System presented in [17].

To compute the actual behavior of a varying input velocity, Johnson [18] used the work-energy relation, that is,

Σwork done by forces = Σkinetic energy produced by velocity.

He expressed the velocity in the obtained relation in terms of discretized displacements by the finite differences method [8], and then solved the resulting relation for the angular velocity to get the recurrence formula of the angular velocity. Starting from the initial velocity, he finally obtained the angular velocity with respect to cam angle increment by solving the recurrence formula. The plotted results are shown in Fig. I.8. The direct sources of varying input velocity, such as torsional vibration of cam, backlash and clearance, and flexible cam shaft, were not considered.

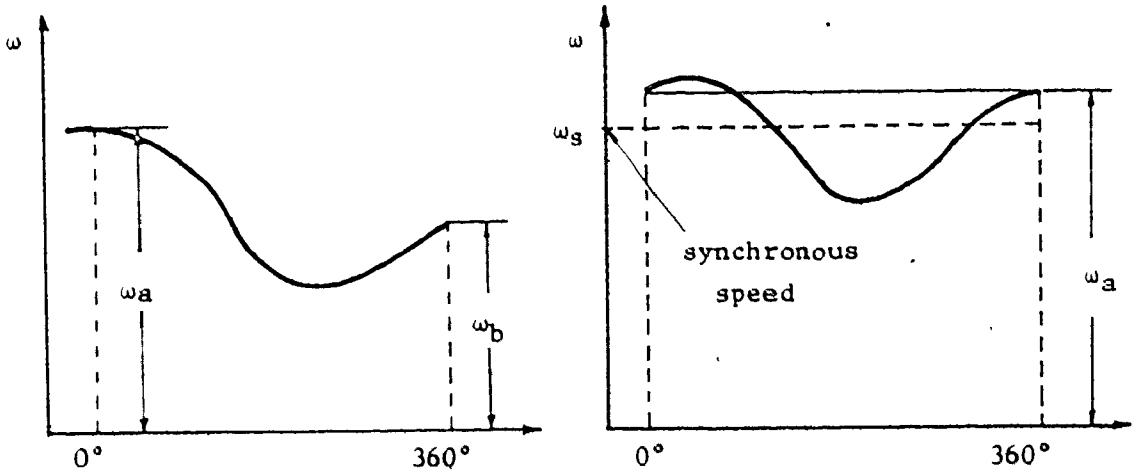

A) when started with ω_a. B) when operation is steady state.

Fig. I.8. Typical Examples of the Variation of Cam Angular Velocity obtained in [18].

By using a very simple one degree of freedom model with no damping (Fig. I.9), Baumgarten [19] proposed a method of calculating the preload force necessary to prevent the separation or jump of the follower. The minimum contact pressure was used as the criterion for jumping without considering the exact contact condition, while contact pressure was unreasonably defined since no total system flexibility was considered. In the freebody diagram, the weight of the follower should not be included since it is cancelled by an initial deflection of the spring. Only the rise cycle was considered; the return cycle was neglected.

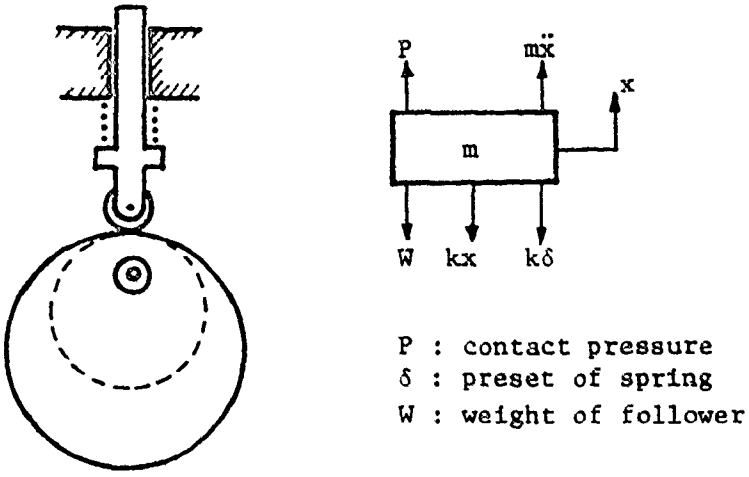

Fig. I.9. One Degree of Freedom Dynamic Model used in [19] for the Calculation of Preload Force.

Introducing a boxcar diagram shown in Fig. I.10, which consists of a springless mass connected by a massless spring and backlash, Goodman [20] demonstrated, as an example, the dynamic effects of backlash existing in a washer mechanism whose major parts consist of a

belt and gears.

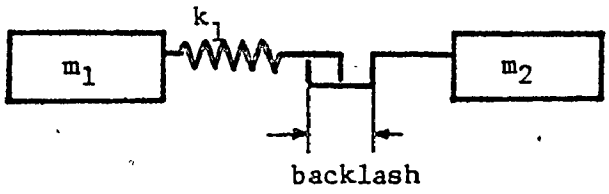

Fig. I. 10. A Boxcar Diagram used in [20] for the Analysis of Backlash.

Knappe [21] was the first to utilize the probabilistic theory and random numbers for the analysis of tolerance, taking a slider-crank mechanism as an example. The approach is as follows:

1. The output is expressed as a function of independent variables and inputs,

$$y = G (x_1, x_2, \ldots x_n),$$

and by differentiating it,

$$dy = \frac{\partial G}{\partial x_1} dx_1 + \frac{\partial G}{\partial x_2} dx_2 + \cdots \frac{\partial G}{\partial x_n} dx_n .$$

2. Assume $\Delta y \approx dy$ and $\Delta x_i \approx dx_i$,

then,

$$\Delta y = \frac{\partial G}{\partial x_1} \Delta x_1 + \frac{\partial G}{\partial x_2} \Delta x_2 + \cdots \frac{\partial G}{\partial x_n} \Delta x_n ,$$

where Δy and Δx_i are the tolerances of output and x_i respectively.

3. After obtaining Δy, the frequency distribution of the output is computed by the Monte Carlo method, sampling from the generated random numbers.

To compare two popularly used motion curves, the cycloidal and modified trapezoidal curves, Allais [22] chose the same model as that used by Hebeler [16]. From the results of the comparison, he found that the modified trapezoidal yields lower peak forces when $n > 7$, while the cycloidal has the advantage where $3 < n < 6$, in which n is the ratio of the cam rise time to the natural period.

Eiss [23] extended the one degree of freedom model suggested by Mercer and Holowenko [12] to a two degree of freedom model (Fig. I.11), in which the previously used assumptions were maintained so as to alleviate the complex mathematical problem. He provided in simple tabular form the follower responses to six acceleration pulses, while demonstrating how the parameters of a two degree of freedom model can be selected to give the minimum vibration amplitude.

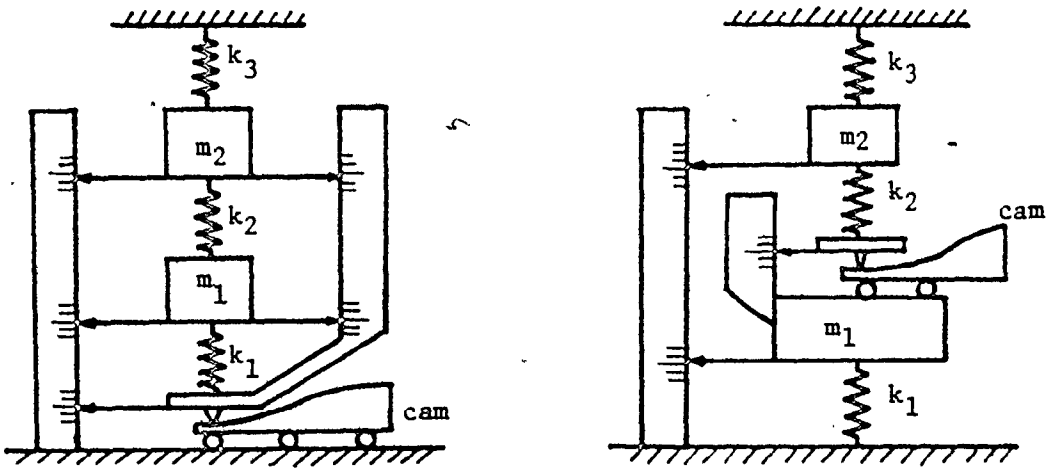

Fig. I.11. Two Degree of Freedom Dynamic Models used in [23].

Erisman [24] used the Fourier series for generating continuous cam lifts and accelerations of flexible automotive valve linkages. To make dimensionless analysis possible, he chose a generalized and oversimplified motion equation,

$$y_v'' = \omega^2 (y_c - y_v)$$

where

y_v = dynamic valve lift

y_v'' = dynamic valve acceleration

y_c = cam lift.

Using a dimensionless design parameter, he explained how to synthesize the cam profile and match it to flexible linkages. He also discussed the design of the spring utilizing the dimensionless design parameter, and suggested that the natural frequency of the spring (Appendix E) should have a ratio of at least 13/1 with the cam shaft speed.

To simplify the mathematical process of optimizing a cam profile to produce minimum residual vibration, Kwakernaak and Smit [25] used a simple one degree of freedim model with no damping. In order to formulate the optimization problem, they attempted two versions of the formulation, which were i) a quadratic problem formulation, and ii) a linear programming formulation, and compared them by their numerical solutions. The optimized profile compared favourably with the well known cycloidal profile.

Brittain and Horsnell [26] provided a numerical method for calculating the former profile which is used in a cam copy grinding

machine shown in Fig. I.12. The effect of grinding wheel wear and of machine setting errors on the profile of a production cam were investigated. To compensate for the grinding wheel wear, a change in the former roller diameter was suggested.

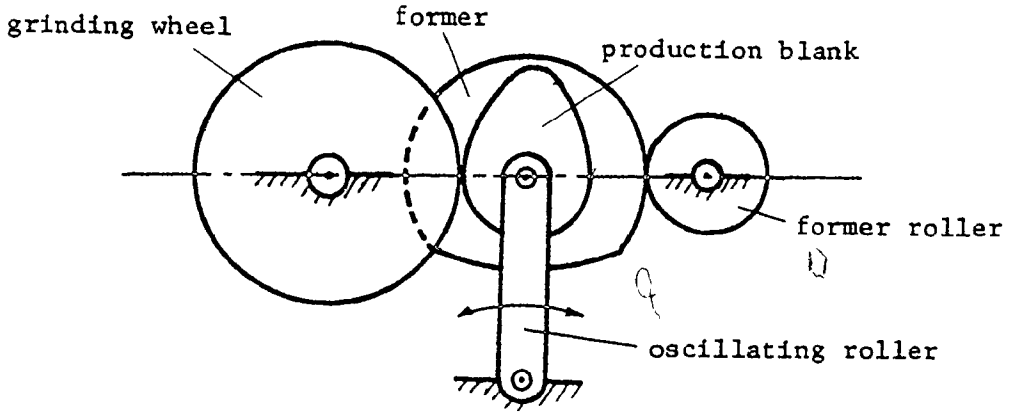

Fig. I.12. Diagram of a Cam Copy Machine Presented in [26].

To analyse the effects on a 4-Bar linkage of the radial clearance at the link joints and the tolerance on link lengths, Garrett and Hall [27] took an approach similar to the one used by Knappe [21], but expanded the output function through the Taylor series, and analysed the 3σ mobility band (variance of follower link displacement). This was considered to be an improved approach.

Emphasizing that non-constant cam angular velocity significantly affects the motion of the follower, Fawcett and Fawcett [28] asserted that the angular velocity is subjected to small amplitude periodic variations caused by the torsional vibration of the cam shaft, as well as

the non-uniform transfer of angular velocity through power transmitting devices. Confining their analysis to the vibrational effect of a flexible cam shaft whose vibration is induced from subharmonic resonances, they investigated the effects of small amplitude vibration of the camshaft purely by harmonic analysis. The follower linkage was assumed to be rigid with no dynamic effects.

Bagci [29] indicated that the use of the first half (rise period) of a cycle of cam rotation yields unreliable information for the complete response analysis of the cam-follower system. Hence, he used a full cycle of the cam motion program (rise-dwell-return-dwell) based on a one degree of freedom model to investigate the dynamic behavior of three motion programs - the trapezoidal, parabolic, and another trapezoidal program whose maximum acceleration is the same as that of the parabolic. It was found that the follower system experiences beats during the consecutive cycles of the cam rotation, that some cam speeds match critical speeds of the follower system, and that a motion program favorable for one speed is not necessarily good at a different speed.

After finding analytically the time response of a linear one degree of freedom system (Fig. I.13.) to a series of typical acceleration pulses, Oledzki [30] studied the corresponding responses of a nonlinear (spring, backlash) system on digital and analog computers. He found that dwell periods in the follower motion are always accompanied by free vibrations with random beats if backlash is present in a kinematic pair, and that the beats do not occur if the spring pro-

perties of the linkage are nonlinear. The following assumptions were made :

1. A positive drive was used (no jumping or separation).
2. The angular velocity of the cam is constant.
3. Cam profile is perfect (zero tolerance).

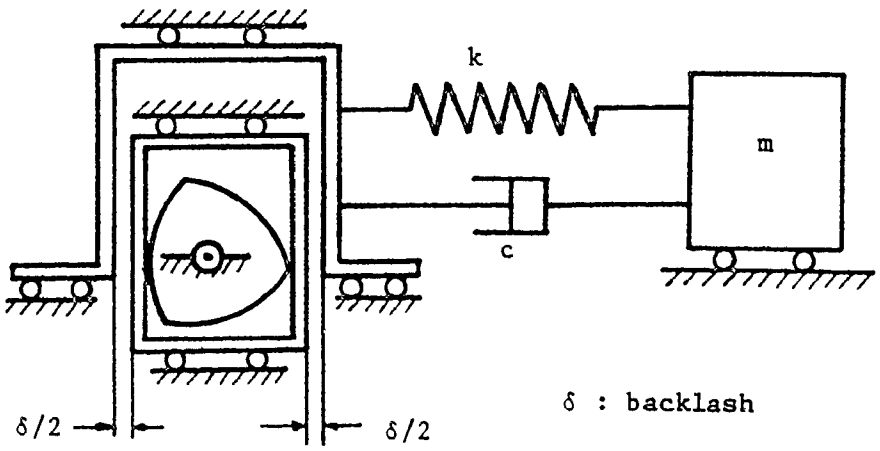

Fig. I. 13. One Degree of Freedom Dynamic Model used in [30].

Solving a simple and general motion equation of a one degree of freedom system by harmonic analysis, Wiederrich and Roth [31] attempted to obtain a motion program which gives low vibration characteristics by controlling the harmonic content of the imposed motion. They found that motions with discontinuous acceleration, i.e. infinite jerk, have low vibration over a wide range of operating speeds. This is a significant contradiction of generalizations about the bad vibration characteristics of motions with high values of jerk. They took a purely mathematical approach (harmonic analysis) without

considering the actual physical phenomena such as contact condition, jump or separation, system flexibility, etc.

Kawasaki et al. [32] discussed how to copy a production cam on a grinding copy machine from a model cam, and suggested a method for calculating by computer the lift error of the cam profile, which is caused by three principal factors - the diameter of the cam grinding wheel, the precision of the model cam profile, and process errors. They analysed the effects of each factor on the lift error.

Weber, in CAM TECH bulletin No. 1 [33] explains a procedure for cutting a cam profile in practice using a curvilinear interpolation with a third degree polynomial, and a conversion from operational coordinates (expressing cam profile as a function of cam angle) to geometric (expressing cam profile in conventional polar coordinates). The advantage of coordinate transformation was demonstrated in cutting a cam having an oscillating follower on either straight-line duplicating machines or N/C machines. This bulletin also shows how to measure the normal, ordinate and abscissa deviations of a cam profile by a sweep method in which the types of follower are considered. In Bulletin No. 11, Weber gives a method of connecting the trade curves (standard motion curves) between two discontinuous points by utilizing a curve function expressed in a finite Fourier series, to improve the dynamics of the system and give a continuous analytical expression.

Adding a linear damper to the one degree of freedom model used by Mercer and Holowenko [12], and using the model shown in Fig. I. 14, Chen and Polvanich [34] investigated the response characteristics of

the follower in terms of nondimensional primary and residual shock response spectra, which are generally adopted for characterizing the dynamic response and damping potential of a structural system.
The shock response spectra are again applied to a two degree of freedom system (Fig. I. 15) to increase the accuracy of the results. The investigation was based on constant cam angular velocity, no jumping, a knife edge follower, and an arbitrary value of damping coefficient. Moreover, each cycle of the periodic motion of the cam was treated as a pulse. In their subsequent paper [35], the linear damper was replaced by a nonlinear damper and the same investigation was carried out.

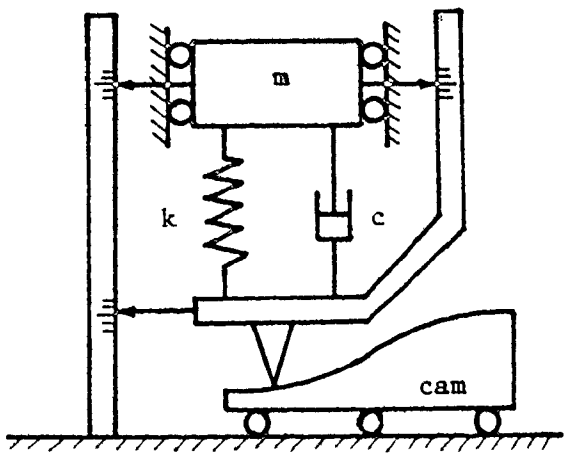

Fig. I. 14. One Degree of Freedom Dynamic Model used in [34].

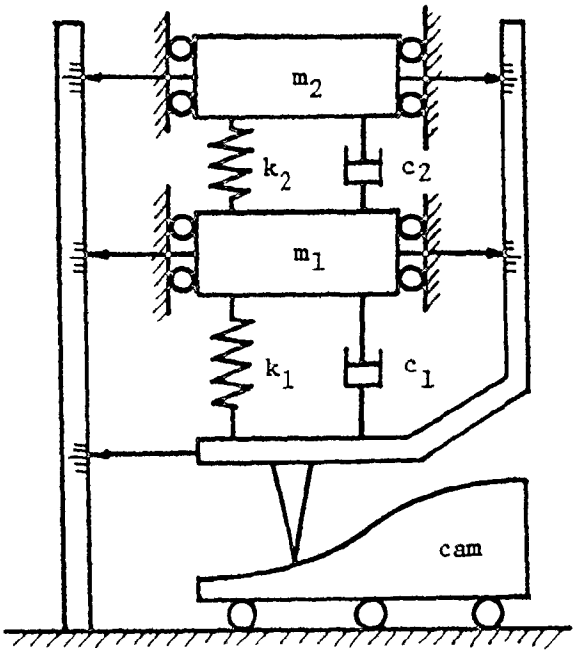

Fig. I. 15. Two Degree of Freedom Dynamic Model used in [34].

Dhande and Chakraborty [36] applied the same approach as that used by Garrett and Hall [27] for analysing the effect of tolerances in the cam-follower system on the displacement output curve. In their analysis, the dynamic behavior of the cam system was not taken into consideration at all. The work was based on the geometry of the cam-follower mechanism and probabilistic theory.

Rao and Raghavachàryulu [37] proposed a method of determining the jump characteristics of cam-follower systems through the use of an

experimental model. Using this model, they examined the jump characteristics of SHM (simple harmonic motion), parabolic, cycloidal and polynomial cams with respect to different spring stiffnesses. It was found that the SHM and parabolic motion cams give better performance than the cycloidal and polynomial cams. The reason for this contradictory discovery was not given, but it can be explained well from the work done by Kim and Newcombe [38], who investigated the tolerance effect of a cam-follower system on time responses, applying the maximum likelihood theory to the finite difference method. Their investigation showed that for the translating roller follower type cam, the sensitivity of the SHM and parabolic curves to tolerance (profile error) is less than that of the cycloidal and polynomial curves. The investigation, however, showed that for the oscillating roller follower cam the former curves are more sensitive to tolerance than the latter.

Di Benedetto [39] proposed three methods of synthesizing a cam profile kinematically for a prescribed jerk pattern which is continuous and has a relatively low peak. The methods commonly use the displacement-jerk recurrence formula obtained from i) the finite differences method, ii) the finite differences and numerical integration method, and iii) the Euler-MacLaurin formula simplified to form a trapezoidal rule. As the time responses are given by discrete numbers, and the numerical integration procedure repeatedly involves truncation and round-off errors, the profile obtained is regarded as being less practical than the known standard motion curves expressed

as functions.

Koster [40] studied the dynamics of a flexible follower driven by a flexible shaft. He obtained the response to the cycloidal cam curve of a representative one degree of freedom model (Fig. I. 16) with a variable fictitious angular velocity. Damping effects were neglected for mathematical convenience.

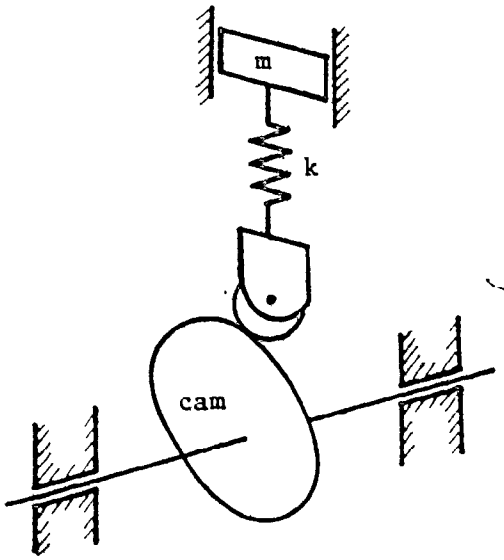

Fig. I. 16. One Degree of Freedom Dynamic Model used in [40].

To provide a fundamental "rule of thumb" for the dynamic system of a cam-follower mechanism, Matthew and Tesar [41] used a one degree of freedom model (Fig. I.17), introducing a shape factor (s) which is equivalent to the cam profile and controlled by the parameters (μ_m, μ_c and μ_k) of the system's dynamic properties.

$$s = \frac{m}{k}\ddot{y} + \frac{c_r}{k}\dot{y} + \frac{k+k_r}{k}y = \frac{m}{k}\omega^2 y'' + \frac{c_r}{k}\omega y' + \frac{k+k_r}{k}y = a_m y'' + a_c y' + a_k y$$

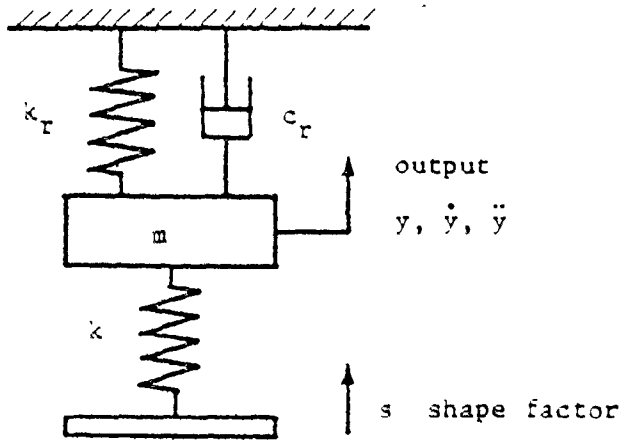

Fig. I. 17. One Degree Freedom Dynamic Model used in [41].

It is often difficult or impossible for a single degree of freedom model to represent the real physical behavior of a system. Therefore, in a second paper [42], Matthew and Tesar changed their one degree of freedom model to a two degree of freedom model shown in Fig. I.18, by distributing the mass, spring and dashpot through the use of distribution parameters. To increase the number of degrees of freedom without considering a real mechanism or system is, however, regarded as a purely mathematical manipulation since it normally has no physical meaning. In a subsequent work [43], Matthew and Tesar discussed the effects of errors which might be introduced into the one degree of freedom model suggested by them in [41], and the effects of errors in the distribution parameters which were used to distri-

bute the dynamic properties in their second work [42]. In addition, they provided the means of calculating errors due to transient vibrations and inertia force vibrations. Throughout their work, they assumed a theoretically perfect cam profile.

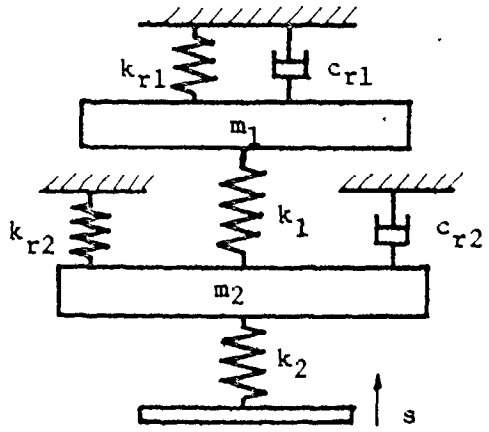

Fig. I. 18. Two Degree of Freedom Dynamic Model used in [42].

Koster [44] investigated the effect of non-constant angular velocity, due to backlash in the driving system and a flexible camshaft, on the dynamics of the cam mechanism, using a four degree of freedom model (Fig. I. 19). The motion-governing equations were derived by the use of the transmission ratio (the kinematic transfer function of the linkage), which relates an infinitesimal rotation

of the output member to the infinitesimal rotation of the input. He solved the motion equations by a computer simulation language called COSILA, which was developed by Philips-Electrologica in the Netherlands. A perfect cam profile was assumed, and no consideration was given to the contact condition between cam and follower or to the jump phenomenon.

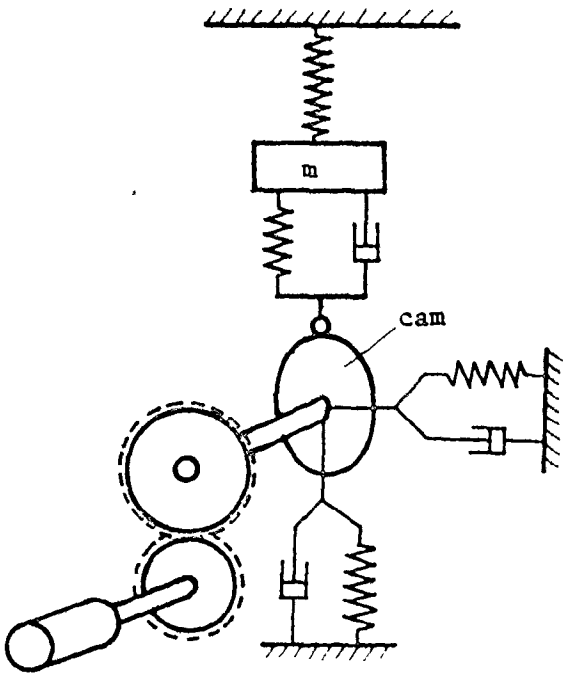

Fig. I. 19. Four Degree of Freedom Dynamic Model used in [44] to Analyse the Various Cam Speeds.

In solving vibration problems in a loom, shown in Fig. I.20, which is operated at various speeds by a cycloidal cam, Noortgate

and Fraine [45] learned that the lay vibrates in resonance with some harmonic of the cam profile. To solve this problem, they attempted to obtain a cam contour having a limited number of harmonics, and proposed a method of calculating the coefficients of harmonics satisfying the condition that the frequency of the highest harmonic should be just below the resonance frequency of the lay at the maximum operating speed of the machine.

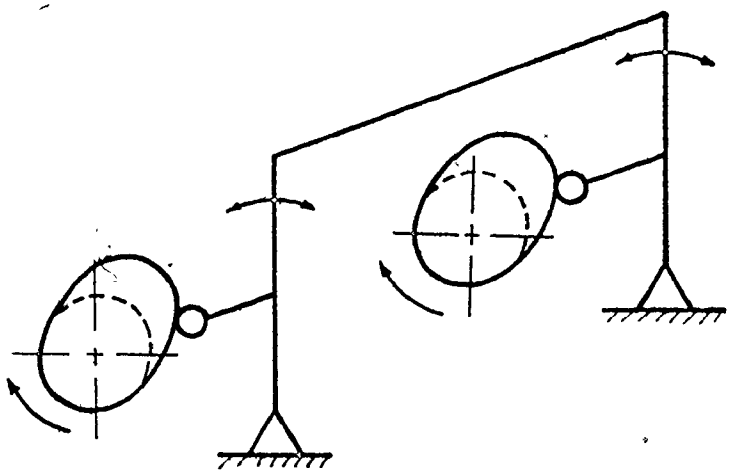

Fig. I. 20 Mechanism of a Loom used in [45].

Ardayfio [46] added a damping to the model used by Koster [40] and solved the differential equation by the finite differences method proposed by Johnson [8].

Smith and Soni [47] attempted to determine the location and magnitude of intermediate cam profile errors. They used the cubic

function of an arc to define the correct intermediate cam profile between the specified cutting points, and from the central difference obtained a recursion formula for the intermediate profile errors. The tips of the scallops (Fig. I.21) were chosen as machine set points (theoretical points).

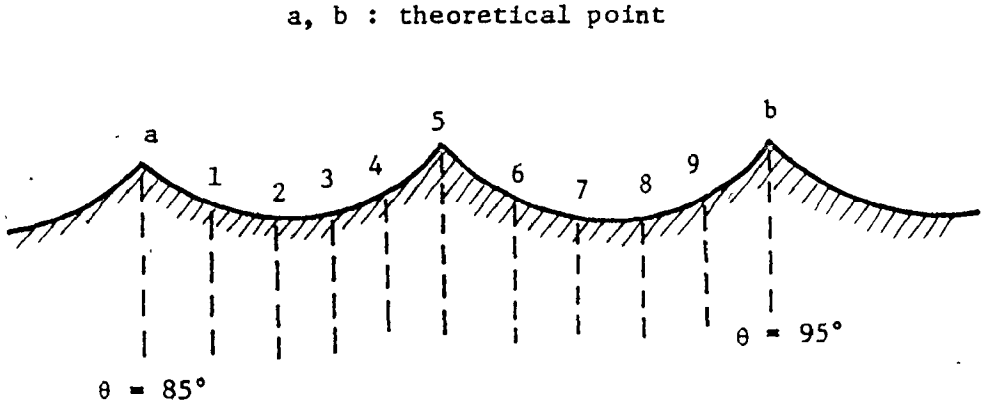

Fig. I. 21. A Part of Cam Profile Simulated in[47].

Using a simplified one degree of freedom model shown in Fig. I.22, Jones and Reeve [48] studied the dynamic behaviors of a family of profiles composed of sinusoidal and constant acceleration segments, which are often called for in a design due to their dynamic properties. The results of the dynamic analysis are presented graphically, and consist of maximum and minimum accelerations, residual vibration, and torque requirement during lift. As the whole analysis was based on the dwell-rise-dwell motion which includes only the rise period of the total cycle, the results are not complete, as discussed by Bagci [29].

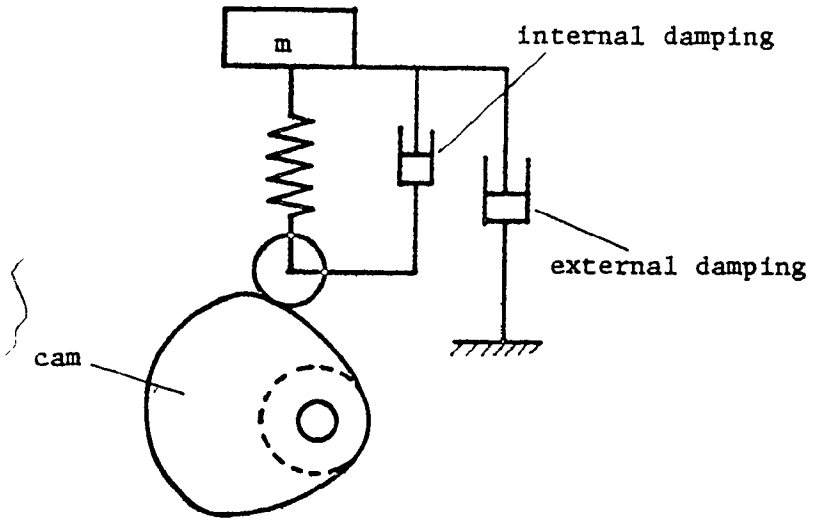

Fig. I. 22. Simplified One Degree of Freedom Model used in [48].

In general practice, the transverse profiles of cams and followers are always imperfect in form and alignment. Beese et al.[49] made a quantitative assessment of the influence of imperfect contact and alignment on the magnitude of contact stresses, and therefore the wear potential, of cam/follower assemblies. In this work it was found that even a very small malfunction of the surface of either the cam or the follower, or small misalignments, seriously reduces the load bearing capability, and that the capability is fundamentally dependant on the geometrical nature of the surface profiles.

Using parabolic and trapezoidal motion programs based on an oscillating roller follower cam mechanism, Giordana et al. [50] investigated the influence on the kinematic analysis of errors in

measuring the cam profile. But they actually investigated the effect of the interpolation error occurring in calculating the second derivative (acceleration) from the measured cam profile, and the effect of the round-off error in computing. To analyse the motion of the oscillating follower from the measured cam profile coordinates, they used the coordinates of a center of curvature at contact point and applied the 4-Bar linkage analogy. This is an indirect analogous approach which is not superior to the vector method [38].

As an extension of their previous work [50], Giordana et al. [51] attempted to study the influence of construction errors on the motion of a cam mechanism based on a purely kinematic analysis, using an oscillating roller follower driven by a parabolic and trapezoidal cam. This work has the following shortcomings:

1. They justified the purely kinematic analysis by reasoning that when the frequencies in the law of motion are much smaller than the frequencies of the limbs of the mechanism, the purely kinematic analysis is acceptable. This justification is hardly adequate since an absence of resonant vibration does not guarantee that there will be no vibration. As far as error analysis is concerned, the dynamic and kinematic analyses should be considered together, since the flexibility of the system does affect the output motion by permitting vibration even though it is not in resonance.

2. To measure the profile of a cam which drives an oscillating roller follower, they used a dial gage which moves in translating

motion. This measurement can be in error because to maintain or keep the probe of the dial gage on the exact contact points between cam and oscillating roller follower (Fig. I.23) is impossible. In other words, the contact points between a cam and an oscillating roller follower are significantly different from those measured by a translating dial gage's small round tip.

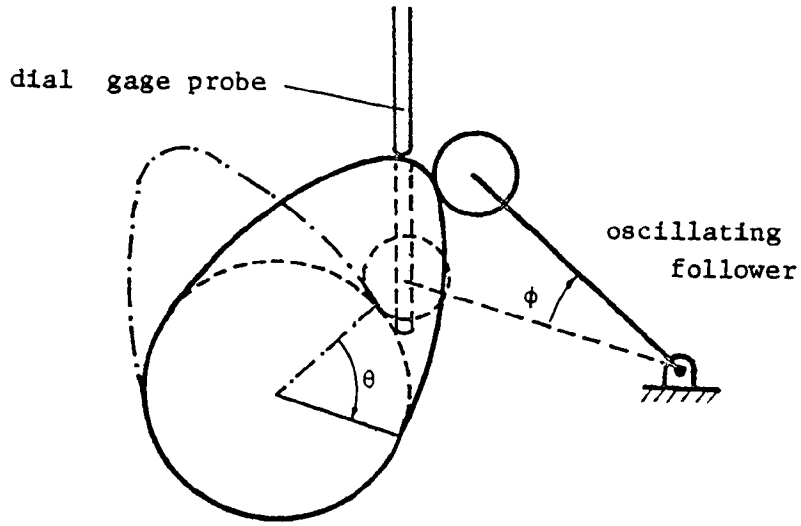

Fig. I. 23. Difference between the Contact Points of Dial Gage Probe and Oscillating Roller Follower with Cam.

3. For the interpolation steps, a 5-degree interval of cam angle was used, which is generally considered too large to obtain accurate results whatever technique is used.

4. As examples of the influence of design approximations they took the case of a cam designed for a translating follower as the cam for an oscillating follower, and used a cam designed by subtracting the roller radius from the cam profile, rather than computing

the envelope of the roller (pitch curve). These cases are considered improper and are not likely to occur.

5. They discussed the effect of variable angular velocity by letting the sum of the elastic potential energy (return spring) and kinetic energy be contant. This approach, however, is considered too rough to be reliable, since the energy equation does not include basic factors causing the variable angular velocity, such as the backlash in a transmitting device, flexible cam shaft, and torsional vibration of the cam.

I.3. Method of Approach

It can be observed from the literature survey that two general approaches have been used to investigate the motion of the follower, i.e. the output. These are : (1) Kinematic and (2) Dynamic. For the kinematic approach, the system has been assumed to be composed of perfectly rigid bodies, and the time responses of the follower became the major concern with respect to a chosen motion curve. In addition to the time responses, the dimensional factors were regarded as important parameters in this approach, especially for the error analysis of the system. The effects of forces were completely excluded in this approach. On the other hand, the dynamic approach has taken the flexibility of the system into consideration, and the main concern is the system vibration. Unlike in the kinematic approach, dimensional factors are normally neglected and a perfectly dimensioned system is assumed. Force analysis on assumed dynamic models is carried out with the objective of minimizing the vibration or avoiding the zone of resonant vibration.

The ultimate purpose of the above two separate approaches is obviously to furnish reliable and useful information concerning the actual behavior of a follower motion driven by a cam. It must, however, be remembered that the actual motion of a follower is a result occurring through the interrelation of all the factors involved in the two separate approaches, such as dimensional, stochastic and deterministic factors, as well as the kinematic and dynamic factors.

Therefore, to provide reliable and useful information on the performance of a follower, it is evident that all possible factors must be included in the investigation, and this can be possible only when the above two separate approaches are implemented simultaneously.

Because of the burdensome mathematics involved, none of the previous investigators has attempted to include all the disturbing factors in the system simultaneously. Some idealizations always had to be made to enable the mathematics to be handled.

It has been pointed out by several investigators [10, 17, 29, 38, 40, 44] that some of these idealizations seriously affect the information obtained and lead to many misconclusions. For instance, the cam speed, which is often considered to be constant, can be quite variable because of the inertia of the driver, flexibility of the cam shaft, the torsional vibration of the cam, and the variation in cam torque due to the motion program itself and follower jumping. As another example, the cam profile, which has always been assumed to be perfectly represented by the theoretical standard motion function, is in fact impossible to manufacture. For instance, for a rise of 1" in 120° with cycloidal motion, the incremental rise or ramp height that is to be built on the cam at 5° into the motion is only 0.00047", and at 7° it is still only 0.0013", which is barely into the range of machine tolerance. This is an inescapable basic fact that has been generally neglected by researchers, and the main objective of this work will be an attempt to include the effects of manufacturing

tolerances as well as all other disturbing factors on the system response. It can also be shown that there is no practical use in investigating 5^{th}, 6^{th} and 7^{th} order polynomial curves because it is practically impossible to produce these on an actual cam profile.

The question is, then, how to approach this compounded problem of studying the actual physical behavior of a cam-follower system more closely and practically without neglecting any significant physical effects of the system. The best initial approach is the use presented here of a simulation technique in which the actual behavior of a cam-follower system is represented by a dynamic and stochastic model. The dynamic and stochastic model was developed through consideration of the previously classified sources of system imperfections.

An eleven degree of freedom cam-follower system has been developed for the dynamic model, and a stochastic model for an actual cam profile has been developed on the basis of a model previously used in a master's thesis project. A mathematical model was implemented by FORTRAN on a PDP 11/34 computer and solved by an up-to-date numerical technique (a refined Runge-Kutta algorithm). The computer and the advanced numerical analysis technique enabled the compounded problem to be solved without significant difficulties economically or mathematically. The results of the simulation, which was continuous with respect to time, were investigated for the influence of system imperfections on the performance of the system, the imperfections being indicated by time responses and inertial responses. Finally, the

results were compared with the results obtained from previous work.

I.4 Objectives

The main objective of this work is to develop an analytical method which will show how the imperfections in a cam-follower system affect the actual performances of the system. The imperfections in the system are to be identified and classified into three categories according to their characteristics. The performances of the system are the outputs from the system, and are also to be divided into two responses according to their nature.

The second objective is to furnish quantitative and qualitative information concerning the influences of system imperfections on the perfomance of the system. The information is to be provided from a computer simulation program which will be developed for the convenient and effective use of any researcher or designer.

Due to the cam-follower system's need for extreme accuracy and its functional complexity, the actual manufacturing and setting up of a system model for any test or experiment would be most difficult and expensive. Even if such a system model were already built, the experimental control of active factors such as cam profile tolerances or roller surface irregularities would be extremely difficult because of their stochastic nature, and to vary them according to several motion programs would be impossibe.

Therefore, in addition to the two major objectives, this work will provide a tool enabling the designer to predict, without setting up the rigorous experimental rig, the actual physical behavior of the system, including the internal as well as the external behavior. The external behavior includes the externally visible motions, such as time (kinematic) responses which can be easily detected by transducers or pick-up devices, and the internal behavior consists of the inertial (dynamic) responses of the system, such as the dynamic stress occurring at the interface of the contact between cam and roller follower while operating, which is almost impossible to detect experimentally.

Throughout this work, the techniques for dynamic and stochastic simulations will be developed, and a method for calculating system dynamic properties, such as the accurate calculation of the spring constant between the two elements of a direct-contact mechanism, will also be presented. The simulation techniques developed will allow the separation of the effects of machining tolerances on both inertial and time responses from those of system flexibility. This was previously thought impossible and has therefore remained unattempted.

CHAPTER II

IMPERFECTIONS IN CAM-FOLLOWER SYSTEMS

Imperfections in a cam-follower system are defined in this work as all the factors existing in a real system which produce a difference between the real output and the theoretical output. Many of these are often avoided in analysis and design to simplify the work and avoid mathematical complexity. To investigate their influence on the performance of the system the leading factors should first be identified, and they are classified here into three general categories according to their nature, as follows :

1. Geometric imperfection
2. Kinematic imperfection
3. Dynamic imperfection.

II.1. Geometric Imperfections

Geometric imperfections are generally the dimensional inaccuracies of a real system as against an ideal system, and the principal factors making up these inaccuracies are tolerances and clearances or backlashes.

II.1.1. Tolerances

Tolerances allow for inaccuracies of manufacture and dimensi-

onal changes in operation, and are given as permissible maximum and minimum variations from the true size. In a broad definition, tolerances cover the variation in mechanical properties resulting from heat treatment and other processing operations, as well as dimensional variation and surface roughness. In this work, however, the investigation will be confined to the dimensional tolerances given or existing on a cam profile.

It is well known that machining tolerance, as one of the design specifications, significantly affects the costs of manufacturing and assembling, but the magnitude of the effects of tolerances on the performance of linkages [21, 27] and especially on cam mechanisms [36, 38] has not been fully investigated. Because of the random nature of manufacturing tolerances, a stochastic approach is required, utilizing the theory of probability. The combination of a stochastic approach and the physical complexity of the kinematic system produces a complex analytical problem, and this is the main reason why the analysis of all-inclusive system errors has not had much investigation.

The kinematic effects of tolerances on the performance (time responses) of cam mechanisms were investigated in depth by Kim and Newcombe [38], who found that the tolerance on a cam profile had a large adverse effect on the performance. This work assumed an idealized mechanism and a rigid system, and is a theoretical study which provides limited information about the effects of

tolerances. But the technique and stochastic model used provide a useful foundation to this work, confirming the association between tolerance and the dynamic behavior of cam-follower systems.

II.1.2. Clearances and Backlash

Unlike tolerances, clearances and backlash are generally introduced as design specifications to allow free motion between two moving parts, as in rotating joints and gears. Tolerances can be reduced indefinitely if cost allows, whereas a certain minimum value of clearance or backlash is compulsory for free motion between parts regardless of the manufacturing cost.

In a cam-follower system, clearance and backlash effects appear at the joints of the follower linkage, the bearings of the cam shaft, follower and driving shaft, and in power transmission devices such as belts and gears. Because clearances and backlash manifest themselves as an uncertainty, their effects should also be analysed by a stochastic method. They also produce impact, vibration and noise as well as affecting the positional accuracy of the mechanism, and a dynamic analysis of their effect is accordingly necessary.

Several investigations have attempted to analyse the effects of clearances and backlash. Dhande and Chakraborty [52] investigated stochastically the clearance effects at the joints of a 4-bar mechanism utilizing the technique employed by Garrett and Hall [27]. For the analysis of dynamic effects of clearances and backlash,

Goodman [20] introduced a box-car diagram, Dubowsky and Freudenstein [53] used an impact pair, and Tesar and Mattew [54] presented a dynamic model for the backlash effects of the positive driven cam-follower system which does not need a return spring. The stochastic technique for the kinematic analysis, and the dynamic model for the dynamic analysis, which were used in their simulation, are provided in Appendix G.

Compared to other imperfections, clearances and backlash have a relatively small effect on the performance of a cam-follower system, and moreover the analysis requires relatively long computing time. On the other hand, they can be reduced so as to be negligible in mechanisms by the use of rigid couplings and preloaded bearings. Therefore the investigation of their effects will be excluded from this work.

II.2. Kinematic Imperfections

Kinematic imperfections are inherent features of cam-follower systems, which have often been idealized in kinematic analysis. They consist of :

1) Variations in angular velocity of the cam
2) Impossibility of cutting the theoretically perfect cam profile
3) Asymmetry between rise and return periods

II.2.1 Non-Constant Angular Velocity of Cam

Cam mechanisms are usually designed with the assumption that the cam rotates ideally with constant angular velocity throughout its whole operation. This assumption introduces errors into the prediction of the actual follower motion, especially in polydyne cam design where the designer is attempting to account for the flexibility of the system. The actual cam speed depends on the flexibility of the cam shaft, torsional vibration, backlash in the power transmission device, and instantaneous torque arising from follower jumping.

The phenomenon of non-constant cam angular velocity produced by instantaneous torque has been investigated by Sarring [17]. To stabilize the velocity, he attempted to counterbalance the torque by adding an extra cam. However, instantaneous torque can be a result of non-constant angular velocity and is not necessarily its cause. Johnson [18] employed the finite difference method to analyse two different models of a rigid cam mechanism : (i) a cam mechanism with known variations in input angular velocity, and (ii) the same mechanism with unknown angular velocity variations. His results were not conclusive. Koster [44] used a more plausible approach by attempting to take all possible sources of input angular velocity variation into account and utilizing a simulation technique. The resulting information was not directly useful.

II.2.2 Impossibility of Cutting the Theoretically Perfect Cam Profile

To satisfy a specific motion requirement, a cam is normally designed by selecting a standard motion curve, or a combination of two or more such curves, (Appendix A) whose kinematic properties are already known to a great extent. Consequently, the performance of the system depends on the chosen motion curves.

To effect the oscillatory motion of the follower a ramp is built up on the base circle of the cam, and a number of standard motion curves have been in traditional use, such as uniform motion, parabolic, simple harmonic, double harmonic, cycloidal, modified trapezoidal, modified sine, and polynomial. These are listed in approximate increasing order. To obtain increasingly smoother acceleration characteristics in the output motion, standard textbooks recommend the selection of a higher order curve. Kinematicians search for ever better motions, and some fairly recent papers have proposed new curves that theoretically have better acceleration characteristics.

However, a most important fact which has rarely been taken into account is that the higher order curves cannot be produced in practice. Because of the limits on machining accuracy the theoretically higher order curve cannot be machined, and the resulting motion may produce no smoother acceleration characteristics than some of the lower order curves. For instance, one of the theoretically better motion curves is the cycloid, but to produce a 25 mm ramp over a 120° cam rotation angle the ramp climbs only 0.006 mm in the first 4°. Therefore the first 4° of the ramp are outside the accuracy range of most machines.

Many people have investigated and developed the standard motion curves. How to synthesize or blend the curves was discussed and suggested by [1, 6, 11, 14, 15, 22, 24, 39], and the dynamic analysis of the curves to avoid a zone of resonant vibration was done by [2, 4, 7, 12, 16, 23, 25, 28, 34], whereas very little investigation on the working behavior of the curves has been carried out.

In this work, the real motion characteristics of each standard curve are studied, including both the effects of tolerances and system flexibility, and their system performances are compared.

II.2.3 Asymmetry between Rise and Return Periods

On the assumption that the return period of the cam motion cycle is point-symmetrical with any rise period, the motion of the follower is usually analyzed by thinking of it as reflection of the rise portion of the standard curve that is being used for the return stroke. This assumption may save calculations, but due to the direction change of the spring force and the possibility of follower jumping (instantaneous change of torque), the motion of the follower during the return period is completely different from the point-symmetrically transformed rise curve. Furthermore, as the follower moves in a cyclic motion, the motion of the return period in a previous cycle affects the rise period in the next cycle.

Thus, an analysis carried out with this assumption leads to false information on the rise period as well as on the return period.

Bagci [29] drew attention to the dangers in this assumption and used a full cycle cam motion program (R-D-R-D) based on a one degree of freedom model to investigate the dynamic behavior of three motion programs (modified trapezoidal, parabolic and another type of trapezoidal). A full cycle of steady state motion should always be chosen and used in the analysis.

In this work, the effect of this assumption is investigated on the performance of cam-follower systems for all the standard motion curves, on the basis of an eleven degree of freedom model.

II.3. Dynamic Imperfections

Dynamic imperfections are the factors affecting the actual dynamic behavior of a system, and are generally neglected or idealized in a theoretical motion analysis or synthesis. They are here sorted into inertia force, flexibility of the system, and energy dissipation.

II.3.1. Inertia Forces

In many of their analyses kinematicians often neglect both translational and rotational inertia forces by assuming that the components of the mechanism of interest are massless. For example, the standard motion programs (Appendix A) which have been derived by kinematicians using the assumption that the mechanism elements have no mass obviously cannot represent the true motion of the follower.

In this work a general technique is developed to account for all the factors affecting the output motion of the follower. As well as considering the manufacturing errors, the dynamic effects of all masses in the system, including 1/3 of the return spring mass (Appendix F), which is often ignored, are taken into account, and both qualitative and quantitative information is provided for the designer.

II.3.2. Flexibility of the system

No real mechanism or system exists which is perfectly rigid. Thus in the vibration analysis of the follower, all the flexibilities in the system must be considered in order to determine the mode of the follower vibration [5, 12, 13, 28, 40] and to avoid resonant zones [23, 24, 42, 45].

The nature of system flexibility can be either nonlinear or linear, depending on whether its relation with the deformation is variable or invariable. The stiffness in the area of contact between cam and follower is actually nonlinear, since it varies according to the location of contact, and is generally regarded as an important factor affecting the life of the cam. The value of this stiffness, however, has been nelgected in analysis, and recently was roughly estimated as a constant value of 100 times the follower linkage stiffness by Shigley [55].

In kinematic analysis, system flexibility is normally ignored in spite of the fact that this imperfection induces follower vibration

and adversely affects its motion. Its inclusion would require a force analysis, which is often thought of as being separate from kinematic considerations.

To obtain its effect on the system performance a dynamic simulation is carried out, and a full cycle chosen from steady state motion must be studied as explained in II.2.3.

In this work, the above mentioned features are all accomplished through a dynamic simulation.

II.3.3. Energy Dissipation

It is obvious that resisting forces always act on the moving or vibrating body and some of the total input energy is dissipated by such forces. Since in a real system energy dissipation affects the dynamic behavior of the system, it is here regarded as an imperfection, in contrast to perfect energy conservation.

The resisting forces which absorb energy are called damping forces, and to bring the analytical results of the performance of the cam-follower system into better agreement with the actual conditions the damping forces must be taken into consideration. These damping forces may arise from several different sources, such as friction between the dry sliding surfaces of the bodies, friction between lubricated surfaces, air or fluid resistance, electric damping, and internal friction due to imperfect elasticity of materials.

In practice, the nature of energy dissipation is so complex that for purposes of analysis the damping forces are very often replaced by an equivalent viscous damping which is expressed in terms of velocity. This equivalent damping is determined in such a manner as to produce the same dissipation of energy per cycle as that produced by the actual resisting forces. If the energy dissipation is proportional to the velocity it is called linear damping, and if not proportional it is called nonlinear damping.

In this work, the two types of energy dissipation are both considered in investigating their effect on the performance of cam-follower systems. For example, the friction damping in the slide bearing of the follower has nonlinear characteristics, since the friction force is varied according to the movement of the follower, and so is the damping force. This nonlinear damping is taken into consideration, together with linear damping such as viscous damping in the cam shaft bearings and motor bearings, air friction on the cam, and structual damping in the follower, drive shaft and camshaft.

Due to the complex nature of damping, exact values are difficult to determine, and this is the most likely reason why the factor of damping or energy dissipation is so often excluded from analysis and synthesis. To enable the investigation of this work to be effective, a technique for calculating the approximate value of each damping coefficient is utilized which provides reasonable values without significant error.

It is reemphasized here that to investigate the effect of one imperfection on the performance of cam-follower systems, all other imperfections must be taken into consideration, because the performance of the system is determined from the compounded interrelation between imperfections.

CHAPTER III

PERFORMANCE OF CAM-FOLLOWER SYSTEM

The performance of any cam-follower system can be described in terms of its real output with respect to the specified output, and in terms of how well it meets operational design constraints such as contact stress, torque, force, noise, vibration and wear. System imperfections as described in the previous section can have a large effect on the performance and in the past have been largely neglected.

Performance will be classified into two general types according to their general nature, as follows :

1. Time Responses
2. Inertial Responses

These are discussed in more detail in the following sections.

III.1. Time Responses

In the design of a cam-mechanism the main objective is usually to have a specific motion response with respect to elapsed time. This is usually a follower displacement versus elapsed time requirement, which is essentially a follower displacement versus cam rotation requirement, since cams almost always run at constant angular velocity, or at a velocity which is timed to the running velocity of the whole machine. For instance, the camshaft on an automobile engine has to lift an intake

valve on every second revolution of the engine.

Sometimes, more complicated motion specifications need to be met, such as requiring the follower to match a certain velocity at a certain point in its stroke, or matching a specific acceleration peak at the end of its stroke to avoid discontinuities in the acceleration curve and infinite jerk. Thus one or more of these responses with respect to time - displacement, velocity, acceleration or jerk - are the factors of interest.

To obtain the theoretical time responses of a cam is a very simple matter, if the standard motion curves are used and imperfections are neglected. The velocity, acceleration and jerk equations are obtained by differentiating a basic displacement equation which is determined by the designer, who usually idealizes the system.

On the other hand, the real motion results from a compounding of the errors in the cam profile, the contact condition between the actual profile and the actual roller surface, the flexibility in all the mechanism elements, the eccentricity of the cam shaft, bearings or base circle, and non-constant angular velocity.

The real motion could be determined experimentally, but with difficulty and high cost. However, the main objective of this project is to determine the relative magnitude of the separate effects of the cam profile errors, i.e. machining tolerances, and this would be impossible to do by experiment alone.

III.2. Inertial Responses

The physical phenomena which arise from the motions of the elements in the cam-follower system, such as forces, torques, stresses, vibration, noise and wear, are classified as inertia responses.

These arise because of the translational and rotational inertias in the system, and the designer must ensure that they are all within the specified limits of his design constraints. If the imperfections in the system are neglected, he must use safety factors based on judgement or experience to account for the excursions of these phenomena from normal values calculated by idealizing the system. These are all important factors which affect the operation, efficiency and life of a system, and it would be beneficial to be able to determine their spectra.

As with the effect of tolerances on the time responses, it would be an almost impossible task to make any meaningful measurements of these phenomena on an experimental basis, and thus the decision was made to resort to a simulation technique.

CHAPTER IV

SIMULATION OF CAM-FOLLOWER SYSTEM

A system is a specific combination of like or unlike elements, arranged in a specified manner such that various inputs or disturbances produce desired responses. To assess the characteristic responses of a cam-follower system to various inputs or disturbances which were regarded as imperfections and specified individually in the previous chapter, a simulation technique has been developed and employed in this work.

Simulation can be used not only for design and analysis, but also to alleviate burdensome procedures in developing or improving a product or system. It is the imitation of the behavior of a real system through the use of a model, and generally deals with two systems: i) the physical system with which engineers are concerned, and ii) the model of the system which is to be studied. The physical system may be a real system that is actually in operation, or it may be only on paper and still in the design stage. The model may itself be another physical system and, in fact, often is. But it can also be a mathematical model.

To simulate the real behavior of a system, two approaches must be taken:

1. A non-stochastic or deterministic approach to account for flexibilities in the system and its dynamic behavior;

2. A stochastic or probabilistic approach to account for the indeterminant factors or uncertainties such as tolerances and backlashes.

Thus, in this work, the simulation of the actual behavior of a cam-follower system will comprise dynamic and stochastic simulations carried out by proper modelling procedures.

IV.1. Dynamic Simulation

The simulated results are greatly dependent on the correct and careful choice of a model, which should be developed with careful consideration of all feasible factors affecting the behavior. In the following sections, a system model is first determined, from which a dynamic model is carefully developed, and the dynamic model is followed by a mathematical model which will enable the computer simulation of the dynamic behavior of the system to be carried out numerically.

Very often authors do not select their models in logical sequence and clearly define the derivation and typical roles of these models. In the following sections an attempt will be made to present the modelling in a logical manner.

IV.1.1. System Model

An infinite number of cam-follower configurations are possible, and it is therefore impossible to simulate them all, nor is it desirable to attempt to simulate any particular configuration or application.

The aim here is to establish a simulation technique that can be applied to all planar cam mechanisms. To this end a representative system was selected, and so designed that it would be relatively easy to manufacture for later experimental work. Also, the design of the model is such that its mechanical properties and constants would be easy to determine.

In addition, two cams were actually manufactured and precisely measured by two cam manufacturing specialist companies so that representative cam profiles could be studied.

The physical system model forms the initial base for the simulation, and it provides the necessary information such as the relationship between the various parts, their geometrical dimensions and their material properties.

All cam-follower systems are commonly composed of five major parts. These are :

1. Driving part (motor, engine)
2. Driven part (cam, camshaft)
3. Power transmitting part between driving and driven parts (gears, belts, chains or couplings)
4. Follower and its subsidiary linkage
5. Load

Accordingly, the proper simulation of the system should consider and include all the five parts so that it may be applied

to any type of cam-follower system without significant modification.

For these reasons, a translating inline roller follower-cam system driven by an eletric motor through a rigid coupling was chosen as a representative cam-follower system model, and sketched in Fig. IV.1. In the system model, a heavy rigid coupling was selected instead of a belt, gear or chain to reduce the circumferential oscillation, and to clearly show the effect of profile tolerances by eliminating the blurring effects of backlash or belt slippage and elasticity. Also a two dimensional disk cam mechanism with a translating roller follower was considered for the simulation because of its popularity and versatility, and because the general contact condition between cam and follower surfaces could be determined theoretically.

IV.1.2 Dynamic Model

To simulate the dynamic behavior of the chosen system model, two kinds of dynamic models can be generally taken into consideration. One is a continuous system with distributed masses and elasticity, and the other is a discrete system with lumped masses connected by weightless springs.

Continuous systems are modelled by assuming them to be composed of homogeneous, isotropic, elastic material, and typical applications are such relatively simple systems as strings, beams, shafts or plates having uniformly distributed properties. A discrete system

can be assumed when the members are massive and stiff, and connected with other members which have relatively small mass but high flexibility. The cam-follower system concerned here is a good example of this latter kind of system, as it consists of lumped masses (motor armature, heavy coupling, cam follower and load) which are connected by relatively light and flexible shafts or rods.

The main reason for assuming the real continuous system to be a discrete system having lumped masses and elasticity is that the behavior of the continuous system is governed by partial differential equations relatively few of which can be solved and then only for restricted boundary conditions. Especially if the system is nonlinear, its analysis is hardly amenable to solution. On the other hand, the motions of a discrete system are given by ordinary differential equations, which can be solved in many cases including nonlinearities.

For these reasons, a dynamic model which consists of lumped masses and elasticity, corresponding to the preditermined physical system model (Fig. IV.1), was chosen to represent the dynamic behavior of the cam-follower system and is shown in Fig. IV.2. The dynamic model has eleven degrees of freedom and is divided into two systems :

1. The three degree of freedom driving or rotational system (Fig. IV.3)
2. The eight degree of freedom driven or translation system (Fig. IV.4)

The torsional dynamic model is shown in Fig. IV.3a, and for ease of

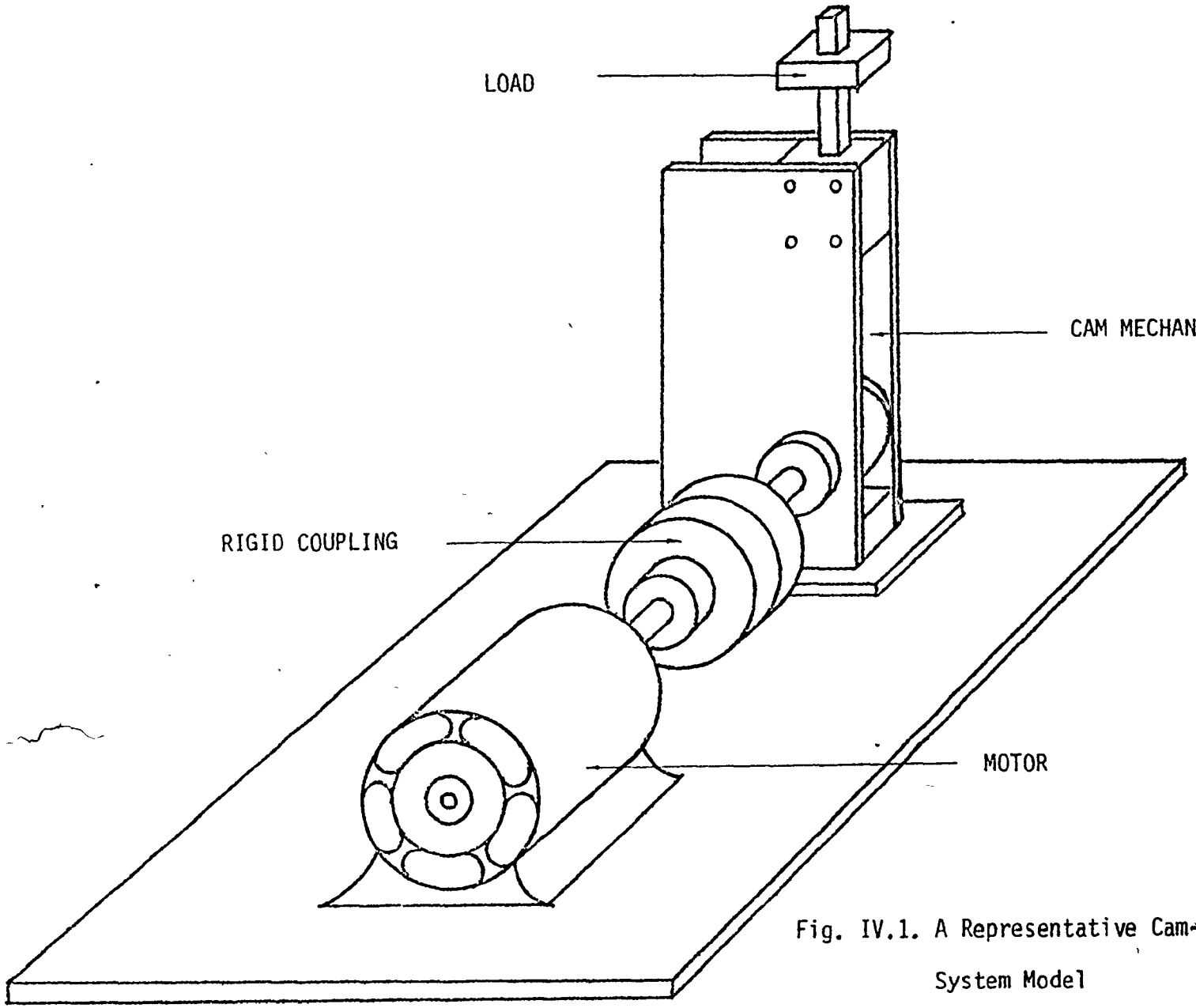

Fig. IV.1. A Representative Cam-Follower System Model

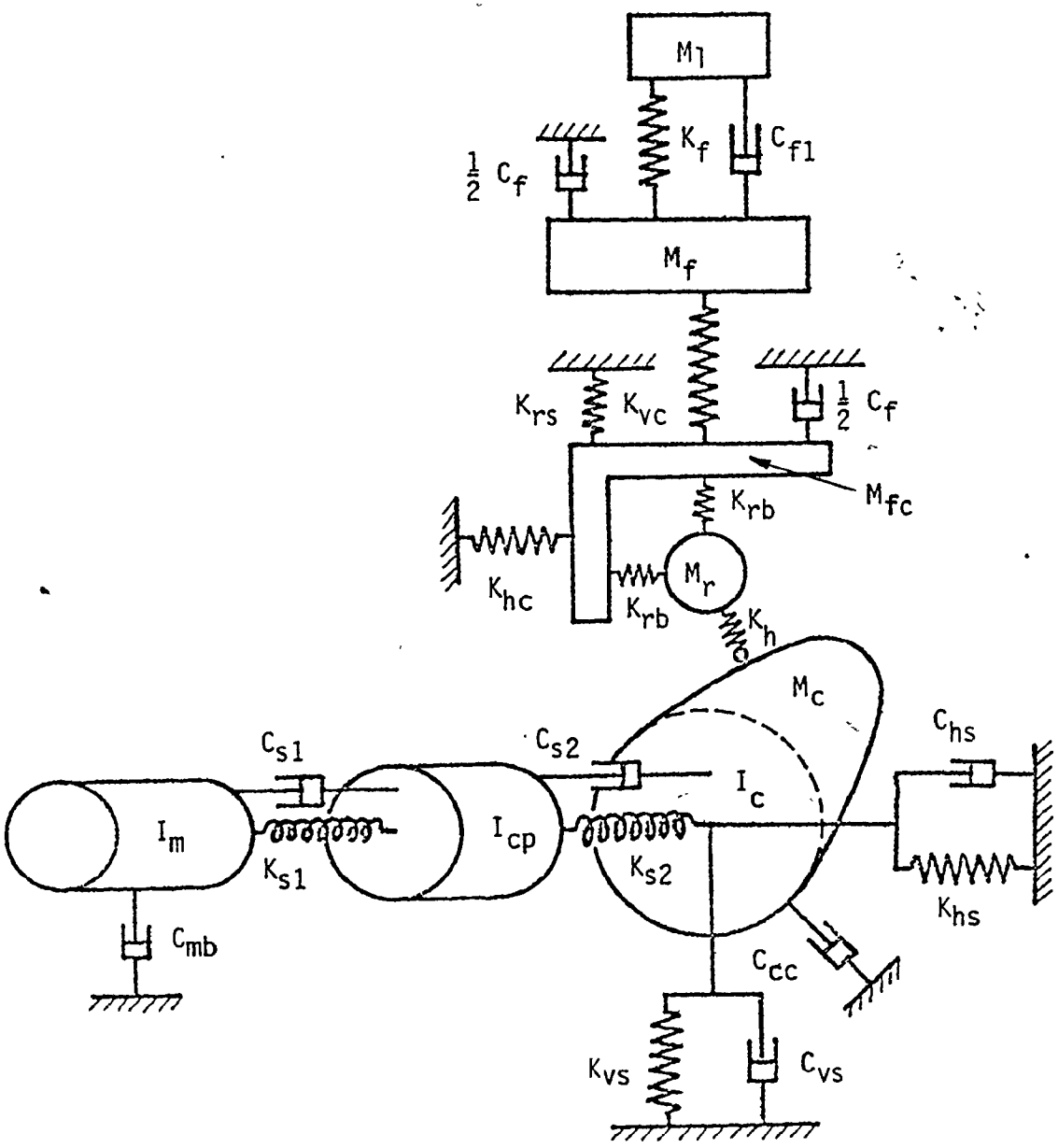

Fig. IV.2. Dynamic Model of Cam-Follower System.

derivation of the mathematical model a linear model equivalent to the torsional model is given in Fig. IV.3b. The latter system is divided into two subsystems according to the vertical (Fig. IV.4a) and horizontal (Fig. IV.4b) motion of the parts. To simulate the actual dynamic behavior as closely as possible, all feasible physical factors, as well as the basic dynamic properties pertaining to the cam follower system, were taken into account, such as :

1. Friction in the follower roller and sliding bearings
2. Cantilever effect of the follower
3. Hertzian contact force and deflection at the cam-follower interface
4. Preload of the return spring
5. Oscillation of the cam shaft
6. Jump phenomena
7. Variations in angular velocity
8. Pressure angle.

The only assumptions made here are :

1. There is no surging in the return spring
2. There is no clearance in the needle bearing of the roller follower
3. Camshaft is supported by preloaded duplex ball bearings to eliminate bearing clearance as well as to endure heavy load or impact.

Since the latter effects can be made insignificant in practice, these

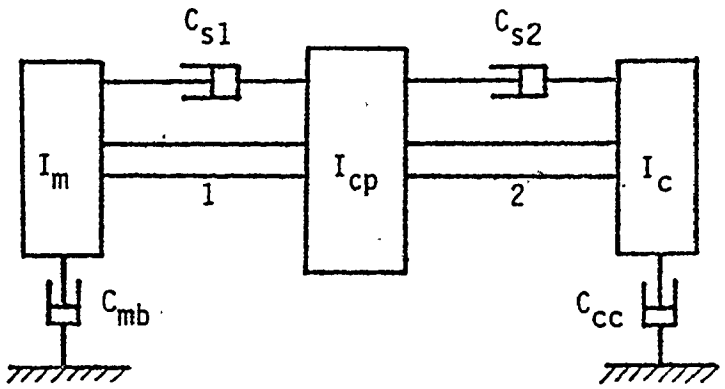

(a) Torsional

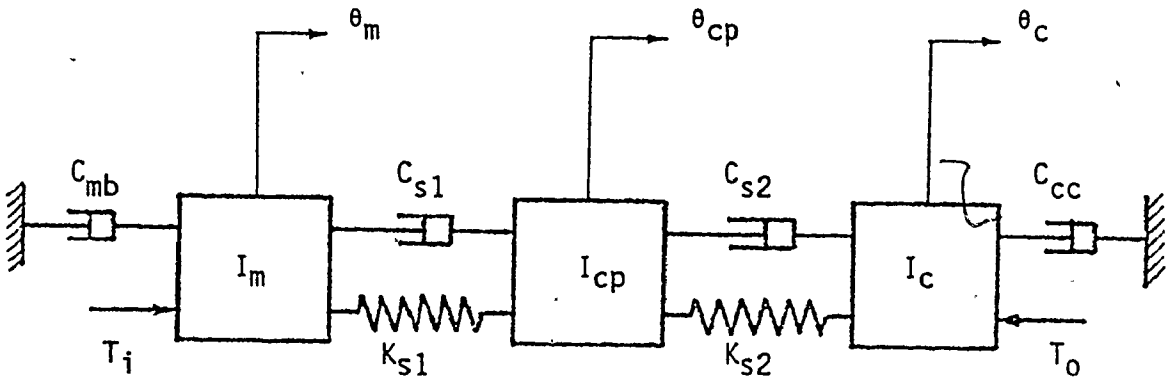

(b) Linear

Fig. IV.3. Dynamic Model of Rotational Subsystem

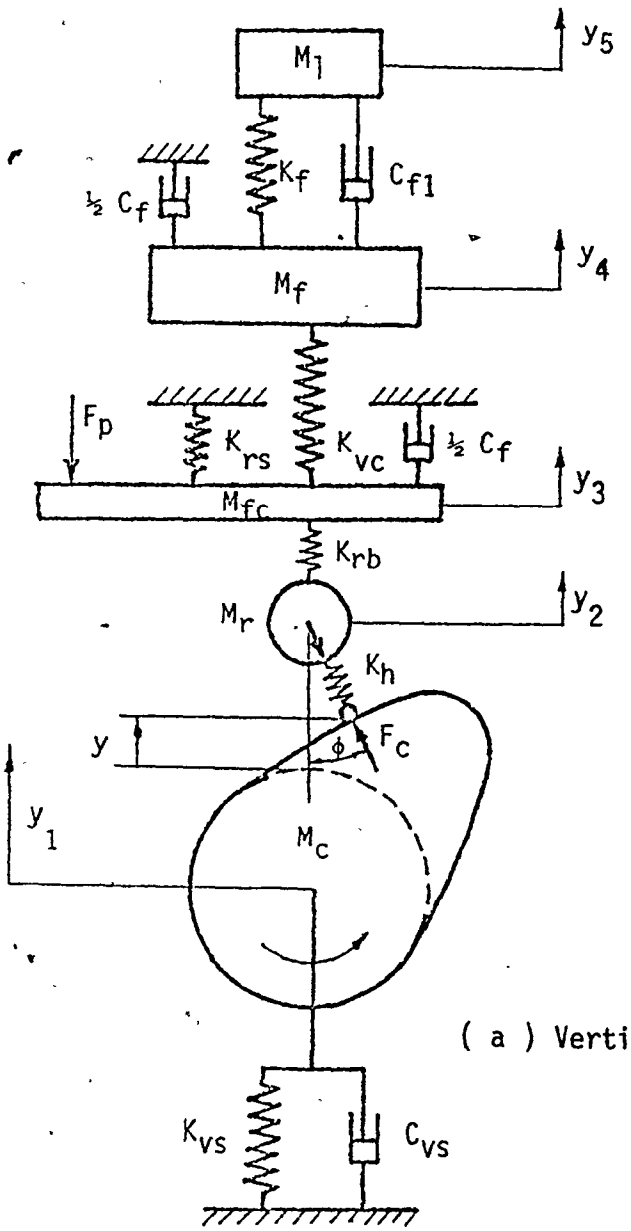

(a) Vertical Motion

(b) Horizontal Motion

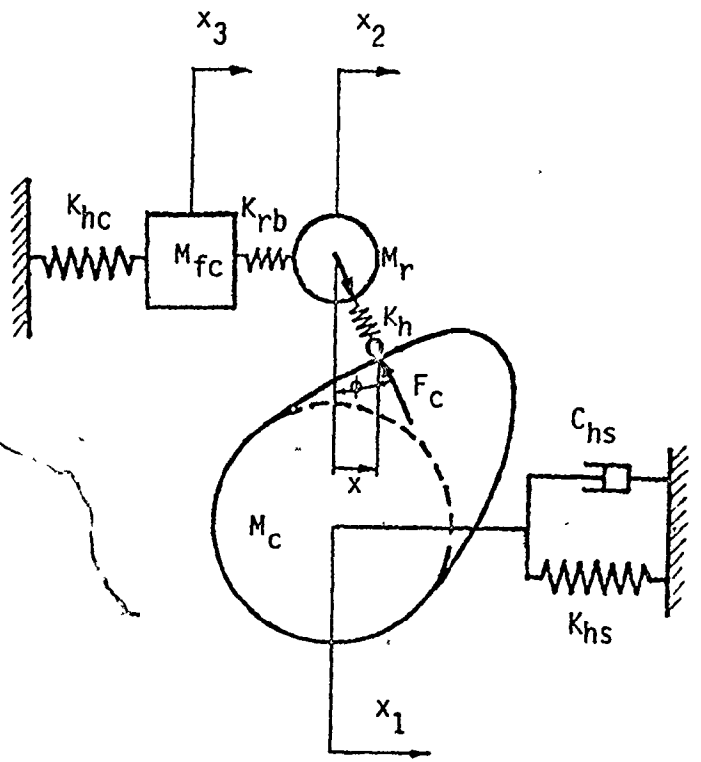

Fig. IV.4. Dynamic Model of Translational Subsystem

assumptions are considered to be reasonable.

IV.1.3 Mathematical Model

The freebody diagrams corresponding to the dynamic models (Figs. IV.3b,4a and 4b) are shown in Figs. IV.5, 6a and 6b respectively.

From Fig. IV.5, the application of equilibrium condition by D'Alembert's principle yields the governing equations of the rotational system as :

$$T_i - C_{mb}\dot{\theta}_m - C_{s1}(\dot{\theta}_m-\dot{\theta}_{cp}) - K_{s1}(\theta_m-\theta_{cp}) = I_m\ddot{\theta}_m$$

$$C_{si}(\dot{\theta}_m-\dot{\theta}_{cp}) + K_{s1}(\theta_m-\theta_{cp}) - C_{s2}(\dot{\theta}_{cp}-\dot{\theta}_c) - K_{s2}(\theta_{cp}-\theta_c) = I_{cp}\ddot{\theta}_{cp}$$

$$C_{s2}(\dot{\theta}_{cp}-\dot{\theta}_c) + K_{s2}(\theta_{cp}-\theta_c) - C_{cc}\dot{\theta}_c - T_o = I_c\ddot{\theta}_c \qquad \text{(IV.1)}$$

where $T_o = \left(\frac{\dot{y}}{\dot{\theta}}\right) F_c \cos\phi$

F_c = contact force between cam and roller

and ϕ = pressure angle

Similarly the equations for the translational system are derived from Figs. IV.6a and 6b :

1. Vertical Movement

$$-K_f(y_5-y_4) - C_{f1}(\dot{y}_5-\dot{y}_4) = M_1\ddot{y}_5$$

$$K_f\,(y_5 - y_4) + C_{f1}\,(\dot{y}_5 - \dot{y}_4) - \frac{1}{2}\,C_f\,\dot{y}_4 - K_{vc}\,(y_4 - y_3) = \frac{d(M_f\,\dot{y}_4)}{dt}$$

$$K_{vc}\,(y_4 - y_3) - F_p - K_{rs}\,y_3 - \frac{1}{2}\,C_f\,\dot{y}_3 - K_{rb}\,(y_3 - y_2) = \frac{d(M_{fc}\,\dot{y}_3)}{dt}$$

$$K_{rb}\,(y_3 - y_2) + F_c\cos\phi = M_r\,\ddot{y}_2 \qquad \text{(IV.2)}$$

$$-F_c\cos\phi - K_{vs}\,y_1 - C_{vs}\,\dot{y}_1 = M_c\,\ddot{y}_1$$

where $M_f = \rho A\,(e_1 + y_3)$

$M_{fc} = \rho A\,(e_2 - y_3)$

ρ = density of follower material

A = cross section area of follower

e_1 , e_2 = distances of follower and its cantilever part respectively

($e_1 + e_2$ = total length of follower)

Note that M_f and M_{fc} are both time variants and

$$\frac{d(M_f\,y_4)}{dt} = \rho A\,\dot{y}_3\,\dot{y}_4 + M_f\,\ddot{y}_4$$

$$\frac{d(M_{fc}\,\dot{y}_3)}{dt} = -\rho A\,\dot{y}_3^2 + M_{fc}\,\ddot{y}_3$$

2. Horizontal Movement

$$K_{rb}\,(x_2 - x_3) - K_{hc}\,x_3 = \frac{d(M_{fc}\,\dot{x})}{dt}$$

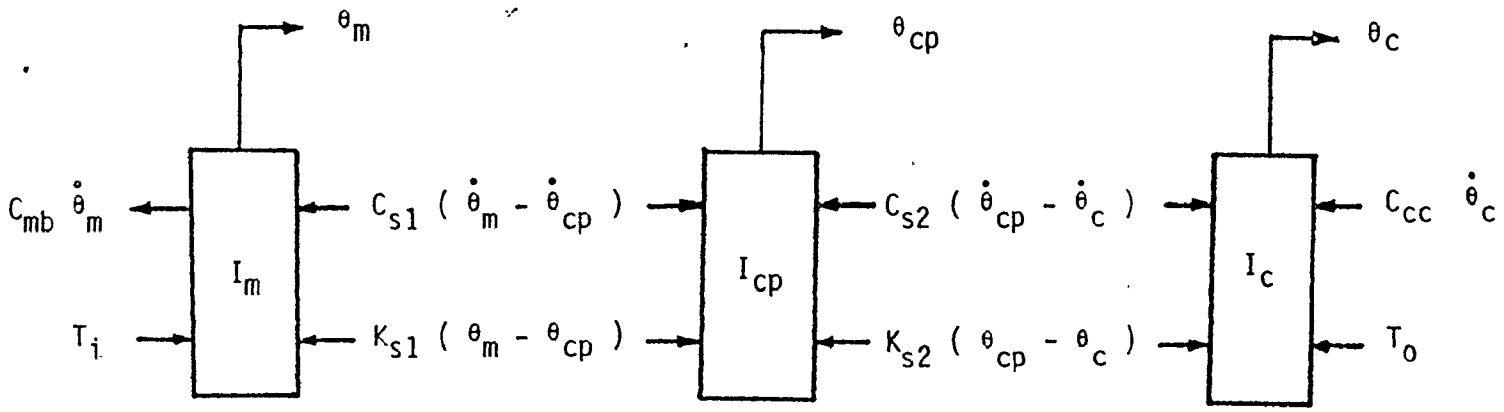

Fig. IV.5. Freebody Diagram of Rotational System

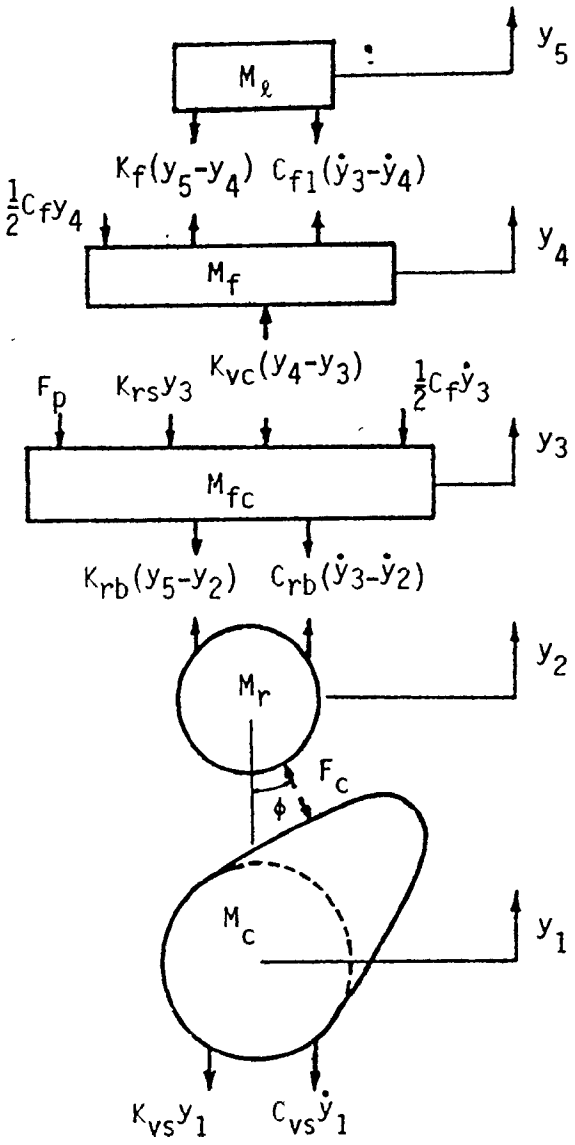

(a) Vertical

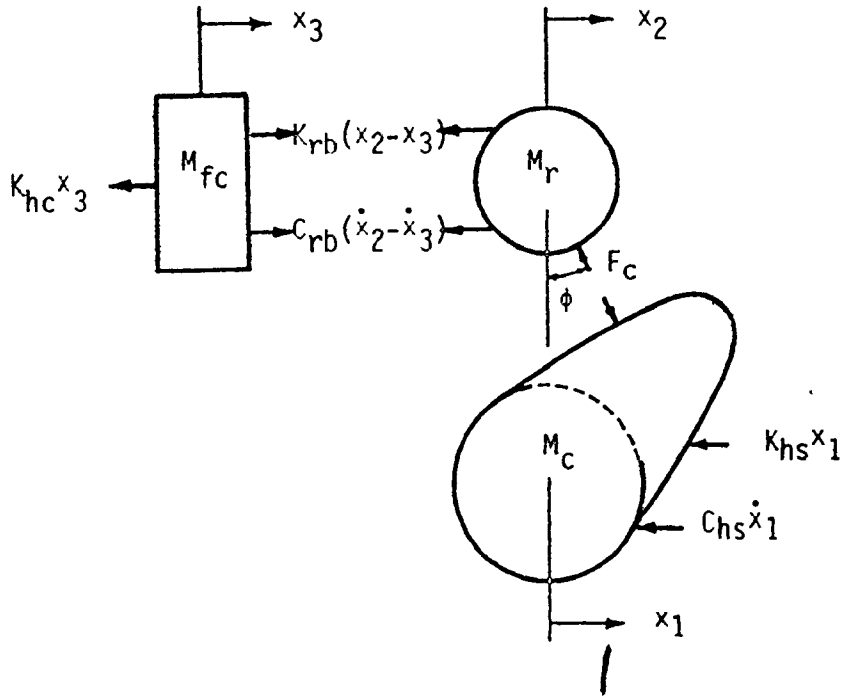

(b) Horizontal

Fig. IV.6. Freebody Diagram of Translational System

$$- K_{rb} (x_2 - x_3) - F_c \sin\phi = M_r \ddot{x}_2$$

$$F_c \sin\phi - K_{hs} x_1 - C_{hs} \dot{x}_1 = M_c \ddot{x}_1 \qquad \text{(IV.3)}$$

where $\frac{d(M_{fc} \dot{x})}{dt} = - \rho A \dot{x}_3 + M_{fc} \ddot{x}_3$

In Equation (IV.2) the damping forces $\frac{1}{2} C_f \dot{y}_4$ and $\frac{1}{2} C_f \dot{y}_3$ are replaced by the friction forces F_1 and F_2 caused by the contact force F_c which will be found later.

IV.2 Stochastic Simulation

Due to the stochastic nature of the machining errors an input representing the actual random nature of the cam profile and the roller surface must be added to the dynamic effects. In this section, as a basic input source, the most probable actual cam profile is first generated within the machining tolerances, considering the actual cam fabricating procedure. The actual motion of the roller itself resulting from the contact between the two irregular surfaces of the cam and roller is then developed by a stochastic technique.

IV.2.1 Machining Process of Cam Profile - Production Cams

When a number of production cams are to be produced, a master cam whose

size is generally larger than the actual cam is first of all cut, and this master cam is then copied in properly reduced scale, thus diminishing further the inevitable errors on the master cam profile. The degree of accuracy needed in high speed machinery particularly requires that a master cam be made at least 4 or 5 times actual size.

The master cam is commonly milled by an NC machine step by step with the increments of cam rotation angle. Aided by a marking compound, a skilled machinist then files or hand-laps the scalloped contour (Fig. IV.7) to a smooth profile joining the machine setting points. With a pantograph device or hydraulic copying mechanism, the final cams of proper size are finish-ground from the master cam.

IV.2.2 Simulation of Actual Cam Contour

To properly simulate the actual profile, the machining methods for the actual cam contour must be taken into account. It is impossible to position the tip of the cutter exactly at a specified point on the profile. It can only be located within an allowable error, namely the tolerance in the x and y direction, which is a two dimensional tolerance as shown in Fig. IV.8.

The resulting profile shape will thus be random within these tolerances. Moreover, due to the scalloped contour obtained from step milling, residual waviness will appear on the profile of the master

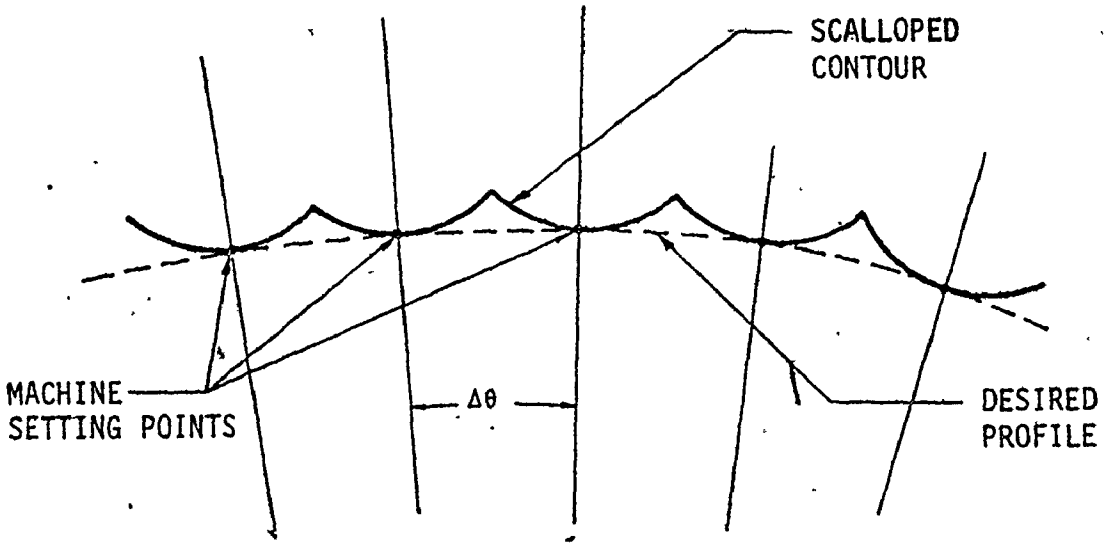

Fig. IV.7. Scalloped Cam Surface

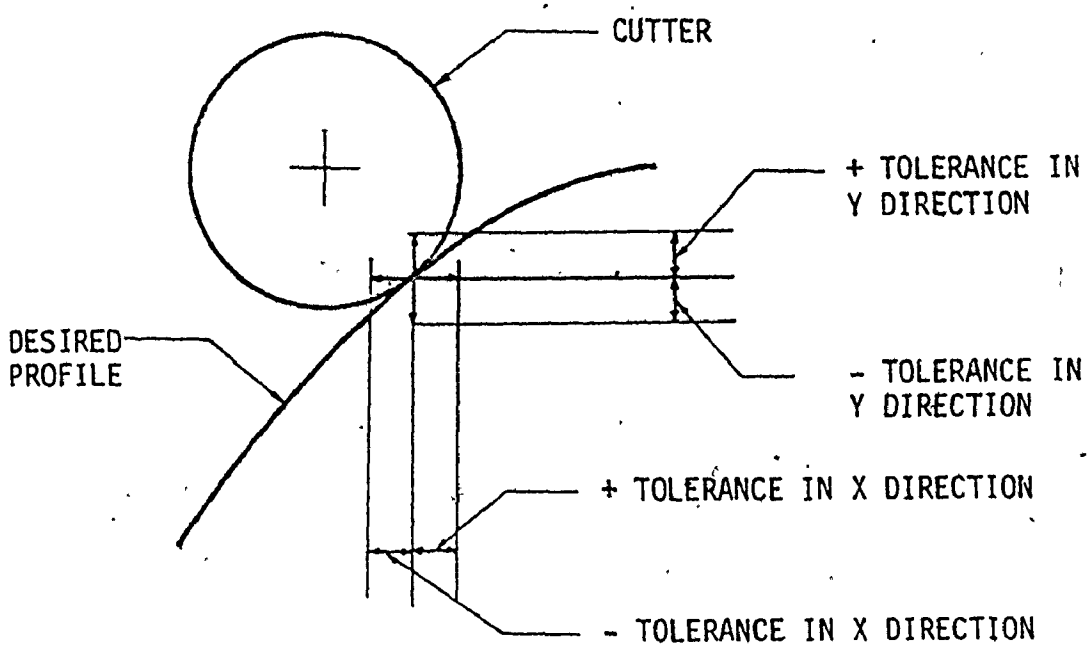

Fig. IV.8. Two Dimensional Tolerance Band for Setting Cutter

cam even after filing or lapping. This residual waviness on the master cam profile will be reproduced on the actual cam. Another source of the waviness on the cam profile is grinding wheel vibration or chattering during the final grinding stage. Therefore, the finally manufactured actual cam profile will be characterized by randomness and waviness.

In addition, the roughness of the cam profile may be included. However, the roughness consists of relatively finely spaced surface irregularities produced by cutting edges and machine tools, and is specified in microinches. Because it will not have any significant effect on the follower motion it is excluded in this simulation, whereas the waviness generally resulting from such factors as machine or work deflections, vibration, heat treatment, or warping strains, consists of irregularities in the nominal surface which are of greater spacing than roughness and is rated in inches (Fig. IV.9).

As any randomness is characterized by its distribution, information about the distribution is necessary to describe the characteristics of cam profile randomness. Whitehouse [56] showed the surfaces produced by milling, turning, grinding and honing have an almost Gaussian (normal) distribution, as given in Fig. IV.10. Applying the Gaussian distribution characteristic to the ground and lapped surface, Elgabry et al. [57] developed a simplified probabilistic model to represent the crests, valleys and facets of the finished surface profile. For a cam profile, which is mainly produced through milling

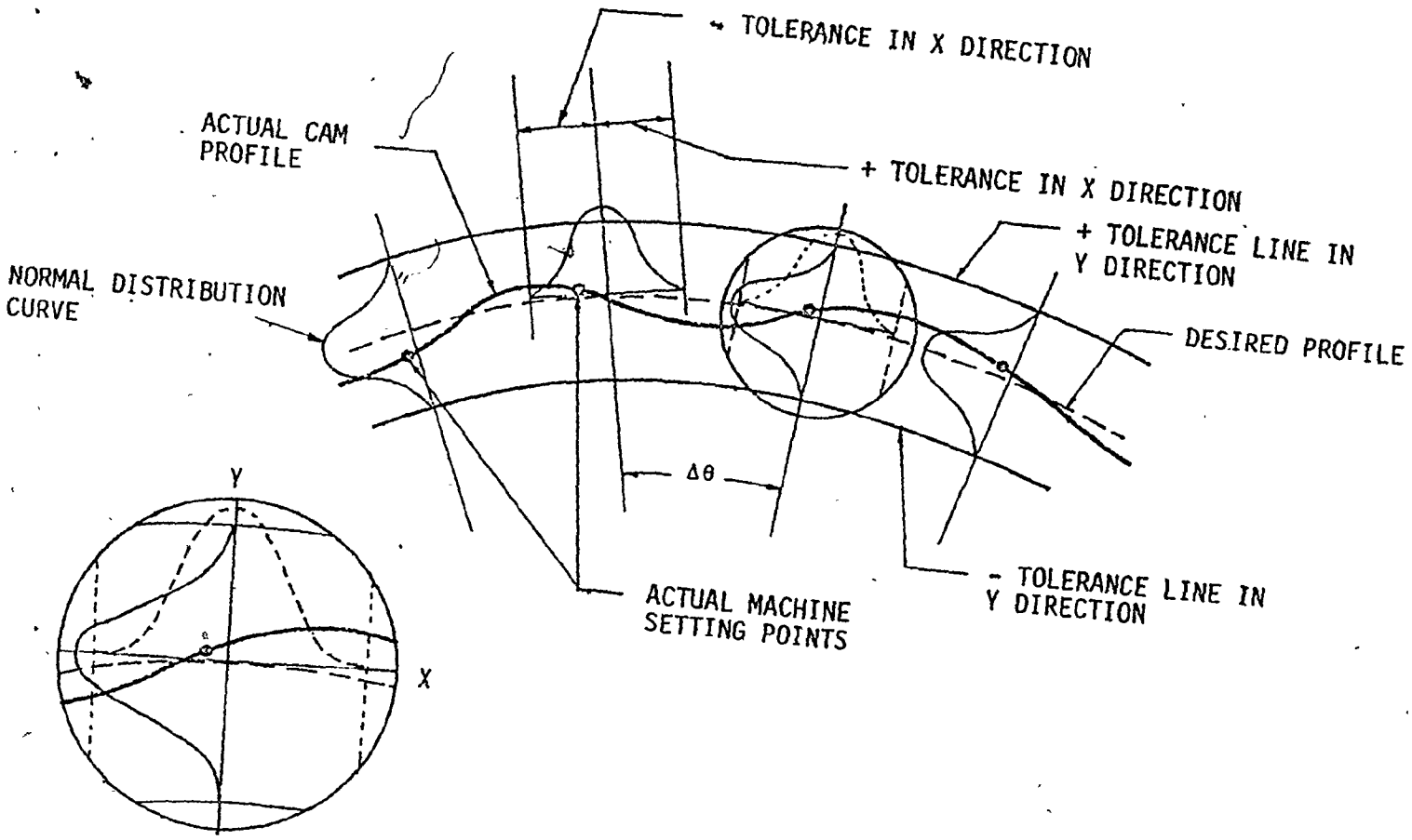

Fig. IV.9. Generation of Cam Profile and Its Waviness Produced by Tolerance Band in Setting Cutter

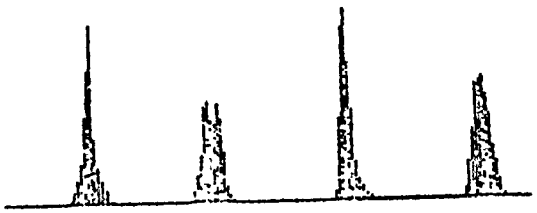

(1) (2) (3) (4)

a. Distribution of Waviness Height by (1) Milling (2) Turning (3) Honing and (4) Grinding

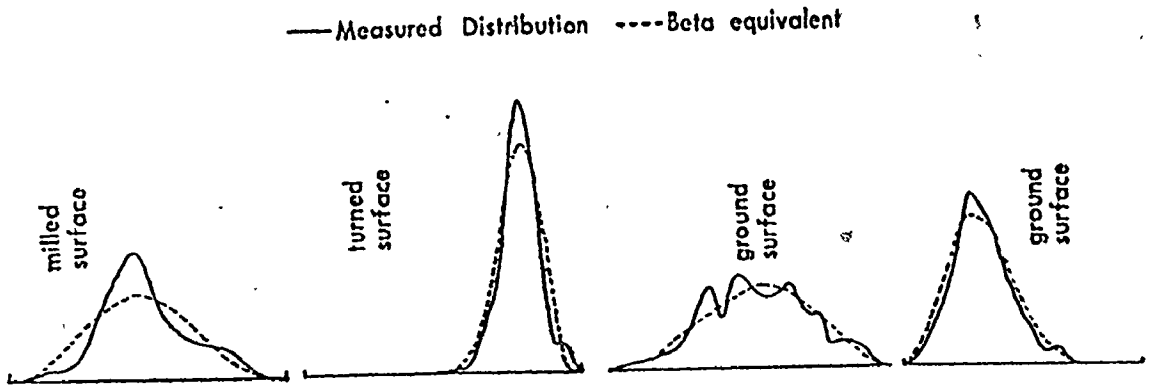

b. Modelling of Distribution Characteristics

Fig. IV.10. Characteristics of Machined Surfaces

and grinding, the randomness can be also described by a Gaussian distribution, and to simulate an actual cam profile this distribution will be utilized.

The waviness, which is the low frequency component of the error function, is described by height (the peak to valley distance) and width (the spacing of adjacent waves). The waviness height is limited by cam profile tolerance, mainly within the standard deviation ($\frac{1}{3}$ of tolerance) from the mean (theoretical) value due to the Gaussian distribution characteristic. The width generally depends upon the incremental cam angle interval, or the abscissa interval of the data for cutter position, which are functions of both cam size and cutter size.

After obtaining this information concerning the two major characteristics of the actual cam profile, it can be simulated on a computer by generating a sequence of uniform random numbers. Using these random numbers, a normally distributed random value is computed with a given mean and standard deviation (Appendix B). For the two dimensional tolerance, two corresponding normally distributed random values are evaluated, thus satisfying the Gaussian distribution characteristic of profile randomness. These two independent values indicate an actual machine setting point and define a point on the actual cam profile. For the whole profile, a series of two such values is generated according to the incremental cam angle interval. In this way, an entire actual cam profile is defined by a series of discrete points, which then need to be connected.

Due to the exclusion of roughness, the actual profile will be smooth and wavy. In fact, an actual working cam profile cannot have microscopic sharp points or surfaces since they are smoothed out by contact with the follower during operation. To smoothly connect the discrete points in view of the waviness, the natural cubic spline function (Appendix C) is adopted, whose continuous and smooth connection provides a proper waviness and simulates the actual cam profile.

IV.2.3 Simulation of Actual Roller Motion

The follower surface will also have some waviness, but generally it will be less than that on the cam profile. However, the contact point between cam and follower will be unknown. Kim and Newcombe [38] used a stochastic technique to determine the motion of the follower not only for disk cams but also for three dimensional cams. This method is summarized in Appendix E.

Assuming a Gaussian distribution of the profile errors, and using stochastic information such as the mean value, standard deviation (σ) and variance, the actual motion of the roller follower is simulated. The points which represent the components of the roller displacement are generated within the 3σ band of the Gaussian distribution, and the theoretical displacement is taken as the nominal (mean) value. A technique similar to that used for generating the cam profile is used to generate these points so that a normally distributed random value is attained. However, one must note that

for this a one dimensional varying tolerance is used (Fig. IV.11), instead of the two-dimensional tolerance of the machine cutter position when generating the cam profile.

The roller displacement curve is made up of lines connecting the discrete points obtained from random values. This curve is the counterpart of the cam profile, and should therefore be continuous. Also, the first and second derivatives are required, and thus the natural spline function was used to fit these discrete points.

It must be emphasized here that in simulating the actual roller displacement the chosen interval or spacing between points is extremely important. The resulting displacement curve has to be differentiated twice, and a small change in the displacement curve has a large effect on the acceleration. For example, if the interval is too small, the displacement will comprise a lot of very small wavy curves (high frequency components of the profile), and the displacement eventually induces unduly oscillating 1st and 2nd derivatives, corresponding to high frequency components which sometimes match with the natural frequency of the follower system, causing resonant vibration of the load. Even though the actual profile is composed of high frequency component curves, the actual roller displacement will not reflect the component curves exactly, because the roller radius is larger than the radius of curvature of these curves. In addition, the Hertzian deformation and cushioning effect between the interface of cam and follower, due to the elastic property of the material, has its effect. On the other hand, if the interval is too large,

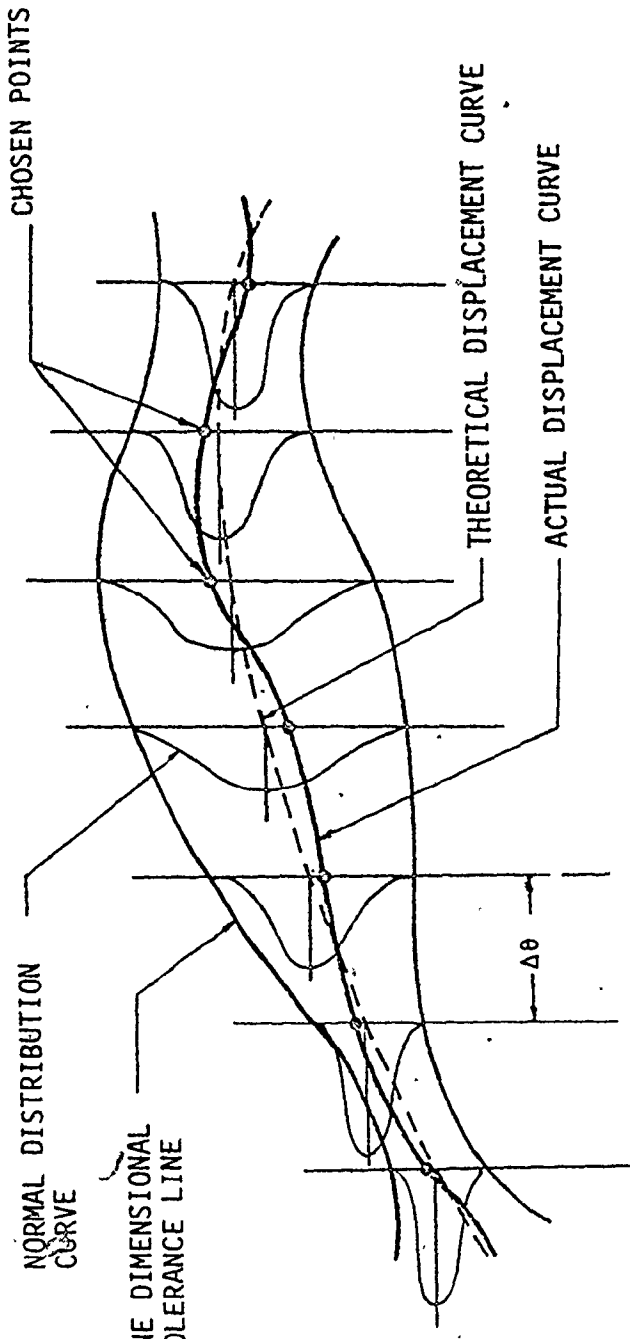

Fig. IV.11. Generation of Actual Displacement

the displacement resulting from the spline curve fitting is located out of the given tolerances, violating the Gaussian distribution characteristic.

Therefore, an optimum interval will exist between the above extreme cases, and to find the optimum value while avoiding the extreme cases the following criteria were used :

1. The interval should be such that the radius of curvature of actual displacement should be at least greater than the radius of the roller ;

2. In choosing the interval, the Gaussian distribution characteristic must be satisfied. This means that the rms of the deviation between the actual and theoretical displacements should be less than or equal to the average standard deviation of the actual displacement.

Generally, and in this particular model, the periods of dwell, rise and return are specified in round numbers of degrees. It is important that the interval value selected should be an integer which will divide evenly into the above periods, so that the end points or conjunction points between different periods are included in the simulated displacement. Therefore, as an additional criterion, it is suggested that :

3. The interval value should be an integer which will divide evenly into each phase or period of the motion included on the cam profile.

The curve generated in this way will represent the actual roller displacement (see Chapter VI), and due to its analytical continuity the roller's remaining motions, such as velocity and acceleration, can be analytically fed back into the dynamic simulation, enabling it to be carried out for the simulation of actual physical behavior of the cam follower system, considering both dynamic and stochastic disturbances.

CHAPTER V

CALCULATION OF DYNAMIC PROPERTIES

V.1 Inertial Masses

For a disk cam, its rotational inertia can be found directly by using polar coordinates, without calculating the center of its mass or applying the parallel axis theorem. The cam profile obtained under the exact contact condition with the roller follower is usually given in cartesian coordinates (Appendix E) as

$$\begin{aligned} x &= (s + s_o) \sin\theta + r_r \cos (\Psi - \theta) \\ y &= (s + s_o) \cos\theta + r_r \sin (\Psi - \theta) \end{aligned} \qquad (V.1)$$

where $s_o = r_b + r_r$

$\Psi = \phi - \frac{\pi}{2}$

By the definition of rotational inertia (polar moment of inertia)

$$I_z = \int r^2 \, dm ,$$

the cam's rotational inertia becomes

$$\begin{aligned} I_z &= \int r^2 (\rho \, t \, r \, dr \, d\theta) \\ &= \rho \, t \int_0^{2\pi} \int_0^{c} r^3 \, dr \, d\theta \end{aligned} \qquad (V.2)$$

where

ρ = mass density

t = thickness of cam

c = upper boundary value of r

This integral is substituted by the relation

$$r^2 = x^2 + y^2 = (s + s_o)^2 + r_r^2 - 2 r_r (s + s_o) \cos \phi \qquad (V.3)$$

and solved to obtain

$$I_z = \rho t \int_o^{2\pi} \frac{1}{4} [(s + s_o)^2 + r_r^2 - 2 r_r (s + s_o) \cos \phi]^2 \, d\theta \qquad (V.4)$$

As s and ϕ are the function of θ, the above integral is in the implicit form with respect to θ, and any attempt to integrate by analytical calculus for the various standard motion curves will be time-consuming. In this work, a numerical integration method is introduced, and the computer program is attached in Appendix I. This provides the area, volume, mass and rotational inertia of the cam for any standard motion programs.

V.2 System Flexibilities

The stiffness of the shaft under torsion is given as,

$$K = \frac{G\,J}{\ell} \qquad (V.5)$$

and the bending stiffness of a shaft which is supported at both ends and has a load at arbitrary distance (a) is found by

$$K = \frac{3\,E\,I\,\ell}{a^2\,b^2} \qquad : \qquad b = \ell - a \qquad (V.6)$$

The spring constant of an element subject to its axial (compressive or tensile) force is calculated from

$$K = \frac{E\,A}{\ell} \qquad (V.7)$$

The follower of a cam mechanism behaves like a cantilever beam at whose free end the lateral component of contact force is applied. The stiffness for this situation is obtained as

$$K = \frac{3\,E\,I}{\ell^3} \qquad (V.8)$$

As the rotational motion of the cam is transferred to its follower through the surface contact between them, the flexibility of the contact region naturally affects the motion transfer. The spring constant for the contact between cam and follower, which has been roughly estimated by Shigley [55], is analytically calculated by utilizing the well known Hertzian stress formula.

For two cylindrical objects having thickness t (Fig. V.1), the width of rectangular contact area w can be obtained from the formula as

$$w = 2\sqrt{\frac{2F}{\pi t}\left[\frac{\frac{1-\nu_1^2}{E_1}+\frac{1-\nu_2^2}{E_2}}{\frac{1}{d_1}+\frac{1}{d_2}}\right]} \qquad (V.9)$$

where

ν_1, ν_2 = Poisson's ratio of materials for cylinders 1 and 2 respectively

E_1, E_2 = Young's modulus of materials for cylinders 1 and 2 respectively

d_1, d_2 = diameter of cylinders 1 and 2 respectively.

From the geometry of circle, the depressed depth h_1 and h_2 are

$$h_1 = r_1 - \sqrt{r_1^2 - \left(\frac{w}{2}\right)^2} \quad \text{and}$$

$$h_2 = r_2 - \sqrt{r_2^2 - \left(\frac{w}{2}\right)^2} \qquad (V.10)$$

Since $K_h = \frac{F}{H}$ where H = total depressed depth, and by assuming F = 1, we finally get for a convex (positive curvature) profile

$$K_h = \frac{1}{h_1 + h_2} \qquad (V.11)$$

and for a concave (negative curvature) profile

$$K_h = \frac{1}{2\,(h_1 - h_2)}$$

In the cam-follower system, r_1 is the radius of the roller and r_2 is the radius of curvature of the cam profile, which varies according to the contact position and is given by :

$$r_2 = \frac{[\,(R_a + y)^2 + (\dot{y}/\omega)^2\,]^{3/2}}{(R_a + y)^2 + 2\,(\dot{y}/\omega)^2 - (R_a + y)\,(\ddot{y}/\omega^2)} - r_1 \qquad (V.12)$$

where $R_a = R_b + r_1$

and R_b = radius of base circle.

V.3 Energy Dissipation

Damping action is caused by a large variety of effects which are difficult to evaluate with certainty, and it is virtually impossible to assign accurate numerical values to each of the possible causes However, if we know the mass and stiffness of each part concerned in a mechanical system, as evaluated in the previous two sections, an estimate of damping can be obtained from the relation of

$$C = 2\,\xi\sqrt{K\,M} \qquad (V.13)$$

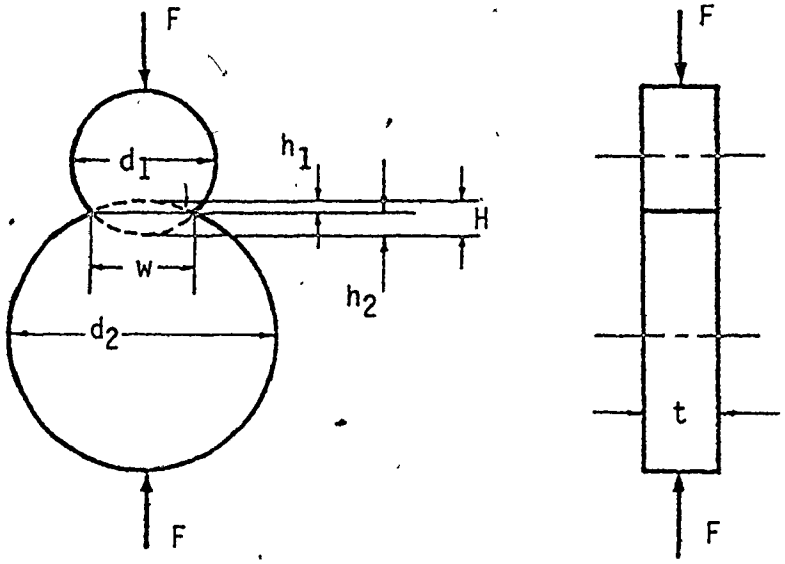

Fig. V.1. Hertzian Contact Between Cam and Follower

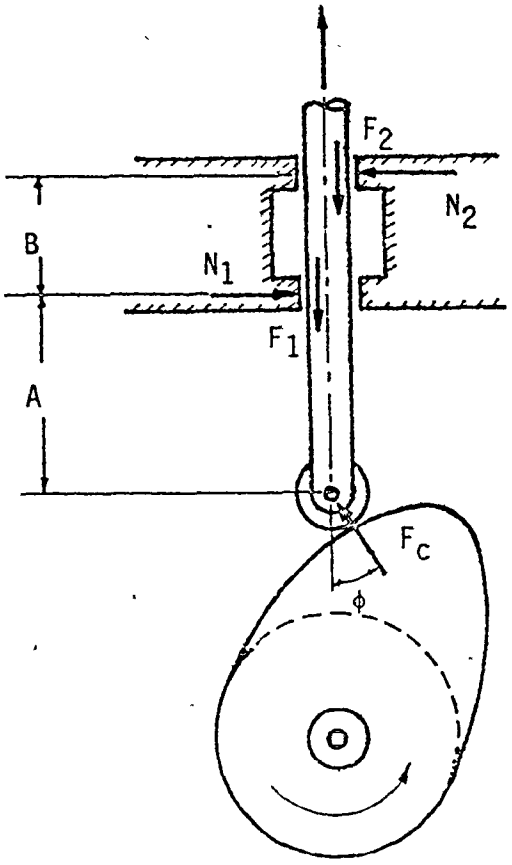

Fig. V.2. Friction Forces in Follower Bearing

where

$$\xi = \frac{C}{C_r} = \text{damping ratio.}$$

The range of ξ for a mechanical system is known to be from 3 % to 15 %, i.e.

$$0.03 \leqslant \xi \leqslant 0.15 \qquad (V.14)$$

and a choice of 0.03 for structual damping and 0.05 to 0.07 for well lubricated machine parts is generally assigned.

By referring to Fig. V.2, the friction forces F_1 and F_2 which will replace respectively the damping forces $\frac{1}{2} C_f \dot{y}_4$ and $\frac{1}{2} C_f \dot{y}_3$ in the mathematical model (Eq. IV.2) are evaluated as follows:

$$\begin{aligned} F_1 &= \mu N_1 \\ F_2 &= \mu N_2 \end{aligned} \qquad (V.15)$$

where μ is the kinetic (sliding) friction coefficient of the follower sliding bearing. From equilibrium conditions (Fig.V.2) :

$$\begin{aligned} N_1 &= \frac{A + B}{B} F_c \sin \phi \\ N_2 &= \frac{A}{B} F_c \sin \phi \end{aligned} \qquad (V.16)$$

where ϕ is the pressure angle and F_c is the contact force which is to be evaluated in the next section.

V.4. Return Spring Preload

The preload in the return spring of a cam-follower system is required to suppress the jump phenomenon of the follower. To determine the preload F_p, let δ_{rs} be the length of spring K_{rs} to be compressed during assembly, and Δ be the compressed length of the series K_{rb}, K_h and K_{vs} after installing the spring K_{rs} (see Fig. IV.6a). Then, from Fig. V.3,

$$F_p = K_t \Delta = K_{rs} (\delta_{rs} - \Delta) \qquad (V.17)$$

where $K_t = \dfrac{K_{rb} K_h K_{vs}}{K_h K_{vs} + K_{rb} K_{vs} + K_{rb} K_h}$,

= total equivalent spring constant of K_{rb}, K_h and K_{vs}

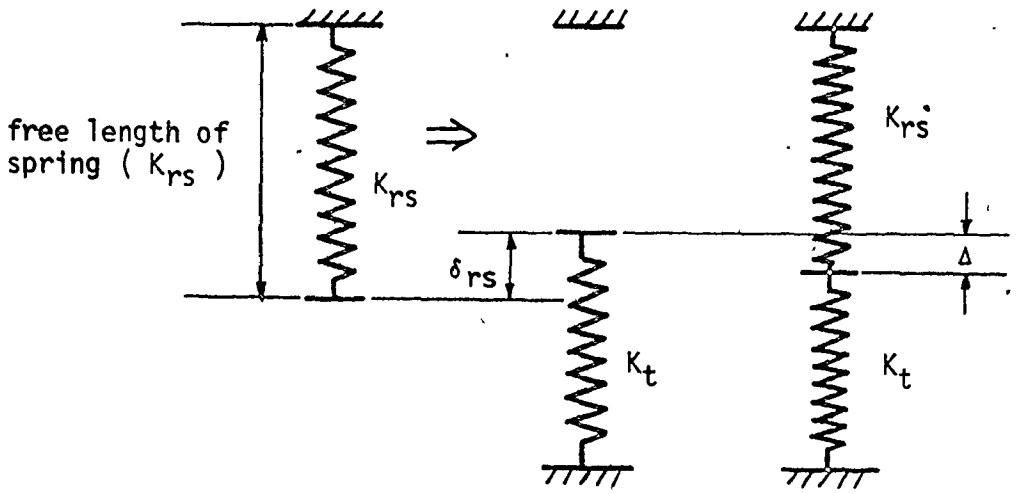

Fig. V.3. Preloading by Return Spring

From Eq. (V.17)

$$\Delta = \frac{K_{rs}\ \delta_{rs}}{K_t + K_{rs}}$$

and

$$F_p = K_t\ \Delta = \frac{K_t\ K_{rs}\ \delta_{rs}}{K_t + K_{rs}} \qquad (V.18)$$

V.5 Contact Force and Jump Criterion

A contact force F_c is obtained by considering the following two cases :

For $y_2 < y + y_1 + \frac{F_p}{K_h}$, contact is maintained between cam and roller and ;

$$F_c = K_h (y + y_1 - y_2) \cos\phi + F_p \cos\phi$$

$$= K_h \left(y + y_1 + \frac{F_p}{K_h} - y_2 \right) \cos\phi \qquad (V.19)$$

and for $y_2 \geq y + y_1 + \frac{F_p}{K_h}$, separation or jump occurs and ;

$$F_c = 0.$$

The condition,

$$y_2 \geq y + y_1 + \frac{F_p}{K_h} \qquad (V.20)$$

is a criterion for jumping.

CHAPTER VI

EFFECTS OF IMPERFECTIONS

VI.1. Data Acquisition

The following principal input data, and other information necessary for simulating the cam-follower system, were obtained from the physical model described in Section IV.1.

1. Basic Inputs

Motion program : D - R - D - R - D

Cam angle interval : Lower Dwell (0 - 30°)

Rise (30° - 180°)

Upper Dwell (180° - 210°)

Return (210° - 360°)

Motion curves : Modified trapezoidal for rise

4-5-6-7 Polynomial for return

Total rise : 1.5 "

Diameter of cam base circle = 3.0 "

Diameter of follower roller = 0.75 "

For a geometrical figure of the cam described above, refer to Fig. VI.1, which shows a full-scale theoretical cam with the dimensions described above.

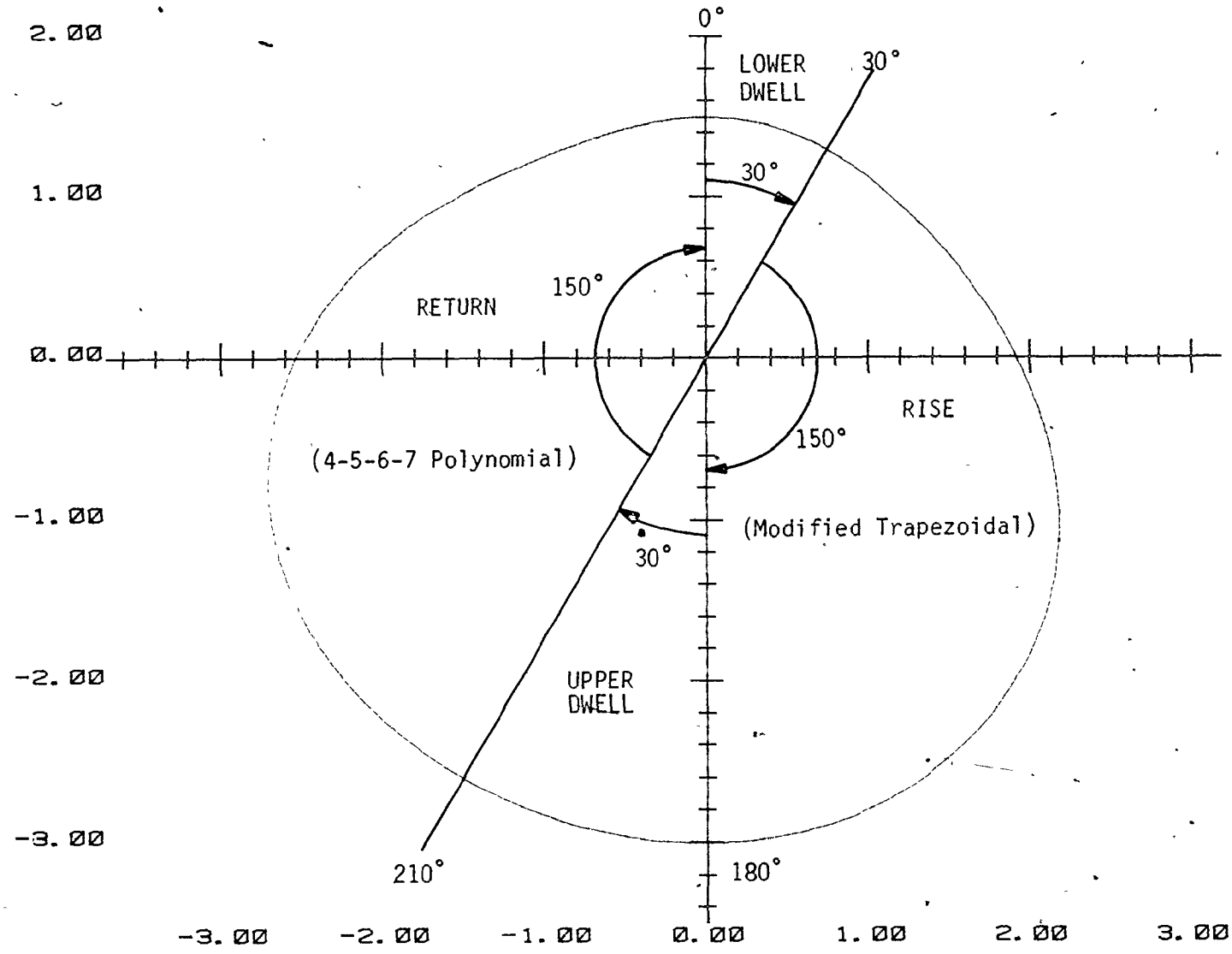

Fig. VI.1. Full-Scaled Theoretical Cam Profile with Specification

2. Dynamic Properties of Cam-Follower System

A) Polar moment of inertia (lb.in.sec^2./rad.)

I_m = 0.0291, I_{cp} = 0.25, I_c = 0.0102

B) Mass (lb.sec^2./in.)

M_l = 0.007764, M_{cs} = 0.0291, M_r = 0.00013

M_f, M_{fc} = internally computed according to the position of follower (nonlinear)

C) Damping coefficient (torsional : in.lb.sec./rad., translational : lb.sec./in.)

C_{mb} = 0.8, C_{s1} = 0.11982, C_{s2} = 0.12

C_{cc} = 1.0, C_{vs} = 4.30474,

C_f, C_{fl} = internally computed according to the position of follower (nonlinear)

D) Spring constant or stiffness (torsional : lb.in./rad., translational : lb./in.)

K_{s1} = 2. x 10^5, K_{s2} = 2. x 10^5

K_{rs} = 60, K_{rb} = 1.5 x 10^6, K_{vs} = 1.48 x 10^6

K_f, K_{vc} = internally computed in accordance with the position of follower (nonlinear)

K_h = internally computed according to contact points (nonlinear)

3. Initial Values

$\dot{\theta}_m = \dot{\theta}_{cp} = \dot{\theta}_c$ = 800 rpm = 83.776 rad./sec.

All other independent variables are set to zero.

4. Other Inputs

δ_{rs} = 0.5 "

Motor Power = 1.75 Hp.

Tolerances - on cam profile = $\pm$ 0.0005 "

- on roller follower = $\pm$ 0.0001 "

Combined tolerance for the nonroundness of camshaft bearings and the nonconcentricity of cam base circle to bearings = $\pm$ 0.001 "

Accuracy of output to be computed by Modified Runge-Kutta algorithm = 0.02 = 2 %

Kinematic friction coefficient = 0.08

Young's modulus (E) = 30 x 10^6 psi

Shearing modulus (G) = 11.4 x 10^6 psi

Poisson's ratio (ν) = 0.295

A typical example of the actual profile is shown in Fig. VI.2, which shows a part of the actual profile magnified 8.4 times. The simulation package can magnify any part of the actual profile by choosing a desired cam angle interval.

VI.2. Validity of Data : Natural Frequencies and Modal Stiffness

To check the validity of data which were analytically obtained based on the reference design, the natural frequencies

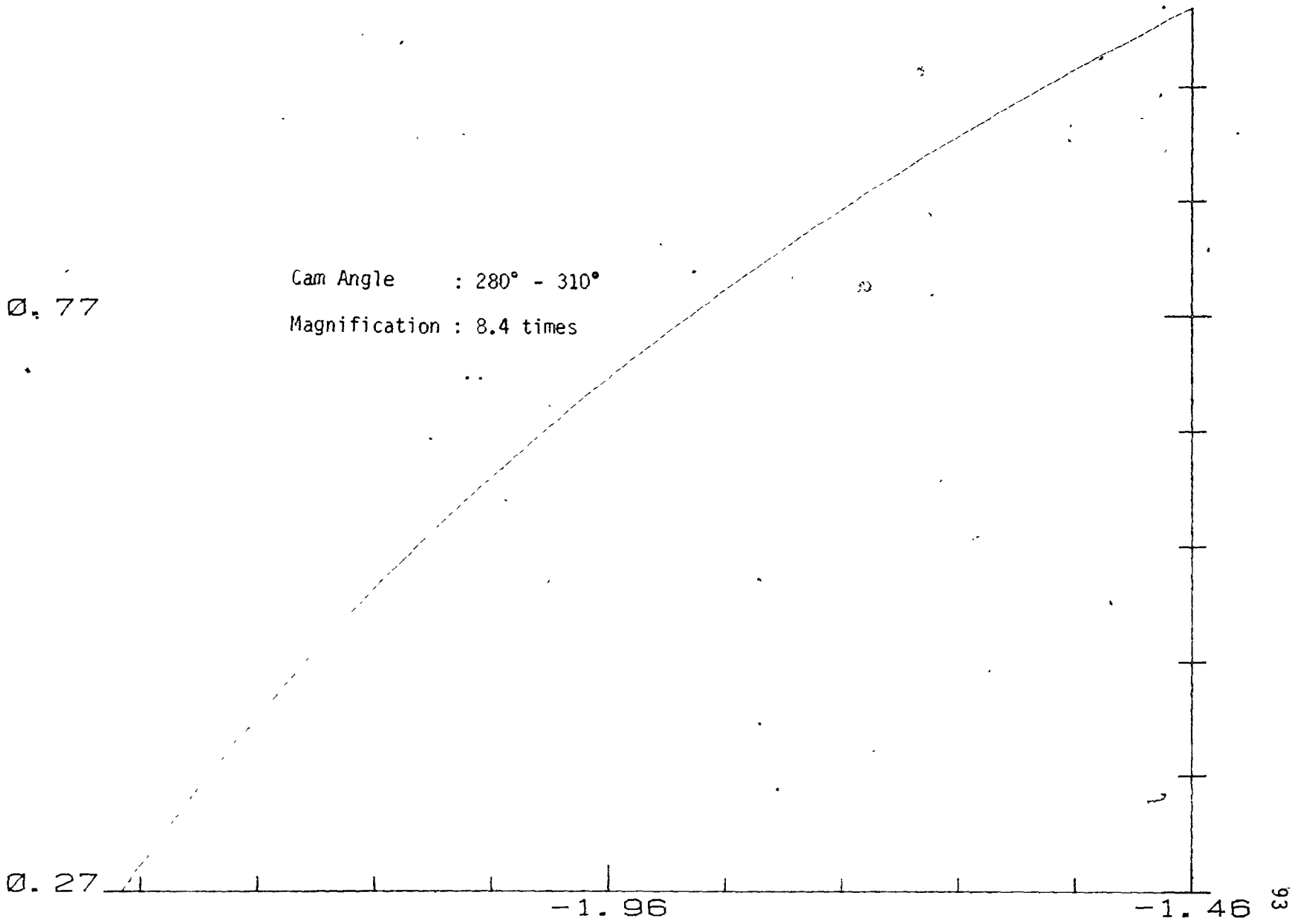

Fig. VI.2. Amplified Actual (Simulated) Cam Profile (inches)

and modal (effective) stiffness of the referred system are calculated by a modal analysis technique. As described in Chapter IV, the developed models include several nonlinearities which were taken into consideration for a closer simulation.

Because the nonlinearities, however, disable the computation of natural frequencies and modal stiffness, they were deliberately removed from the models, especially for the translational system, and the resulting models are shown in Fig. VI.3. Note that the dynamic model of the translational system revised for the modal analysis was reduced to a three degree of freedom model from an eight degree of freedom model. The mathematical model is as follows :

$$
\begin{aligned}
& M_r \ddot{y}_1 - K_{rb} (y_2 - y_1) = F_c \cos \phi \\
& M_f \ddot{y}_2 - C_{f\ell} (\dot{y}_3 - \dot{y}_2) + C_f \dot{y}_2 - K_f (y_3 - y_2) + \\
& K_{rs} y_2 + K_{rb} (y_2 - y_1) = - F_p \qquad \text{(VI.1)} \\
& M_\ell \ddot{y}_3 + C_{f\ell} (\dot{y}_3 - \dot{y}_2) + K_f (y_3 \tau y_2) = 0
\end{aligned}
$$

The dynamic and mathematical models for the rotational system are to be used as they are given in Fig. IV.4 and Eq. (IV.2) respectively.

From the principal method of modal analysis, the procedures to be taken for the calculation of natural frequencies and modal stiffnesses are as follows :

1. Solve the differential equation of a free undamped system

$$[M]\{\ddot{x}\} + [K]\{x\} = 0 \qquad \text{(VI.2)}$$

to obtain the eigen values, λ_i , for angular natural frequencies (A.N.F.) and eigen vectors, $\{x_i\}$, for natural modes (N.M.) ;

$$\begin{aligned} \text{A.N.F.} &= \omega_i = \lambda_i \\ \text{N.M.} &= \{x_i\}_{\omega_i} \end{aligned} \qquad \text{(VI.3)}$$

2. Find a modal matrix, P, by combining each normal mode, and normalize this matrix with respect to the 1st row ;

$$P = \begin{bmatrix} \begin{Bmatrix} x_1 \\ x_2 \\ \cdot \\ \cdot \\ \cdot \\ x_i \end{Bmatrix}_{\omega_1} & \begin{Bmatrix} x_1 \\ x_2 \\ \cdot \\ \cdot \\ \cdot \\ x_i \end{Bmatrix}_{\omega_2} & \cdots & \begin{Bmatrix} x_1 \\ x_2 \\ \cdot \\ \cdot \\ \cdot \\ x_i \end{Bmatrix}_{\omega_i} \end{bmatrix} \qquad \text{(VI.4)}$$

$$= \begin{bmatrix} \begin{Bmatrix} 1 \\ \cdot \\ \cdot \\ \cdot \\ \frac{x_i}{x_1} \end{Bmatrix}_{\omega_1} & \begin{Bmatrix} 1 \\ \cdot \\ \cdot \\ \cdot \\ \frac{x_i}{x_1} \end{Bmatrix}_{\omega_2} & \cdots & \begin{Bmatrix} 1 \\ \cdot \\ \cdot \\ \cdot \\ \frac{x_i}{x_1} \end{Bmatrix}_{\omega_i} \end{bmatrix}$$

3. Finally compute the modal stiffness by using the ortho-

gonality of normal modes to decouple the coupled stiffness matrix [K] :

$$\text{Modal Stiffness} = [P]^T [K] [P] \qquad \text{(VI.5)}$$

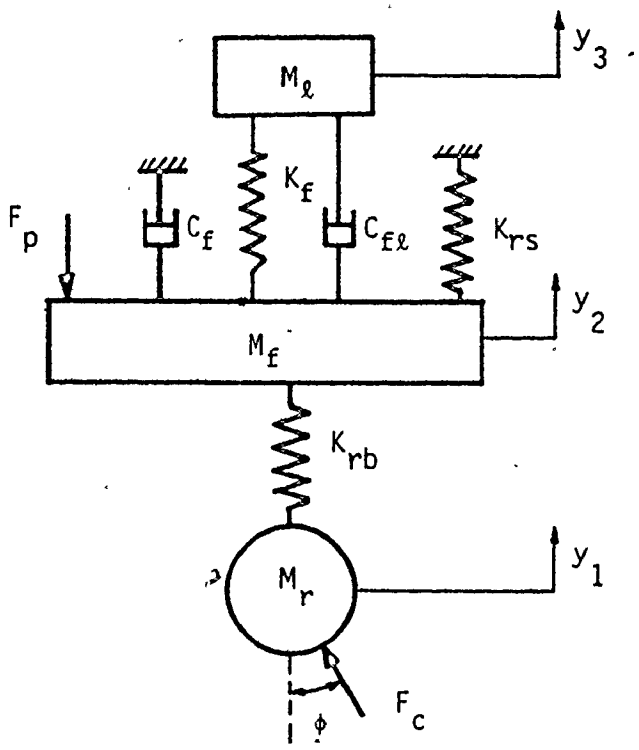

Fig. VI.3. A Dynamic Model with Three Degrees of Freedom of Translational System for Modal Analysis

For easy computer use, the equations (VI.1) and (IV.2) are re-expressed in matrix notation as follows :

For the translational system,

$$\begin{bmatrix} M_r & 0 & 0 \\ 0 & M_f & 0 \\ 0 & 0 & M_\ell \end{bmatrix} \begin{Bmatrix} \ddot{y}_1 \\ \ddot{y}_2 \\ \ddot{y}_3 \end{Bmatrix} + \begin{bmatrix} 0 & 0 & 0 \\ 0 & C_{f\ell}+C_f & -C_{f\ell} \\ 0 & -C_{f\ell} & C_{f\ell} \end{bmatrix} \begin{Bmatrix} \dot{y}_1 \\ \dot{y}_2 \\ \dot{y}_3 \end{Bmatrix} + \begin{bmatrix} K_{rb} & -K_{rb} & 0 \\ -K_{rb} & K_{rb}+K_f+K_{rs} & -K_f \\ 0 & -K_f & K_f \end{bmatrix} \cdot$$

$$\begin{Bmatrix} y_1 \\ y_2 \\ y_3 \end{Bmatrix} = \begin{Bmatrix} F_c \cos\phi \\ \mathcal{L} F_p \\ 0 \end{Bmatrix} \qquad \text{(VI.6)}$$

and for the rotational system

$$\begin{bmatrix} I_m & 0 & 0 \\ 0 & I_{cp} & 0 \\ 0 & 0 & I_c \end{bmatrix} \begin{Bmatrix} \ddot{\theta}_m \\ \ddot{\theta}_{cp} \\ \ddot{\theta}_c \end{Bmatrix} + \begin{bmatrix} C_{s1}+C_{mb} & -C_{s1} & 0 \\ -C_{s1} & C_{s1}+C_{s2} & -C_{s2} \\ 0 & -C_{s2} & C_{s2}+C_{cc} \end{bmatrix} \begin{Bmatrix} \dot{\theta}_m \\ \dot{\theta}_{cp} \\ \dot{\theta}_c \end{Bmatrix} + \begin{bmatrix} K_{s1} & -K_{s1} & 0 \\ -K_{s1} & K_{s1}+K_{s2} & -K_{s2} \\ 0 & -K_{s2} & K_{s2} \end{bmatrix} \cdot$$

$$\begin{Bmatrix} \theta_m \\ \theta_{cp} \\ \theta_c \end{Bmatrix} = \begin{Bmatrix} T_i \\ 0 \\ -T_i \end{Bmatrix} \qquad \text{(VI.7)}$$

The implementation on the PDP 11/34 minicomputer resulted as shown in Table VI.1, and from the table the following are recognized :

1. The normal mode at the lowest natural frequency (897.438 rpm) of the translational system is 1 : 0.99999 : 1, which means

Table VI.1. Results of Modal Analysis for Natural Frequencies & Modal Stiffness

	Translational System (K_{rs} = 100 lb/in)			Rotational System		
N.F. Hertz (rad/sec)	17424.53 (109481.61)	3660.38 (22998.84)	14.95729 (93.97945)	705.95 (4435.63)	419.25 (2634.23)	0.00663 (0.04169)
RPM	1045472.80	219622.81	897.43793	42357.21	25155.06	0.398088
Normalized Modal Matrix. ([P])	1.0	1.0	1.0	1.0	1.0	1.0
	-0.038806	0.954158	0.9999995	-1.86269	-0.009649	1.0
	0.000549	-0.441937	1.0	544.9986	-0.014934	1.0
Modal Stiffness ($[P]^T [K] [P]$)	1620690.5	0.1542968	0.453125	5.9813E10	0.875	-8.0
	-0.0595703	2537052.3	0.125	0.75	2.0388E5	0.006836
	-0.4105444	-0.0078773	100.0035	0.0	0.0	0.0

that the load, follower and roller act like a solid body. This is true because the load and roller are actually attached together to a follower body. Note that the actual operating frequency is 800 rpm, which is below the lowest natural frequency.

2. As the rotational system has one free end, its lowest natural frequency must be zero, and this is verified in the table even though it is not exactly zero (0.04168 rad/sec = 0.0066 Hertz). At a zero natural frequency a system must respond as a rigid body, and results substantiate this with the normal mode (1 : 1 : 1) at the lowest natural frequency.

3. The quantitatively realistic mass and stiffness matrices should provide zero off-diagonal components in the modal mass or stiffness matrices when they are uncoupled. In Table VI.1, this fact is well indicated when the off-diagonal components become negligible compared to the diagonal components.

This analysis shows that the data analytically obtained in the previous section is well within the quantitatively realistic range.

VI.3. Implementation on Computer : Numerical Method

After completing the modelling and assessing the necessary dynamic properties along with additional parameters, the remaining

problem is how to manipulate the mathematical model (simultaneous nonlinear differential equations) to obtain the desired results. The system has more than two degrees of freedom and must be handled numerically. Due to its fast computation, an analog computer is generally used to simulate the dynamic behavior of a system. As this work, however, demands strict accuracy and quantitative information to fulfill the stochastic simulation, a PDP-11/34 digital minicomputer which was available was chosen as a simulator for the cam-follower mechanism.

The numerical methods considered for the solution are classified mainly into two types :

1. Runge-Kutta type
2. Predictor-corrector type

The methods of the former type employ a recurrence formula, and are the most widely used methods for the numerical solution of simultaneous differential equation for the following reasons:

1. Good stability characteristics
2. Easy to program
3. Small per step truncation error
4. Self-starting
5. Variable step size as desired without any complications
6. Widely used and well documented

Their primary drawbacks are:

1. Local error estimates are somewhat difficult to obtain
2. They require more derivative evaluation, taking relatively long computer time.

On the other hand, methods of the latter type consist of two major formulas : one (the predictor) is the formula for a first estimate of the solution, and the other (the corrector) is for the correction of the roughly estimated value by iteration. As an additional formula, the modifier is generally included in order to reduce the number of iterations required for the corrector.

In contrast to the Runge-Kutta type methods, these methods are unstable, non self-starting, relatively difficult to program and to change step size as desired, and have comparatively large per step truncation error, while having advantages such as the easy estimate of error and the relatively small number of formulas needed.

For this particular work, a numerical method of the Runge-Kutta type was selected to solve the mathematical model derived in Chapter IV, because of the significant advantages of these methods over those of the predictor-corrector type. The first drawback of Runge-Kutta type methods was overcome by using the modified Runge-Kutta algorithm (Appendix D) [58, 59], in which the accuracy of computing can be controlled as desired.

VI.4. Analysis of the Effects of Imperfections on System Performance

In the following analysis of results the effects of flexibility alone and the effects of both flexibility and tolerances on the motion are examined. The motion produced by the simulated cam profile, i.e. the profile containing manufacturing errors and including the effects of flexibility in the system, is compared with a theoretically perfect cam, i.e. one with no manufacturing errors and no compliance. Hereafter, these will be referred to as the "actual" (simulated) and "theoretical" cams.

The time responses of the "simulated" cam are compared with the theoretical responses by calculating the root mean square (RMS) of the deviations from the theoretical curves. For the inertial responses such as torque, contact stress and contact force, the average height of the disturbance and maximum and minimum excursions are given.

In Figs. VI.4 to 13 the theoretical cam response curves are shown for comparison with the simulated cam responses. Figs. VI.4 to 5 show the transient and damped behavior of the acceleration during the 1st and 2nd revolution, and Figs. VI.6 to 13 show that it has essentially achieved steady state by the third revolution.

The curves are plotted in different colors so that they may be clearly distinguished.

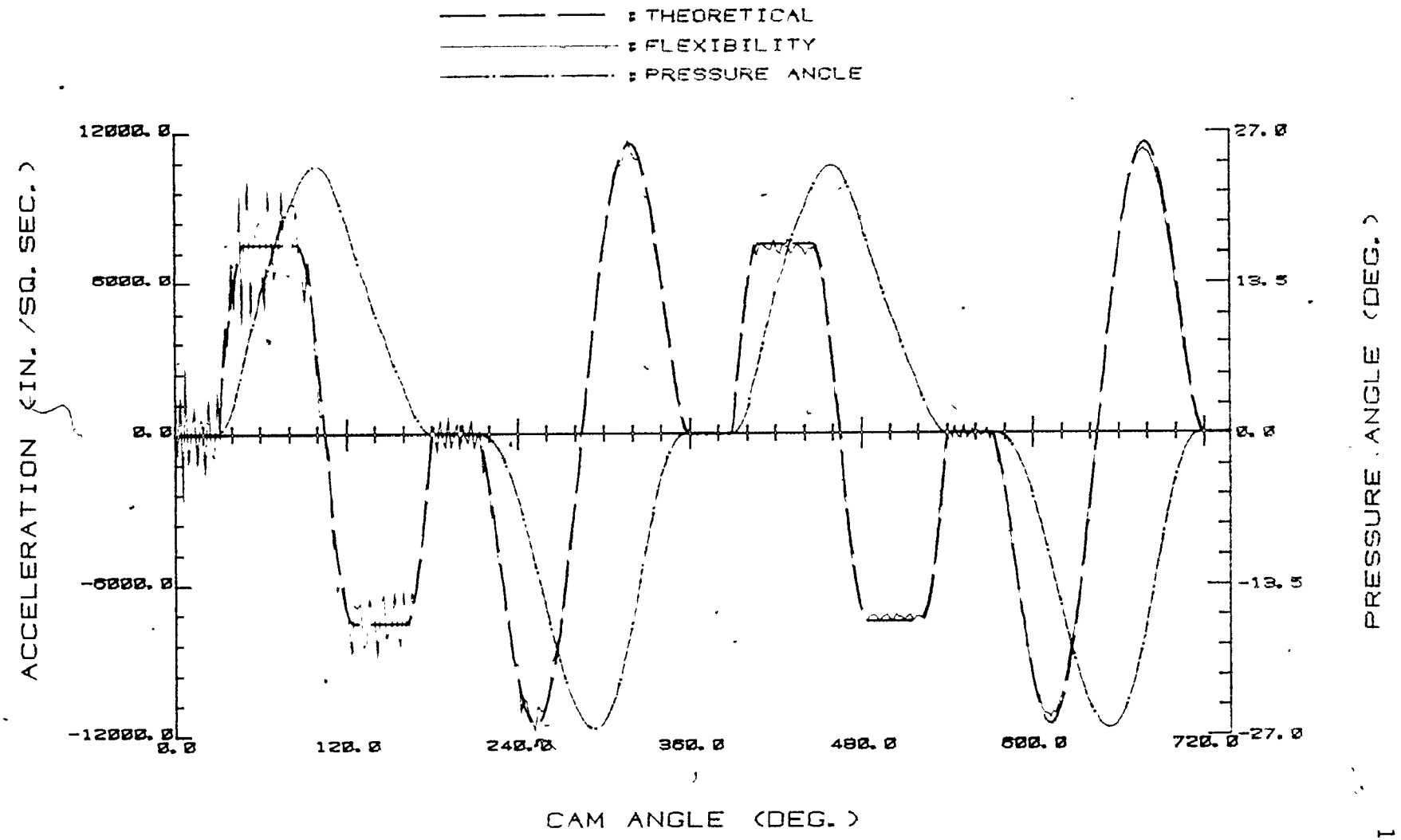

Fig. VI.4. Transient and Damped Behavior of Acceleration for Theoretical Cam for 1st & 2nd Cycle

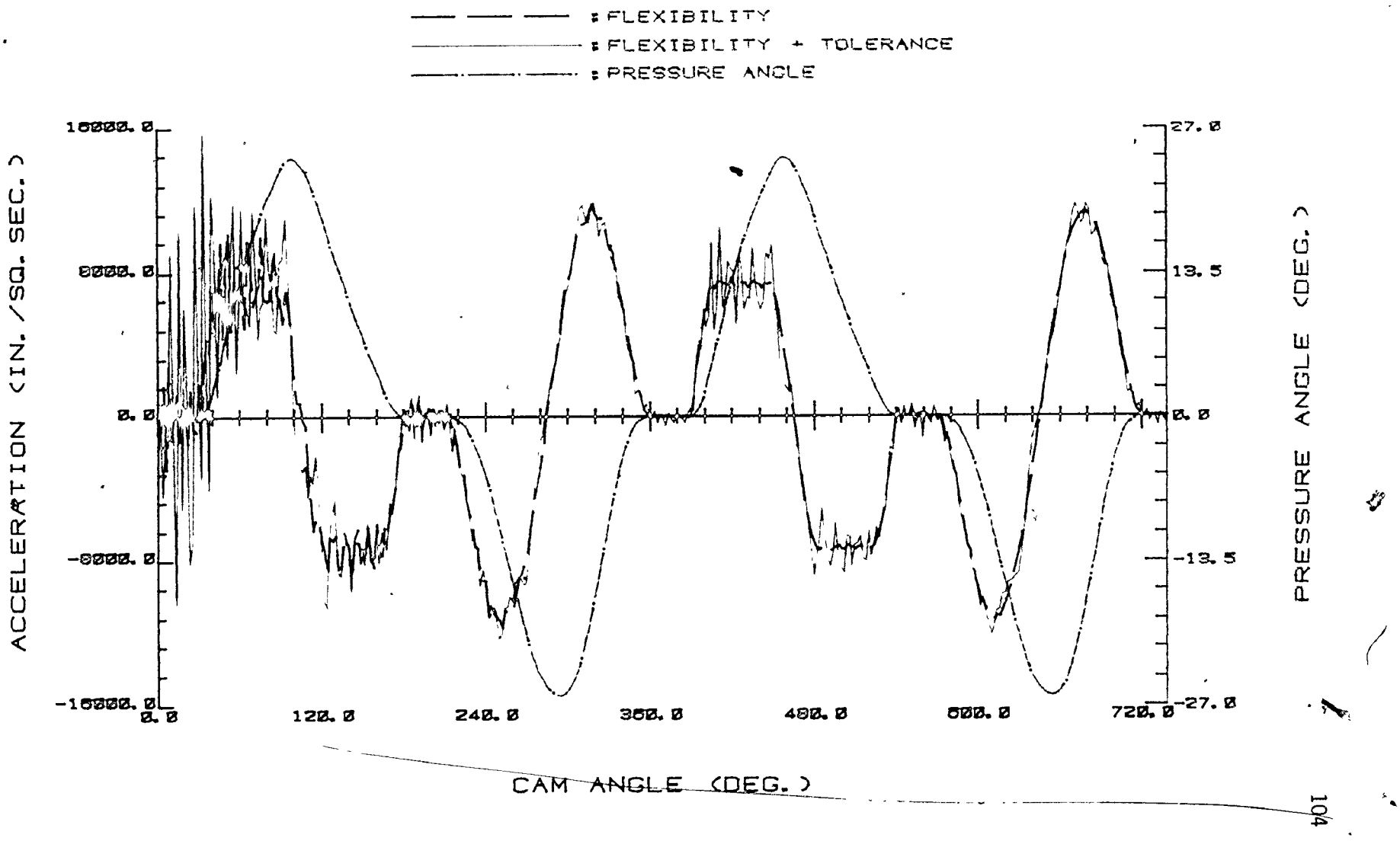

Fig. VI.5. Effects of Both Flexibility and Tolerance on Acceleration & Pressure Angle - Actual Cam

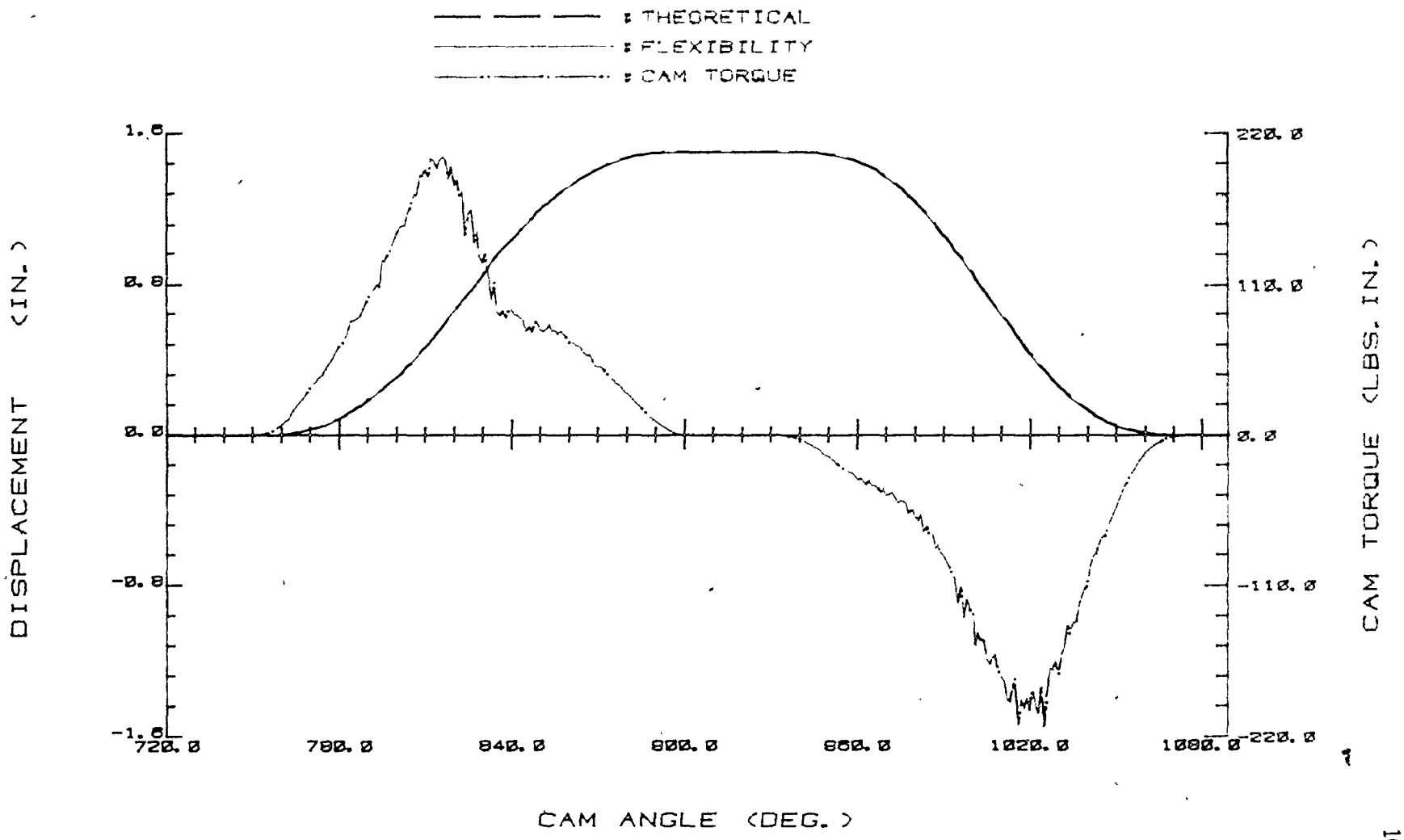

Fig. VI.6. Steady State Behavior of Displacement & Cam Torque - Theoretical Cam

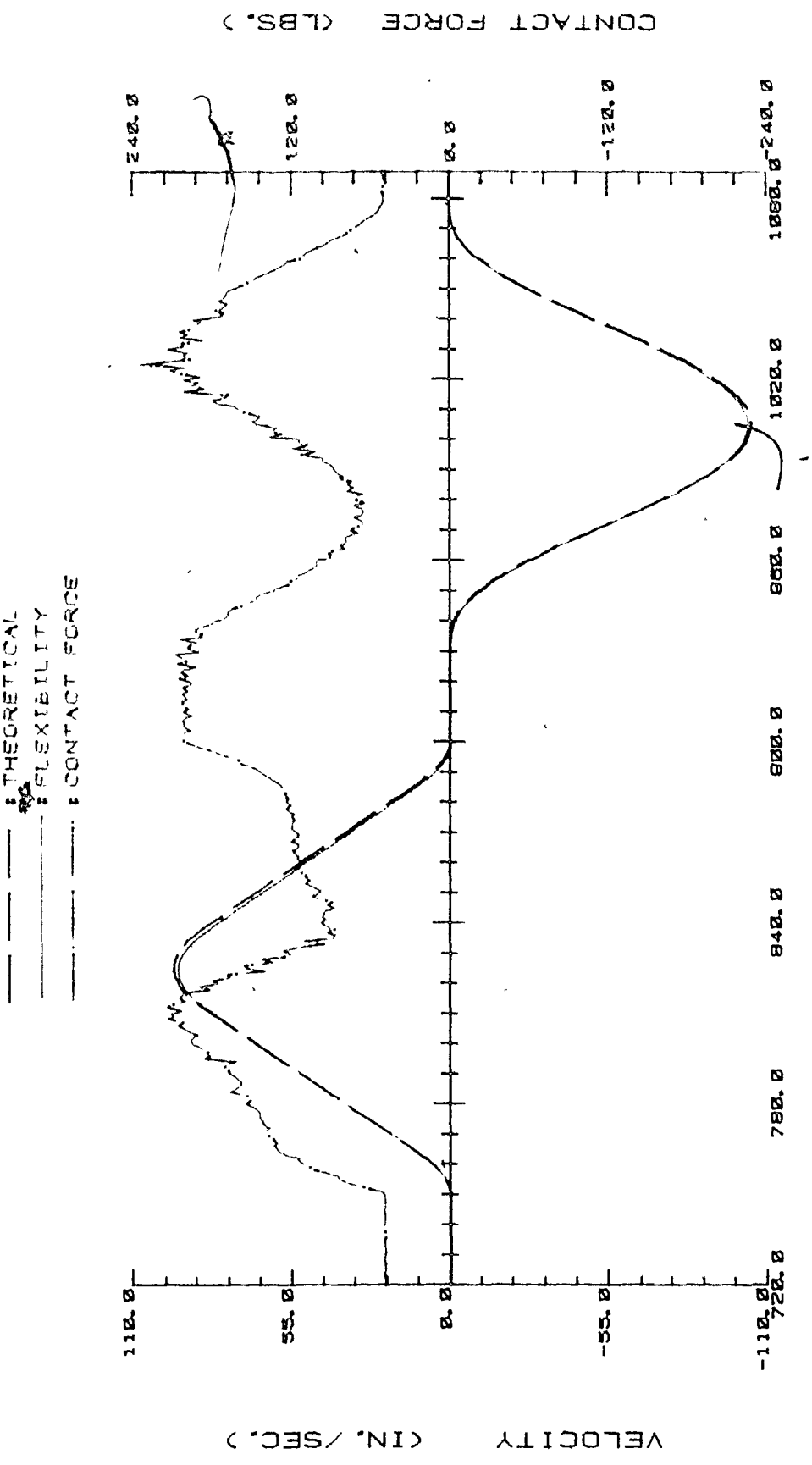

Fig. VI.7. Steady State Behavior of Velocity and Contact Force - Theoretical Cam

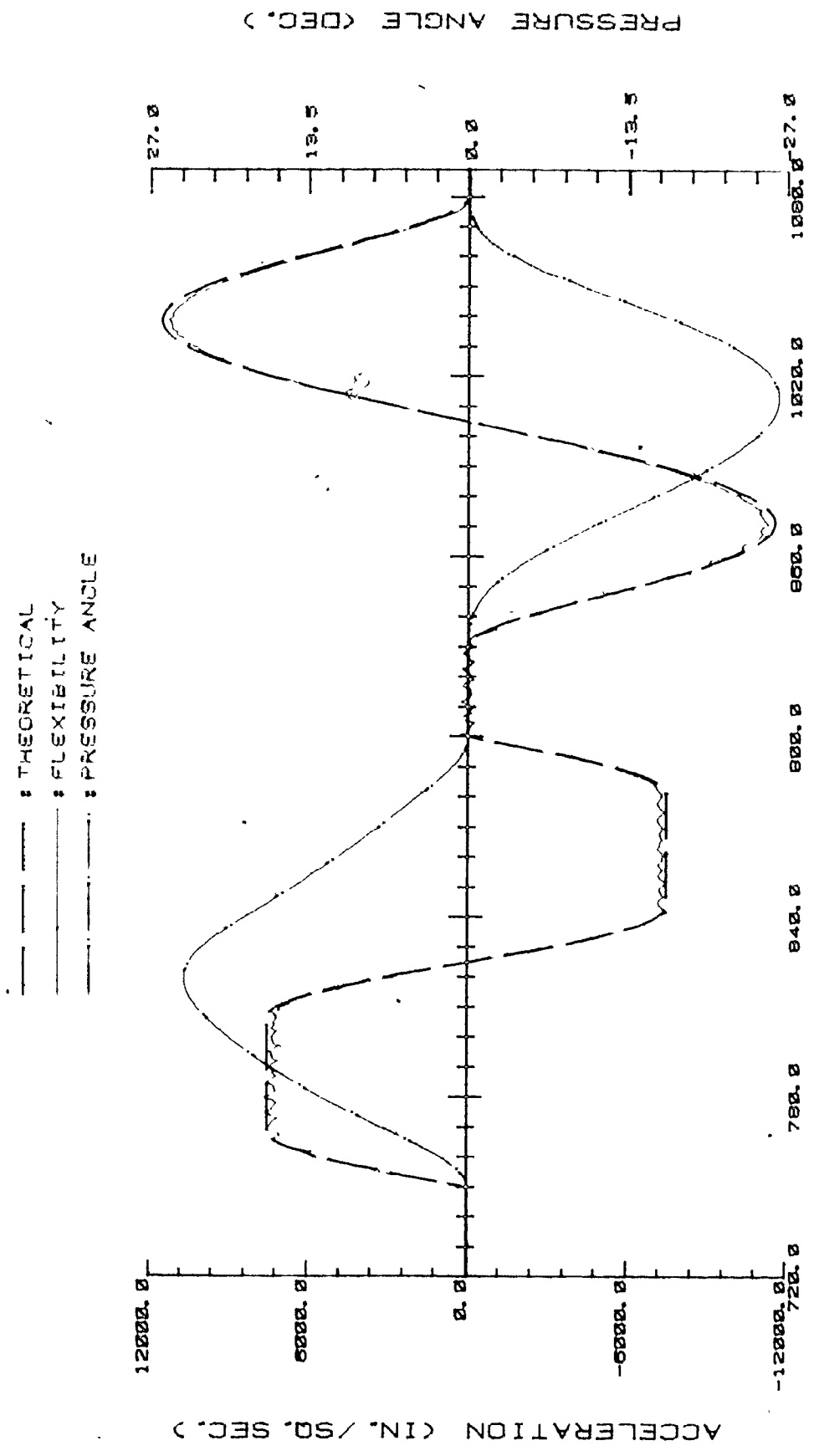

Fig. VI.8. Steady State Behavior of Acceleration & Pressure Angle - Theoretical Cam

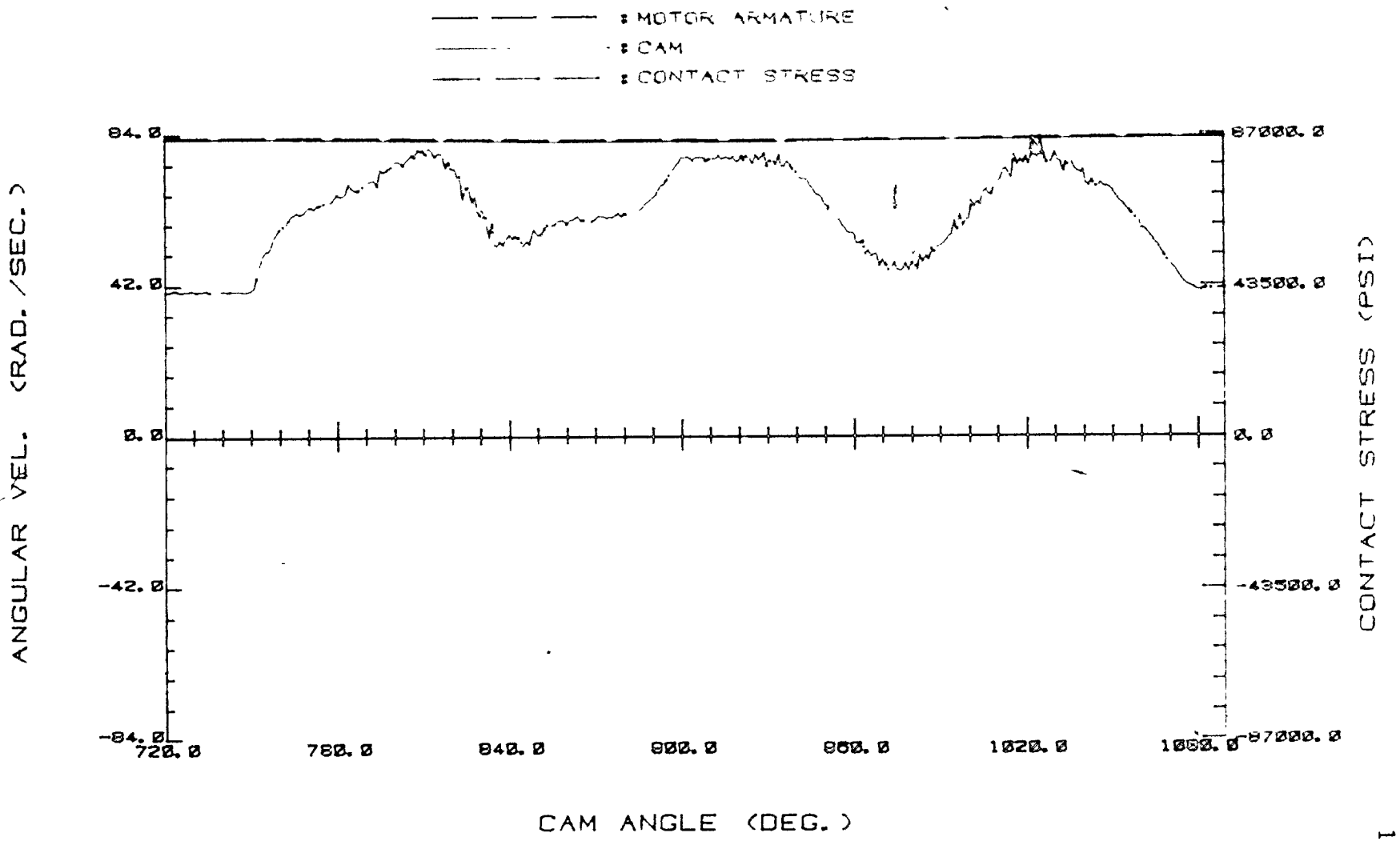

Fig. VI.9. Steady State Behavior of Angular Velocity and Contact Stress - Theoretical Cam

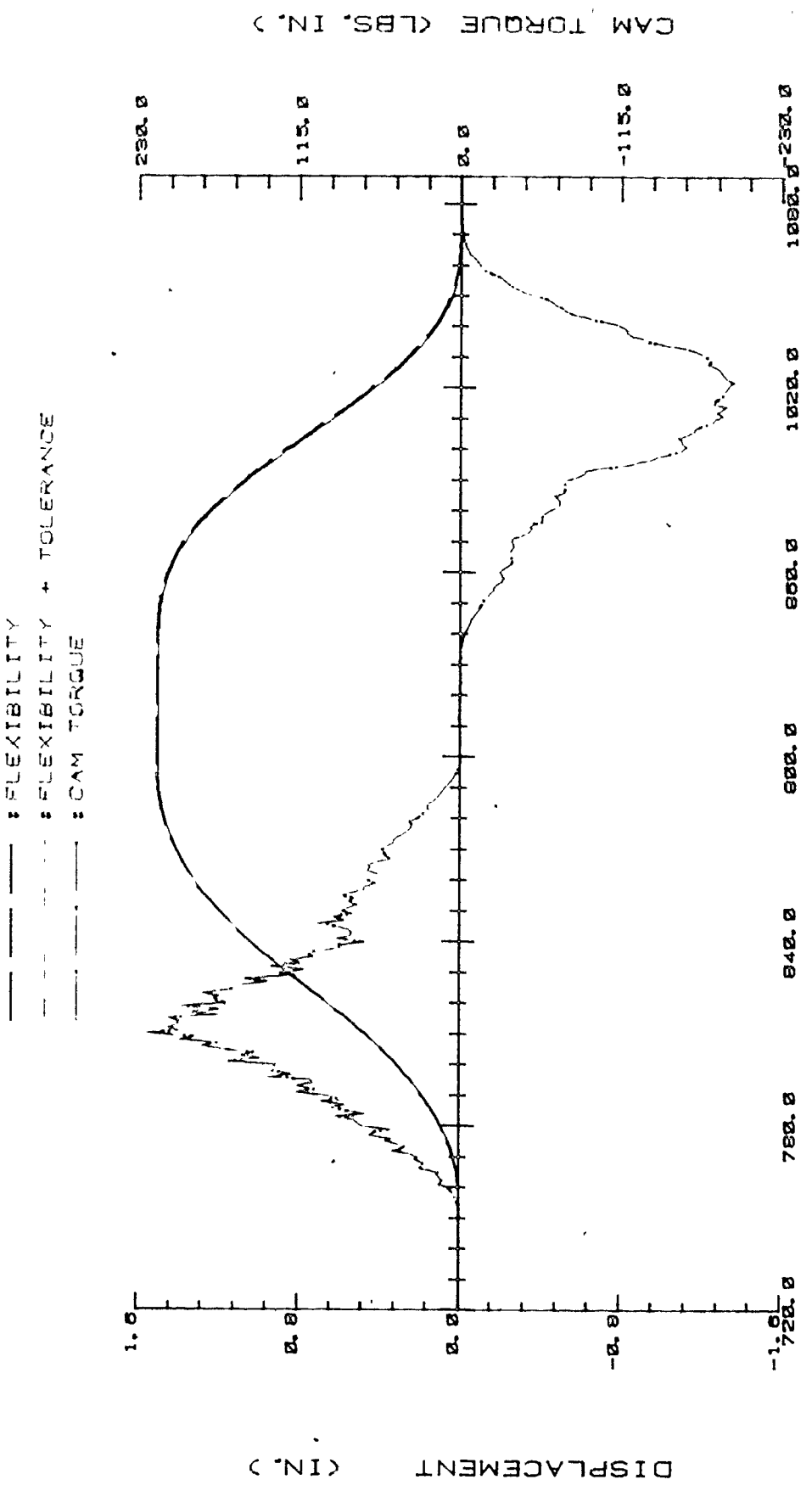

Fig. VI.10. Effects of Flexibility and Tolerance on Displacement & Cam Torque - Actual Cam

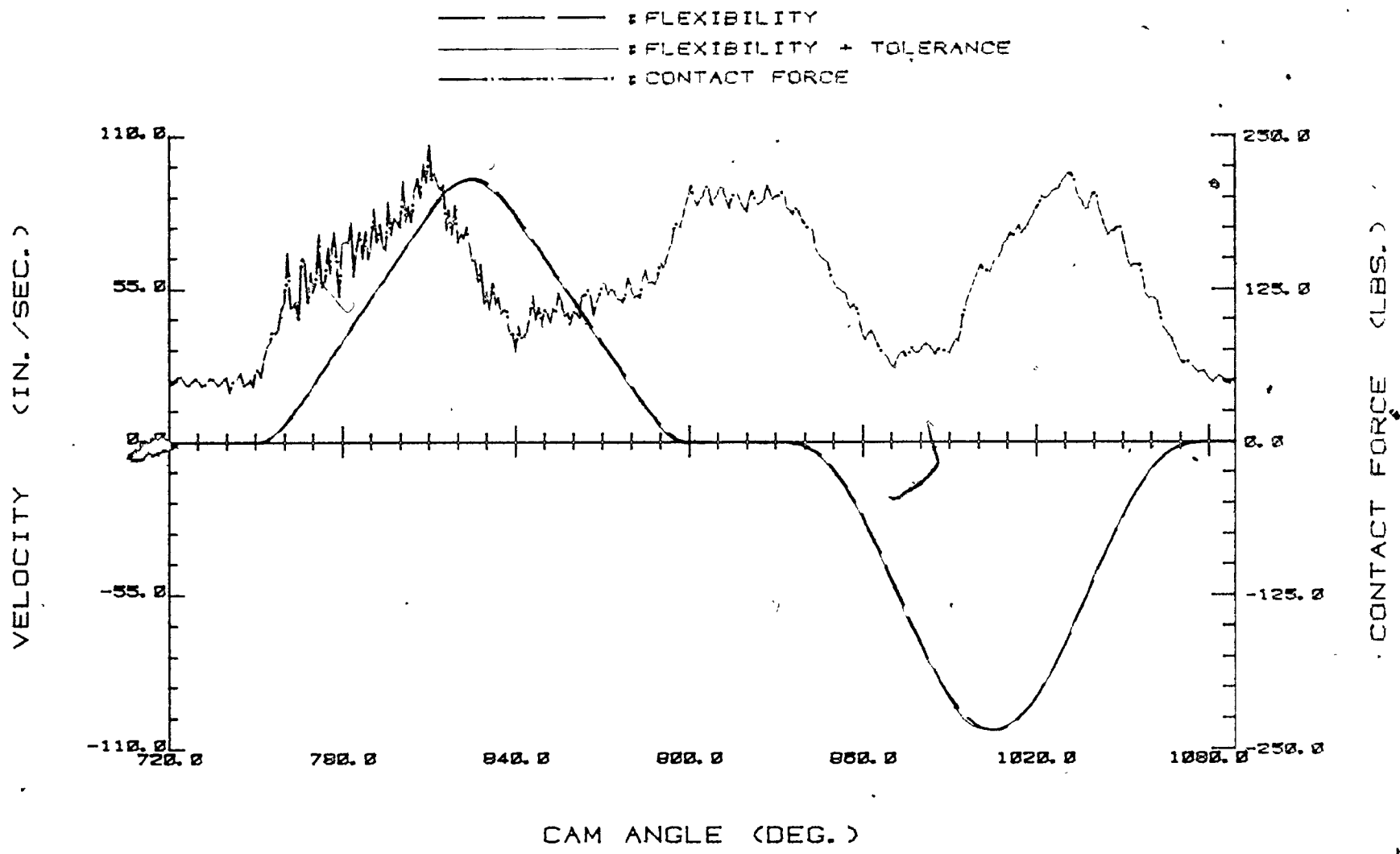

Fig. VI.11. Effects of Flexibility and Tolerance on Velocity & Contact Force - Actual Cam

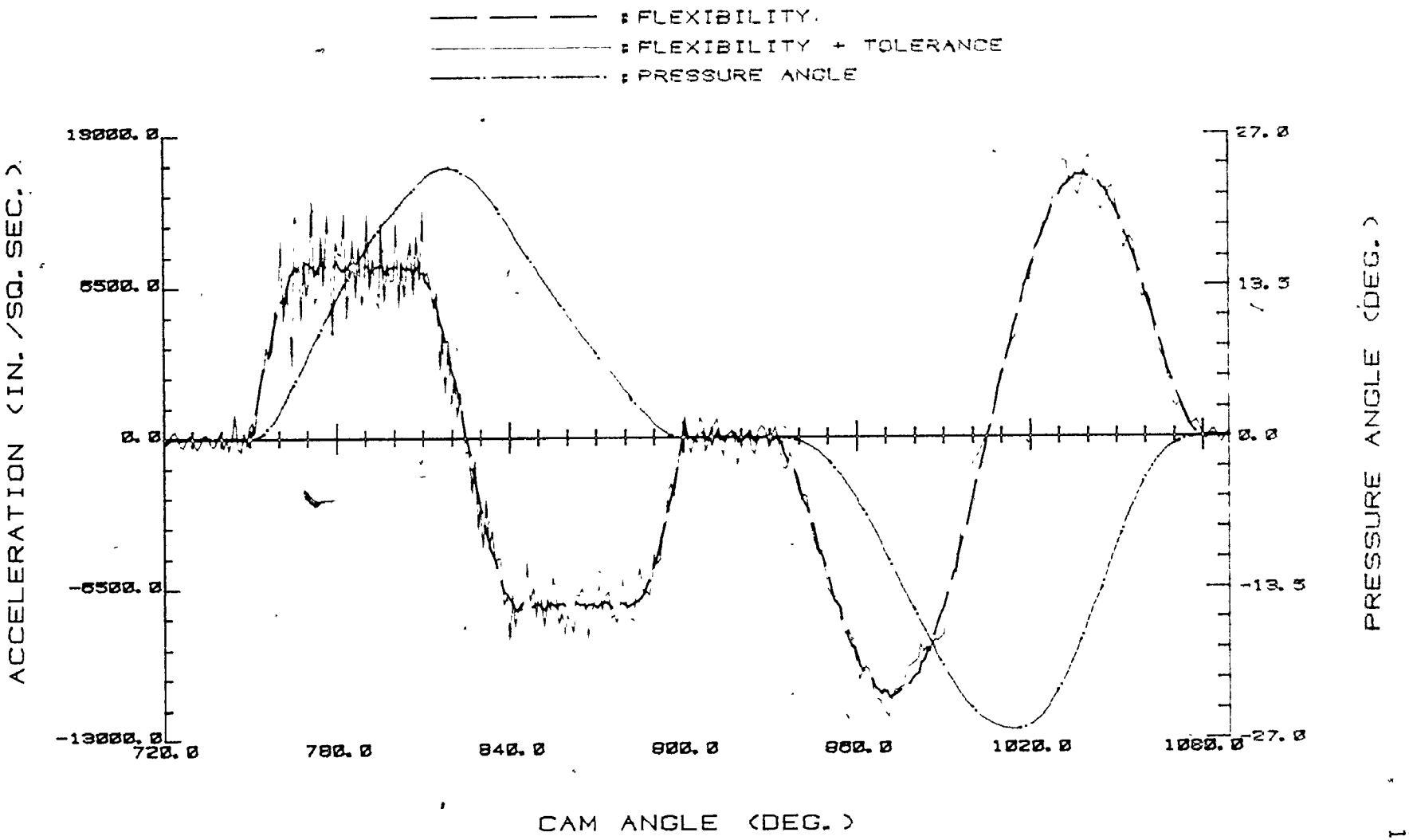

Fig. VI.12. Effects of Flexibility and Tolerance on Acceleration & Pressure Angle - Actual Cam

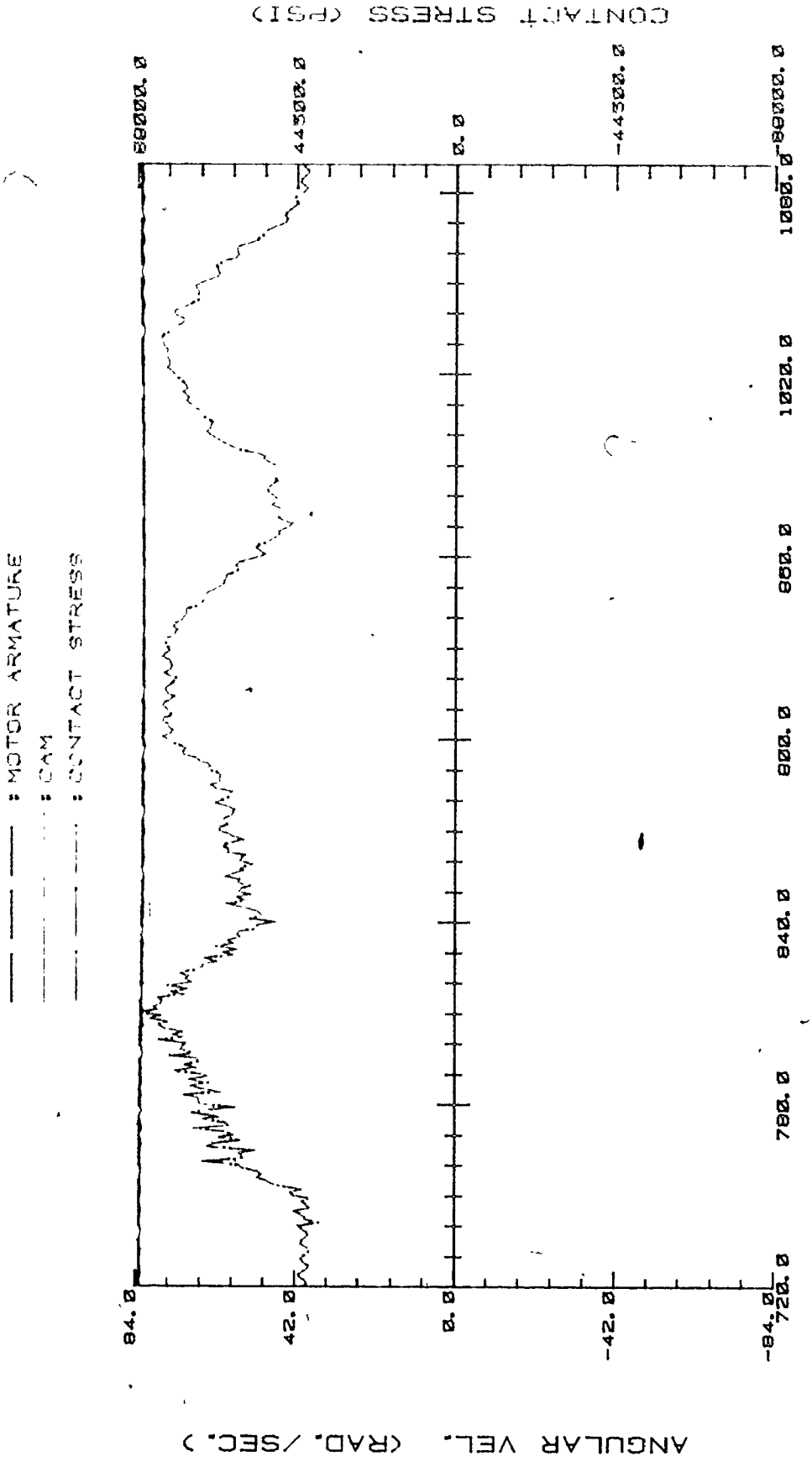

Fig. VI.13. Effects of Flexibility and Tolerance on Angular Velocity & Contact Stress - Actual Cam

VI.4.1. Effects of Geometrical Imperfections : Tolerances

The effects of machining tolerances on the time and inertial responses are summarized numerically in Table VI.2. The system flexibility was kept constant and the tolerance and waviness was varied. In the initial model a modified trapezoidal rise was specified with a 4-5-6-7 polynomial return. It was found that if the 4-5-6-7 polynomial was used for the rise, and the modified trapezoidal motion for the return, a more stable motion was achieved, and in this analysis the sensitivity of this particular cam to changes in tolerance and waviness was investigated.

The waviness is measured in terms of frequency per cam revolution (FPR), and is here defined as the total number of curve portions between the inflection points in a follower displacement curve for a total cam revolution. As shown in Fig. VI.14, this is calculated by taking the first derivative or velocity curve, where the points now become local maximum or minimum and easily counted.

From Table VI.2, the results indicate the following :

1. Tolerance does significantly influence the cam-follower sytem performance and requires more attention than previously given.
2. The magnitude of the tolerance affects the perfomance less adversely than the FPR of the waviness.

Table VI.2. Effects of Tolerances and Resulting Waviness on Time and Inertial Responses

* RMS and AVG are calculated on the whole second cycle (D-R-D-R)

	Tolerances (in.) : cam =	0.0025	0.0005			0.0001
	roller =	0.0005	0.0001			0.00002
	Frequency of Waviness	17/rev.	57/rev.	39/rev.	17/rev.	17/rev.
Displacement	RMS (x 10^{-3})	4.0983	2.0345	1.5616	1.3536	1.2773
Velocity	RMS (x 10^{0})	3.6148	5.2955	2.7901	1.7515	1.4860
Acceleration	RMS (x 10^{3})	3.7696	33.1816	9.5289	1.7078	1.5389
Angular Velocity	RMS (x 10^{-1})	6.5973	44.4730	41.1881	5.7737	5.8004
Jumping	Rise	no	yes	yes	no	no
	Return	no	yes	no	no	no
Cam Torque (lb. in.)	Rise (AVG)	79.9229	80.1424	81.3914	80.1864	79.7707
	Return (AVG)	-73.4545	-72.6805	-73.3859	-73.4844	-73.4706
	Maximum	253.0	307.0	240.8	236.0	233.0
Contact Force (lb.)	AVG (x 10^{2})	1.3074	1.2673	1.3153	1.3068	1.3057
	Max. (")	2.52	3.50	2.70	2.356	2.32
Contact Stress (psi)	AVG (x 10)	0.6341	0.5521	0.6297	0.6346	0.6342
	Max. (")	0.90	1.022	0.940	0.882	0.864

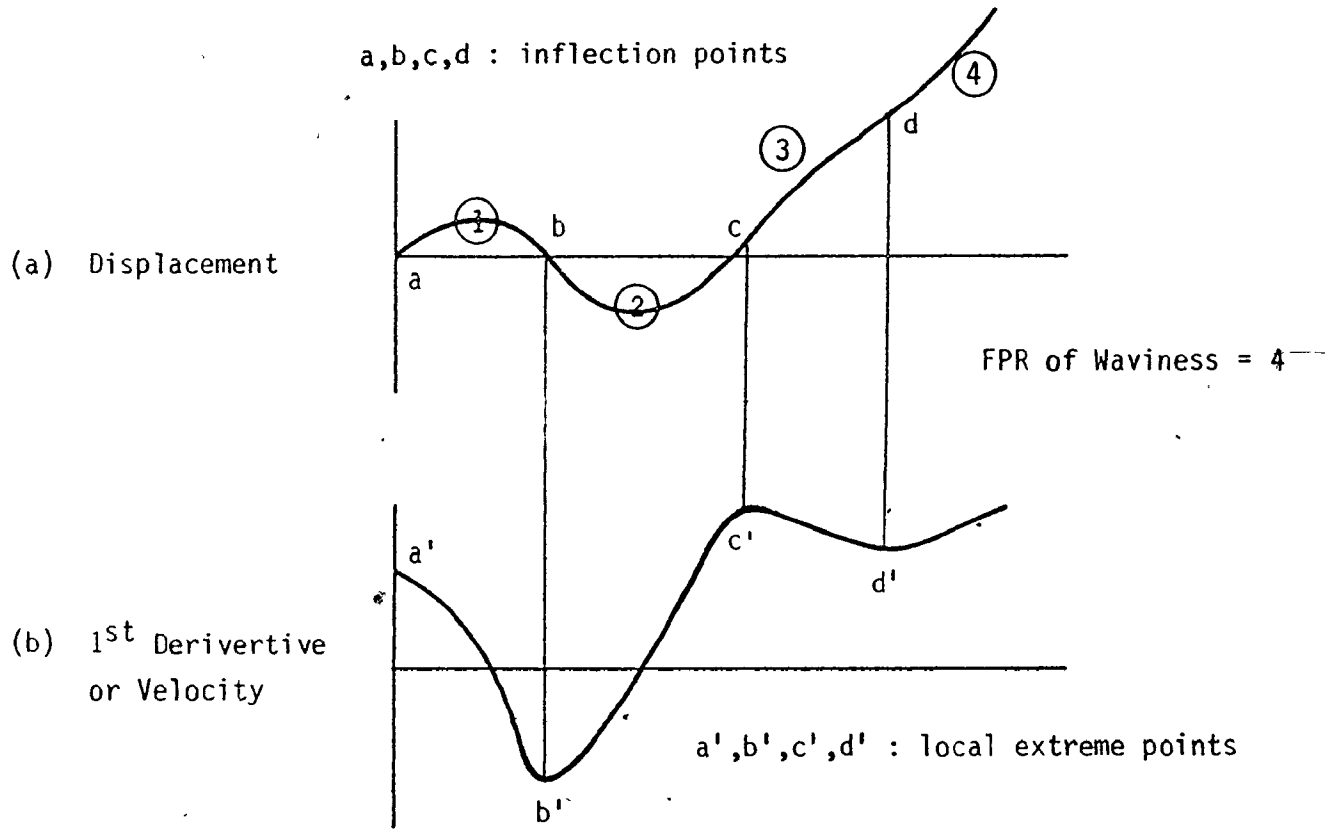

Fig. VI.14. Calculation of FPR of Waviness.

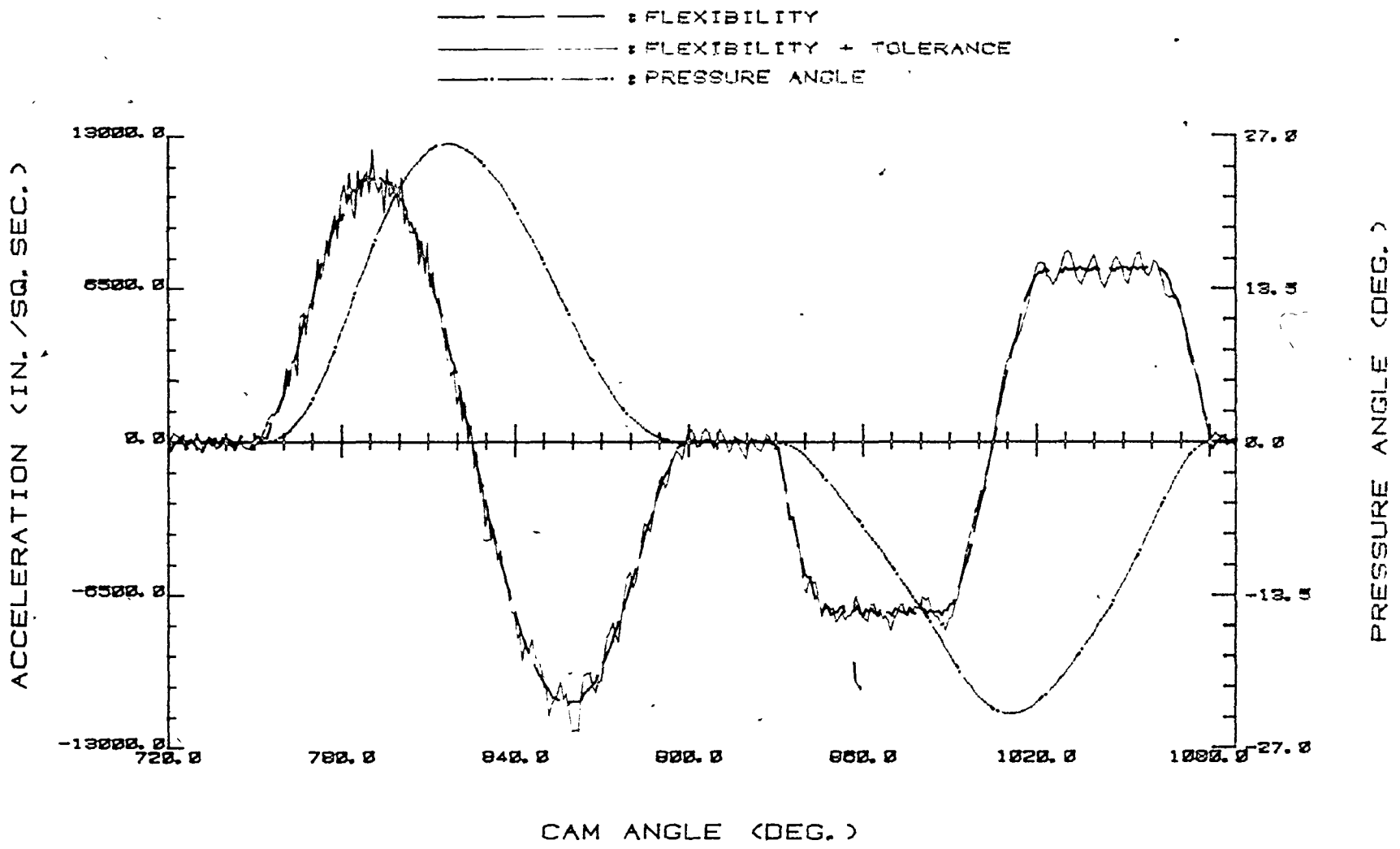

Fig. VI.15. Tolerance (cam:0.0005, roller:0.0001) and Waviness (17/rev.) Effect on Acceleration and Pressure Angle : Rise = 4-5-6-7 Polynomial, Return = Modified Trapezoidal

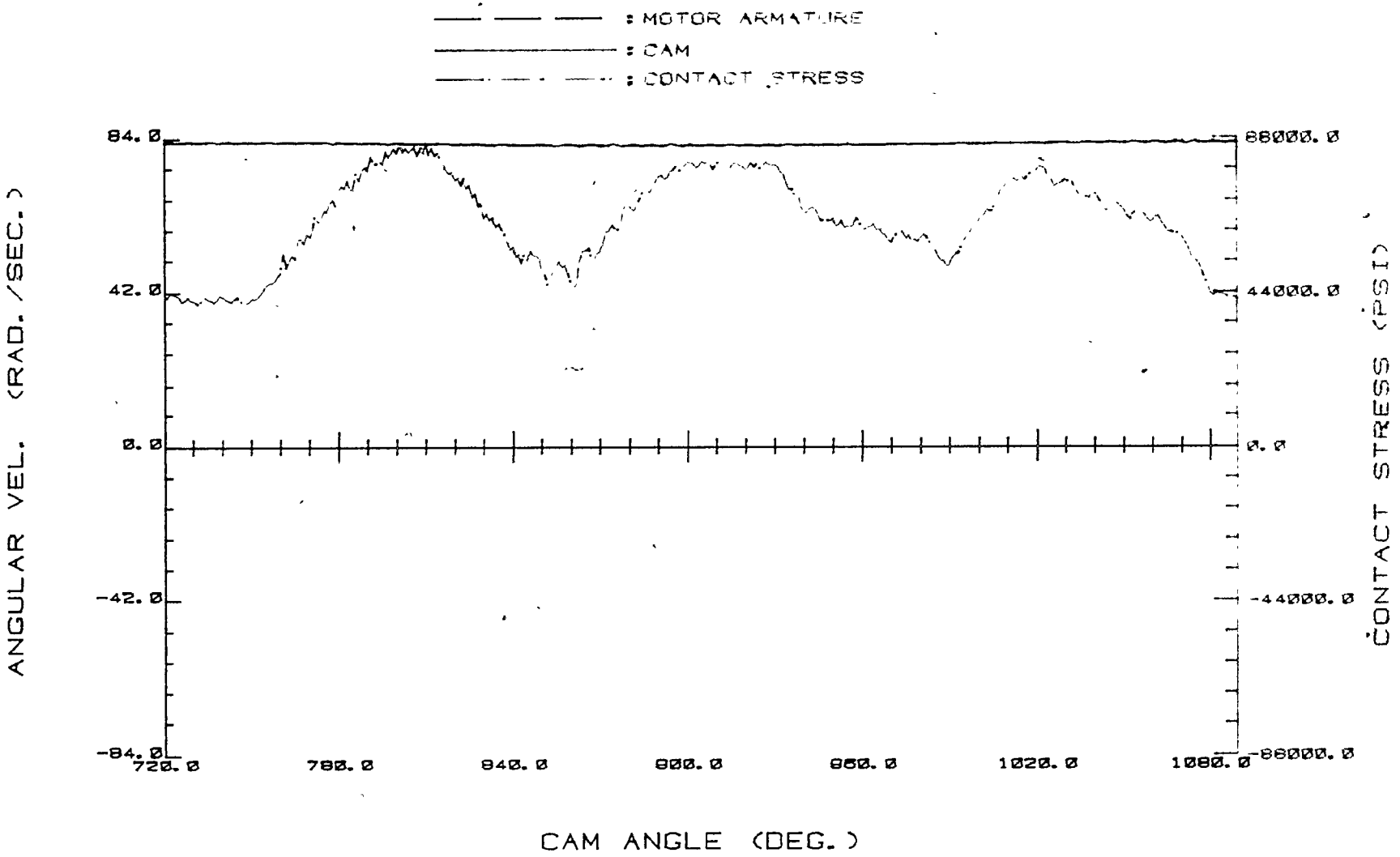

Fig. VI.16. Tolerance (cam : 0.0005, roller : 0.0001) and Waviness (17/rev.) Effect on Angular Velocity and Contact Stress : Rise = 4-5-6-7 Polynomial, Return = Modified Trapezoidal

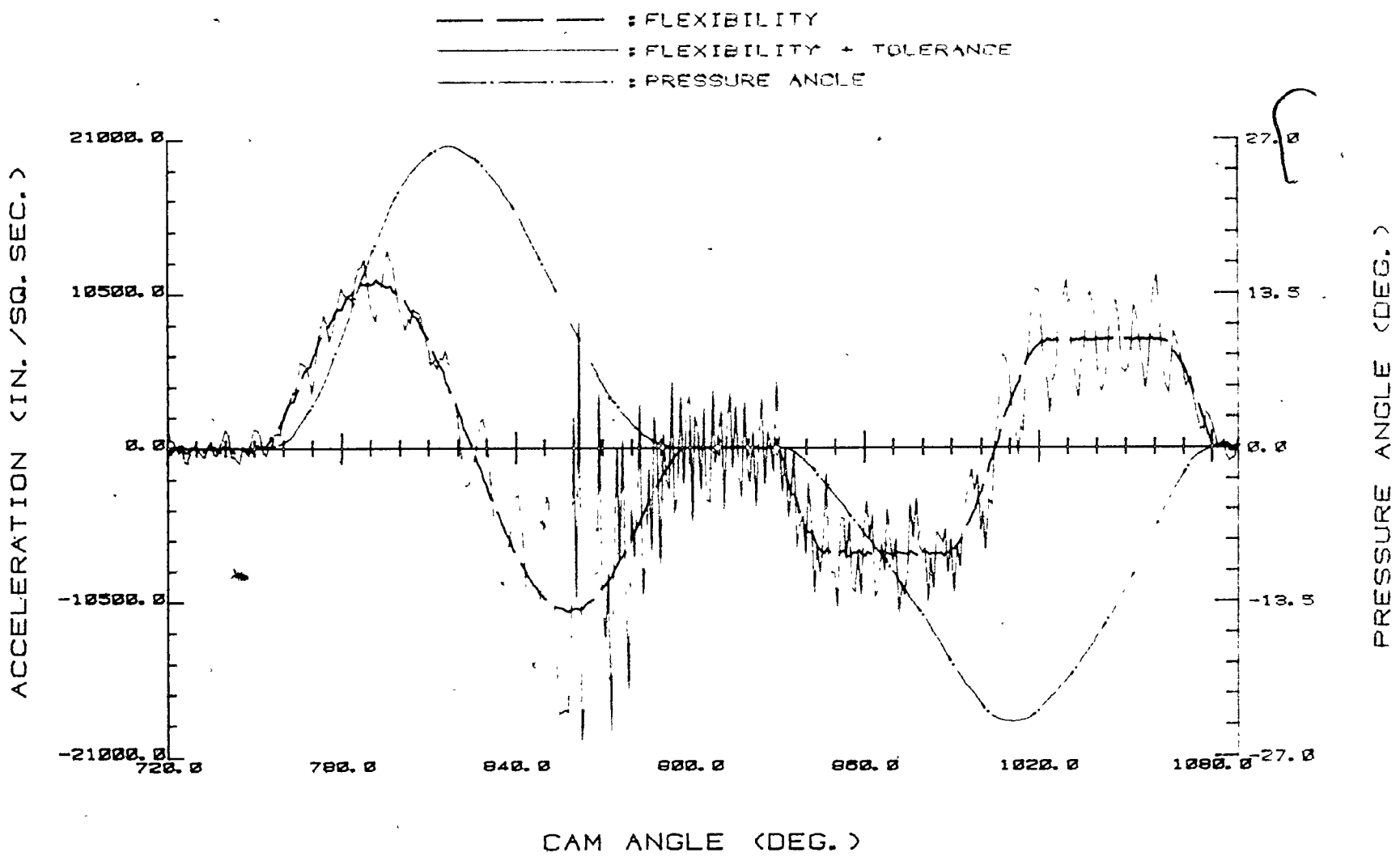

Fig. VI.17. Tolerance (cam : 0.0005, roller : 0.0001) and Waviness (39/rev.) Effect on Acceleration and Pressure Angle : Rise = 4-5-6-7 Polynomial, Return = Modified Trapezoidal

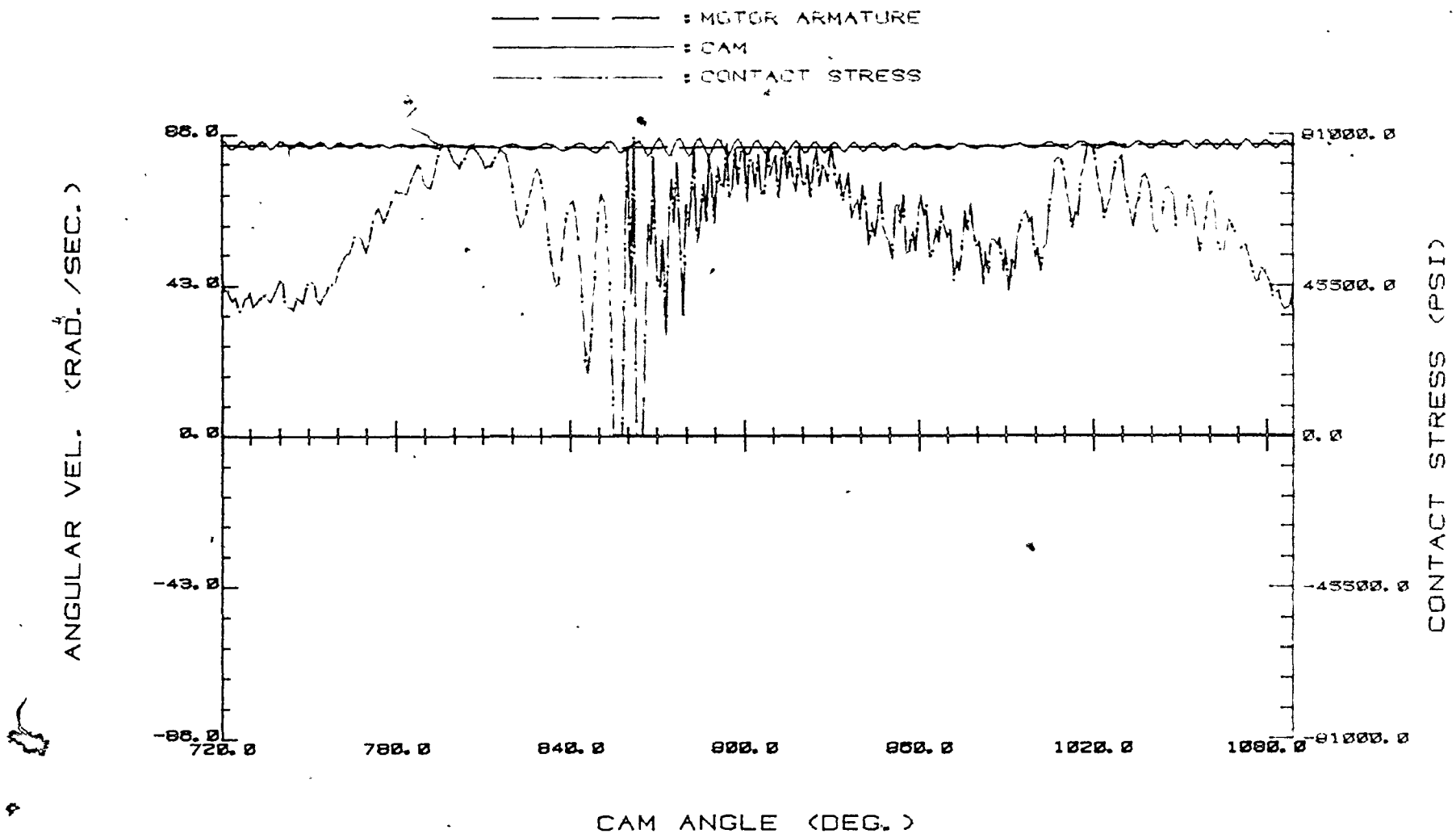

Fig. VI.18. Tolerance (cam : 0.0005, roller : 0.0001) and Waviness (39/rev.) Effect on Angular Velocity and Contact Stress : Rise = 4-5-6-7 Polynomial, Return = Modified Trapezoidal

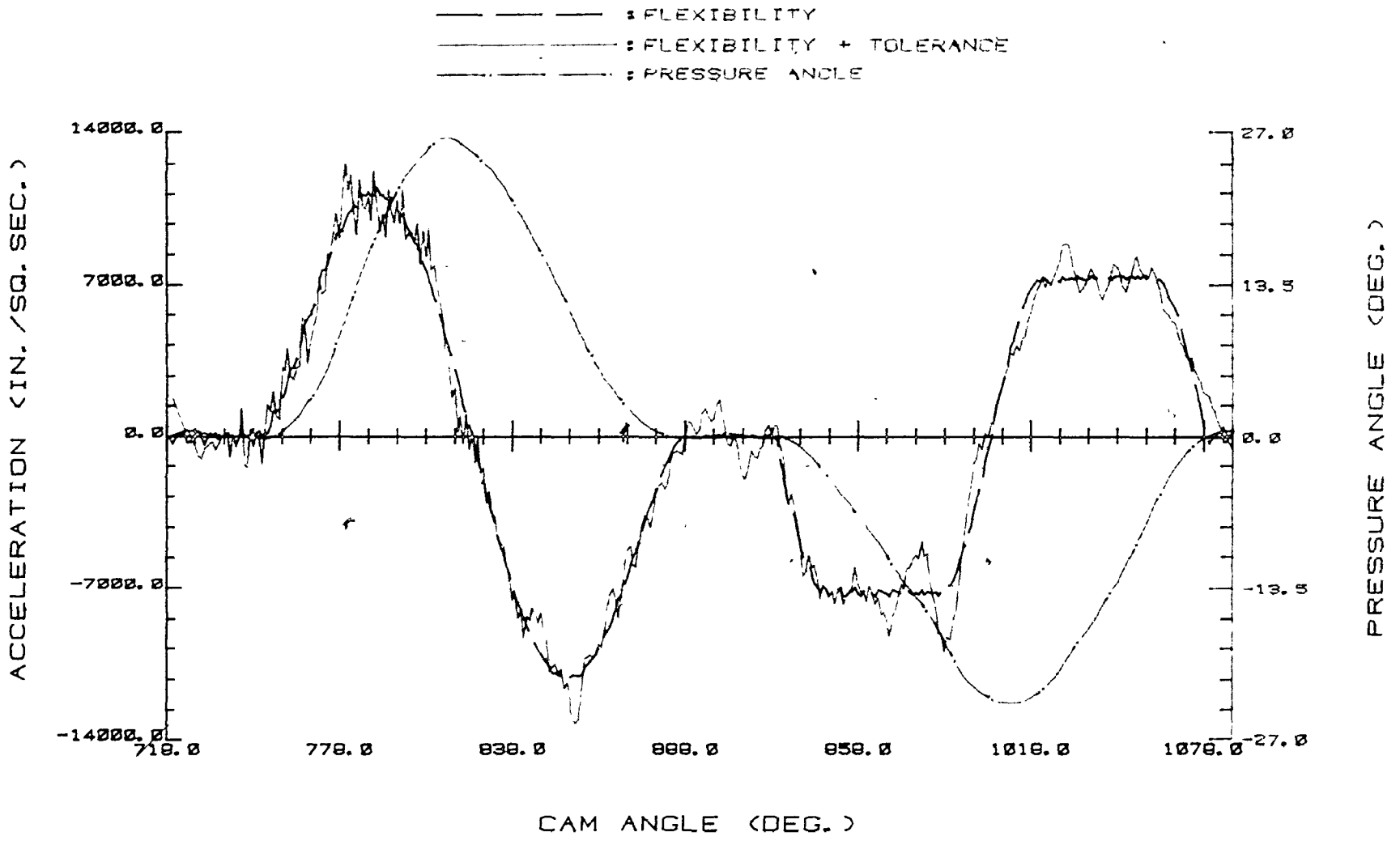

Fig. VI.19. Tolerance (cam : 0.0025, roller : 0.0005) and Waviness (17/rev.) Effect on Acceleration and Pressure Angle : Rise = 4-5-6-7 Polynomial, Return = Modified Trapezoidal

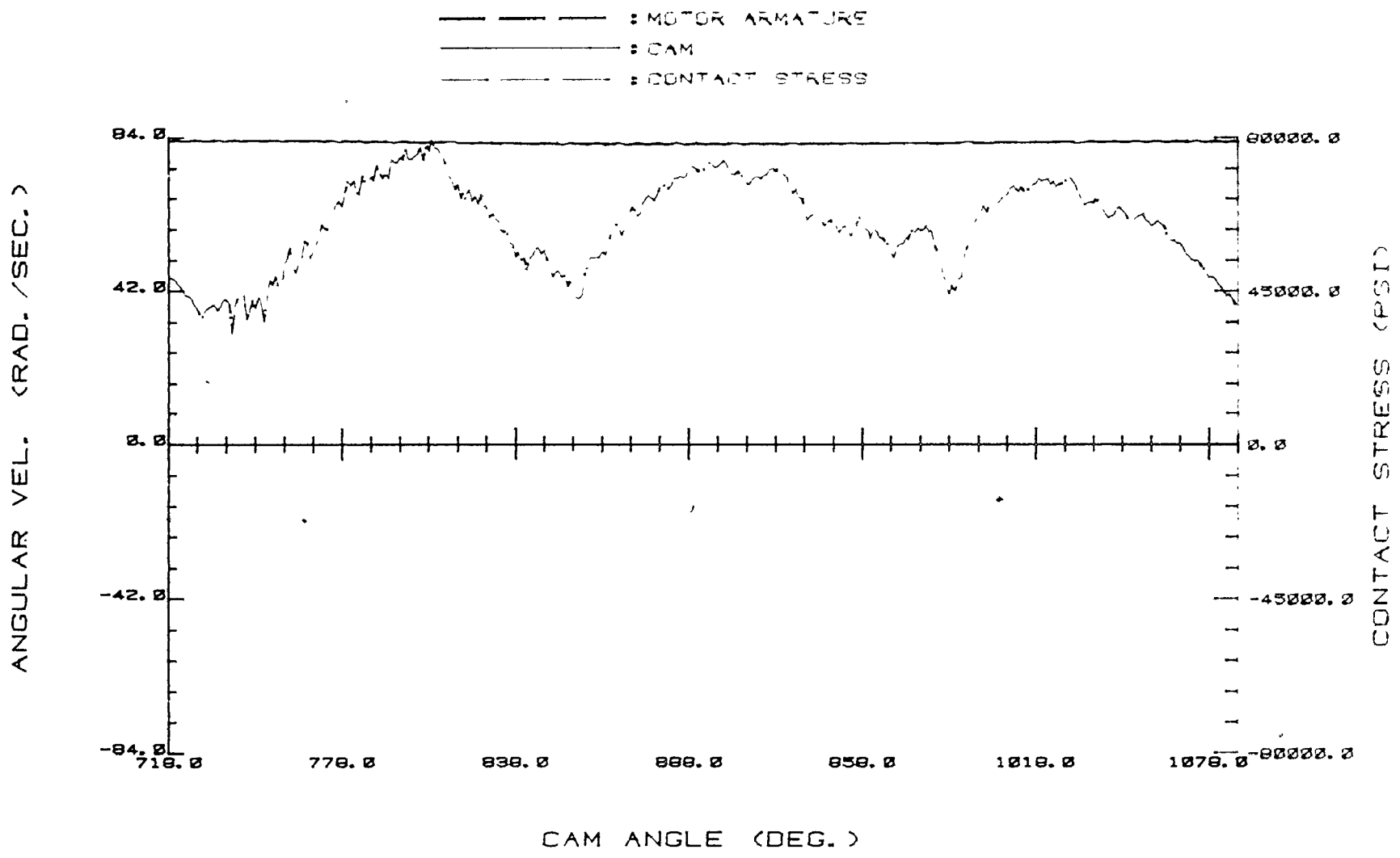

Fig. VI.20. Tolerance (cam : 0.0025, roller : 0.0005) and Waviness (17/rev.) Effect on Angular Velocity and Contact Stress : Rise = 4-5-6-7 Polynomial, Return = Modified Trapezoidal

3. A fairly rough profile can be accepted for a relatively good performance only if the FPR of its waviness is kept low;
4. The FPR of the profile's waviness affects the time responses, especially the acceleration and angular velocity, more severely than the inertial responses. Note that an increase in the FPR quickly causes the follower to jump, which results in unacceptable performance.

These results are well illustrated in Figs. VI.15-20, where they are illustrated graphically in different colours. In Fig. VI.17, the widely broken intervals in the pressure angle graph and corresponding zero contact stress indicate regions in the motion where jumping of the follower is occurring.

VI.4.2. Effects of Kinematic Imperfections

A. Relative Sensitivity of the Various Standard Motion Programs to Flexibility and Tolerances

The same system flexibility and tolerance (including waviness) was applied to cams using each of the standard motion programs, so that the sensitivity of the various standard programs to these system defects could be assessed. First, a theoretically perfect cam surface (theoretical cam) was employed so that the effect of flexibility alone could be determined, and then a simulated actual cam surface which included

tolerance and waviness was used to determine sensitivity to both flexibility and tolerance.

Table VI.3 shows the effects of flexibility alone (theoretical cam) on the time responses and Table VI.5 shows the effects of both flexibility and tolerance (actual cam). Table VI.4 shows the results of the theoretical cam on inertial responses, and Table VI.6 the results of the actual cam on the inertial responses. The second cycle of rotation was investigated, and the RMS was calculated for each of the four motion periods D-R-D-R. To obtain a comparison index, these RMS values for each period were summed and shown in the last column as an overall sensitivity index.

The rise and return periods of the 1st cycle were also taken into consideration to investigate the transient vibration behavior, damping rate and stability of each program. For the inertial responses, the rise and return period are chosen only from the 2nd cycle, to analyse under the steady state operating condition the torque requirement, power feedback and pitting tendency of each program.

For the investigation of the effects on the time responses, the acceleration only was presented in the tables, since it is the most sensitive to any imperfection, although the other responses such as displacement or velocity were given equal consideration in the investigation. In Table VI.9, the characteristics of theoretical motion programs are summarized for reference.

From Tables VI.3-4, the effects of each theoretical curve on

Table VI.3. Effects of the Various Standard Motion Curves on Acceleration due to System Flexibility

RMS = root mean square of (Accel. by Flexibility - Theoretical Accel.)

	Low Dwell	Rise		High Dwell	Return		Sensitivity to Flexibility ($\Sigma[RMS]_{II}$)
	II cycle $(RMS)_{II}$	I cycle $(RMS)_{I}$	II cycle $(RMS)_{II}$	II cycle $(RMS)_{II}$	I cycle $(RMS)_{I}$	II cycle $(RMS)_{II}$	
Straight Line	2.3161	4.0	7.2	1.940	4.8	5.9	17.3560
Parabolic	0.3599	0.529	0.405	0.5249	0.3569	0.419	1.7088
SHM	0.3177	0.17	0.32	0.4183	0.244	0.26	1.3160
Cubic 1	1.472	2.40	4.4	9.293	3.7	6.2	21.3650
Cubic 2 (2-3 Poly.)	0.4212	0.20	0.35	0.5114	0.30	0.31	1.5926
DHC	0.0611	0.093	0.054	0.6344	0.47	0.37	1.1195
Cycloidal	0.0174	0.110	0.016	0.0133	0.023	0.0172	0.0639
Trapezoidal	0.0264	0.114	0.032	0.0222	0.038	0.033	0.1136
Modified Trapezoidal	0.0248	0.117	0.0155	0.0202	0.025	0.0175	0.0780
3-4-5 Poly.	0.0245	0.116	0.0150	0.0197	0.025	0.017	0.0762
4-5-6-7 Poly.	0.0017	0.101	0.0169	0.0010	0.0243	0.0186	0.0382
Modified Sine	0.0266	0.119	0.0147	0.0223	0.0278	0.0167	0.0803

* unit : (x 10^4) inch/sec^2

Table VI.4. Effects of the Various Standard Motion Curves on Inertial Responses due to System Flexibility

	RISE					RETURN				
	Torque (lb.in.)	Contact Force (lb.)		Contact Stress (psi)		Torque (lb.in.)	Contact Force (lb.)		Contact Stress (psi)	
	avg.(max.)	min.	max.	min.	max.	avg.(max.)	min.	max.	min.	max.
Straight Line	136.52 (4400)	0	3744	0	345600	-66.11 (-3916)	0	3900	0	360000
Parabolic	75.338 (233)	0	233	0	87120	-73.59 (-300)	37	304	33000	99000
SHM	78.2 (155)	42	222	37600	84600	-72.6 (-137)	42	189	37600	79900
Cubic 1	98.8 (870)	0	2403	0	277300	-96.5 (-2870)	0	2990	0	288000
Cubic 2 (2-3 Poly.)	77.47 (154)	42	222	37600	84600	-73.132 (-135)	43	189	38800	79900
DHC	79.67 (208)	44	213	38000	83300	-73.12 (-232)	0	256	0	91500
Cycloidal	79.2 (185)	48	203	42400	80750	-73.6 (-168)	48	203	42400	80750
Trapezoidal	78.9 (191)	50	218	43000	83600	-73.38 (-176)	50	205	43000	80960
Modified Trapezoidal	78.8 (200)	46	212	41500	83000	-73.32 (-188)	46	201	41500	80300
3-4-5 Poly.	78.81 (163)	47	202	42000	81900	-73.137 (-152)	47	202	42000	78400
4-5-6-7 Poly.	80.49 (222)	51	229	42600	86600	-73.349 (-204)	51	214	42600	82140
Modified Sine	77.94 (148)	46	200	41500	74700	-73.31 (-141)	46	189	41500	72630

the system flexibility can be observed as follows :

1. Transient Vibration

The programs are listed in order of increased vibration :

DHC, 4-5-6-7 Polynomial, Cycloidal, Trapezoidal, 3-4-5 Polynomial, Modified trapezoidal, Modified sine, SHM, 2-3 Polynomial (Cubic 2), Parabolic, Cubic 1, Straight line

This indicates that the program having a smoother acceleration in the rise period of the initial cycle has less transient vibration.

2. Sensitivity to Shock

The index for the sensitivity of each program to shock

$$= [(RMS_I - RMS_{II}) / RMS_I]_{rise} + [(RMS_I - RMS_{II}) / RMS_I]_{return}.$$

The smallest index indicates the least sensitivity, and the programs are listed in the order of increasing sensitivity :

Cubic 1, Straight line, SHM, Cubic 2, Parabolic, DHC, Trapezoidal, 4-5-6-7 Polynomial, Cycloidal, Modified trapezoidal, 3-4-5 Polynomial, Modified sine

This indicates that the larger the step in acceleration

the more sensitive to shock the program is, and in the case of no step, the sensitivity becomes proportional to the peak acceleration of the program.

3. Stability of Programs under the Same Operational Condition

Unstable programs : Straight line, Parabolic, SHM, Cubic 1, Cubic 2 (2-3 Polynomial)

Stable programs : DHC, Cycloidal, Trapezoidal, Modified trapezoidal, 3-4-5 Polynomial, 4-5-6-7 Polynomial, Modified sine

The unstable programs have larger steps in acceleration and are more sensitive to shock than those of the stable programs.

4. Jump Phenomena

Jump in rise : Parabolic

Jump in return : DHC

Jump in both periods : Straight line, Cubic 1

5. Maximum Torque Requirement

Programs are listed in the order of the increasing torque requirement :

Modidied sine, Cubic 2 (2-3 Polynomial), SHM, 3-4-5 Polynomial, Cycloidal, Trapezoidal, Modified trapezoidal, DHC, 4-5-6-7 Polynomial, Parabolic, Cubic 1, Straight line

It is noted that the program whose peak acceleration is skewed to the left side needs a smaller power requirement. (See Table VI.9 for a comparison between the 2-3 polynomial and Cubic 1.)

6. Power Feedback

For purposes of seeking the program which gives the best economy in input energy, the power feedback during the return period is important, and the programs are listed below in order of the smallest to the largest feedback :

SHM, Cubic 2 (2-3 Polynomial), 3-4-5 Polynomial, Modified sine, Modified trapezoidal, 4-5-6-7 Polynomial, Trapezoidal, Parabolic, Cycloidal

The above order was chosen by considering the magnitude of the average negative torque in the return period, but it is noted that there is no considerable difference between programs. (The programs generating jumps for the return period were excluded).

7. Pitting Tendency

Pitting is the main factor impairing the life of a cam and the pitting tendency of each program is examined by referring to the maximum contact stress during a revolution. The programs are listed below in order of increasing pitting tendency :

Modified trapezoidal, Trapezoidal, 3-4-5 Polynomial*, Cycloidal*, Modified sine*, SHM*, Cubic 2*, Parabolic, DHC*, Cubic 1, Straight line

* : pitting in upper dwell; remainder : pitting in rise period

8. Sensitivity to Flexibiltiy

The sensitivity of each program to the system flexibility is measured by the total RMS ($\Sigma[RMS]_{II}$) of the entire 2nd revolution (D-R-D-R), and listing in order of increasing sensitivity we have :

4-5-6-7 Polynomial, Cycloidal, 3-4-5 Polynomial, Modified trapezoidal, Modified sine, Trapezoidal, DHC, SHM, Cubic 2, Parabolic, Straight line

Having small sensitivity to system flexibility means that the particular program has good dynamic characteristics by yielding a smooth acceleration and providing a finite value of jerk.

In Tables VI.5-6, it is recognized that the combined effects of system flexibility and tolerance are significantly greater than the effects of the system flexibility alone and results are elaborated upon below :

1. Transient Vibration

Table VI.5. Effects of the Various Standard Motion Curves on Actual (Flexibility + Tolerance) Acceleration

RMS = root mean square of (Actual Accel. - Theoretical Accel.)

	Low Dwell	Rise		High Dwell	Return		Sensitivity to Tolerance
	II cycle $(RMS)_{II}$	I cycle $(RMS)_{I}$	II cycle $(RMS)_{II}$	II cycle $(RMS)_{II}$	I cycle $(RMS)_{I}$	II cycle $(RMS)_{II}$	$(\Sigma[RMS]_{II} - SF)$
Straight Line			not	workable			
Parabolic	0.2028	0.4286	0.1879	0.1375	0.1039	0.1183	-1.0623
SHM	0.2158	0.538	0.208	0.2277	0.116	0.105	-0.5610
Cubic 1	2.382	3.30	5.23	4.625	5.52	3.50	-5.628
Cubic 2 (2-3 Poly.)	0.2447	0.655	0.256	0.2724	0.155	0.125	-0.6945
DHC	0.0228	0.400	0.103	0.3490	0.155	0.144	-0.5007
Cycloidal	0.0244	0.391	0.0614	0.0448	0.0913	0.0465	0.1132
Trapezoidal	0.0258	0.350	0.141	0.0477	0.0950	0.0901	0.1910
Modified Trapezoidal	0.0258	0.342	0.122	0.0477	0.0615	0.0518	0.1693
3-4-5 Poly.	0.0315	0.335	0.108	0.0530	0.0589	0.0459	0.1622
4-5-6-7 Poly.	0.0260	0.458	0.0723	0.0412	0.0598	0.0526	0.1539
Modified Sine	0.0358	0.328	0.124	0.0715	0.0599	0.0502	0.2012

* unit : (x 10^4) inch/sec^2 , SF : Sensitivity to Flexibility (Table VI.3)

Table VI.6. Effects of the Various Standard Motion Curves on Inertial Responses due to Flexibility + Tolerance

	RISE					RETURN				
	Torque (lb.in.)	Contact Force (lb.)		Contact Stress (psi)		Torque (lb.in.)	Contact Force (lb.)		Contact Stress (psi)	
	avg.(max.)	min.	max.	min.	max.	avg.(max.)	min.	max.	min.	max.
Straight Line			not	workable						
Parabolic	77.717 (226)	34	230	33000	86400	-73.287 (-212)	73	218	52000	84000
SHM	77.679 (140)	37	224	45120	84600	-73.134 (-127)	94	154	54050	73320
Cubic 1	62.778 (1155)	0	3300	0	331500	-61.262 (-882)	0	1650	0	331200
Cubic 2 (2-3 Poly.)	76.787 (139)	20	225	44000	84000	-72.999 (-121)	92	150	54000	69600
DHC	79.575 (198)	24	208	29680	81900	-73.547 (-180)	24	196	29680	80100
Cycloidal	79.326 (207)	55	221	43700	84100	-73.776 (-163)	55	204	43700	79200
Trapezoidal	78.7475 (221)	53	238	42940	88930	-73.893 (-175)	53	207	42940	81960
Modified Trapezoidal	78.7470 (218)	40	243	39100	89700	-73.893 (-176)	48	195	41400	80500
3-4-5 Poly.	78.294 (187)	48	206	42050	81780	-73.620 (-145)	54	188	43500	81200
4-5-6-7 Poly.	79.832 (241)	47	234	39200	88200	-73.537 (-174)	48	218	41650	84300
Modified Sine	77.604 (175)	55	216	43700	82600	-73.438 (-140)	55	194	43700	79800

In order of increasing vibration :

Modified sine, 3-4-5 Polynomial, Modified trapezoidal, Trapezoidal, cycloidal, DHC, Parabolic, 4-5-6-7 Polynomial, SHM, Cubic 2, Cubic 1

2. Sensitivity to Shock

In order of increasing sensitivity :

Cubic 1, Parabolic, Trapezoidal, SHM, Modified sine, Modified trapezoidal, Cubic 2, DHC, 3-4-5 Polynomial, 4-5-6-7 Polynomial, Cycloidal

3. Stability

Unstable programs - Parabolic, Cubic 1

Stable programs - all programs except the unstable programs and straight line.

4. Jump Phenomena

No program produces jump except the straight line and the Cubic 1, which have jumps in both the rise and return periods.

5. Torque Requirement

In order of increased torque requirement :

Cubic 2, SHM, Modified sine, 3-4-5 Polynomial,

DHC, Cycloidal, Modified trapezoidal, Trapezoidal, Parabolic, 4-5-6-7 Polynomial, Cubic 1

6. Power Feedback

In order of increasing power feedback :

Cubic 2, SHM, Parabolic, Modified sine, 4-5-6-7 Polynomial, DHC, 3-4-5 Polynomial, Cycloidal, Trapezoidal & Modified trqpezoidal, (Cubic 1 was excluded due to the jump)

7. Pitting Tendency

In order of increased pitting tendency :

Cycloidal, Modified trapezoidal, 3-4-5 Polynomial, Trapezoidal, Modified sine*, 4-5-6-7 Polynomial, DHC*, SHM*, Cubic 2*, Cubic 1, * : pitting in upper dwell; remainder : pitting in rise period.

8. Sensitivity to Tolerance

To measure the sensitivity to tolerance alone, the total RMS for the effects of flexibility is subtracted from the total RMS for the actual (flexibility + tolerance) effect, i.e. the sensitivity to tolerance is

$$[\ \Sigma\ (RMS)_{II}\ ]_{actual} - [\ \Sigma\ (RMS)_{II}\ ]_{flexibility}$$

In the order of increasing sensitivity :

Cubic 1, Parabolic, Cubic 2, SHM, DHC, Cycloidal, 4-5-6-7 Polynomial, 3-4-5 Polynomial, Modified trapezoidal, trapezoidal, Modified sine

The effect of tolerance on the following basic programs, Parabolic, SHM, Cubic 1, Cubic 2, and DHC, became negative, which means that the tolerance actually diminished the undesirable vibration induced in the theoretical cam, i.e. cam surface with no tolerance.

The above two observations were tabulated in Tables VI.7-8 respectively, and by comparing the effects on the theoretical cams and the actual cams, which carry the machining tolerance, the following conclusions are summarized :

1. The basic motion programs such as straight line, Parabolic, SHM, and Cubic 1 (2-3 Polynomial), whose dynamic performance is theoretically very poor, are less sensitive to tolerance, and their poor dynamic performance is even compensated by tolerance under the actual operating conditions. Note that jumping which occurred on the theoretical cams disappeared when tolerance was introduced, and unstable programs became stable.

2. Contrary to the basic programs, the advanced motion programs such as Cycloidal, Modified trapezoidal, 4-5-6-7 Polynomial, and Modified sine are very sensitive to the tolerance even though they have very good theoretical dynamic characteristics. Therefore, to maintain this

Table VI.7. Comparison of Motion Curves - Flexibility Effects

* Numbers were given in the order of increasing effect. S : stable, U : unstable

	Transient Vibration	Sensitivity to Shock	Stability	Jumping		Torque Requirement	Power Feed-back	Pitting Tendency	Sensitivity to Flexibility
				rise	return				
Straight Line	12	11	U	yes	yes	12	-	12	11
Parabolic	10	8	U	yes	no	10	8	9	10
SHM	8	10	U	no	no	3	1	7	8
Cubic 1	11	12	U	yes	yes	11	-	11	12
Cubic 2 (2-3 Poly.)	9	9	U	no	no	2	2	8	9
DHC	1	7	S	no	yes	8	-	10	7
Cycloidal	3	4	S	no	no	5	9	5	2
Trapezoidal	4	6	S	no	no	6	7	2	6
Modified Trapezoidal	6	3	S	no	no	7	5	1	4
3-4-5 Poly.	.5	2	S	no	no	4	3	3	3
4-5-6-7 Poly.	2	5	S	no	no	9	6	4	1
Modified Sine	7	1	S	no	no	1	4	6	5

Table VI.8. Comparison of Motion Curves - Combined (Flexibility + Tolerance) Effects

* Numbers were given in the order of increasing effect. S : stable, U : unstable

	Transient Vibration	Sensitivity to Shock	Stability	Jumping		Torque Requirement	Power Feed-back	Pitting Tendency	Sensitivity to Tolerance
				rise	return				
Straight Line	not comparable but most likely worst curve								
Parabolic	7	10	U	no	no	9	3	6	2
SHM	9	8	S	no	no	2	2	9	4
Cubic 1	11	11	U	yes	yes	11	-	11	1
Cubic 2 (2-3 Poly.)	10	5	S	no	no	1	1	10	3
DHC	6	4	S	no	no	5	6	8	5
Cycloidal	5	1	S	no	no	6	8	1	6
Trapezoidal	4	9	S	no	no	8	9	4	10
Modified Trapezoidal	3	6	S	no	no	7	9	2	9
3-4-5 Poly.	2	3	S	no	no	4	7	3	8
4-5-6-7 Poly.	8	2	S	no	no	10	5	7	7
Modified Sine	1	7	S	no	no	3	4	5	11

Table VI.9. Characteristics of Theoretical Motion Programs

* M.O.I = moment of inertia

	Velocity		Acceleration		Jerk		Pressure Angle (max.)	Cam	
	curve	max.	curve	max. (min.)	curve	max. (min.)		Area	M.O.I
Straight Line	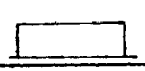	1.0 v		∞		∞ (- ∞)	1.0 P	1.118 A	1.131 M
Parabolic	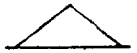	2.0 v		1.0 a		∞ (- ∞)	1.85 P	1.139 A	1.230 M
SHM		1.57 v	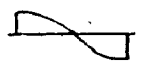	1.23 a	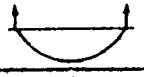	∞ (-1.29j)	1.5 P	1.136 A	1.213 M
Cubic 1	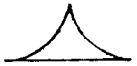	3.0 v		3.0 a		2.0 j (0.0)	2.5 P	1.153 A	1.288 M
Cubic 2 (2-3 Poly.)		1.5 v	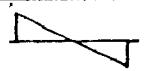	1.5 a	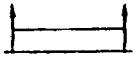	∞ (-1.0 j)	1.45 P	1.134 A	1.206 M
DHC	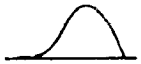	2.04 v	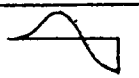	1.388 a (-2.47 a)	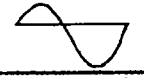	1.7 j (-3.53j)	1.88 P	1.0 A	1.0 M
Cycloidal		2.0 v	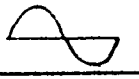	1.57 a	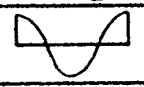	3.29j (-3.29j)	1.85 P	1.146 A	1.258 M
Trapezoidal	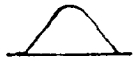	2.0 v		1.33 a		3.55j (-3.55j)	1.85 P	1.145 A	1.254 M
Modified Trapezoidal		2.0 v	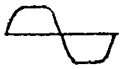	1.22 a	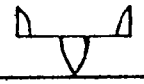	5.12j (-5.12j)	1.85 P	1.1438A	1.2485M
3-4-5 Poly.		1.875v	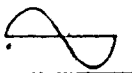	1.44 a		5.0 j (-2.5 j)	1.75 P	1.143 A	1.2480M
4-5-6-7 Poly.		2.19 v	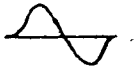	1.88 a	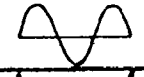	3.5 j (-4.375j)	1.986 P	1.150 A	1.275 M
Modified Sine		1.76 v	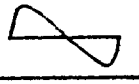	1.38 a	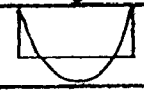	5.79j (-1.93j)	1.663 P	1.141 A	1.237 M

theoretical dynamic performance as it is, the machining accuracy should be such that cam profiles are maintained as close to the theoretical profile as possible.

3. It is reaffirmed that the tolerances exert a considerable influence on the system performance, which has been directly estimated from the theoretical behavior of motion programs. (Note that there are significant changes in the orders between the effects of the theoretical program and the actual program.)

4. The most practical and theoretically best program is found to be a cycloidal curve, a practically better program is a 3-4-5 polynomial, and a good program is a modified trapezoidal curve.

B. Influences of Nonconstant Angular Velocity of Cam

It is important to maintain the angular velocity of any cam as constant as possible by having a high inertia and stiff camshaft in the system. However, for the reasons described in Chapter II, it is virtually impossible to maintain an absolutely constant angular velocity, and some variation occurred in the physical model set up for this simulation.

Table VI.10 shows the numerical variation, and Figs. VI.21 to 26 show this in graphical form. To investigate the effect of angular

Table VI.10. Effect of Non-constant Angular Velocity of Cam on Time Response

A : accel., D : decel., # : jump occurs

Spring Constant (lb/in)		Period		Angular Velocity (AORD*) %			Accel. (RMS) x 10^4	Impact Force (AVG) x 10^2
				Motor	Coupling	Cam		
PARABOLIC	80	Dwell (I)		0.3972	0.3992	1.5268	0.3599	0.7679
		Rise	A	0.6083	0.6098	1.0707	0.3969	0.6243
			D#	1.3333	1.3313	1.8329	0.4139	1.5294
		Dwell(II)		1.5121	1.5201	1.7010	0.5249	1.0158
		Return	A	1.4288	1.4268	1.4329	0.3591	0.7617
			D	0.8831	0.8827	1.9492	0.4706	1.5809
CYCLOIDAL	55	Dwell (I)		0.7374	0.7471	1.8088	0.2685	1.0820
		Rise	A	0.9280	0.9266	1.1588	0.2163	0.7690
			D#	1.3548	1.3545	1.3119	0.6172	0.3560
		Dwell(II)#		1.4062	1.4072	1.4415	1.0282	1.3270
		Return	A#	1.4323	1.4333	1.4618	0.5242	0.9080
			D	1.1575	1.1560	1.6746	0.3701	1.1430
	80	Dwell (I)		0.4039	0.4010	0.3959	0.0165	0.0242
		Rise	A	0.5975	0.5996	0.6524	0.0124	0.0305
			D	1.2274	1.2267	1.1760	0.0153	0.5982
		Dwell(II)		1.3412	1.3418	1.3437	0.0130	0.6796
		Return	A	1.3205	1.3198	1.2770	0.0177	0.6335
			D	0.8708	0.8709	0.9127	0.0133	0.4450

* AORD : Average of Relative Deviation from the initial angular velocity (= 83.776 rad/sec)

velocity variation, theoretically perfect cam profiles were chosen, two different motions were compared, and the return spring rate was varied in one of these motions.

In Figs. 21-26, it is recognized that the primary and principal cause of the significant non-constant angular velocity of the cam is the impact between cam and follower, which is mostly generated by poor dynamic characteristics of the motion program (Figs. 21-22) and from jumping of the follower arising from an insufficient return spring force (Figs. 23-24). As the impact disturbs the rotation of the cam, this disturbance is fed back through the elastic cam shaft, gears, belts or couplings, which may include backlash, and circumferential vibration occurs resulting in a variance in angular velocity.

The nature of the variance in angular velocity is analyzed as follows : At the instant when there is a follower jump during the rise period, the angular velocity of the cam is momentarily increased by the torque from a power source because of no contact or zero load between cam and follower. While the zero load leads to zero torque, the follower under spring force returns from the jump to contact with the cam giving it an impact. The impact suddenly diminishes the increasing angular velocity of the cam and also generates a reverse momentary torque on the cam since the impact is against the cam rotation. During the return period, the angular velocity and the torque are increased by the impact since its direction is the same as the cam rotation.

As all the time responses except displacement are the function

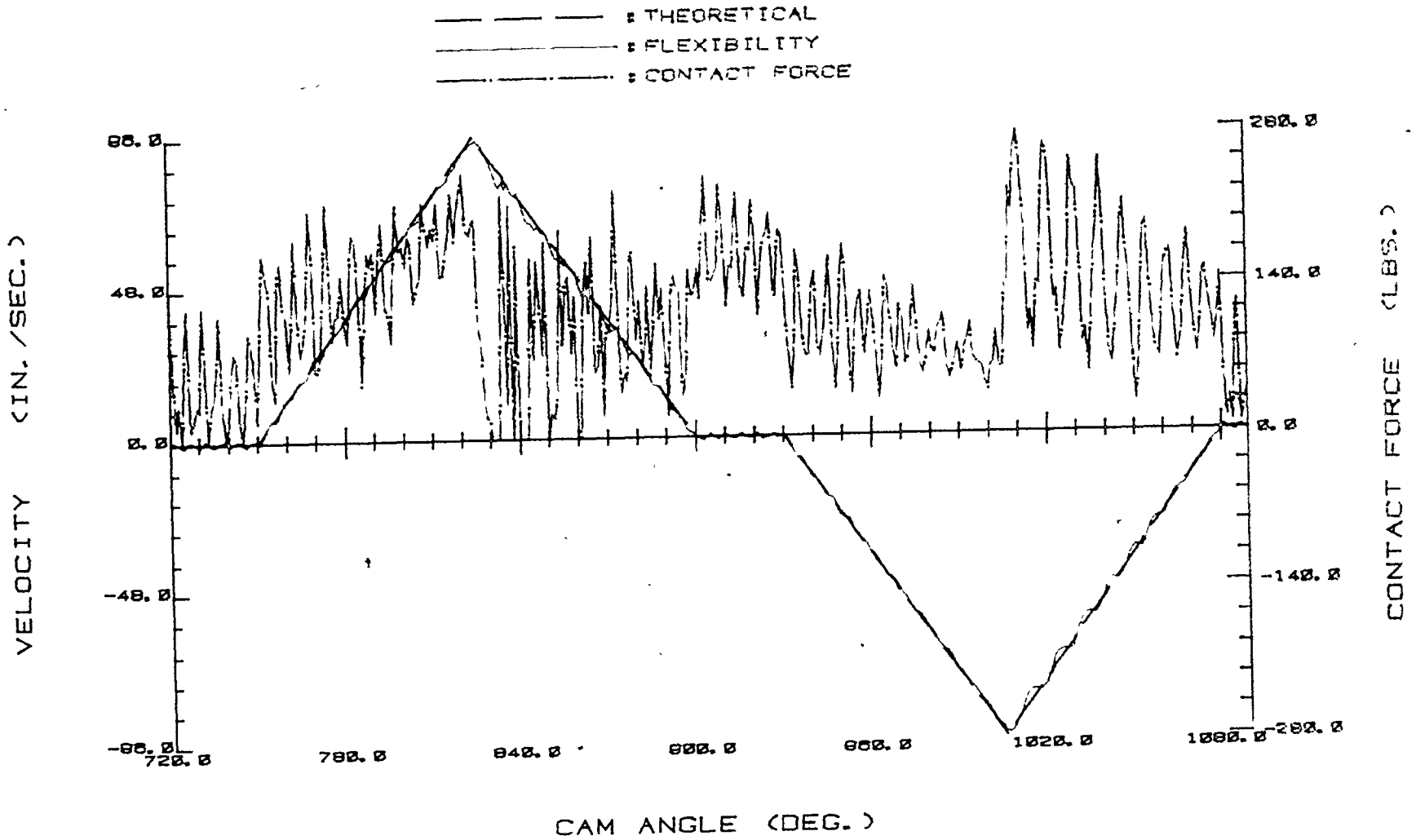

Fig. VI.21. Velocity and Contact Force for the Parabolic Motion Program : Effect of Variable Angular Velocity (Spring Stiffness = 80 lb/in)

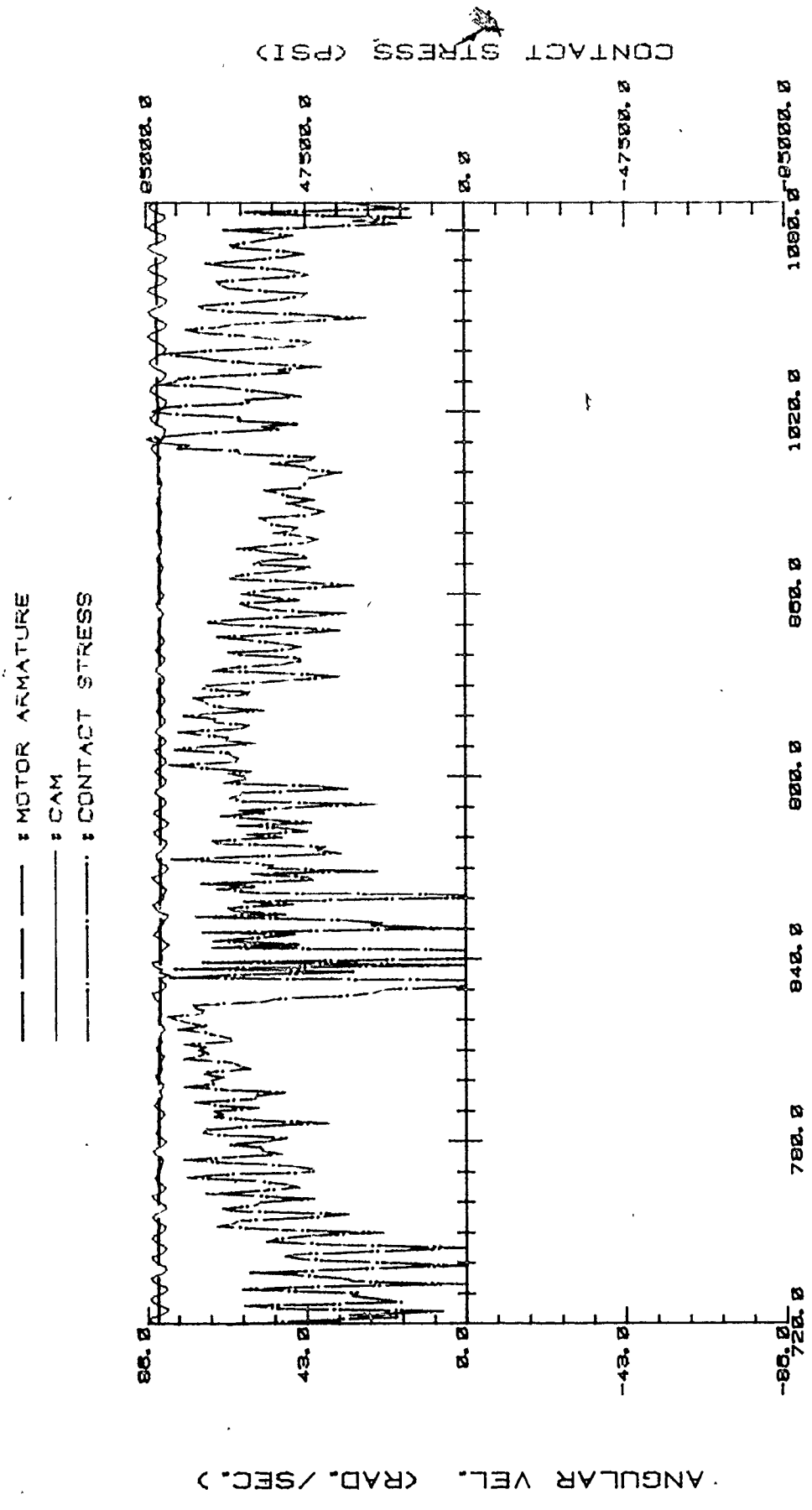

Fig. VI.22. Angular Velocity and Contact Stress for the Parabolic Motion Program : Effect of Variable Angular Velocity (Spring Stiffness = 80 lb/in)

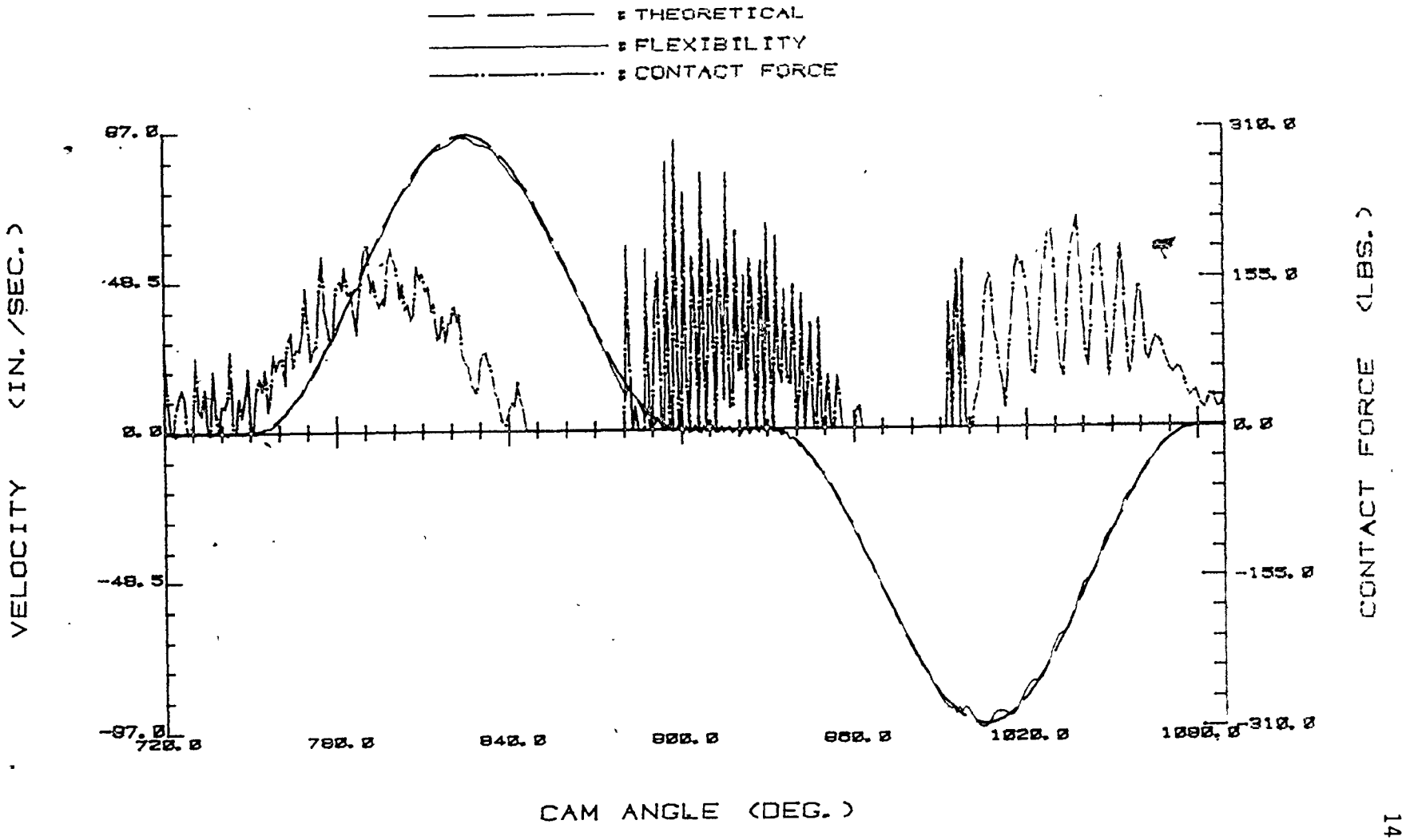

Fig. VI.23. Velocity and Contact Force for the Cycloidal Motion Program : Effect of Variable Angular Velocity (Spring Stiffness = 55 lb/in)

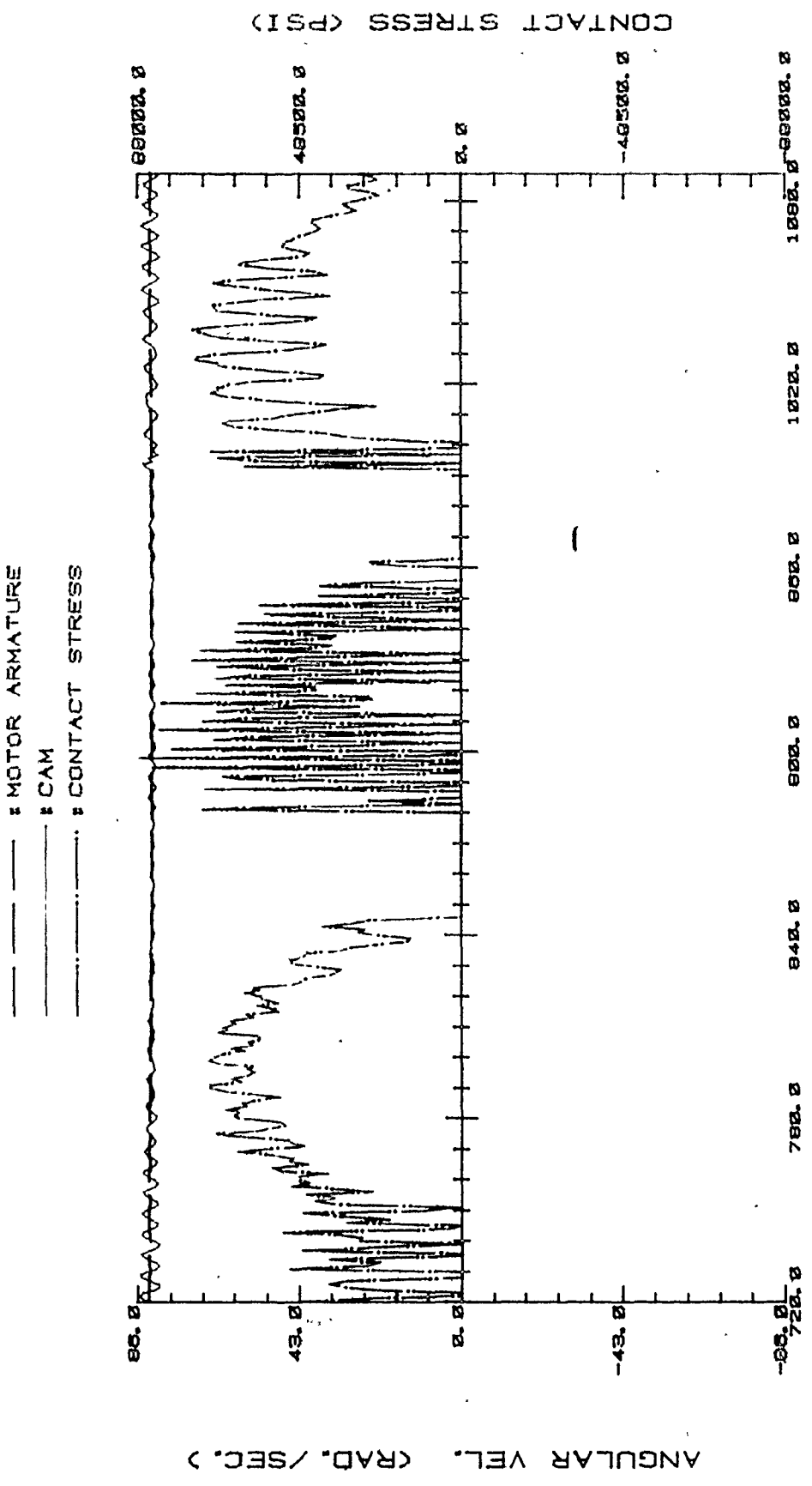

Fig. VI.24. Angular Velocity and Contact Stress for the Cycloidal Motion Program : Effect of Variable Angular Velocity (Spring Stiffness = 55 lb/in)

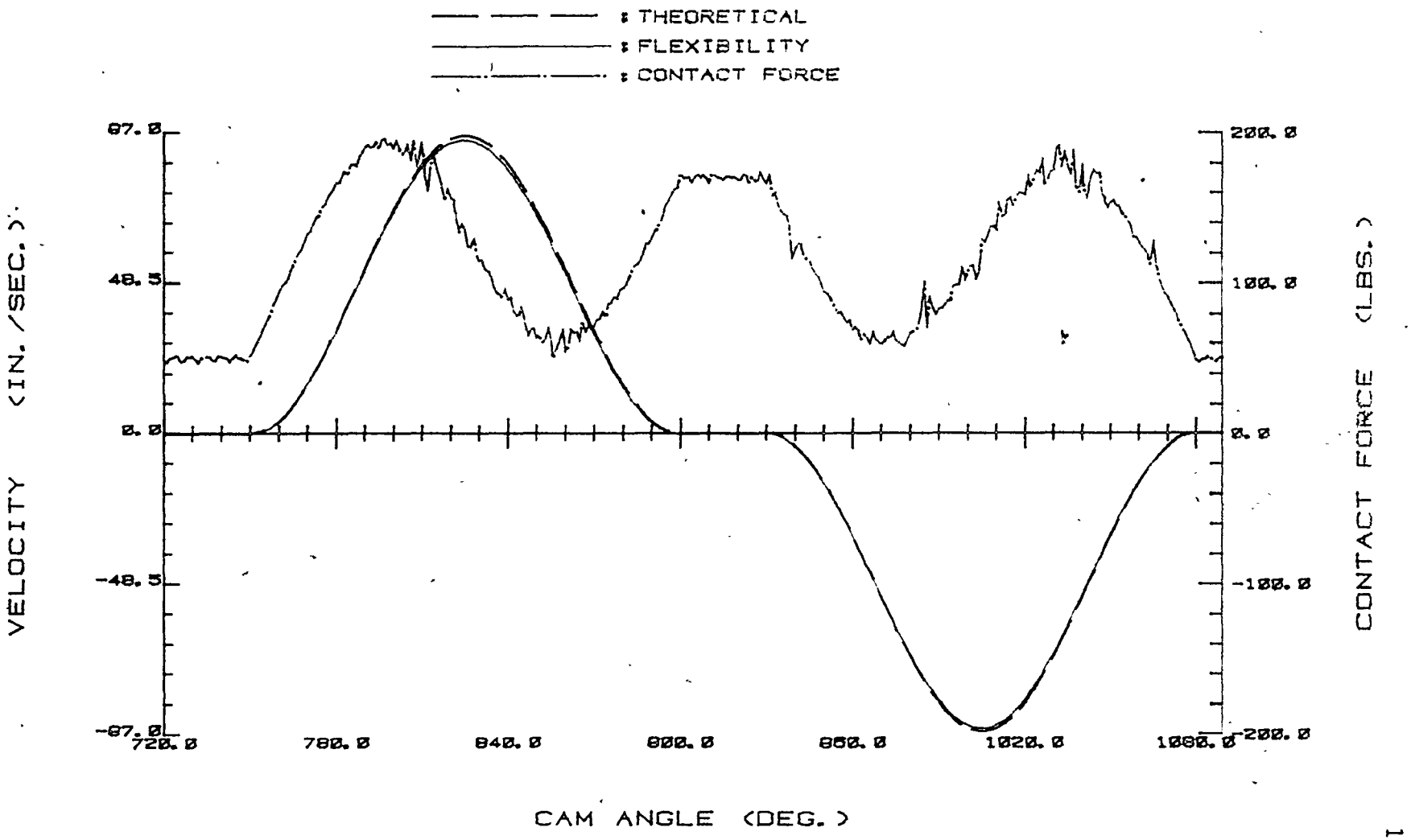

Fig. VI.25. Velocity and Contact Force for the Cycloidal Motion Program : Effect of Variable Angular Velocity (Spring Stiffness = 80 lb/in)

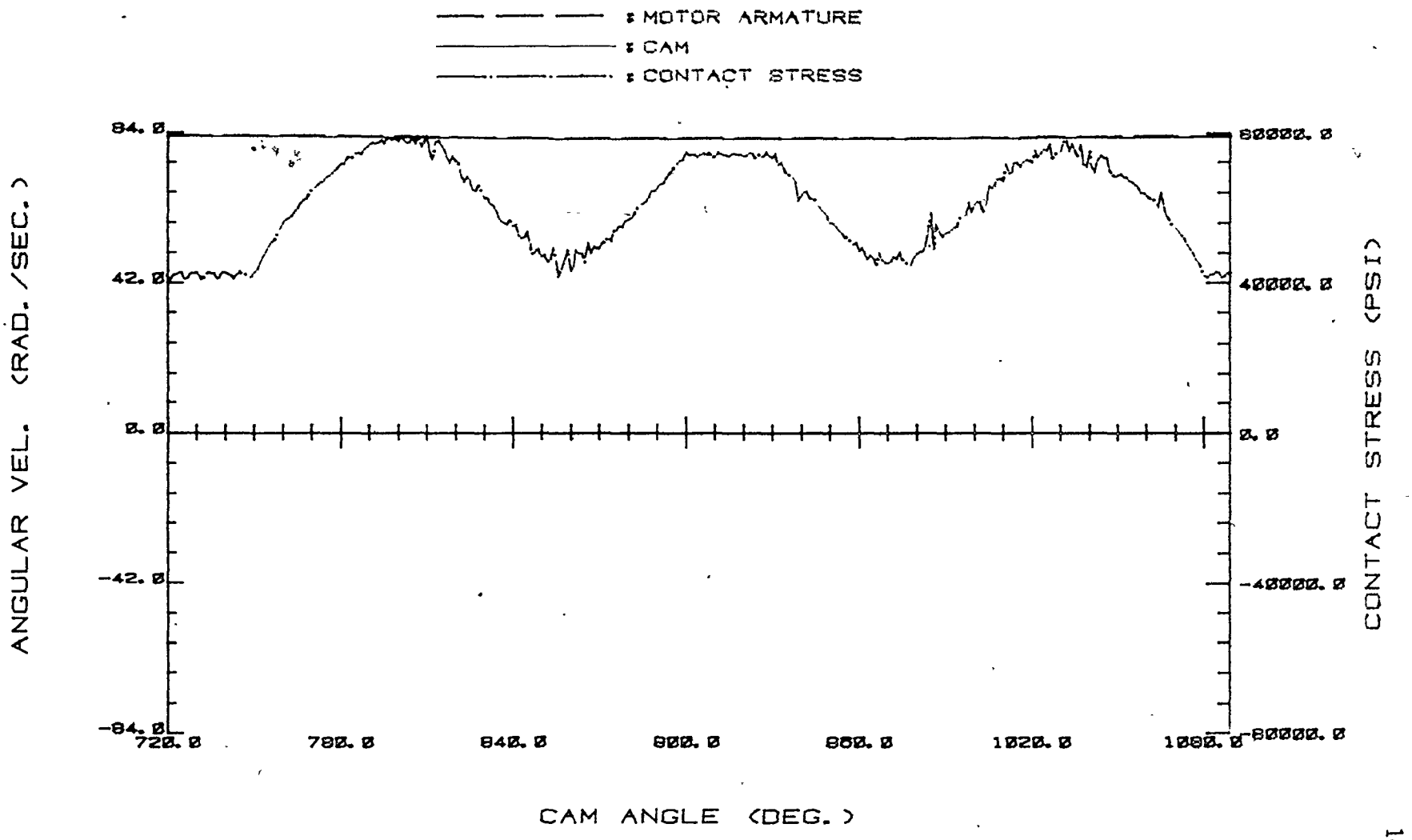

Fig. VI.26. Angular Velocity and Contact Stress for the Cycloidal Motion Program : Effect of Variable Angular Velocity (Spring Stiffness = 80 lb/in)

of angular velocity of the cam, they are considerably affected by the variation of angular velocity. However, although acceleration is an important design parameter, only the acceleration which is the most sensitive to angular velocity variation is investigated here.

In the typical case of 800 rpm (Table VI.10), the parabolic program, which has poor dynamic characteristics, caused the follower to jump during the rise period (due to the abrupt and great change of acceleration), altering the angular velocity by 1.95 % in the average of relative deviation (AORD) from the initial angular velocity. It is found that the period just after the period in which the jump occurs suffers from a significant variation of angular velocity and acceleration, while the maximum variation of angular velocity happens at the period of maximum impact. Note that the small % percentage change of angular velocity greatly affects the acceleration even though it is in turn influenced by the system flexibility and nonlinearity. Table VI.10 also illustrates the effect of insufficient return spring force in a cam mechanism using cycloidal motion, as compared to a mechanism using a spring strong enough to resist jumping. The reduction in angular velocity variation and acceleration with the greater spring rate is clearly evident.

To avoid these adverse effects, the angular velocity at the cam must be kept as constant as possible, and the following are suggested corrective measures :

1. Reduce the impact between cam and follower by providing the proper spring force or employing a suitable motion

program according to the operating speed of the cam.

2. Stiffen the power transmitting shaft and reduce the allowance or backlash in the power transmitting device as much as possible.
3. Introduce a flywheel which has a large moment of inertia, such as a heavy coupling, to diminish the feedback effect of the momentary impact, while supplying power sufficient to drive the heavy inertia.

C. Asymmetry between Rise and Return Periods

Asymmetry between rise and return periods has been briefly discussed in Chapter II, and the numerical verification can easily be recognized from Tables VI.3-6, which clearly exhibit the significant differences in time and inertial responses between the rise and return periods for various motion programs.

Fig. VI.27(a) shows a theoretical acceleration curve for a D-R-D-R cycle, with the signs of positive and negative acceleration indicating a smooth motion program such as cycloidal or 3-4-5 polynomial. Due to the symmetry of the acceleration shape, as well as the other time responses between the two periods, one usually designs a cam mechanism taking only one period, commonly the rise period, into consideration.

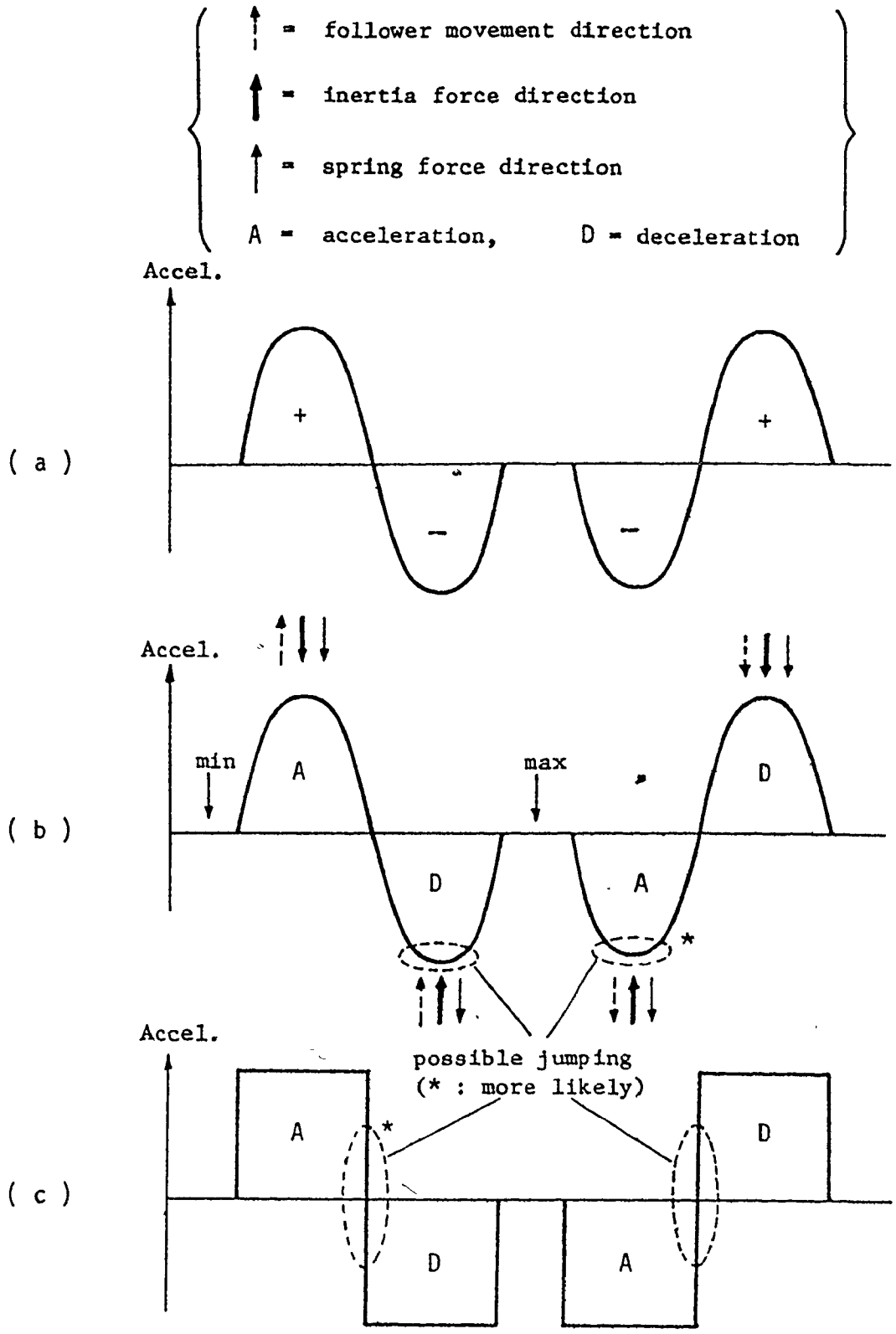

Fig. VI.27. Relationship between Inertia Force, Spring Force and Follower Movement

But it must be noted that the negative acceleration during the return period is not a deceleration but actually an acceleration, since the direction of the follower movement is downward, i.e. negative. Likewise, the positive acceleration of the period is in fact a deceleration. This physical recognition indicates the virtual asymmetry between the two periods, which significantly changes the performance during both periods and therefore needs to be considered in addition to the exciting forces which directly influence the performance.

Fig. VI.27(b) shows the directions of the inertia and spring forces for each acceleration and deceleration part, together with the direction of the follower movement. The direction of inertia force during the acceleration is opposite to the follower motion, and during the deceleration it is in the same direction. During the accelerating part of the same period, a difference between the inertia and spring forces is applied to the follower in the same or opposite direction to it, depending on the magnitude of the forces. If the inertia force is greater than the spring force, the direction of the resulting force would be the same as the follower's, and jump would occur, which is most undesirable; but when the spring force is greater than the inertia force, the direction becomes opposite to the follower movement, preventing it from jumping. This is the reason why the spring force should be designed to be greater than the inertia force during the rise period.

On the other hand, the direction of the resulting force during the accelerating part of the return period is opposite to that during

the decelerating part of the rise period, due to the change of the follower motion. In other words, if the inertia force is greater than the spring force, the direction of the resulting force becomes opposite to the follower movement, causing it to jump. If, however, the inertia force is smaller than the spring force, the resulting force is in the same direction as the follower motion, forcing the follower to contact with the cam. During the decelerating part of the return period, the combined force of the inertia and spring forces is applied to the follower. This is similar to the rise period, but because this force is in the same direction as the follower movement, the impact or contact force/stress is less significant than in the rise period.

Having realized the general governing principles of cam-follower behavior, one must also be aware of the fact that a jump occurs more easily during the return period than in the rise period (Fig. VI.28). Both periods are subjected to an equal exciting force (the difference of the inertia and spring forces), but for a jump to occur in the rise period the follower must push up the spring further due to the advancing cam, whereas in the return period the follower may simply stay still, since the cam itself falls off from the follower. Extra force is needed to push the spring up, thus a jump in the rise period is less likely than in the return period; and although jump can occur during the rise period, its duration will be much shorter than during the return period (Fig. VI.29). Consequently, this indicates that the spring force should be calculated for the return period rather than for the rise period.

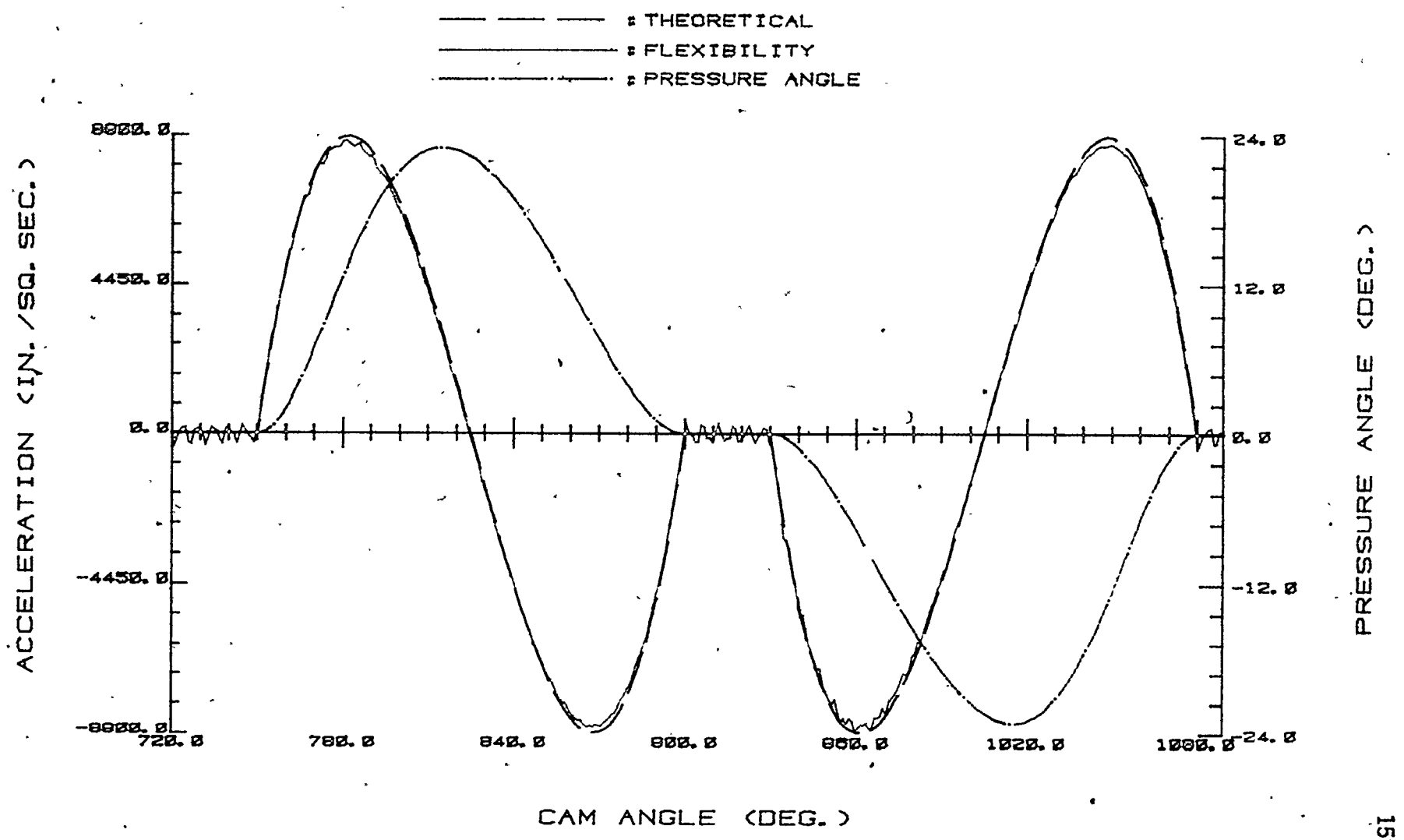

Fig. VI.28. Asymmetricity between Rise & Return Periods on 3-4-5 Polynomial Motion Program
(Spring Stiffness = 60 lb/in)

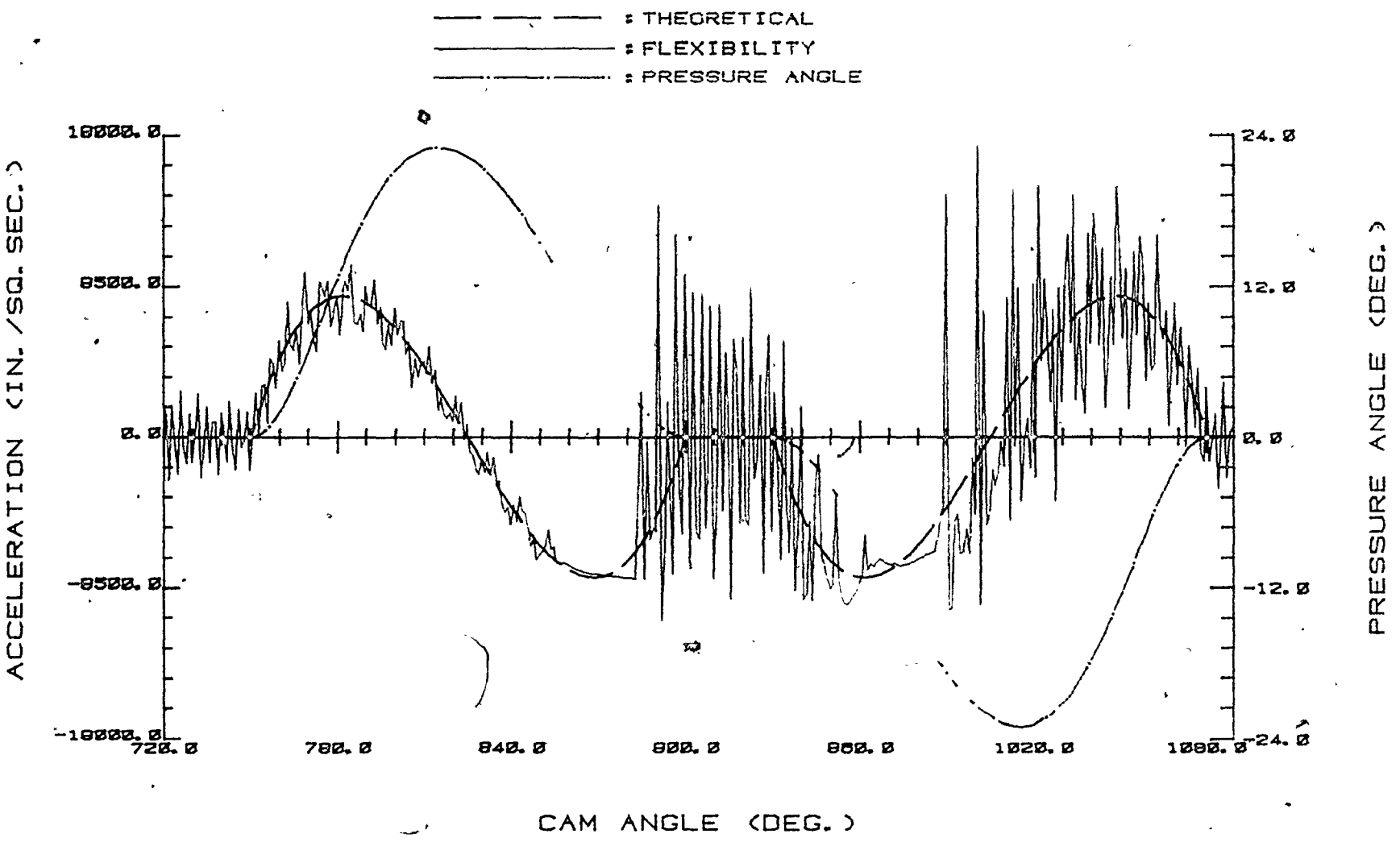

Fig. VI.29. Asymmetricity between Rise & Return Periods on 3-4-5 Polynomial Motion Program
(Spring Stiffness = 50 lb/in)

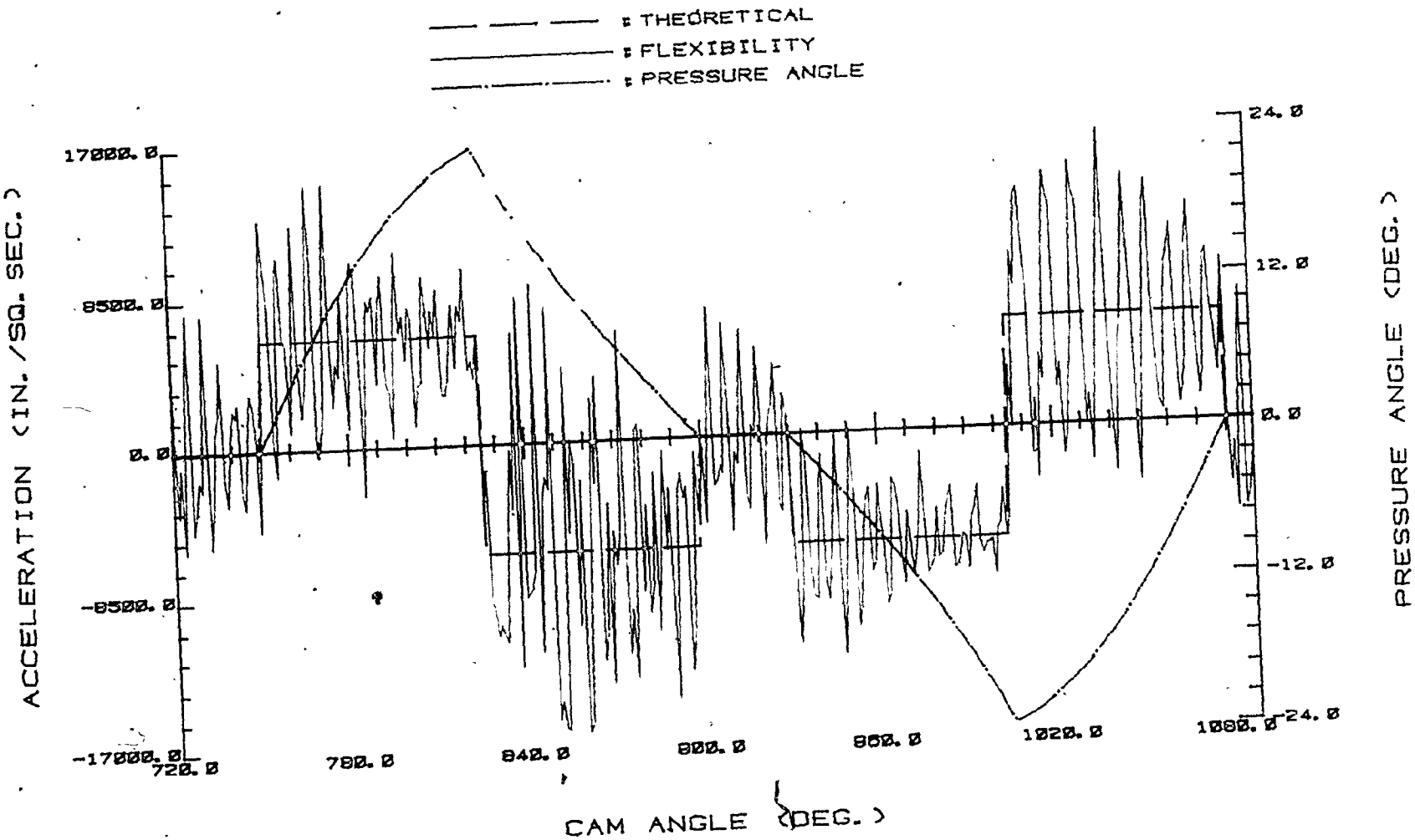

Fig. VI.30. Asymmetricity between Rise & Return Periods on Parabolic Motion Program
(Spring Stiffness = 80 lb/in)

Fig. VI.27(c) shows the theoretical acceleration curve for parabolic motion, with the directional relation of the exciting forces and the follower motion. As seen in the figure, the parabolic program has an abrupt and large initial deceleration (twice the peak acceler ation) in the middle of both rise and return periods. Due to this sudden initial deceleration, the parabolic and cubic 1 programs, which have a similar but larger abrupt initial acceleration in the middle of both periods (refer to Table VI.9), are exceptions to the analysis in the previous paragraph. In other words, these two programs produce a jump more easily during the rise period than during the return period (Fig. VI.28), because during the rise period the inertia force induced from the initial large deceleration is applied to the follower, as it moves up, in the same direction. Thus, the inertia force separates the follower from the cam by pushing it away from the cam whereas during the return period the inertia force, having the same magnitude as in the rise period, is applied to the falling follower, forcing it to contact with the cam. From this phenomenon, the asymmetry between the rise and return periods can also be observed. To suppress jumping, it is obvious from Figs. VI.27(c) and 30 that the spring force should be calculated from the rise period by using twice the peak deceleration for parabolic or cubic 1 motion.

The above analysis of the asymmetry between the rise and return periods was carried out based on the theoretical cam. For the actual cam, the asymmetry between the two periods becomes more serious because the effects of tolerance, added to the system flexibility, cause a

greater deviation in the performance between the rise and return periods.

As a result of the asymmetry between the rise and return periods, the following effects are noted:

1. A jump, the most undesirable factor in system performance, is most likely to occur at the decelerating part of the rise period and at the accelerating part of the return period.
2. Except for the parabolic and cubic 1 programs, a jump is more likely to occur during the return period than in the rise period.
3. The spring force should be calculated from the return period acceleration for all motion programs except the parabolic and cubic 1. To avoid a jump during the return period as far as possible when two different programs are to be used, the program having a higher peak acceleration or deceleration should be used for the rise period.

VI.4.3. Effects of Changes in System Dynamics

Based on the reference design described in Section VI.1, the effects of changes in the dynamics of the cam-follower system on its performance are investigated by decreasing or increasing one of the dynamic characteristics from 10 % to 30 %, while keeping the remainder the same as in the reference design. In Tables VI.11-12, the effects on the performance of a theoretical and an actual cam are presented numerically by the root mean square (RMS) of the derivation from theoretical values during a full revolution (D-R-D-R) for the time responses, and the average (AVG) for the inertial responses.

In Figs. VI.31-35, the effects are graphically presented for easy visualization and are analysed in detail below :

A. Effect of Changes in Inertia

Displacement - No significant influence, but an increase of inertia gradually worsens the time response for a theoretical cam, and rapidly worsens it for an actual cam, due to the waviness arising from machining tolerances.

Velocity - Slight influence; an increase in inertia improves this time response.

Deceleration - Significant influence; appreciable change in inertia leads to rapid worsening of this time response.

Table VI.11 Effects of Changes (± 10 %) in Dynamic Characteristics on Time & Inertial Responses

		System as Designed	Mass (Inertia)		Damping		Stiffness	
			10 % decrease	10 % increase	10 % decrease	10 % increase	10 % decrease	10 % increase
Displacement RMS (x 10^{-3})	T	0.79047	0.77966	0.80321	0.79221	0.78862	0.86828	0.72708
	A	1.47070	1.53736	1.75568	1.68347	1.55837	1.66322	1.54085
Velocity RMS (x 10^{0})	T	1.38409	1.50124	1.28881	0.64995	2.13475	1.37396	1.3870
	A	1.84587	1.96158	1.75772	1.24410	2.55839	1.85479	1.83869
Acceleration RMS (x 10^{3})	T	0.29295	0.23662	0.33878	0.29100	0.29470	0.27910	0.31675
	A	0.66738	0.48636	0.64185	0.61835	0.56013	0.66603	0.50340
Angular Velocity RMS (x 10^{0})	T	0.22968	0.20285	0.27165	0.25319	0.21346	0.23896	0.19537
	A	0.57489	0.40675	0.72238	0.64006	0.54333	0.66255	0.42119
Contact Stress AVG (x 10^{5})	T	2.53833	2.54150	2.53577	2.53581	2.53995	2.53929	2.53530
	A	2.53630	2.54365	2.53314	2.53904	2.53710	2.53877	2.54020

RMS & AVG calculated over a whole cam revolution including D-R-D-R

T : theoretical cam, A : actual cam

Table VI.12 Effects of Changes (± 30 %) in Dynamic Characteristics on Time & Inertial Responses

		System as Designed	Mass (Inertia)		Damping		Stiffness	
			30 % decrease	30 % increase	30 % decrease	30 % increase	30 % decrease	30 % increase
Displacement RMS (x 10^{-3})	T	0.79047	0.76310	0.83019	0.79608	0.78527	1.08952	0.63061
	A	1.47070	1.50732	1.72748	1.75955	1.66487	1.85336	1.59207
Velocity RMS (x 10^{0})	T	1.38409	1.85436	1.09657	1.03276	3.63438	1.36214	1.39062
	A	1.84587	2.29802	1.63784	1.5484	4.02033	1.84265	1.82660
Acceleration RMS (x 10^{3})	T	0.29295	0.65376	0.66042	0.63046	1.05501	0.30367	0.27601
	A	0.66738	1.46756	2.16292	2.06739	1.75176	0.49692	0.43443
Angular Velocity RMS (x 10^{0})	T	0.22918	0.14550	0.42199	0.21657	0.19376	0.28018	0.20199
	A	0.57489	0.23461	1.06444	1.06525	0.49969	0.83750	0.27922
Contact Stress AVG (x 10^{5})	T	2.53833	2.55226	2.52502	2.53720	2.54498	2.53856	2.54270
	A	2.53630	2.54435	2.52217	2.53738	2.54026	2.53568	2.53605

RMS & AVG calculated over a whole cam revolution including D-R-D-R

T : theoretical cam, A : actual cam

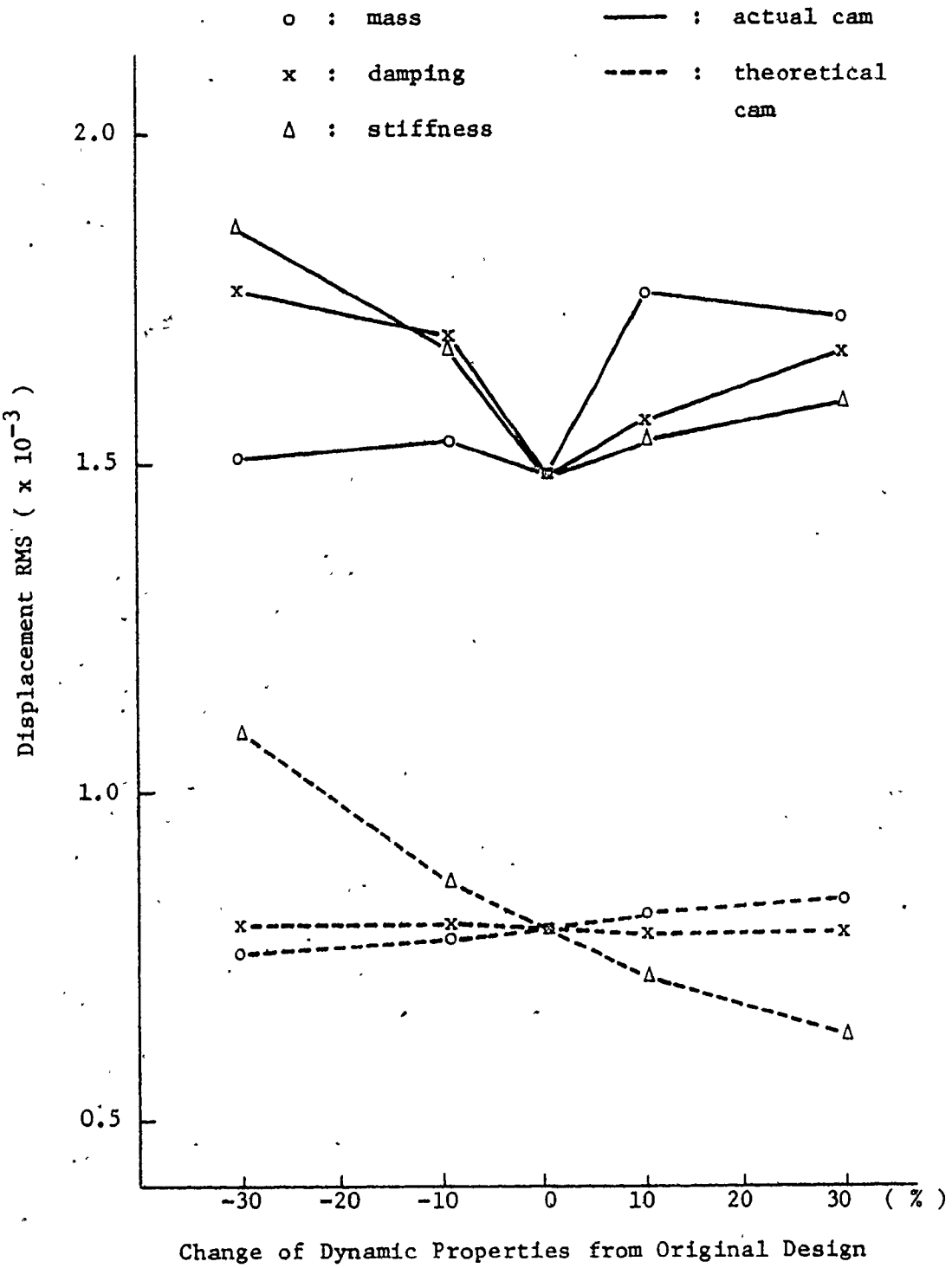

Fig. VI.31. Effect of Changes in Dynamic Characteristics on Displacement

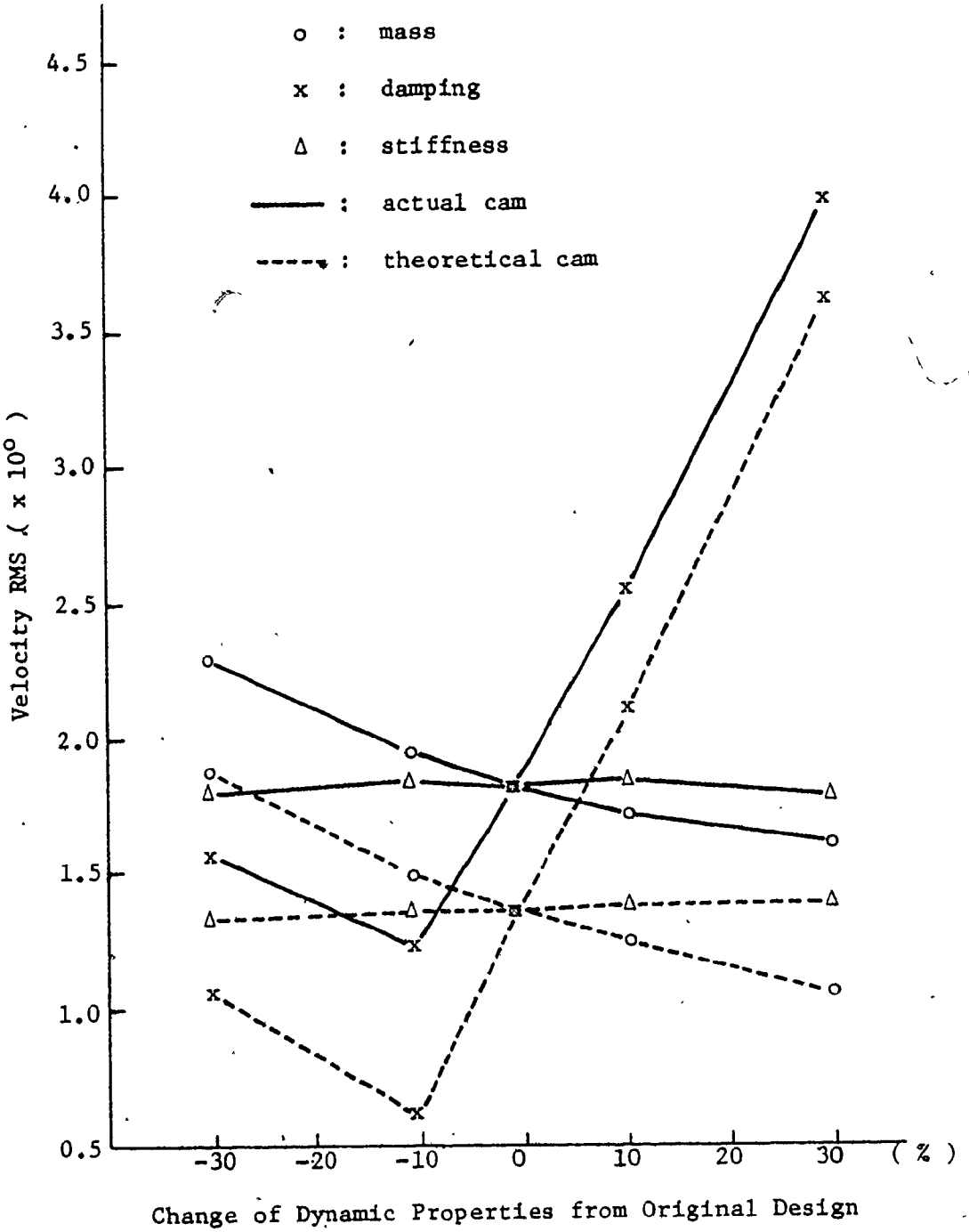

Fig. VI.32. Effect of Changes in Dynamic Characteristics on Velocity

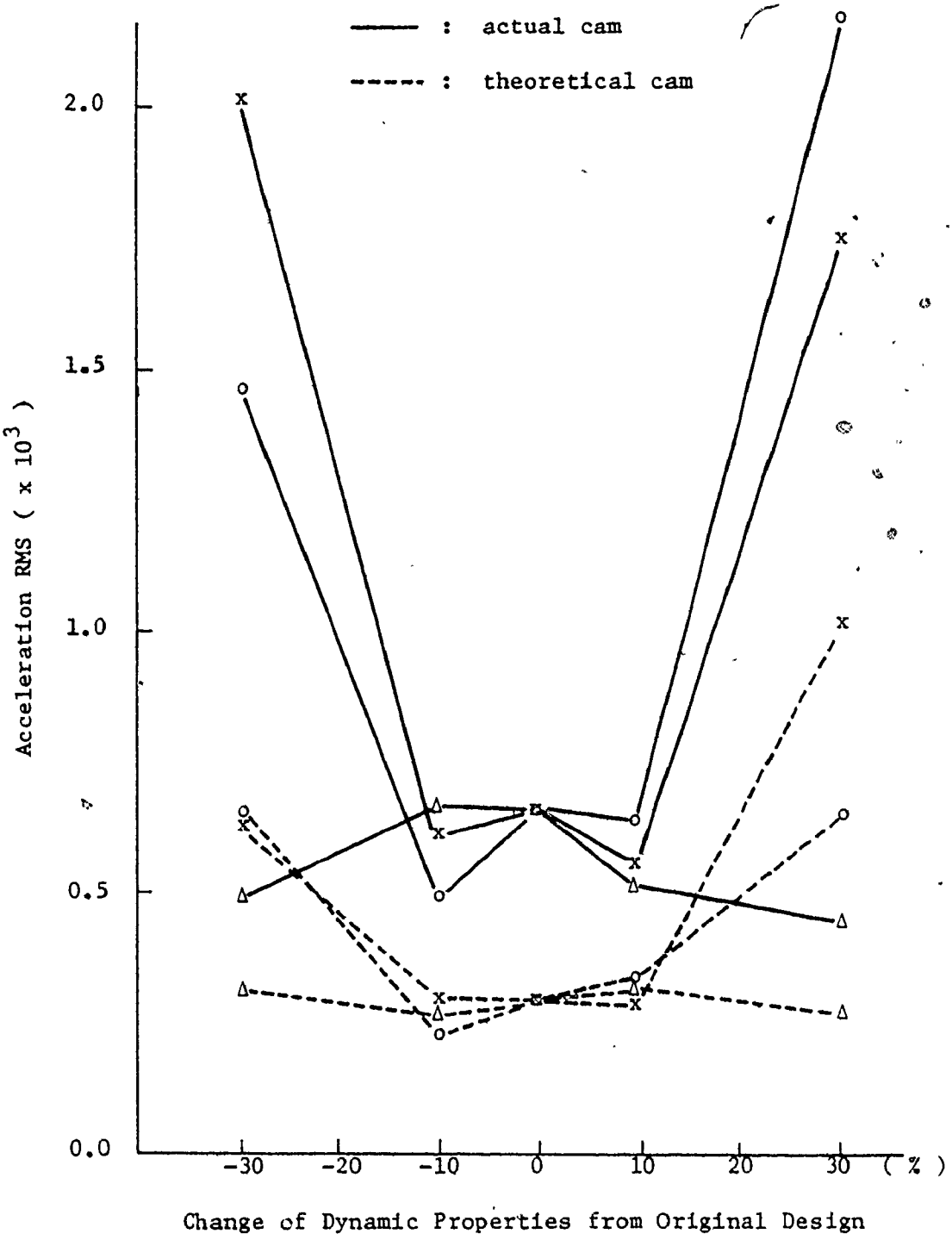

Fig. VI.33. Effect of Changes in Dynamic Characteristics on Acceleration

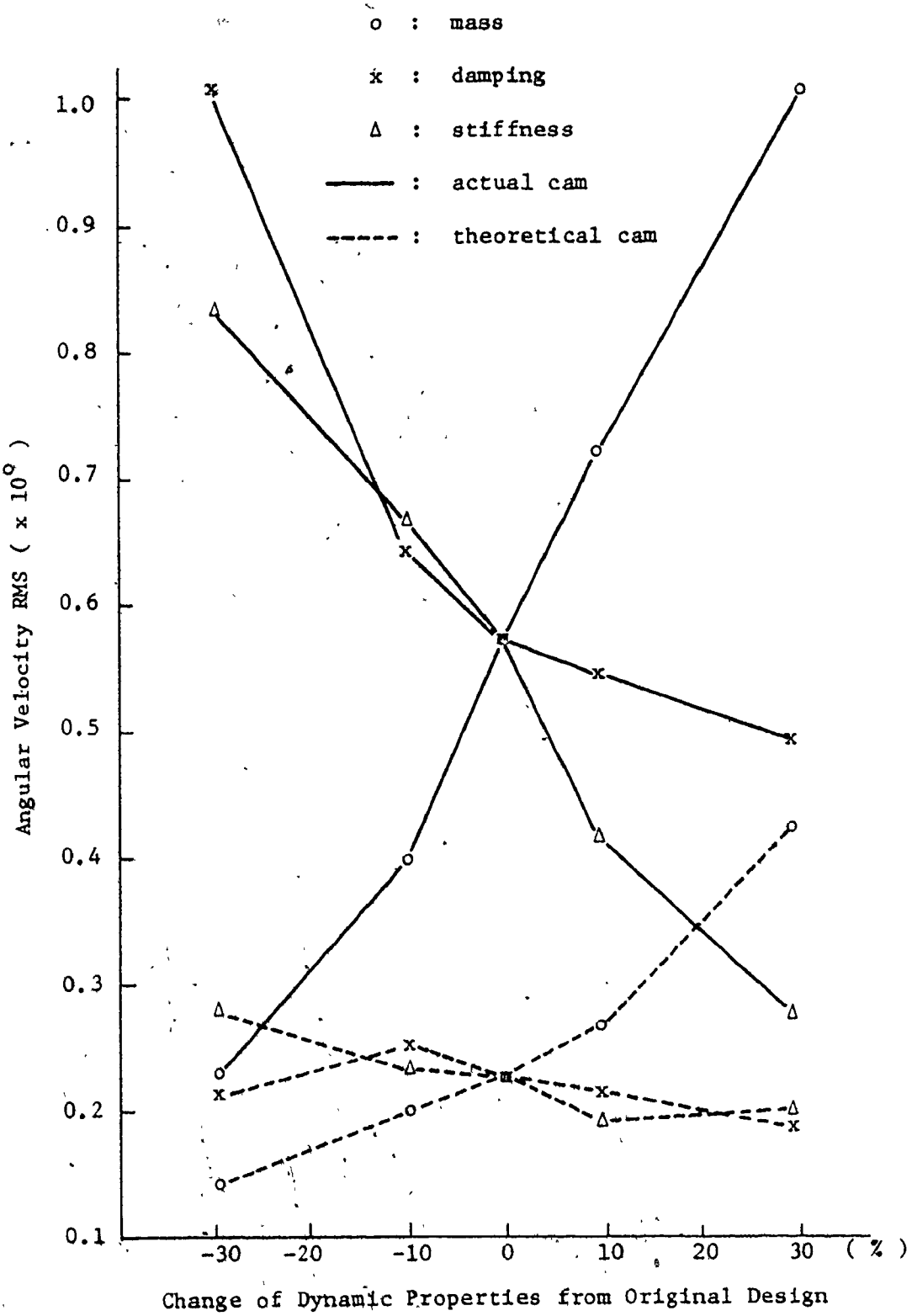

Fig. VI.34. Effect of Changes in Dynamic Characteristic on Angular Velocity

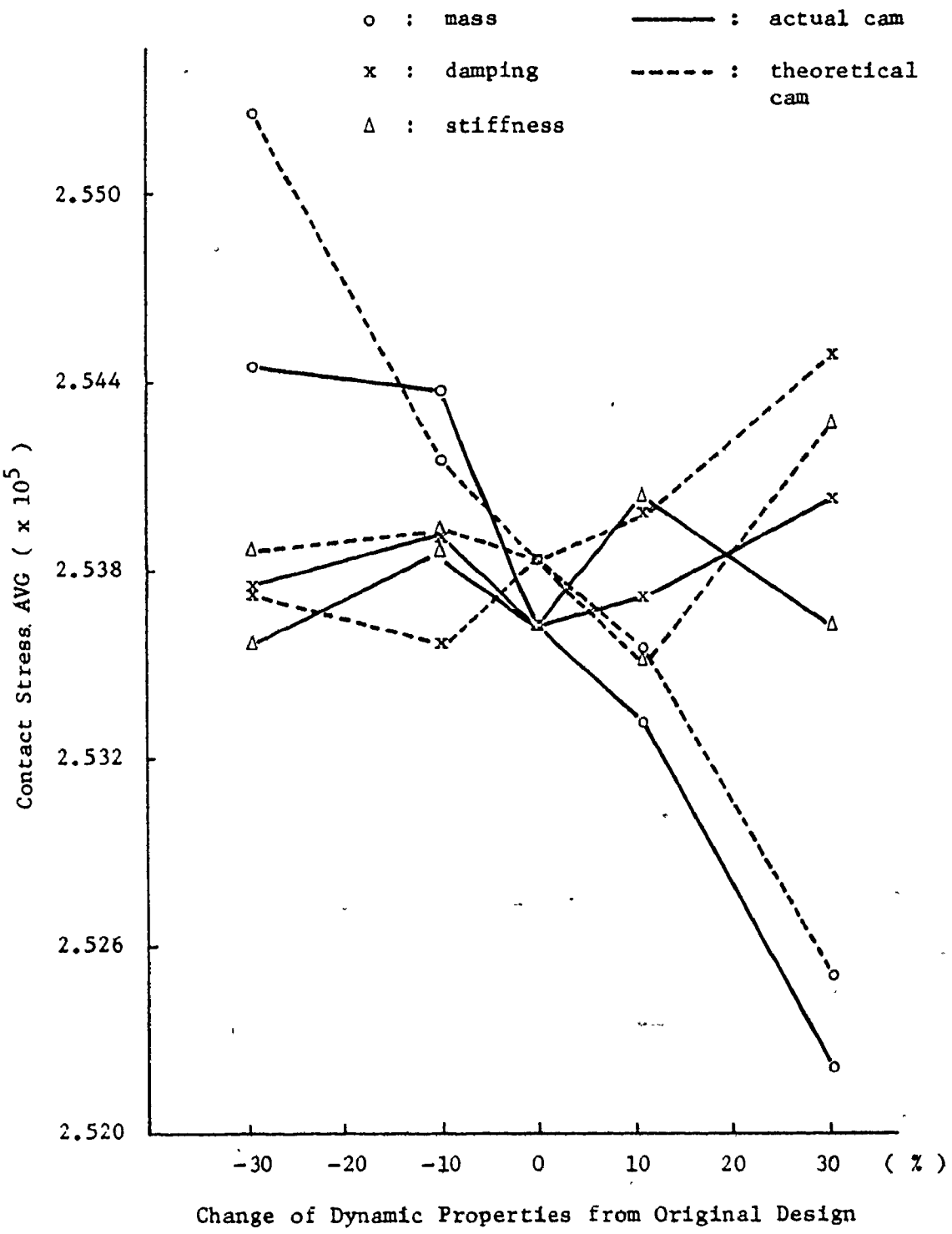

Fig. VI.35. Effect of Changes in Dynamic Characteristics on Contact Stress

Angular velocity - An increase markedly worsens this time response.

Contact Stress - An increase of inertia improves this inertial response by reducing it rapidly.

From this analysis, it is noted that an increase of inertia is generally undesirable for the time responses, but it favourably affects the inertial responses. Therefore, this factor needs to be optimized, and this need becomes obvious from its effect on acceleration.

B. Effect of Changes in System Stiffness

Displacement - For a theoretical cam the response apparently improves as stiffness is increased, but for an actual cam no improvement is observed due to the waviness arising from machining tolerances.

Velocity - No influence.

Acceleration - No significant influence, but an increase in stiffness improves this time response.

Angular velocity - An increase of system stiffness significantly stabilizes the angualr velocity of the actual cam, but has little effect on the theoretical cam.

Contact Stress - Small fluctuations only.

From these results, it is obvious that the more rigid a system is, the more its performance is improved.

C. Effect of Changes in Damping

Displacement - No influence observed for the theoretical cam, but an increase in damping worsens this response on an actual cam due to the waviness arising from machining tolerances.

Velocity - Significant influence when damping is increased.

Acceleration - This response rapidly worsens on increase of damping (The influence of damping on this response is similar to that of inertia).

Angular velocity - An increase in damping improves this response for the actual cam, but for the theoretical cam the effects are not significant.

Contact Stress - On increase of damping, this inertial response also increases, deteriorating the performance.

From this analysis, it is found that changes in damping for a theoretical cam have little influence on the system performance, except for the velocity of the follower and the contact stress, which are considerably worsened by an increase of damping. On the other hand, the angular velocity of the cam is rapidly stabilized as the damping increases.

From the above three investigations of the effects of changes

in dynamic characteristics, the following general conclusions can be drawn.

1. An incorrect choice or miscalculation of one dynamic property by as much as 30 % does not cause an appreciable deviation in any of the simulated outputs. Note the relatively small changes in RMS values for each response.
2. The effect of a change in any dynamic property is very small in comparison to the effects of the machining tolerances on the displacement.
3. Acceleration is the most sensitive of the time responses to any disturbance in the system. Variations in inertia and damping cause a rapidly worsening response, whereas an increase in system stiffness reduces fluctuations in the acceleration.

VI.5. Analysis of Errors in Simulation Results

The four main sources of errors in this simulation process are as follows :

1. Error in calculation of dynamic properties from the model
2. Error in representation of cam profile and actual roller displacement by stochastic simulation
3. Errors caused by the numerical methods used for the solution of differential equations
4. Computer round-off error

All dynamic properties were calculated from well known and proven theories or formulas as seen in Chapter V. In the previous section a sensitivity analysis was carried out, and it was discovered that a deviation of as large as 30 % did not appreciably affect the results. This is a large error, but it is one that has been accepted in engineering practice for the calculation of the safety factor. It is used here as an error bound, and deviations are not likely to occur outside this, as shown in Section VI.2.

To obtain some appreciation of the error that might arise in simulating the cam profile, two real cams were designed according to the specification given in Section VI.1 and manufactured by Cam Commercial Co. in Chicago. These were precisely measured by a quality control technician of Eonic Cam Design and Manufacturing Co. in Detroit, using

their computerized measuring machine. The results of this measurement are presented in Fig. VI.36 by plotting the deviations of the real cam from the theoretical cam with respect to cam angle. Although the initially ordered tolerance (±0.001 inch) was not satisfied at all (this fact indicates the extreme difficulty of precision cam profile cutting), the measured data graphically illustrate the general nature of errors that can arise in cutting a cam profile. Note from Fig. VI.36 that as the pressure angle increases the deviation of the actual cam from the theoretical one becomes negative, due to the corresponding pressure increment between the cam surface and its cutter, which forces the cutter to overcut.

To compare the analytically predicted deviation in the stochastic simulation with the actual deviation, the absolute values of the deviation measured from the real cam were multiplied by a certain weight in order to compensate for the gap between the two different tolerances, and plotted in non-dimensional units together with the predicted deviation as shown in Fig. VI.37. From Fig. VI.37, the two deviation curves are found to be nearly identical to each other, indicating that no significant error was involved in the actual roller displacement simulation. The maximum error between the two deviations was found to be as small as 5%.

The error from the third source is caused by the numerical algorithm used to solve the differential equations. With this in mind, the modified Runge-Kutta algorithm (Appendix D) was chosen because it maintains the accuracy of the calculation within a previously given error bound. All calculations done to solve the simultaneous nonlinear

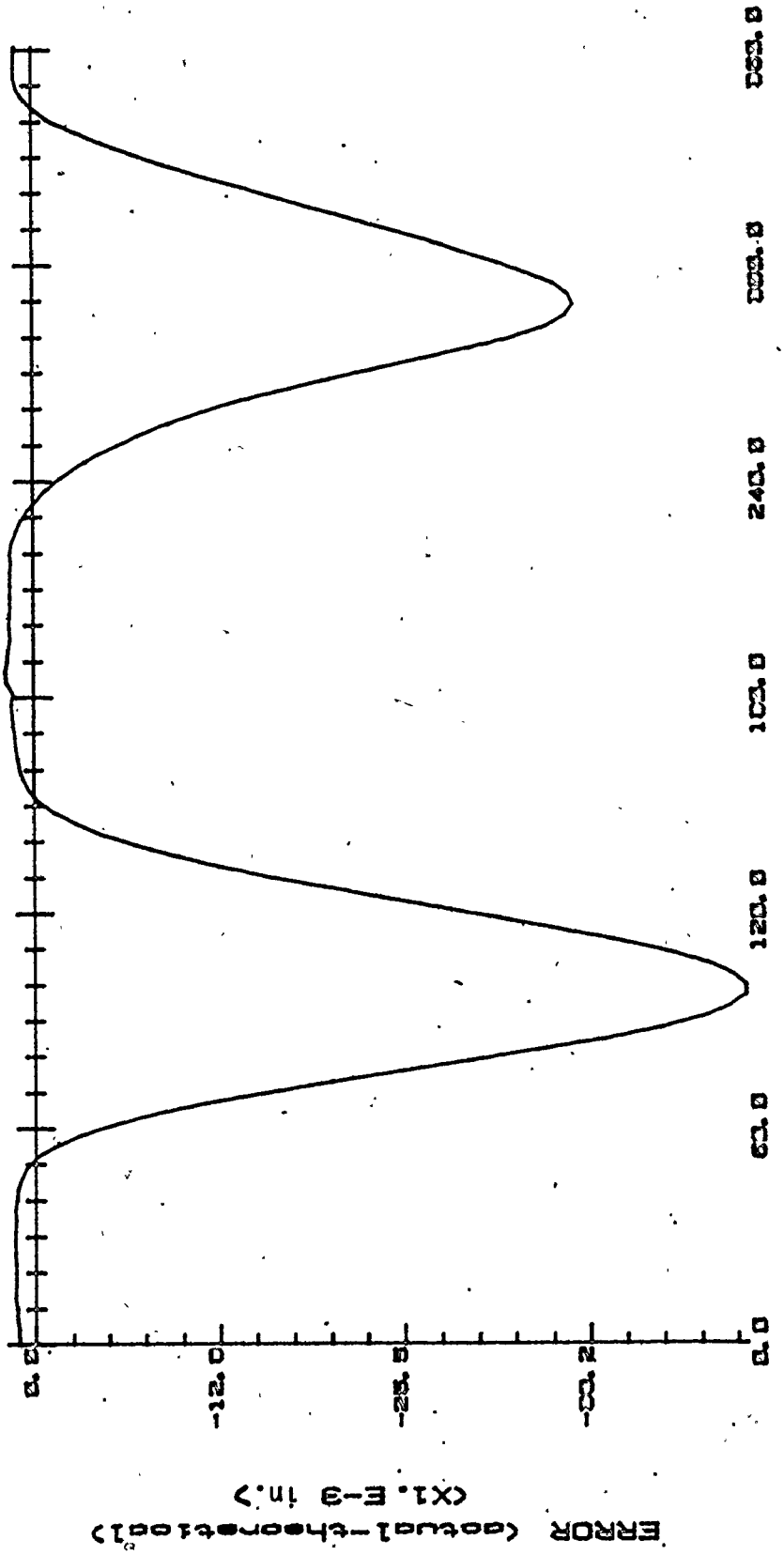

Fig. VI.36. Deviation between Real and Theoretical Roller Displacement.

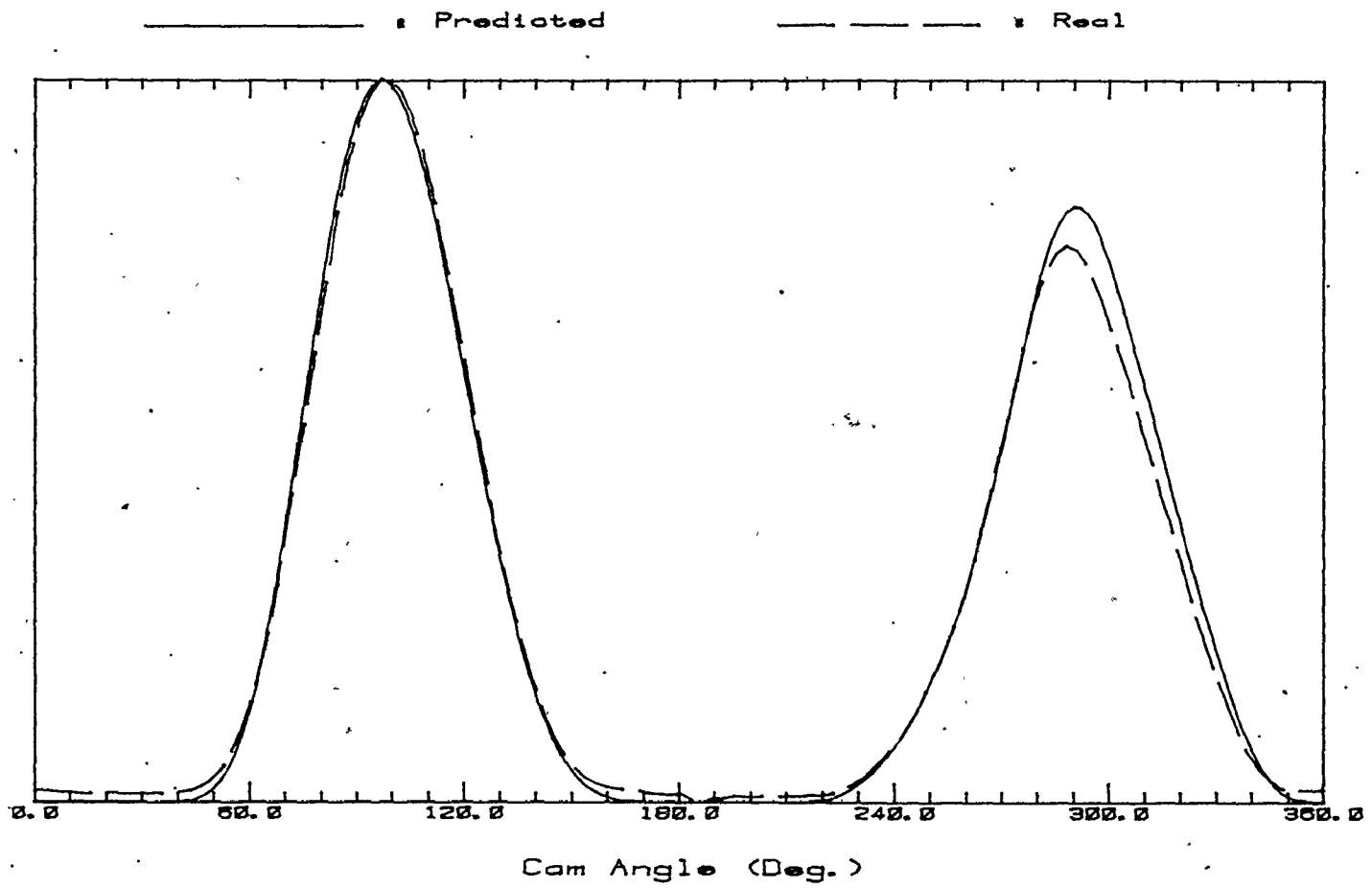

Fig. VI.37. Comparison of the Predicted Deviation used for the Simulation of Actual Roller Displacement to the Real Deviation of Real Roller Displacement.

differential equations were executed by setting the maximum relative error to 2% (Section VI.1). This is an optimum error bound, since a smaller bound noticeably increases the computing time, whereas a larger one yields unreliable results. It is also to be noted that the smaller error bound requires more iterations, thus increasing the computing error by accumulation.

The fourth source of error arises from the computer itself, specifically by the limited number of "bytes" (group of adjacent binary digits operated on as a unit by the computer) used for computation. This is the error due to the hardware system, whereas the error in the third source is due to the software system. Depending on the computer employed, the precision of a computation varies according to the byte number used for the computation, especially when a large number of iterations are required. The final results will carry an accumulated error due to truncation and round-off errors. Because this simulation requires a large number of iterations, the double precision feature was employed wherever a particularly large number of iterations was required. However, the double precision feature has the drawback of doubling the computing time. This was overcome by installing a floating point hardware system which will be described in next chapter. The number of iterations taken during simulation is difficult to determine, and the direct calculation of the magnitude of this error is extremely difficult. As an indirect way of assessing this error, the steady state acceleration responses of the 4th, 5th and 6th cycles, which should be identical, were obtained by running the computer continuously. This is shown in Figs. VI.38,

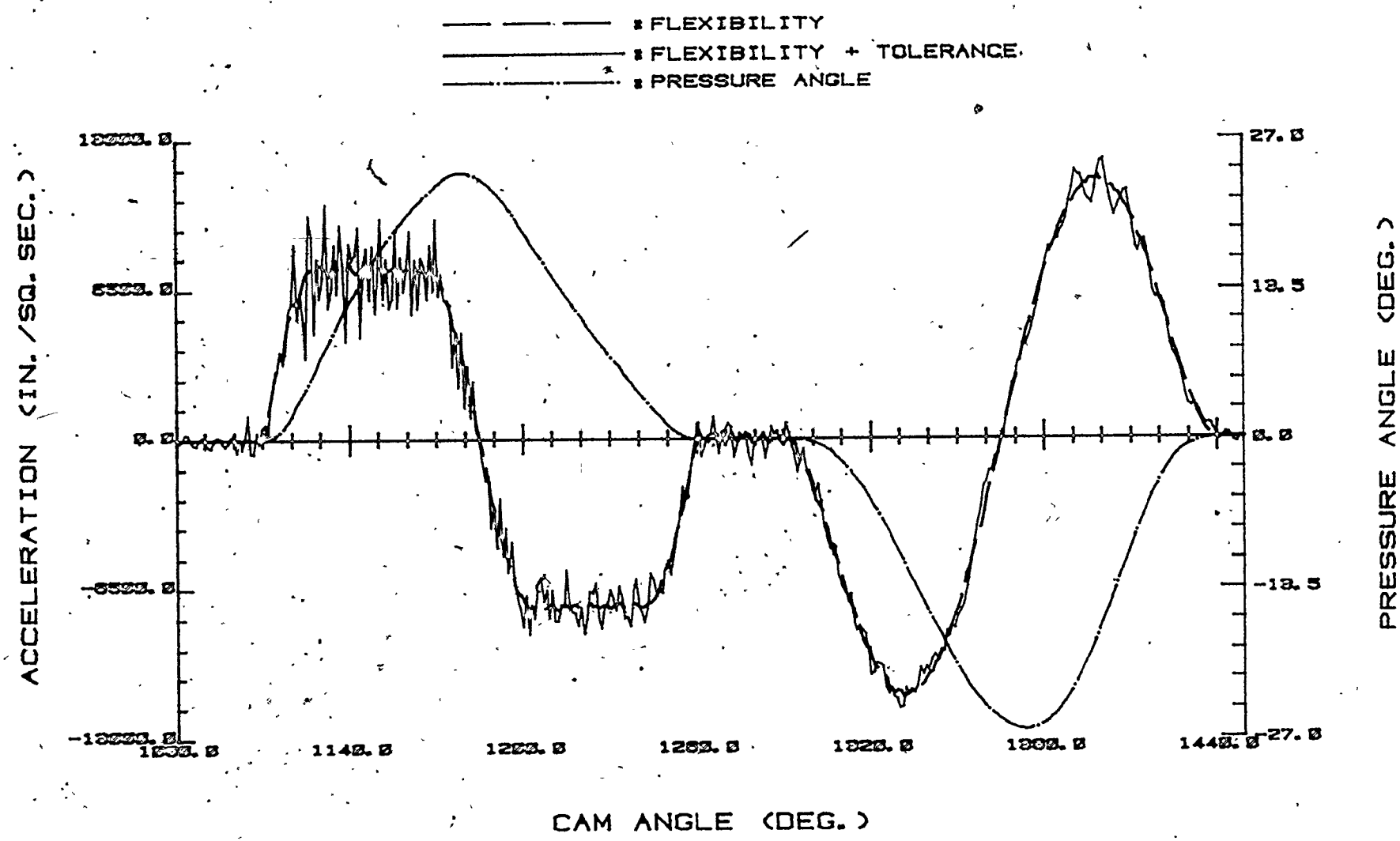

Fig. VI.38. Steady State Acceleration Response and Pressure Angle of 4th Cycle.

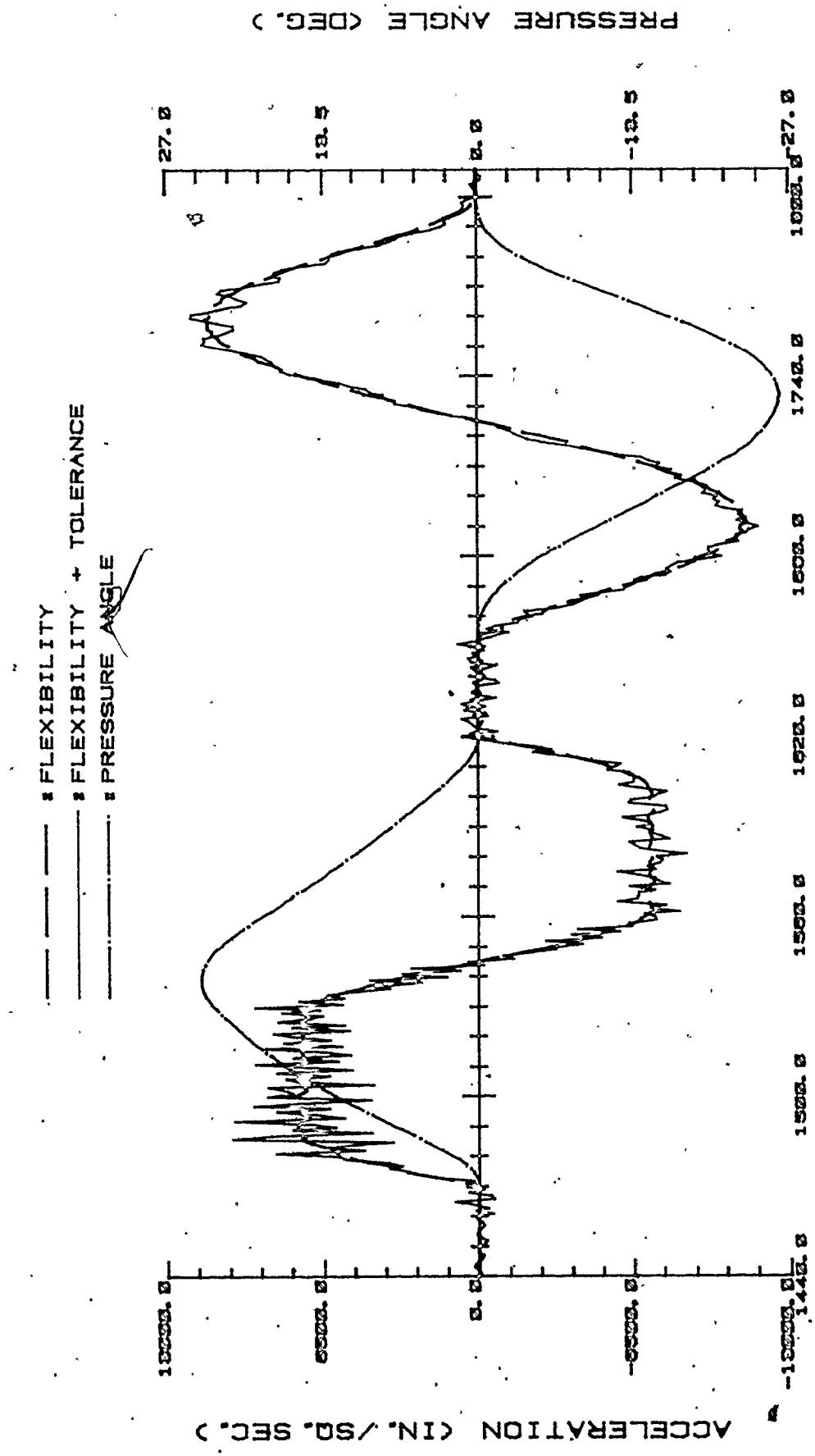

Fig. VI.39, Steady State Acceleration Response and Pressure Angle of 5th Cycle.

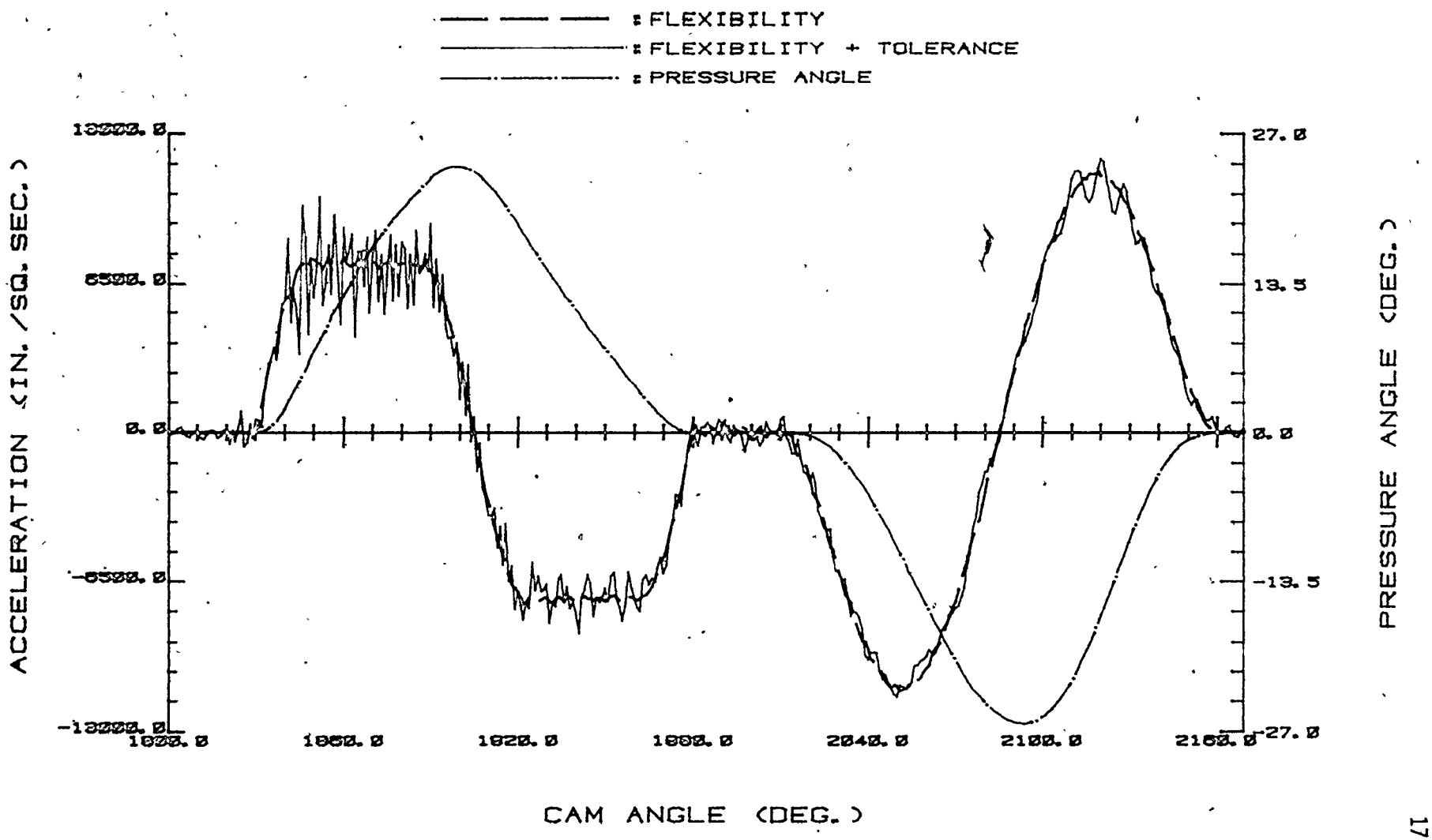

Fig. VI.40. Steady State Acceleration Response and Pressure Angle of 6th Cycle.

39, and 40 respectively. From the figures, it is recognized that the three acceleration curves are almost identical. By comparing the acceleration of the 3rd cycle with that produced in the 6th it was determined that the maximum error between the two curves is about 1%.

The estimated maximum error from each error source is summarized in Table VI.13, and the combined total error is calculated by a statistical method as follows :

Table VI.13 Maximum Error of Error Source in Simulation

	1	2	3	4
Error Source	Dynamic Properties	Roller Displacement	Numerical Algorithm	Computation by Computer
Maximum Error	30 %	5 %	2 %	1 %

Assuming a normal distribution for each error and a linear relation between each error source, then

$$y = a x_1 + b x_2 + c x_3 + d x_4 \qquad (VI.8)$$

where y = combined error source

x_i = error source of i th

a, b, c, and d = weighting coefficients,

The resultant error in the simulation can statistically be assessed by a maximum likelihood method as

$$\mu_y = a\,\mu_{x_1} + b\,\mu_{x_2} + c\,\mu_{x_3} + d\,\mu_{x_4}$$

$$\sigma_y = \sqrt{a^2\,\sigma^2_{x_1} + b^2\,\sigma^2_{x_2} + c^2\,\sigma^2_{x_3} + d^2\,\sigma^2_{x_4}} \qquad (VI.9)$$

in which

μ = mean or nominal value

σ = standard deviation.

Since

$$a = b = c = 1,$$

$$\mu_{x_1} = \mu_{x_2} = \mu_{x_3} = \mu_{x_4} = 0,$$

and

$$\sigma_{x_i} = \frac{(\text{Maximum Error})_{x_i}}{3},$$

from Eq. (VI.9)

$$\mu_y = 0$$

$$\sigma_y = \sqrt{\left(\frac{0.3}{3}\right)^2 + \left(\frac{0.05}{3}\right)^2 + \left(\frac{0.02}{3}\right)^2 + \left(\frac{0.01}{3}\right)^2}$$

$$= 0.102$$

Hence, the best possible value of error in the simulation results (E_{sr}) is estimated by

$$E_{sr} = \mu_y \pm \frac{0.6745\ \sigma_y}{\sqrt{n}} \quad : \quad n = \text{sample size} = 4$$

$$= \pm\ 0.0342 = \pm\ 3.4\ \%$$

Thus it is concluded that, since the maximum error bound is likely to be 6.8%, the computer simulation results are reliable and valid.

VI.6. Comparison with the Results of Previous Work

VI.6.1 The Effect of Cam Profile Manufacturing Errors

As far as could be determined from the literature survey included in Chapter I, very little work has been done on the effect of cam profile manufacturing errors on the follower output. The most closely related work was done by Kim and Newcombe [38], who developed a computer simulation technique to examine the results of the tolerance in manufacturing the cam profile on the follower displacement, velocity and acceleration. Their results generally agree with those obtained here, but their work was based on an idealized, perfectly rigid system, and the effect of system flexibility was neglected. However, the system examined here was stiff, and the effects of the manufacturing errors dominated the combined effects of manufacturing errors and flexibility.

Nourse [60] discusses advances made in cam profile measurement and evaluation particularly in respect to the automotive industry, and the use of computers in aiding the measurement task. He describes the practice of specifying cam profile tolerances as follows :

> The tolerance consists of two kinds of statements : first, there is a maximum allowable deviation (or bandwidth) from which the profile 'as made' can be permitted to depart from the design profile. Normally, this bandwidth changes with the location along the profile. The second kind of statement is a profile waviness specification. The intent of this tolerance is to limit the rate at which the profile 'as made' can be permitted to deviate from the design values.

Typical tolerances might be as follows :

Bandwidth specification = ± 0.0010 inch

Waviness specification = 0.0001 in./deg.

The information on profile waviness is particularly related to this work.

Tesar and Mattew [54] include in their text an appendix, "Cam Manufacture", in which profile errors and their effects, are discussed in a general way. They state that it is the waviness that causes acceleration errors, and that the waviness error is very unpredictable since it depends on so many factors in the manufacturing. This helps to substantiate the use of the stochastic technique employed here.

VI.6.2 Work on Non-Constant Angular Velocity of Cam

Some extensive work was carried out by Sarring [17], Johnson[18], Fawcett and Fawcett [28] and Koster [44] on the effect of variations in cam angular velocity. A source of angular velocity variation is instantaneous torque change or galloping. This was well elaborated by Sarring [17]. The variation of angular velocity (Fig. I.8) plotted by Johnson [18] is quite large, but its general behavior is in accord with the results of this work. The harmonic analysis done by Fawcett and Fawcett [28] showed the vibrational effect of a flexible cam shaft. A highly idealized approach was used, but the resulting principal effects were in close approximation to the results obtained here. Koster [44] did not draw

conclusive results on the effect of this imperfection, but he showed the possibility of a dynamic simulation of a cam-follower system on a digital computer employing a dynamic model (Fig. I.19) which is basically similar to the model used in this work.

VI.6.3 Work on the Asymmetry of Rise and Return Periods

Bagci [29] investigated the effect of this imperfection and prescribed the use of a full cycle of the cam-follower motion program. His results obtained on the basis of a full cycle of cam motion agree well with the results obtained by simulation in this work. The evidence for the necessity of investigating a full cycle has been discussed and illustrated at length numerically as well as graphically in this work.

VI.6.4 Work on Comparison of Standard Motion Programs

As mentioned early in Chapter I, Gagne [2] and Mitchell [3] performed an entirely experimental analysis on the performance of several motion programs. The overall shape of the time responses obtained from their experiments matches well with the simulated responses here, even though there are slight dissimilarities between the responses due to the differences in dimensions and dynamic properties of the two systems. The suggestions given by Gagne [2] and the

results obtained by Mitchell [3] generally agree with the deductions of this work.

VI.6.5 Investigation of Changes in System Dynamics

It was found from the literature survey in Chapter I that a lot of work has been done on the dynamics of cam-follower systems. However, these investigations were consistently aimed at system vibration, in attempting to minimize the vibration or avoid the zone of resonant vibration. Practically no work has been done on the effect of changes in cam-follower system dynamics as investigated here. In fact, previous work usually employed a conventional harmonic analysis method, and thus investigations into the effect of changes in cam-follower system dynamics could not be taken into account. The simulation technique used here, taken as a systems approach, has enabled the investigation of the effect of changes in the dynamics of the cam-follower system on its performance. This is a new contribution and thus no comparison with previous work can be made.

CHAPTER VII

DISCUSSION AND CONCLUSION

VII.1 Discussion

The digital minicomputer (PDP 11/34), the major tool used to solve the simulation problem, has limitations because of its small main memory and its relatively slow computing speed. In this work, the drawback of the small memory was overcome by 1) utilizing an overlay technique, in which the parts of a computer program share the available memory in such a way that when one part is complete it is overlaid (and therefore erased) by the other, 2) separating the lengthy plotting program from the main program, and 3) transferring a large amount of data generated during intermediate computing steps to magnetic disk storage. The problem of slow computing speed was solved by installing a floating point hardware system that enables the CPU (central processing unit) of the computer to speed up the computation of multiplication and division which takes most of the computing time. In this particular simulation, the installation of the hardware system increased the computation speed by 2.5 times the original speed ; a average of 10 hours taken to simulate two revolutions of a cam was reduced to about 4 hours.

In the simulation, the surging effects of the return spring were neglected, on the assumption that :

1. A spring having high natural frequency is used
2. The Fourier harmonics of the cam contour are relatively small

These two assumptions are easily achievable in practice, and there will be no noticeable error caused by spring resonant vibration or surging. If spring surging is known to be a significant problem, the governing equations presented in Appendix F should be introduced in the mathematical model, since they take the dimensions and material properties of the spring into consideration. However, the introduction of these equations into the simulation will significantly increase the computing time, especially the time needed to reach a steady state condition.

In the calculation of the stiffness, K_h, due to Hertzian deflection using Eqs. (V.9-10), the contact force, F, was assumed to be unity because it is difficult to express this in explicit nonlinear form. Thus, at any contact point equivalent linear springs were assumed. To support this assumption, some calculations were made on an example comparing the contact forces obtained based on linear springs with those obtained when nonlinear springs were used. The results are shown in Table VII.1(a), and it can be seen that the differences are sufficiently small so as not to affect the overall results.

Because the radii of curvature of the cam and follower surfaces vary the stiffness at various points of contact will vary and this is treated as a nonlinearity in this work. This nonlinearity is much more pronounced than that due to Hertzian deflection at any point as shown in Table VII.1(b).

Table VII.1(a). Calculations of Contact Forces, Total Deflections and Stiffnesses

Data used : Poisson's ratio of materials (ν_1, ν_2) = both 0.295
Young's modulus of materials (E_1, E_2) = both 30×10^6 psi
Diameter of roller (d_1) = 0.75"
Diameter of cam curvature (d_2) = 3.0"
Thickness of cam (t) = 0.25"
Range of contact Force (F) = 1 - 350 lbs.

Actual Contact Force (F, lbs.) based on Nonlinear Springs	1	50	100	150	200	250	300
Total Deflection ($h_1 + h_2$) ($\times 10^{-5}$ inches)	0.01550002	0.00775005	1.5500208	2.3250469	3.1000833	3.8751301	4.6501874
Stiffness (K_h) ($\times 10^6$ psi)	6.451612	6.4515696	6.4515262	6.4514829	6.4514396	6.4513962	6.4513095
Contact Force (F, lbs.) based on Linear Springs	1	50.00033	100.00133	150.00301	200.00535	250.00836	300.01205

Table VII.1(b). Stiffnesses along Different Radii of the Actual Roller and Cam Contour Curvature

When the actual force, F = 100 lbs.,

Diameter of Roller (d_1)	0.015	0.075	0.15	0.75
Diameter of Cam Curvature (d_2)	150.0	30.0	15.0	3.0
Stiffness (K_h, $\times 10^6$ psi)	6.4449407	6.4502859	6.4509593	6.4515262

To simulate the actual cam profile and roller displacement, normally distributed numbers were used for sampling. The basic background priniciple is the central limit theorem, based on the asymptotic behavior of the Gaussian distribution (Appendix B). The other alternative for sampling is to use the Monte Carlo simulation technique, which may give a closer approximation to the Gaussian distribution. However the sampling will be greatly increased due to the requirement of a large sample size for confidence.

In the stochastic simulation, two difficulties arose because of the typical characteristics of the spline function (Appendix C). The spline function fitting requires an increasing order in its abscissae to effect the interpolation, and the rectangular coordinates for the actual cam profile had to be rearranged so as to put the x-coordinates in increasing order. This rearrangement was accomplished by dividing the profile into 3 parts as shown in Fig. VII.1(a) : 1st part - 0° to 90°, 2nd - 90° to 270°, and 3rd - 270° to 360°. The first and third parts no longer have the order problem since their x-coordinates are in increasing order, but the second part does because its x-coordinates are in decreasing order. To simulate the profile here the sign of the coordinates was changed to produce an increasing order.

The other characteristic of the spline function is that, during fitting of a data set by the function, a final data point is not involved in the interpolation between nodes. In the simulation of the actual roller displacement, this characteristic causes a step between the initial and final points of the displacement curve when the end point of a return period is connected to the starting point of the lower dwell,

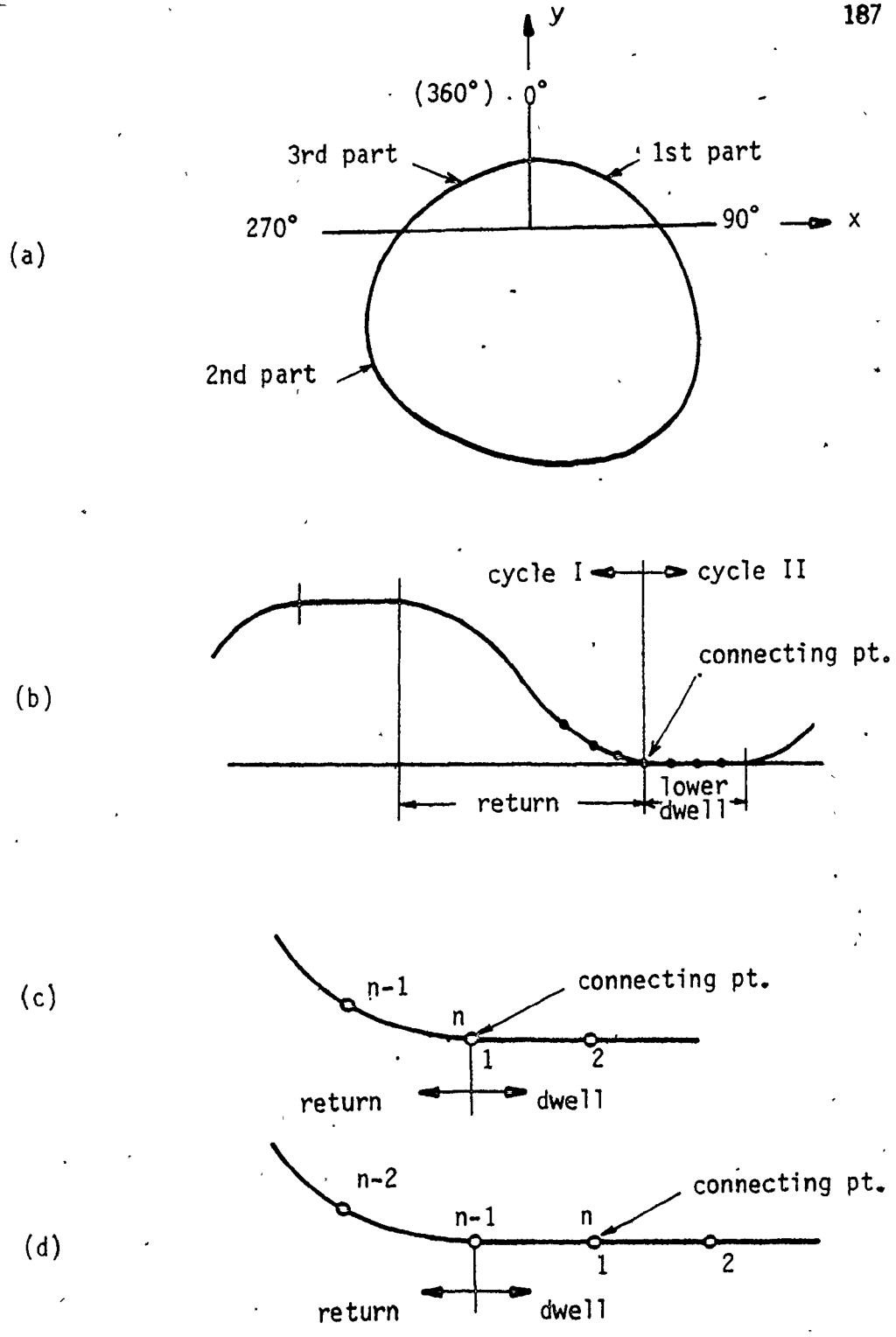

Fig. VII.1. Fitting of Spline Function for Cam Profile and Actual Roller Displacement.

as illustrated in Fig. VII.1(b). It was found that the step increases when the connection is done between two nodes on curves with different slopes, such as the direct connection between a return and a lower dwell period as shown in Fig. VII.1(c). To make this step as small as possible the connection was done during the lower dwell period, so that two nodes on the same slope can be smoothly connected (Fig. VII.1(d)) and the simulated cam profile for the next cycle will be an exact repeat. Since the simulation starts at the beginning of the lower dwell, the order of nodes was rearranged after the connection back to the original order as shown in Fig. VII.1(c).

In a real system there will exist some non-roundness in the cam shaft bearing and eccentricity between the cam base circle and the bearings. These imperfections are both stochastic in nature, and deviate the roller follower displacement from the theoretical. The effect is similar to that of dimensional tolerances. A method derived in my masters thesis [61] for a cam with an offset translating roller follower was applied in this simulation. The effect of the offset distance was handled stochastically using a tolerance and a nominal distance, and the effects of non-roundness and eccentricity can be accounted for in a similar way.

An inline roller follower has been considered here, so that the nominal value for the offset due to non-roundness and eccentricity is zero, and a tolerance of $\pm$ 0.001" is used as described in Section VI.1.

After equalizing the FPR (Frequency Per Revolution) of a simulated profile's waviness with the FPR (= 29) of a manufactured profile's waviness, the follower's performance was simulated, and the

comparison of the simulated acceleration with a theoretical one is presented in Fig. VII.2 as one of the results of the simulation. It is recognized from the figure that the relatively large value (≒ 29) of the FPR of waviness induced a considerable fluctuation in the acceleration curve, and the excessively large deviations (0.003" - 0.05") from the theoretical profile displaced the acceleration curve from the theoretical one, causing it to be skewed. To improve the acceleration, the FPR of waviness was deliberately reduced from 29 to 18 while maintaining the same tolerance. The result is shown in Fig. VII.3, from which it is found that the fluctuations were significantly suppressed, but the previous skew shape still remained due to the unchanged large deviation.

When one is examining the acceleration curves, the steepness of the theoretical curve tends to obliterate the variations in real vibratory motion from the theoretical curve, and the steeper the curve the greater this effect. This phenomenon is analysed as follows :

The vibratory motion of an object is the oscillating movement of the object with respect to its equilibrium position, and is recorded with respect to time. Therefore, the mode of vibration will naturally be altered if the equilibrium position changes from its initial position. In Fig. VII.4, the effect of this position change is illustrated for three cases : 1) no change, 2) change due to a continuous upward movement, and 3) change due to a continuous downward movement.

When an exciting force is applied to the mass, the vibration for

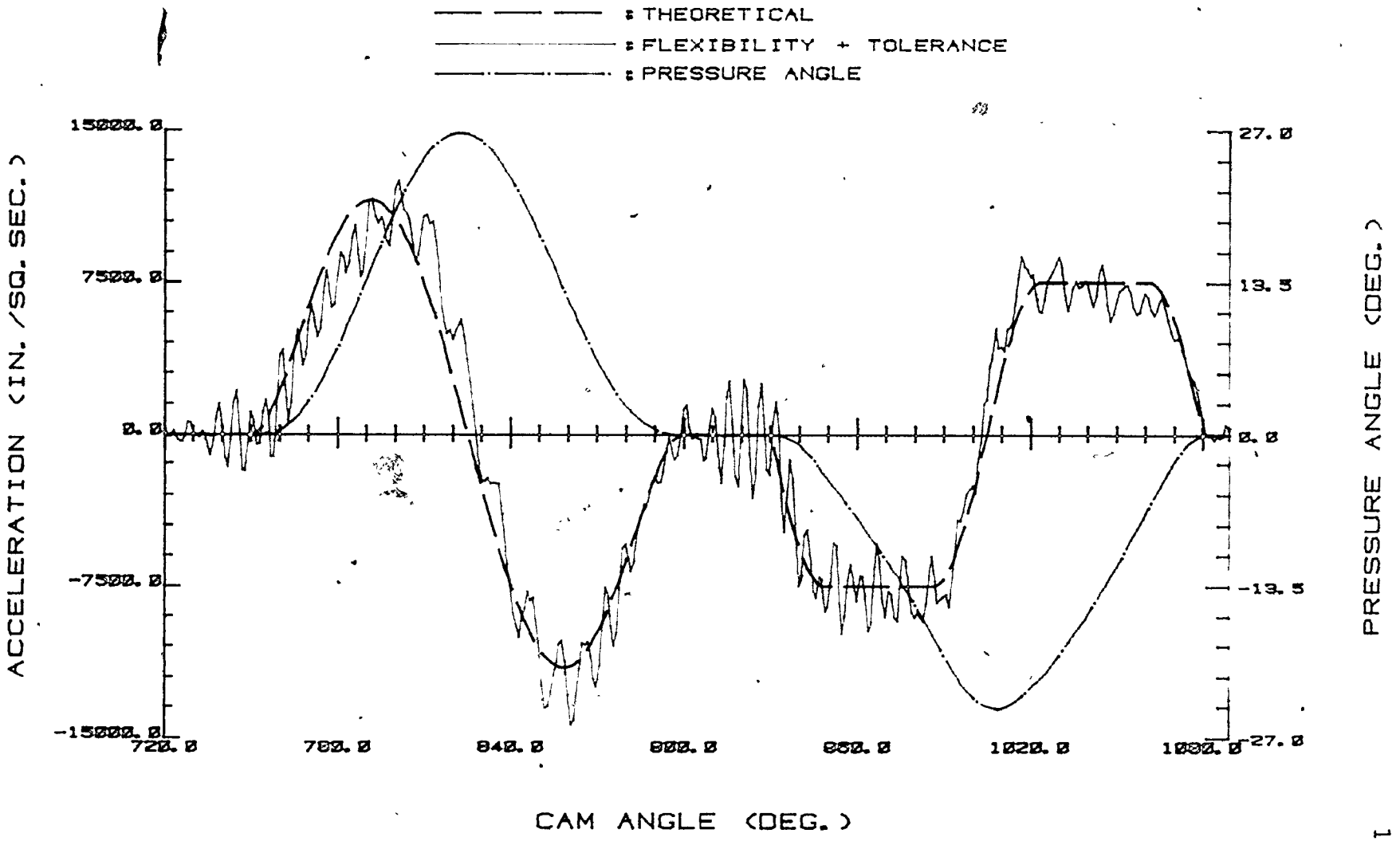

Fig. VII.2. Steady State Acceleration Response Simulated on the Profile of Real Cam Model (FPR = 29).

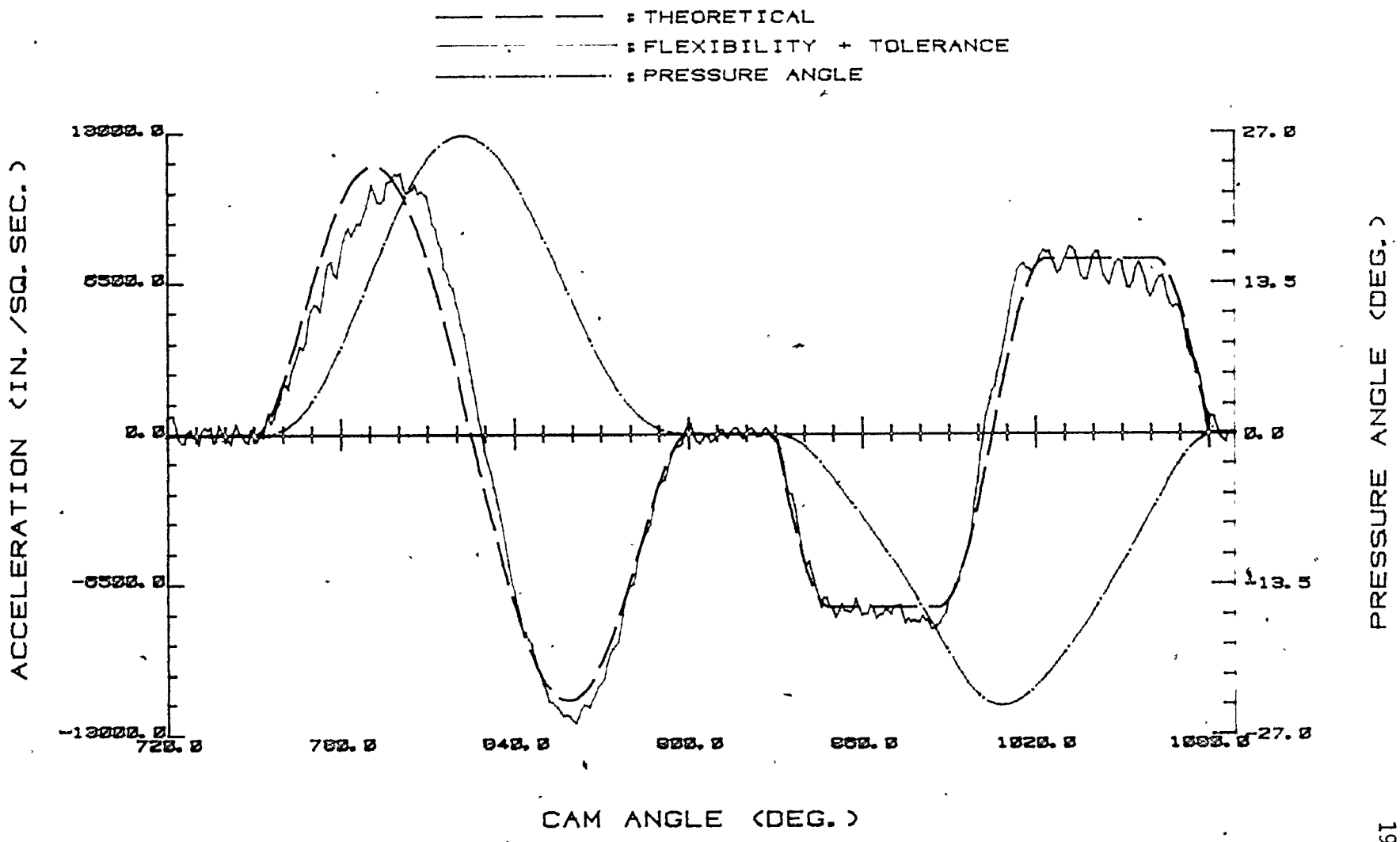

Fig. VII.3. Steady State Acceleration Response Simulated on the Profile of Real Cam Model with Reduced FPR (= 18).

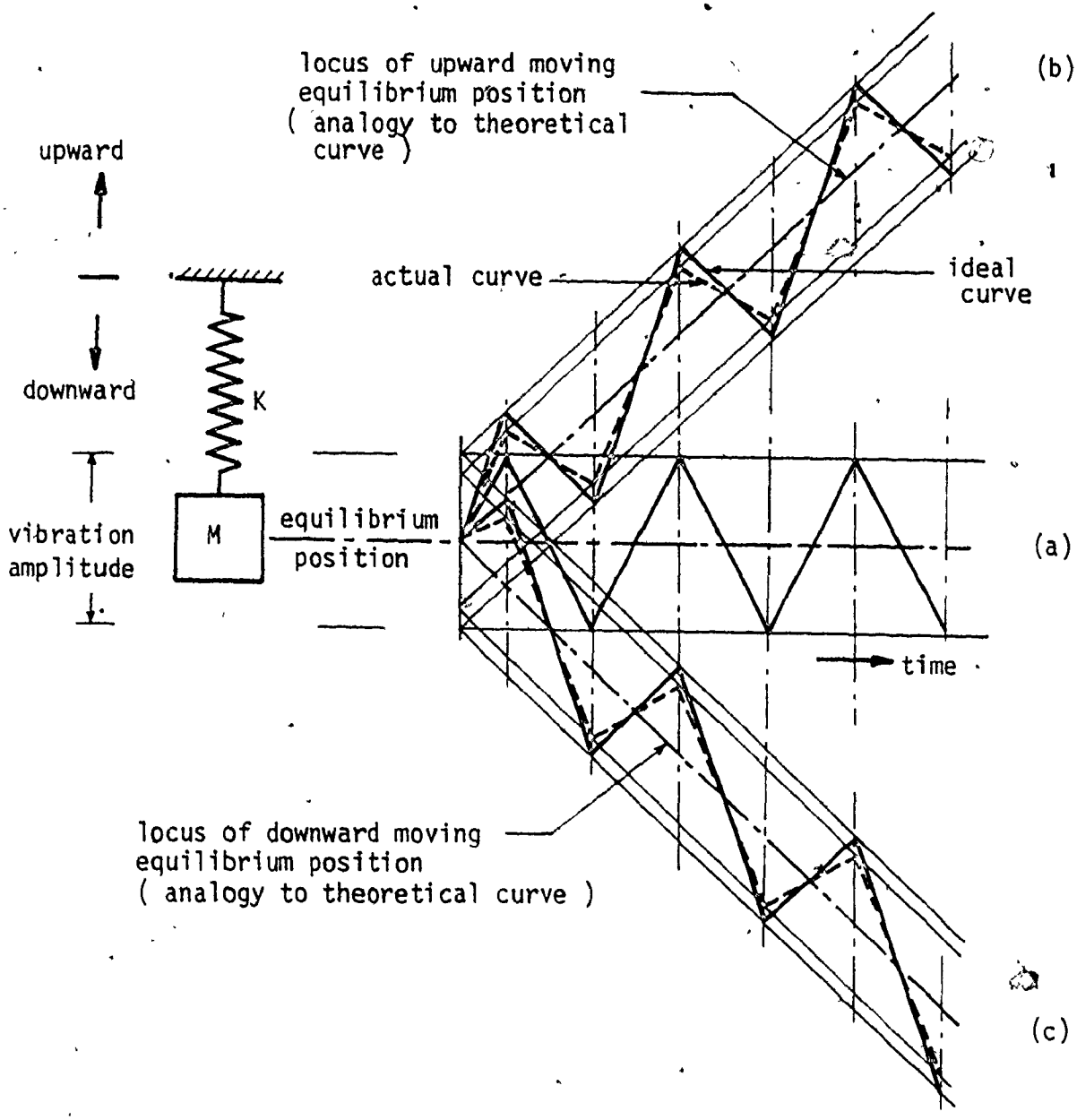

Fig. VII.4. Variation in Vibrational Mode due to the Change of Equilibrium Position. (Attenuating Effect of the Steepness on Vibration)

a fixed equilibrium position is uniform, as shown in Fig. VII.4(a), if little or ideally no damping is assumed. (It is noted that for explanation purposes, a linear saw-tooth vibration was assumed instead of the actual sinusoidal vibration.) But, for the two cases of equilibrium position change, the uniform oscillatory motion is no longer attained, as shown in the two time histories, Fig. VII.4(b) and (c). For the ideal case, the displacement of the equilibrium position is simply added to the amplitude of the horizontal vibration, and the resultant vibration becomes the curve drawn as a solid line. Therefore the deviation from the equilibrium position is the same as that of the horizontal vibration. For an actual case, however, kinetic energy is consumed by the movement of the equilibrium position (actually the movement of the frame), and due to this consumption the vibrational amplitude of the mass is shortened, consequently obliterating the variation in vibratory motion, as indicated by the dashed lines. The greater the moving speed, i.e. the steeper the slope of the locus, the greater the kinetic energy consumption, and the shorter the amplitude of the mass, letting the vibratory motion approach closer to the locus of the equilibrium position.

The locus of the moving equilibrium position and the vibration along the locus can be analogous respectively to the theoretical curve and the real motion on it in the cam-follower system response. From this analogy it is concluded that the steepness of the theoretical curve tends to obliterate (attenuate) the variations in real vibratory motion from the theoretical curve, and the steeper the curve the greater this effect.

To corroborate this, one is referred to the vibration caused by the modified trapezoidal motion in Fig. VI.12. During the first 1/8 of the curve, which is in cycloidal motion, the variation in the acceleration response is observed to be less than that on the remainder of the curve, which is parabolic and a region of theoretical constant acceleration where one would expect more uniform motion. It is hypothesized that during the first 1/8 of the motion, energy is absorbed and the vibration is attenuated, while during the remainder of the motion the acceleration is theoretically constant, and vibration from the original impact is free to continue except for the small system damping. In addition, waviness on this portion of the curve will freely superimpose its forcing effect. This phenomenon requires further investigation and is beyond the scope of this project.

VII.2. Conclusion

This work involved an investigation of the effects of imperfections in a cam-follower system on the system performance, and was carried out by a simulation technique so as to provide more refined information - quantitative as well as qualitative - for the design and manufacture of cam-follower systems. All factors which have an effect of the accuracy of the output motion of the follower link were taken

into account. A perfect cam profile is impossible to achieve in practice, and this fact has generally been neglected in previous research and in design procedures. The effects of waviness in the cam profile, and flexibility or compliance in the mechanism components, were regarded as system imperfections, and the time and inertial responses of the follower as the system output. An eleven degree of freedom dynamic model of a cam-follower system including its drive system was developed, and the dynamic simulation based on this model was combined with a stochastic simulation to handle the random nature of the machining tolerances, which have a considerable effect on the actual output. The lengthy simulation program was implemented on a PDP 11/34 minicomputer, by employing a refined Runge-Kutta numerical algorithm and overlay technique to fulfil the time based continuous simulation of the system's physical behavior.

To simulate the physical output of the system as closely as possible to reality, various analytical methods to assess the preloading of the return spring, contact force, jump criterion, and the spring constant between cam and follower were developed, by taking into consideration the nature of the contact surface which typically belongs to a general contact mechanism.

The validity of the simulation results was checked on the basis of four main error sources. The estimated maximum % error of each source is as follows :

1. Dynamic properties - by modal analysis (natural frequen-

cy and modal/effective stiffness) - 30 %

2. Cam profile and actual roller displacement generated from stochastic simulation - by comparing with manufactured model cams - 5 %
3. Numerical algorithm - by controlling total absolute and relative error - 2 %
4. Computing accuracy of computer - by comparing the performance of 3rd cycle with those of 4th, 5th and 6th cycles - 1 %

These analytical checks were carried out in lieu of the experimental validation which is not within the scope of this work. From the error analysis, the error in the simulation results was found to be less than $\pm$ 3.42 %, and this small error bound confirms that the analysed effects of imperfections are all reliable and valid. In addition to this analytical error check, the validity of the results was double-checked by collating them with those of previous investigations.

The original contributions of this work to the field of knowledge in the design and manufacture of cam-follower systems are summarized as follows :

1. A simulation system has been developed for cam-follower systems which allows all possible factors causing errors in the output function to be taken into account. This simulation technique allows the reseacher to examine the separate or combined effects of such factors as waviness in the cam profile, compliance in the various links, or variations in angular velocity, whereas in the past some

of these had to be neglected because they could not be handled together.

Using this technique, the simulated actual output motions of several cam-follower systems with trial rise-return motion designs, including all possible error sources, have been produced for the first time. Through necessity, the machined surfaces of the cam profiles have been simulated stochastically. However, if actual profile data were available it could be entered into the system to produce an accurate forecast of the output motion, and as a check on the nature of the simulated profiles two cams were manufactured by cam specialist companies, one of which was measured on their computerized high precision profile checking machine.

2. In particular this work has examined the effects of waviness in cam profiles which occurs within the necessary tolerance bands that must be allowed in machining a profile in practice.

   It has not been possible to examine the result of this imperfection in cam profiles in the past either separately or together with other imperfections such as flexibility.

   It must also be stated here that it would be difficult, if not impossible, to obtain this information by experimental means, because it is impossible to manufacture a perfect cam

profile or perfectly rigid system which could be used as a reference system so that the separate effects of flexibility and waviness could be determined. Any measurements that could be made would necessarily include both of these effects. There would also be the difficulty of determining the exact position of the cam due to variations in angular velocity and relating this to the errors in output due to the other factors.

3. The tendency in engineering design is towards greater refinement of analytical models with the objective of greater precision in the prediction of system performance. This work is regarded as a contribution towards the simulation of general contact mechanisms such as gears or Geneva mechanisms, including the stochastic nature of the machined surface of the contact profiles.

From the results of this simulation work it has been possible to draw the following conclusions on cam design and manufacture :

1. The machining accuracy consists of two major components :

   a) The deviation of the actual mean profile or pitch surface from the theoretical pitch curve
   b) The waviness which is superimposed on the pitch surface.

   As the deviation of the pitch surface away from the theoretical increases, the output or performance curve is transverse-

ly distorted or skewed away from the theoretical curve, whereas the waviness as specified by frequency per revolution (FPR) causes the performance curve to fluctuate vertically about the theoretical curve in a vibratory manner.

Although uniform tolerance is often specified for the machine manufacturing the cam profile, the machining errors are not uniform around the profile because of the change in pressure angle which proportionally changes the force exerted between profile and cutter. Thus, maximum deviation occurs at maximum pressure angle, and an overcut occurs as indicated by the negative deviation in Fig. VI.36.

To minimize these deviations the following recommendations are made : The cam designer should assign a smaller tolerance to those areas on the profile having a large pressure angle, such as on the mid-rise and return slopes. Also, it would be feasible to install a constant force device on the profile cutting machine.

It has been observed that the waviness tends to produce a greater vibratory effect when it exists on profile arcs of low or zero slope such as in dwell periods, as illustrated in Fig. VII.4. Consequently, the FPR of the waviness should be kept as small as possible in these areas.

Increased waviness frequency (FPR) causes a greater impairment in the output motion than the magnitude of the tolerance.

2. The basic motion programs such as straight line, parabolic, SHM, and cubic 1 (2-3 polynomial), whose dynamic performance are theoretically very poor, are less sensitive to tolerance than the higher order curves, and their poor dynamic performance is in some cases even improved by the effect of the machining tolerance. It was interesting to find that jumps caused by a theoretically perfect profile of the basic motion programs disappeared when tolerance was introduced, and unstable motions actually became stable. By contrast, the advanced motion programs such as cycloidal, modified trapezoidal, 4-5-6-7 polynomial, and modified sine are very sensitive to the tolerance although they have very good theoretical dynamic characteristics. Therefore, to maintain this theoretically superior dynamic performance in practice, a strict machining accuracy is demanded to cut the cam profile as close as possible to the theoretical value. This means that a mathematically improved motion program does not necessarily guarantee its theoretically predicted performance unless a rigorous cutting precision is obtained. In other words, the effort to further improve or develop theoretical performance by new mathematical motion functions will be in vain if the theoretical profiles demand impractical or extremely accurate cutting. In all aspects, the cycloidal, 3-4-5 polynomial and modified trapezoidal curves were found to have the best overall performance under relatively large

tolerances.

3. A primary source of variation in the angular velocity of the cam was found to be the impact between the cam and its follower induced by the poor dynamic characteristics of a selected motion program or by jumping of the follower arising from insufficient spring force. Variation in the angular velocity of a cam is an inertial response as exemplified by rotational vibration of the cam. As the angular velocity of the cam has a direct input to the time responses such as velocity and acceleration of the follower, a small variation such as 2 % of the design velocity significantly affects the time responses, especially the acceleration, which is proportional to angular velocity by the power of 2.

   To keep the angular velocity of the cam as constant as possible, the following recommendations are made :

   a) Reduce the impact between cam and follower by providing a proper spring force or employing a motion program adequate to its operating speed.
   b) Stiffen the power transmitting shaft and reduce the allowance or backlash in the power transmitting device as much as possible.
   c) Use a large flywheel effect in the rotating system and supply sufficient power to overcome the inertia.

4. The general behavior of the follower motion is essentially

governed by the direction change of its exciting forces (spring force and inertia force) with respect to its movement, as illustrated in Fig. VI.27. As the result of these direction changes, an asymmetry between the rise and return period occurs, and follower jump, if imminent, will occur at the deceleration part of the rise period or at the acceleration part of the return period. When the same program is used for both return and rise periods, follower jump is more likely to occur in the return period, except for the parabolic and cubic 1 program, for which follower jump is more likely during the rise period due to the instantaneous change of their accelerations. Therefore, to prevent follower jump, a spring force must be calculated from the return period for all motion programs except the parabolic and cubic 1. When a different program is employed for each period, it is proposed that a program with a lower peak acceleration be employed for the return period to decrease the jump during the period.

5. An increase of system inertia is generally undesirable for the time responses but is beneficial for inertial responses, and consequently it is suggested that the system inertia be optimized in respect to time and inertial responses. For this particular model it was observed that an increase in system stiffness or rigidity improved the performance, i.e. the displacement, velocity and acceleration curves were smoother, and the cam angular velocity became more stable.

This occured with very little increase in contact stress.

On checking the sensitivity of this model to changes in dynamic properties such as inertia and damping, variations of up to 30 % did not appreciably affect the results of the simulation.

REFERENCES

[1] Dudley, W. M., "A New Approach to Cam Design", Mach. Des., July 1947, PP. 143-148.

[2] Gagne, A. F., "Design of High Speed Cam", Mach. Des., July 1950, PP. 108-111.

[3] Mitchell, D. B., "Tests on Dynamic Response of Cam-Follower System", Mech. Eng., Vol. 72, 1950, PP. 467-471.

[4] Neklutin, C. N., "Designing Cams for Controlled Inertia and Vibration", Mach. Des., June 1952, PP. 143-160.

[5] Barkan, P., "Calculation of High-Speed Valve Motion with a Flexible Over-head Linkage", SAE Trans., Vol. 61, 1953, PP. 687-700.

[6] Stoddart,D. A., "Polydyne Cam Design", Mach. Des. 25, P. 121 (Jan. 1953) ; P. 146 (Feb. 1953) ; P. 149 (March, 1953).

[7] Kloomok,M. & Muffley,R. V., "Plate Cam Design with Emphasis on Dynamic Effects", Prod. Eng., Feb. 1955, PP. 156-162.

[8] Johnson,R. C., "Method of Finite Differences for Cam Design", Mach. Des. 27, Nov. 1955, PP. 195-204.

[9] Rothbart,H. A., Cams - Design, Dynamics and Accuracy, John Wiley, New York, 1956.

[10] Johnson, R. C., "How Profile Errors Affect Cam Dynamics", Mach. Des., Feb. 7, 1957, PP. 105-108.

[11] Kloomok,M. & Muffley,R. V., "Computers Simplify Solutions of Polynomial Cam Curves", Prod. Eng., March 1957, PP. 196-202.

[12] Mercer, S. Jr. & Holowenko, A. R., "Dynamic Characteristics of Cam Forms Calculated by the Digital Computer", ASME Trans., Nov. 1958, PP. 1695-1705.

[13] Johnson,R. C., "The Dynamic Analysis and Design of Relative Flexible Cam Mechanisms Having More than One Degree of Freedom", ASME Trans., J. of Eng. for Ind., Nov. 1959, PP. 323-331.

[14] Okcuogly,S. A., "An Application of Polydyne Cam Design", Trans. of 6th Cong. on Mech., Oct. 10-11, 1960, PP. 44-47.

[15] Weber,T. Jr., "Filter Theory Applied to Cam Dynamics", (Ref. [12], PP. 48-54).

[16] Hebeler,C. B., "Design Equations and Graphs for Finding the Dynamic Response of Cycloidal-Motion Cam Systems", Mach. Des., Feb. 2, 1961, PP. 102-107.

[17] Sarring,E. G., "Torque Compensation for Cam Systems", Trans. of 7th Conf. on Mech., Oct. 8-10, 1062, PP. 179-185.

[18] Johnson,R. C., "Analysis and Design of Cam Mechanisms Having a Varying Input Velocity", (Ref. [17], PP. 213-218).

[19] Baumgarten,J. R., "Preload Force necessary to Prevent Separation of Follower from Cam", (Ref. 17 , PP. 213-218)

[20] Goodman,T. P., "How to Calculate Dynamic Effect of Backlash", Mech. Des., May 23, 1963, PP. 150-157.

[21] Knappe,L. F., "A Technique for Analysing Mechanism Tolerances", Mach. Des., April 25, 1963, PP. 155-157.

[22] Allais,D. C., "Cycloidal vs Modified Trapezoidal Cams", Mach. Des., Jan. 31, 1963, PP. 93-96.

[23] Eiss, N. S. Jr., "Vibration of Cams Having Two Degrees of Freedom", ASME Trans., J. of Eng. for Ind., Nov. 1964, PP. 343-350.

[24] Erisman, R. J., "Automotive Cam Profile Synthesis and Valve Gear Dynamics from Dimensionless Analysis", SAE Trans., 1967, PP. 128-149.

[25] Kwakernaak, H. and Smit, J., "Minimum Vibration Cam Profiles", J. Mech. Eng. Sci., Vol. 10, No. 3, 1968, PP. 219-227.

[26] Brittain, J. H. C. & Horsnell, R., "A Prediction of Some Causes and Effects of Cam Profile Errors", Proc. Instr. Mech. Engrs., 1967-68, Vol. 182, P+3L, PP. 145-151.

[27] Garrett, R. E. and Hall, A. S., "Effect of Tolerance and Clearance in Linkage Design", ASME Trans., J. of Eng. for Ind., Feb. 1969, PP. 198-202.

[28] Fawcett, J. N. and Fawcett, G. F., "The Effect of Cam Vibration on Follower Motion", Comm. of the 3rd World Congress for the Theory of Mach. & Mech., Sept. 13-20, 1971, PP. 147-160.

[29] Bagci, C., "Stop Designing and Testing Cam-Follower Systems Using the Rise Portions of the Displacement Programs Only", (Ref. 28, PP. 347-364).

[30] Oledzki, A., "Some Dynamic Properties of Systems with Cam Mechanisms", Mech. and Mech. Theory, Vol. 8, 1973, PP. 543-554.

[31] Wiederrich, J. L. & Roth, B., "Dynamic Synthesis of Cams Using Finite Trigonometric Series", ASME Trans., J. of Eng. for Ind., Feb. 1975, PP. 287-293.

[32] Kawasaki, Y. et al., "Lift Error on Grinding Cam Profile", Annals of the CIRP, Vol. 24/1/1975, PP. 253-258.

[33] "CAM TECH" #1 and #11, Technical Bulletins from Cam Technology Inc., Elmsford, N. Y., 1975.

[34] Chen, F. Y. & Polvanich, N., "Dynamics of High-Speed Cam-Driven Mechanisms, Part 1 : Linear System Models", ASME Trans., J. of Eng. for Ind., Aug. 1975, PP. 769-776.

[35] Ibid., "Part 2 : Nonlinear System Models", PP. 777-784.

[36] Dhande, S. G. & Chakraborty, J., "Mechanical Error Analysis of Cam-Follower Systems - A Stochastic Approach", I. Mech. E., 1975, PP. 957-962.

[37] Rao, J. S. & Raghavacharyulu, E., "Experimental Determination of Jump Characteristics in Cam-Follower System", (Ref. [35], PP. 951-955)

[38] Kim, H. and Newcombe, W. R., "Stochastic Error Analysis of Cam Mechanism", Mech. and Mach. Theory, Vol. 13, 1978, PP. 631-641.

[39] Di Benedetto, A., "Some Methods of Kinematic Synthesis of Cam Profiles for Prescribed Jerk Pattern", (Ref. [35], PP. 963-968)

[40] Koster, M. P., "Effect of Flexibility of Driving Shaft on the Dynamic Behavior of a Cam Mechanism", ASME, 74-DET-48.

[41] Mattew, G. K. & Tesar, D., "One Degree of Freedom Cam System Synthesis and Analysis", J. of Mech. and Mach. Theory, March 1974.

[42] Mattew, G. K. & Tesar, D., "The Design of Modeled Cam Systems, Part I : Dynamic Synthesis and Chart Design for the Two Degree of Freedom Model", ASME Trans., J. of Eng. for Ind., Nov. 1975, PP. 1175-1180.

[43] Ibid., "Part II : Minimization of Motion Distortion due to Modelled Errors", PP. 1181-1189.

[44] Koster, M. P., "Digital Simulation of the Dynamics of Cam Followers and Camshafts", I. Mech. E., 1975, PP. 969-974.

[45] Noortgate, L. V. & Fraine, J. D., "A General Computer Aided Method for Designing High Speed Cams Avoiding the Dangerous Excitation of the Machine Structure", Mech. and Mach. Theory, Vol. 12, No. 3, 1977, PP. 237-245.

[46] Ardayfio, D., "Dynamics of High Speed Cam Mechanisms with Damped Flexible Followers Driven by Flexible Cam Shafts", ASME 76-DET-63, 1977.

[47] Smith, D. L. & Soni, A. H., "Simplified Design & Evaluation of Cam Surfaces", Proc. of the 5th OSU Appl. Mech. Conf., Nov. 6-9, 1977.

[48] Jones, J. R. & Reeve, J. E., "Dynamic Response of Cam Curves Based on Sinusoidal Segment", Cams and Cam Mechanisms, Mech. Eng. Publications Ltd., 1978, PP. 14-24.

[49] Beese, J. G. et al., "Imperfections in Cam Profiles and Cam-Follower Alignment : Influence on Wear Potential", (Ref. [48], PP. 136-140)

[50] Giordana, F. et al., "On the Influence of Measurement Errors in the Kinematic Analysis of Cams", Mech. and Mach. Theory, Vol. 14, 1978, PP. 327-340.

[51] Giordana, F. et al., "The Influence of Construction Errors in the Law of Motion of Cam Mechanisms", Mech. and Mach. Theory, Vol. 15, 1980, PP. 29-45.

[52] Dhande, S. G. and Chakraborty, J., "Analysis and Synthesis of Mechanical Error in Linkages - A Stochastic Approach", ASME Trans., J. of Eng. for Ind., Aug. 1973, PP. 672-676.

[53] Dubowsky, S. and Freudenstein, F., "Dynamic Analysis of Mechanical Systems with Clearances, Part 1 : Formation of Dynamic Model", ASME Trans., J. of Eng. for Ind., Feb. 1971, PP. 305-309.

[54] Tesar, D. & Matthew, G. K., The Dynamic Synthesis, Analysis and Design of Modeled Cam Systems , Lexington Books, D. C. Heath and Company, 1976.

[55] Shigley, J. E., Simulation of Mechanical Systems , McGraw-Hill, New York, 1967.

[56] Whitehouse, D. J., "Approximate Methods of Assessment of Surface Topography Parameters", Annals of the CIRP, Vol. 25/1/1976, PP. 461-465.

[57] Elgabry, A. A., Osman, M. O. M. and Sankar, T. S., "A Simplified Probabilistic Model for Two-Dimensional Profile Characterization of Surfaces Machined by Finishing Processes", CSME Trans., Vol. 5, No. 3, 1978-79, PP. 155-164.

[58] England, R., "Error Estimates for Runge-Kutta Type Solutions to Systems of Ordinary Differential Equations", Comput. J., Vol. 12, May 1969, PP. 166-170.

[59] Chai, A. S., "A Fifth-Order Modified Runge-Kutta Integration Algorithm", SIMULATION, Vol. 18, Jan. 1972, PP. 21-27.

[60] Nourse, J. H., "Recent Developments in Cam Profile Measurement and Evaluation", SAE Paper No.964A, 1965.

[61] Kim, H. R., "Stochastic Analysis of Manufacturing Errors in Cam Mechanisms", M. Eng. Thesis, Dept. Mech. Eng., McMaster Univ., Hamilton, Ont., 1977.

APPENDIX A

FOLLOWER MOTION PROGRAMS

Nomenclature

y = displacement of follower

v = velocity of follower

a = acceleration of follower

j = jerk of follower

h = total follower rise

θ = cam angle

β = total cam angle for 'h'

———— : displacement

------ : velocity

———— : acceleration

———— : jerk or pulse

A.1 Simple Polynomial Curves

1. Straight line (constant velocity) curve

$y = h\theta/\beta$

$v = h\omega/\beta$

$a = 0$

$j = 0$

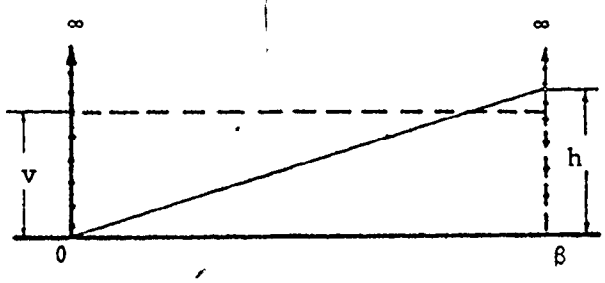

Fig. A.1-1. Straight line (constant velocity) curve

2. Parabolic (constant acceleration) curve

$$\theta=0-\beta/2 \begin{cases} y = 2h(\frac{\theta}{\beta})^2 \\ v = 4h\omega\theta/\beta \\ a = 4h\omega^2/\beta^2 \\ j = 0 \end{cases} \qquad \theta=\beta/2-\beta \begin{cases} y = h[1-2(1-\frac{\theta}{\beta})^2] \\ v = 4h\omega(1-\frac{\theta}{\beta})/\beta \\ a = -4h\omega^2/\beta^2 \\ j = 0 \end{cases}$$

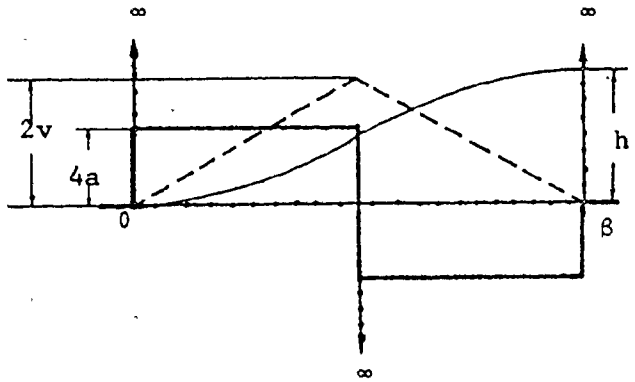

Fig. A.1-2. Parabolic (constant acceleration) curve

3. Cubic (constant pulse) No.1 curve

$$\theta=0-\beta/2\begin{cases} y = 4h(\theta/\beta)^3 \\ v = 12h\omega(\frac{\theta}{\beta})^2/\beta \\ a = 24h\omega^2(\frac{\theta}{\beta})/\beta^2 \\ j = 24h(\omega/\beta)^3 \end{cases} \qquad \theta=\beta/2-\beta\begin{cases} y = h[1-4(1-\frac{\theta}{\beta})^3] \\ v = 12h\omega(1-\frac{\theta}{\beta})^2/\beta \\ a = -24h\omega^2(1-\frac{\theta}{\beta})/\beta^2 \\ j = 24h(\omega/\beta)^3 \end{cases}$$

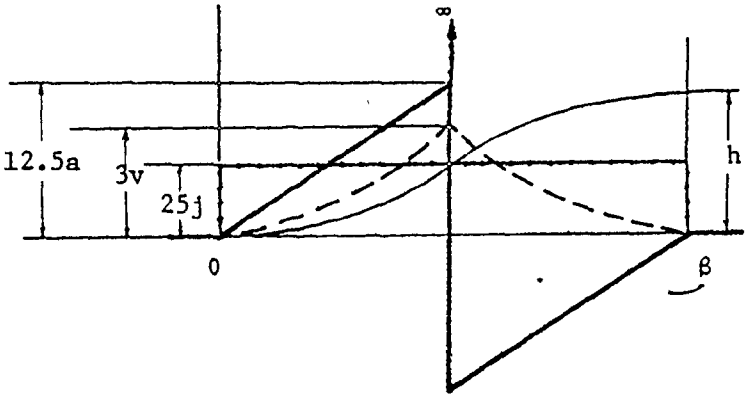

Fig. A.1-3. Cubic (constant pulse) No.1 curve

4. Cubic (constant pulse) No.2 curve

$$y = h\theta^2(3-\frac{2\theta}{\beta})/\beta^2$$
$$v = 6h\theta\omega(1-\frac{\theta}{\beta})/\beta^2$$
$$a = 6h\omega^2(1-\frac{2\theta}{\beta})/\beta^2$$
$$j = -12h(\omega/\beta)^3$$

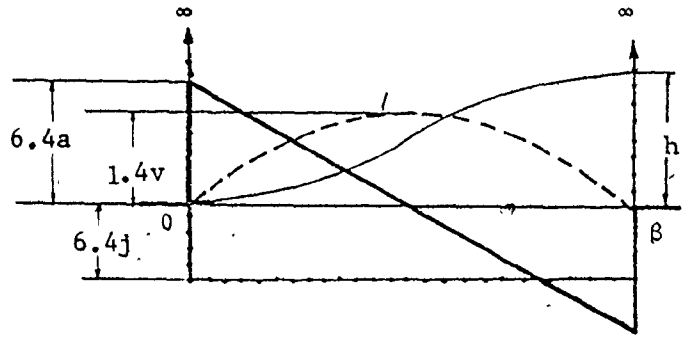

Fig. A.1-4. Cubic (constant pulse) No.2 curve

A.2 Trigonometric Curves

1. Simple harmonic motion (crank) curve

$$y = \frac{h}{2} \left(1 - \cos \frac{\pi\theta}{\beta} \right)$$

$$v = \frac{h\pi\omega}{2\beta} \cdot \sin \frac{\pi\theta}{\beta}$$

$$a = \frac{h}{2} \left(\frac{\pi\omega}{\beta}\right)^2 \cdot \cos \frac{\pi\theta}{\beta}$$

$$j = -\frac{h}{2} \left(\frac{\pi\omega}{\beta}\right)^3 \cdot \sin \frac{\pi\theta}{\beta}$$

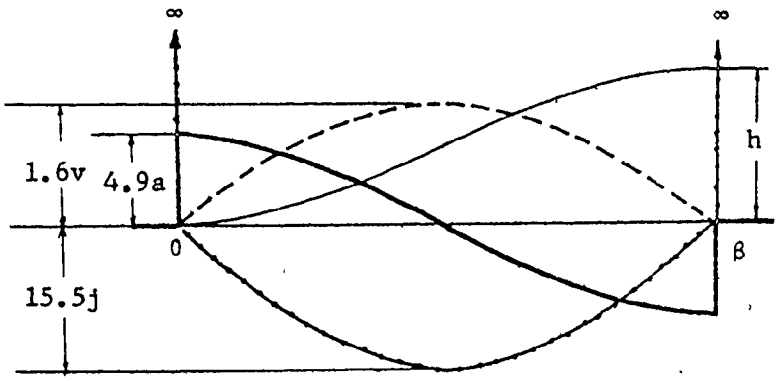

Fig. A.2-1. Simple harmonic motion (crank) curve

2. Double harmonic curve

$$y = \frac{h}{2} \left[\left(1 - \cos \frac{\pi\theta}{\beta}\right) - \frac{1}{4} \left(1 - \cos \frac{2\pi\theta}{\beta}\right) \right]$$

$$v = \frac{h}{2} \frac{\pi\omega}{\beta} \left(\sin \frac{\pi\theta}{\beta} - \frac{1}{2} \sin \frac{2\pi\theta}{\beta}\right)$$

$$a = \frac{h}{2} \left(\frac{\pi\omega}{\beta}\right)^2 \cdot \left(\cos \frac{\pi\theta}{\beta} - \cos \frac{2\pi\theta}{\beta} \right)$$

$$j = \frac{h}{2} \left(\frac{\pi\omega}{\beta}\right)^3 \cdot \left(-\sin \frac{\pi\theta}{\beta} + 2 \sin \frac{2\pi\theta}{\beta} \right)$$

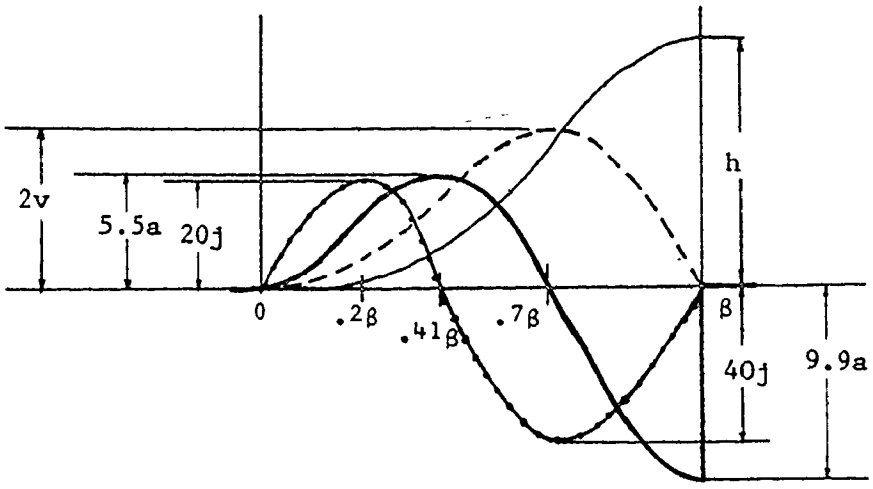

Fig. A.2-2. Double harmonic curve

3. Cycloidal (sine acceleration) curve .

$$y = \frac{h}{\pi} \left(\frac{\pi\theta}{\beta} - \frac{1}{2} \sin \frac{2\pi\theta}{\beta} \right)$$

$$v = \frac{h\omega}{\beta} \left(1 - \cos \frac{2\pi\theta}{\beta} \right)$$

$$a = 2h\pi \left(\frac{\omega}{\beta}\right)^2 \cdot \sin \frac{2\pi\theta}{\beta}$$

$$j = 4h\pi^2 \left(\frac{\omega}{\beta}\right)^3 \cdot \cos \frac{2\pi\theta}{\beta}$$

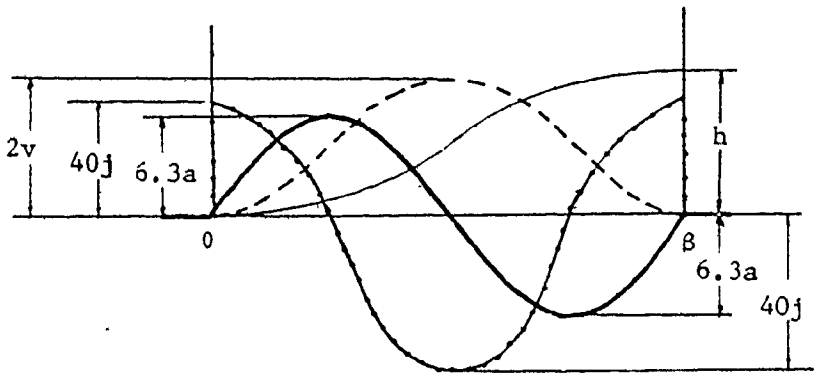

Fig. A.2-3. Cycloidal (sine acceleration) curve

4. Modified sine curve

$\theta = 0 - \beta/8$:

$$y = \frac{h}{4(\pi+4)} \left[4\pi\left(\frac{\theta}{\beta}\right) - \sin\frac{4\pi\theta}{\beta} \right]$$

$$v = \frac{h\pi\omega}{(\pi+4)\beta} \left(1 - \cos\frac{4\pi\theta}{\beta} \right)$$

$$a = \frac{4h\pi^2\omega^2}{\beta^2(\pi+4)} \sin\frac{4\pi\theta}{\beta}$$

$$j = \frac{16h\pi^3\omega^3}{\beta^3(\pi+4)} \cos\frac{4\pi\theta}{\beta}$$

$\theta = \beta/8 - \beta/2$:

$$y = \frac{h}{4(\pi+4)} \left[4\pi\left(\frac{\theta}{\beta}\right) - 9\cos\left(\frac{4\pi\theta}{3\beta} - \frac{\pi}{6} \right) + 8 \right]$$

$$v = \frac{h\pi\omega}{(\pi+4)\beta} \left[1 + 3\sin\left(\frac{4\pi\theta}{3\beta} - \frac{\pi}{6} \right) \right]$$

$$a = \frac{4\,h\pi^2\omega^2}{(\pi+4)\beta^2} \cos\left(\frac{4\pi\theta}{3\beta} - \frac{\pi}{6} \right)$$

$$j = -\frac{16h\pi^3\omega^3}{3(\pi+4)\beta^3} \sin\left(\frac{4\pi\theta}{3\beta} - \frac{\pi}{6} \right)$$

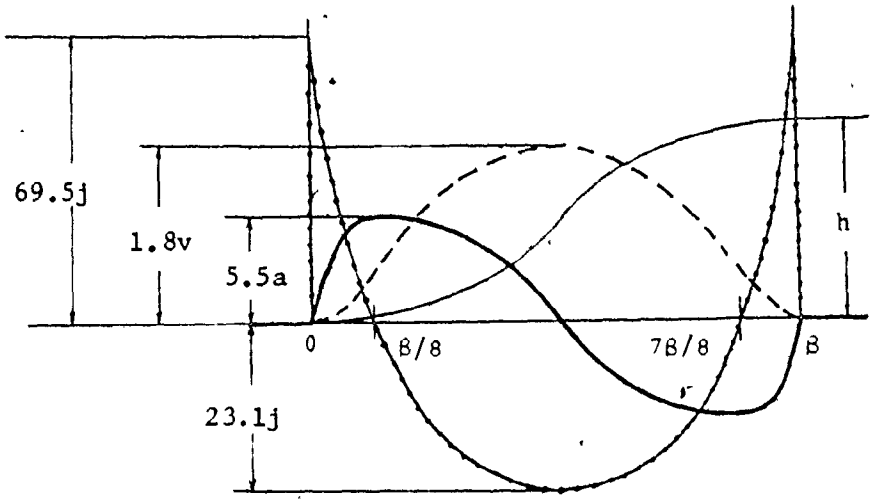

Fig. A.2-4. Modified sine curve

A.3 Combination Portions of Basic Curves

1. Trapezoidal acceleration curve

$\theta = 0 - \beta/8$:

$$y = \frac{64}{9} h \left(\frac{\theta}{\beta}\right)^3 \quad , \qquad v = \frac{64}{9} \frac{\omega h}{\beta} \left(\frac{\theta}{\beta}\right)^2$$

$$a = \frac{128h}{3} \frac{\theta \omega^2}{\beta^3} \quad , \qquad j = \frac{128h}{3} \left(\frac{\omega}{\beta}\right)^2$$

$\theta = \beta/8 - 3\beta/8$:

$$y = h \left[\frac{1}{72} - \frac{1\theta}{3\beta} + \frac{8}{3}\left(\frac{\theta}{\beta}\right)^2\right]$$

$$v = \frac{h\omega}{\beta} \left(- \frac{1}{3} + \frac{16\theta}{3\beta} \right)$$

$$a = \frac{16h}{3}\left(\frac{\omega}{\beta}\right)^2 \quad , \qquad j = 0$$

$\theta = 3\beta/2 - \beta/2$:

$$y = h \left[\frac{7}{18} - \frac{10}{3} \frac{\theta}{\beta} + \frac{32}{3} \left(\frac{\theta}{\beta}\right)^2 - \frac{64}{9} \left(\frac{\theta}{\beta}\right)^3\right]$$

$$v = \frac{h\omega}{\beta} \left[-\frac{10}{3} + \frac{64}{3} \frac{\theta}{\beta} - \frac{64}{3} \left(\frac{\theta}{\beta}\right)^2\right]$$

$$a = \frac{h\omega^2}{\beta^2} \left(\frac{64}{3} - \frac{128}{3} \frac{\theta}{\beta} \right)$$

$$j = - \frac{128\ h}{3} \left(\frac{\omega}{\beta}\right)^3$$

2. Modified trapezoidal acceleration curve

$\theta = 0 - \beta/8$:

$$y = 0.0972461\ h[4\ \frac{\theta}{\beta} - \frac{1}{\pi}\ \sin\ (4\pi\frac{\theta}{\beta})]$$

$$v = 0.3889845\ \frac{h\omega}{\beta}[1 - \cos\ (4\pi\frac{\theta}{\beta})]$$

$$a = 4.888124\ \frac{h\omega^2}{\beta^2}\ \sin\ (4\pi\frac{\theta}{\beta})$$

$$j = 61.425977\ \frac{h\omega^3}{\beta^3}\ \cos\ (4\pi\frac{\theta}{\beta})$$

$\theta = \beta/8 - 3\beta/8$:

$$y = h\ [2.444\ (\frac{\theta}{\beta})^2 - 0.222\ \frac{\theta}{\beta} + 0.007234]$$

$$v = \frac{h\omega}{\beta}\ [\ 4.888124\frac{\theta}{\beta} - 0.222\ ]$$

$$a = \frac{h\omega^2}{\beta^2}\ \ 4.888124\ ,\qquad j = 0$$

$\theta = 3\beta/8 - \beta/2$:

$$y = h\ [1.611\frac{\theta}{\beta} - 0.0309544\ \sin\ (4\pi\frac{\theta}{\beta} - \pi) - 0.3055077]$$

$$v = \frac{h\omega}{\beta}\ [\ 1.611 - 0.3889845\ \cos\ (4\pi\frac{\theta}{\beta} - \pi)]$$

$$a = 4.888124\ \frac{h\omega^2}{\beta^2}\ \sin\ (4\pi\frac{\theta}{\beta} - \pi)$$

$$j = 61.425977\ \frac{h\omega^3}{\beta^3}\ \cos\ (4\pi\frac{\theta}{\beta})$$

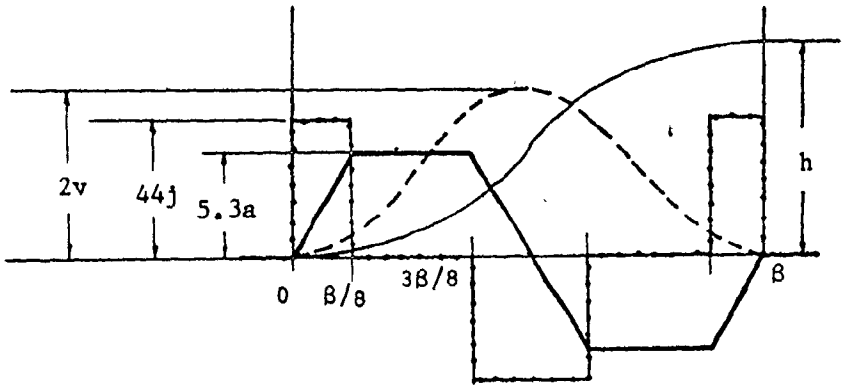

Fig. A.3-1. Trapezoidal acceleration curve

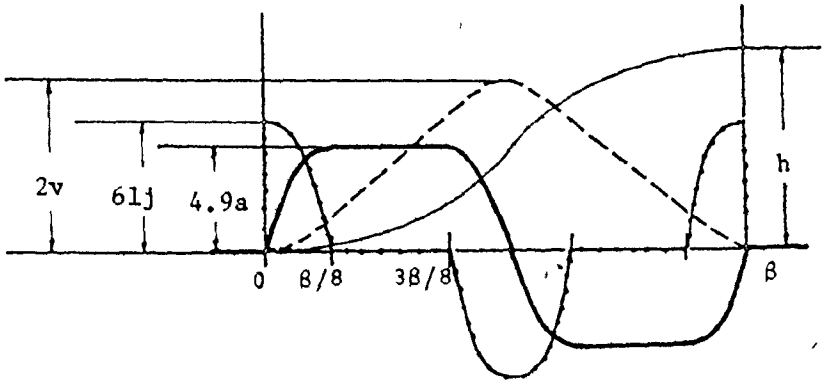

Fig. A.3-2. Modified trapezoidal acceleration curve

A.4 Polynomial Curves

1. 2-3 polynomial

exactly same as the cubic (constant pulse) No.2 curve.

2. 3-4-5 polynomial

$$y = h\ [10(\tfrac{\theta}{\beta})^3 - 15(\tfrac{\theta}{\beta})^4 + 6(\tfrac{\theta}{\beta})^5]$$

$$v = \frac{h\omega}{\beta}\ [\ 30(\tfrac{\theta}{\beta})^2 - 60(\tfrac{\theta}{\beta})^3 + 30(\tfrac{\theta}{\beta})^4\ ]$$

$$a = \frac{h\omega^2}{\beta^2}\ [\ 60(\tfrac{\theta}{\beta}) - 180(\tfrac{\theta}{\beta})^2 + 120(\tfrac{\theta}{\beta})^3\ ]$$

$$j = h(\tfrac{\omega}{\beta})^3\ [\ 60 - 360(\tfrac{\theta}{\beta}) + 360(\tfrac{\theta}{\beta})^2\ ]$$

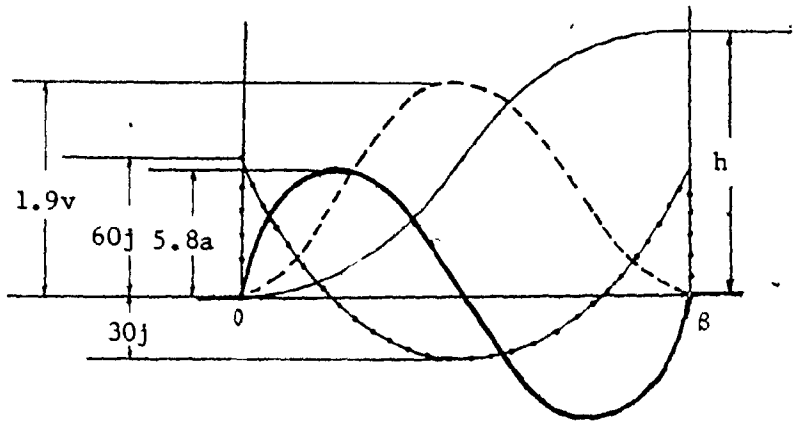

Fig. A.4-2. 3-4-5 polynomial

3. 4-5-6-7 polynomial

$$y = h\ [\ 35(\tfrac{\theta}{\beta})^4 - 84(\tfrac{\theta}{\beta})^5 + 70(\tfrac{\theta}{\beta})^6 - 20(\tfrac{\theta}{\beta})^7\ ]$$

$$v = \frac{h\omega}{\beta}\ [\ 140(\tfrac{\theta}{\beta})^3 - 420(\tfrac{\theta}{\beta})^4 + 420(\tfrac{\theta}{\beta})^5 - 140(\tfrac{\theta}{\beta})^6\ ]$$

$$a = \frac{h\omega^2}{\beta^2}\ [\ 420(\tfrac{\theta}{\beta})^2 - 1680(\tfrac{\theta}{\beta})^3 + 2100(\tfrac{\theta}{\beta})^4 - 840(\tfrac{\theta}{\beta})^5\ ]$$

$$j = \frac{h\omega^3}{\beta^3}\ [\ 840(\tfrac{\theta}{\beta}) - 5040(\tfrac{\theta}{\beta})^2 + 8400(\tfrac{\theta}{\beta})^3 - 4200(\tfrac{\theta}{\beta})^4\ ]$$

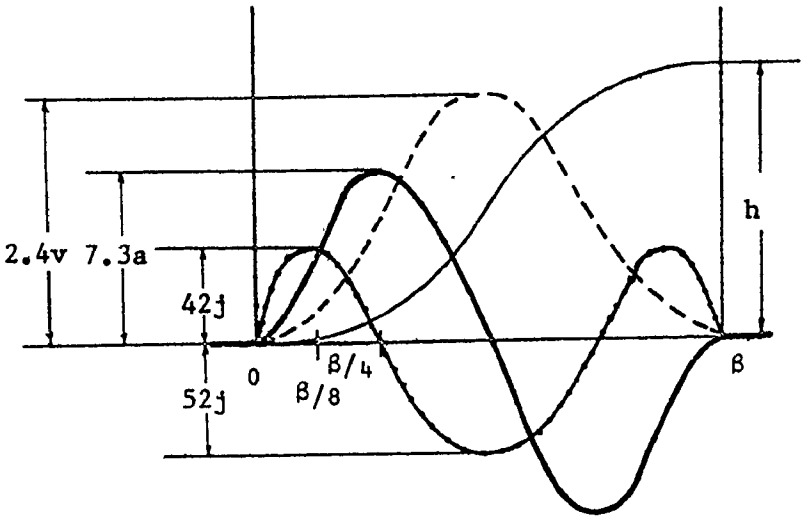

Fig. A.4-3. 4-5-6-7 polynomial

A.5 Equations for Return Period

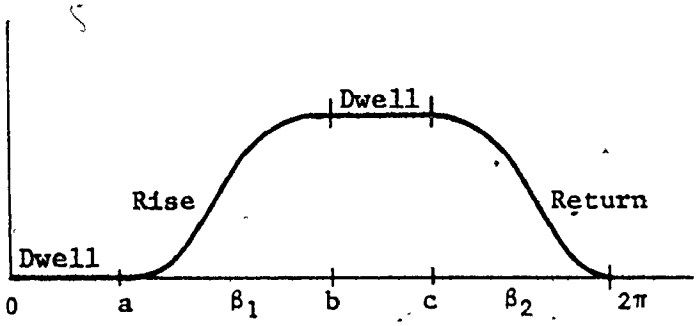

Fig. A.5-1. D-R-D-R motion program of total cycle

Displacement : Replace θ in the rise displacement equation by $-(\theta - \beta_2 - c)$ and β by β_2.

Velocity : First derivative of the resulting displacement or negative velocity of rise period.

Acceleration : Second derivative of the resulting displacement or sign-changed acceleration of rise period.

Jerk or Pulse : Third derivative of the resulting displacement or sign-changed jerk of rise period.

APPENDIX B

GENERATION OF NORMALLY DISTRIBUTED RANDOM NUMBERS

An approximation to normally distributed random numbers Y can be found from a sequence of uniform random numbers* using the formula :

$$Y = \left(\sum_{i=1}^{k} X_i - \frac{k}{2} \right) / \left(k/12 \right)^{\frac{1}{2}} \qquad \text{(B-1)}$$

where

X_i = a uniformly distributed random number ($0<X_i<1$)

k = numbers of X_i

Y approaches a true normal distribution asymptotically as k approaches infinity. If k is chosen as 12 to reduce execution time on computer, Eq.(B-1) becomes

$$Y = \sum_{i=1}^{12} X_i - 6.0 \qquad \text{(B-2)}$$

The adjustment for the required mean and standard deviation is then*

$$\bar{Y} = \sigma Y + \mu \qquad \text{(B-3)}$$

where

$\bar{Y}$ = required normally distributed random number

σ = given standard deviation

μ = given mean value .

---

* Hamming, R. W., " Numerical Methods for Scientists and Engineers ", McGraw-Hill, N.Y., 1962, pp.34 & 389.

APPENDIX C

MATHEMATICAL SPLINE FOR SMOOTHING DATA

Smoothing data actually means the interpolation of intervals produced by discrete data to generate continuous functions. A generally used polynomial interpolation has the drawback of producing approximations that may be excessively oscillatory between the knots or junction points. To smooth out this excessive oscillatory behavior, the mathematical analog of a spline may be utilized.

Splines are long thin strips of wood or some other materials used much like French curves by draftsmen to fit a smooth curve between specified points. The mathematical spline is the result of replacing the draftsman's spline by its small pieces and then approximating the latter by a piecewise cubic (generally a different cubic between knots) with matching slopes for adjoining pieces and also matching higher derivatives at the points of interpolation ; the mathematical spline is continuous and has continuous first and second derivatives.

To derive a mathematical model for the spline, the properties of a draftsman's spline are described and denoted mathematically as shown in Table C-1. Since by the property 3 in Table C-1, S(x) is a cubic polynomial for $x_i \leq x \leq x_{i+1}$, its second derivative S"(x) must be linear, and by the linear interpolation formula we obtain

$$S''(x) = S''(x_i) + \frac{x - x_i}{x_{i+1} - x_i}\left(S''(x_{i+1}) - S''(x_i)\right) \qquad (C\text{-}1)$$

Table C-1. Properties of Spline

No	Properties	Mathematical Description
1	Spline must pass through knots.	$S(x_i)=f_i$, i=1, 2, ··· n where x_i=distinct data points $S(x_i)$=spline function f_i=function value at x.
2	Spline does not break, nor does it bend into sharp angle.	S(x), S'(x) and S"(x) are continuous on [a,b].
3	Thin beam theory shows that between knots, spline approximates a cubic polynomial.	In each subinterval $[x_i, x_{i+1}]$, S(x) is a cubic polynomial.
4	Spline assumes the slope that minimizes its potential energy (The potential energy is approximately proportional to curvature i.e. to second derivative).	If F(x) is any other function that satisfies properties 1, 2 and 3, then $\int_a^b S''(x)\,dx \leq \int_a^b F''(x)\,dx$ and $S''(a)=S''(b)=0$.

By integrating Eq.(C-1), we get

$$S'(x)=S'(x_i)+(x-x_i)S''(x_i)+\frac{S''(x_{i+1})-S''(x_i)}{2(x_{i+1}-x_i)}(x-x_i)^2. \qquad (C\text{-}2)$$

The integration of Eq.(C-2) and the property 1 give us

$$S(x)=f_i+S'(x_i)(x-x_i)+\tfrac{1}{2}(x-x_i)^2S''(x_i) + \frac{S''(x_{i+1})-S''(x_i)}{6(x_{i+1}-x_i)}(x-x_i)^3. \qquad (C\text{-}3)$$

To simplify Eqs.(C-2) and (C-3), let $S''_i = S''(x_i)$ and $h_i = x_{i+1} - x_i$. Replace i by i-1 and set $x = x_i$ in Eq.(C-2) to obtain

$$S'(x_i) = S'(x_{i-1}) + \frac{1}{2}(S''_i + S''_{i-1})\, h_{i-1} \qquad (C\text{-}2)'$$

Set $x = x_{i+1}$ in Eq.(C-3), and solve it for $S'(x_i)$ to get

$$S'(x_i) = \frac{f_{i+1} - f_i}{h_i} - \frac{h_i}{6}S''_{i+1} - \frac{h_i}{3}S''_i \qquad (C\text{-}4)$$

If $S''(x_i)$ is known for $i = 1, 2, \cdots n$, then from Eq.(C-4) and (C-3), $S(x)$ can be evaluated for any value of $x \in [a,b]$.

To get the values of $S''(x_i)$ taking property 3 into account, equate Eq.(C-2)' and Eq.(C-4) to obtain

$$S'(x_{i-1})+\frac{1}{2}(S''_i+S''_{i-1})h_{i-1}=\frac{f_{i+1}-f_i}{h_i}-\frac{h_i}{6}S''_{i+1}-\frac{h_i}{3}S''_i \qquad (C\text{-}5)$$

Now, replace i by i-1 in Eq.(C-4) and substitute the resulting expression for $S'(x_{i-1})$ into Eq.(C-5), then the result is

$$h_{i-1}S''_{i-1}+2(h_{i-1}+h_i)S''_i+h_iS''_{i+1}=6\left(\frac{f_{i+1}-f_i}{h_i}-\frac{f_i-f_{i-1}}{h_{i-1}}\right) \qquad (C\text{-}6)$$

which holds for $i = 2, 3, \cdots n-1$.

Note that this is a set of n-2 linear equations for the unknowns $S''_2, S''_3, \cdots S''_{n-1}$. The values for S_1 and S''_n are determined by property 4. Once S''_i are, thus, solved for $i = 1,2, \cdots n$, the mathematical spline function $S(x)$ can be evaluated at any $x \in [a,b]$ by using Eqs.(C-3) and (C-4).

APPENDIX D

COMPARISON OF RUNGE-KUTTA METHOD WITH MODIFIED RUNGE-KUTTA ALGORITHM

To solve a system of 1st order ordinary differential equations of form $\dot{y}=dy/dt=F(y,t)$,

Runge-Kutta	Modified Runge-Kutta
	$t_1=t_o+h,\ t_2=t_1+h=t_o+2h$
$a_1=hF(y_o,t_o)$	$a_1=hF(y_o,t_o)$
$a_2=hF(y_o+\frac{1}{2}a_1,t_o+\frac{1}{2}h)$	$a_2=hF(y_o+\frac{1}{2}a_1,t_o+\frac{1}{2}h)$
$a_3=hF(y_o+\frac{1}{2}a_2,t_o+\frac{1}{2}h)$	$a_3=hF(y_o+\frac{1}{4}(a_1+a_2),t_o+\frac{1}{2}h)$
$a_4=hF(y_o+a_3,t_o+h)$	$a_4=hF(y_o-a_2+2a_3,t_o+h)$
$y_1=y_o+(a_1+2a_2+2a_3+a_4)/6$	$y_1=y_o+\frac{1}{6}(a_1+4a_3+a_4)$
	$a_5=hF(y_1,t_1)$
	$a_6=hF(y_1+\frac{1}{2}a_5,t_1+\frac{1}{2}h)$
	$a_7=hF(y_1+\frac{1}{4}(a_5+a_6),t_1+\frac{1}{2}h)$
	$Error=\frac{1}{90}(-a_1+4a_3+17a_4-23a_5+4a_7-B)+O(h^6)$
	where
	$B=hF(y_o+\frac{1}{6}[-a_1-96a_2+92a_3-121a_4+144a_5+6a_6-12a_7],t_2)$
	If Error$\leq$Absolute error + Relative error $*y_1$,
	$y_2=y_1+\frac{1}{6}(a_5+4a_7+hF[y_1-a_6+2a_7],t_2)$

APPENDIX E

STOCHASTIC ANALYSIS OF FOLLOWER MOTION DUE TO THE SURFACE TOLERANCES OF CAM AND ITS FOLLOWER

In a system, the general expression of the output y_2 in relation to the input y_1 and its variables (x_1, x_2, ... , x_n) can be written as

$$y_2 = f (x_1, x_2, \dots , x_n, y_1) \qquad (E.1)$$

When, based on the stochastic model (Fig. E.1) of a general cam-follower system, the input variables (x_1, x_2, ... , x_n) are treated as random variables, y_2 becomes a dependent random variable for a fixed value of y_1. Then, the behavior of the output variable y_2 can be studied by considering it as a random variable for a series of fixed values of y_1 in its range.

Expanding Eq.(E.1) in Taylor series about the mean value of x_i's gives

$$y_2 = f (\mu_1, \mu_2, \dots, \mu_n, y_1) + \sum_{i=1}^{n} \frac{\partial f (\mu_1, \mu_2, \dots, \mu_n, y_1)}{\partial x_i} (x_i - \mu_i)$$

$$+ \frac{1}{2} \left[\sum_{i=1}^{n} \frac{\partial^2 f (\mu_1, \mu_2, \dots, \mu_n, y_1)}{\partial x_i^2} (x_i - \mu_i)^2 + 2 \dots \right] + \dots \qquad (E.2)$$

where μ_1 = mean values of x_i's .

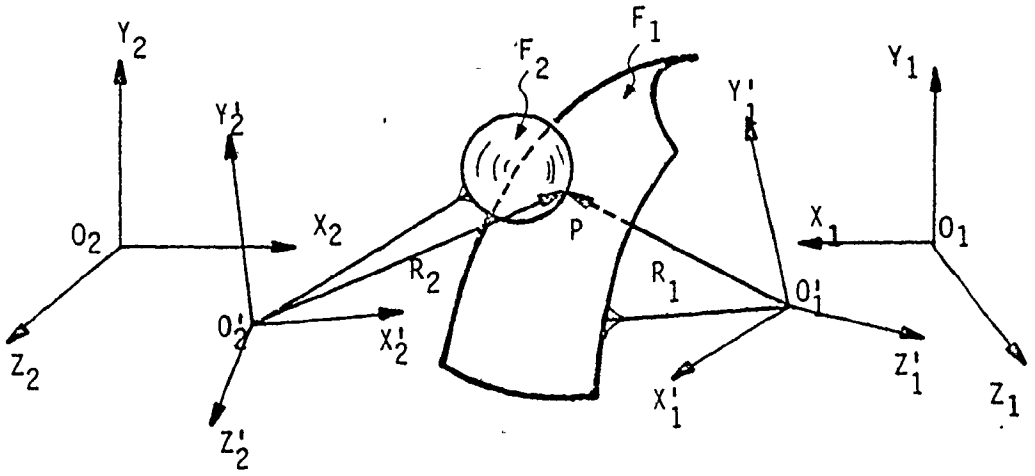

Fig. E.1. Schematic Diagram of a General Cam-Follower System.

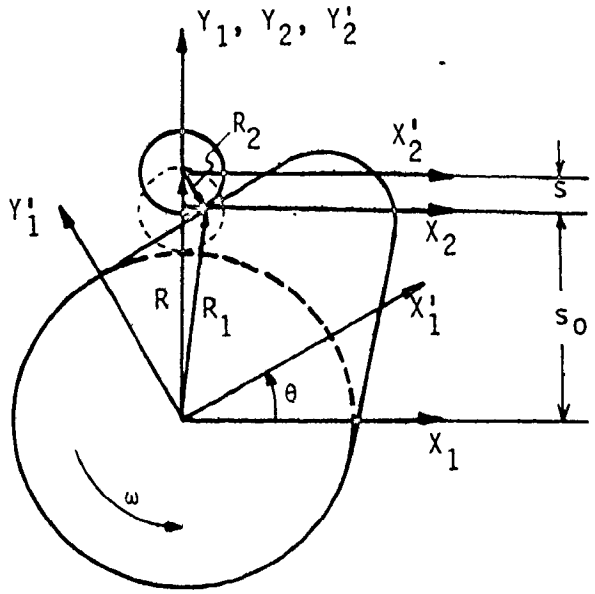

Fig. E.2. Disk Cam with a Translating In-line Roller Follower.

Taking the mean values at both sides of Eq.(E.2), and neglecting the higher terms than second term, yields

$$\mu_{y_2} = f (\mu_1, \mu_2, \cdots , \mu_n, y_1) \qquad (E.3)$$

The variance is obtained from the equation

$$\sigma^2_{y_2} = E [(y_2 - \mu_{y_2})^2] = E [y_2^2] - \mu^2_{y_2} \qquad (E.4)$$

Substituting Eqs. (E.2) and (E.3) into Eq. (E.4), and deleting the higher term than second term, gives

$$\sigma^2_{y_2} = \sum_{i=1}^{n} \left[\frac{\partial f (\mu_1, \mu_2, \cdots , \mu_n, y_1)}{\partial x_i} \right]^2 \sigma_i^2 \qquad (E.5)$$

where σ_i = standard deviation of x_i's

From Eqs. (E.3) and (E.5), the stochastic information (mean value, standard deviation and variance) of output can be obtained.

For example, by applying matrix algebra and vector analyis to the disk cam with a translating in-line roller follower (Fig. E.2), the cam profile is expressed in cartesian coordinates as

$$\begin{aligned} x &= (s + s_o) \sin \theta + r \cos (\psi - \theta) \\ y &= (s + s_o) \cos \theta + r \sin (\psi - \theta) \end{aligned} \qquad (E.6)$$

where

$$\psi = \cos^{-1}\left[\frac{x\cos\theta - y\sin\theta}{r}\right] = \phi - \frac{\pi}{2}$$

and ϕ = pressure angle.

Now, from Eq. (E-6)

$$s = x\sin\theta + y\cos\theta - r\sin\psi - s_o \qquad (E.7)$$

This is the required relation between input variables (x, y and r) and output variable (s) for a fixed value (θ) and is equivalent to Eq. (E.1).

Then

$$\frac{\partial s}{\partial x} = \sin\theta - r\cos\psi\,\frac{\partial\psi}{\partial x}$$

$$\frac{\partial s}{\partial y} = \cos\theta - r\cos\psi\,\frac{\partial\psi}{\partial y} \qquad (E.8)$$

$$\frac{\partial s}{\partial r} = -r\cos\psi\,\frac{\partial\psi}{\partial r} - \sin\psi - \frac{\partial s_o}{\partial r}$$

in which

$$\frac{\partial\psi}{\partial x} = \frac{\cos\theta}{r\,k_2}, \qquad \frac{\partial\psi}{\partial y} = \frac{-\sin\theta}{r\,k_2}$$

$$\frac{\partial\psi}{\partial r} = \frac{y\cos\theta - x\cos\theta}{r^2\,k_2}, \qquad \frac{\partial s_o}{\partial r} = 1$$

$$k_2 = (1 - k_1^2)^{\frac{1}{2}} \quad \text{and} \quad k_1 = \frac{y\sin\theta - x\cos\theta}{r}.$$

From Eqs. (E.3), (E.5) and (E.8), the stochastic information for the roller follower displacement is obtained. The information concerning the velocity and acceleration of the follower is found by applying the finite difference method, compensated by the maximum likelihood theory, to the previously obtained information concerning the displacement.

APPENDIX F

SPRING VIBRATION

F.1. Inclusion of Spring Mass

Assuming that a spring with a small mass of its own deforms like a massless spring and the deformation of its free end is

$$y (\ell, t) = y_o \sin \omega t \ .$$

We obtain the deformation at a distance x from the clamped end as

$$\dot{y} (x, t) = y_o \omega \frac{x}{\ell} \cos \omega t \ .$$

The kinetic energy K of a spring of length ℓ at the instant when $\cos \omega t = 1$ is

$$K = \frac{1}{2} y_o^2 \omega^2 m_1 \int_o^{\ell} \frac{x^2}{\ell^2} dx = \frac{1}{2} y_o^2 \omega^2 \frac{m_1 \ell}{3} = \frac{1}{2} y_o^2 \omega^2 \frac{m}{3} \qquad (F.1)$$

where m_1 = mass per unit length

$m = m_1 \ell$ = entire mass.

Eq. (F.1) indicates that the kinetic energy of the spring including its mass can be approximated by a massless spring of the

same shape with a concentrated mass at the free end equal to 1/3 the mass of the real spring. However, this assumption introduces a small error, since the deformation of the real spring is not the same as the massless spring because its mass generates an inertia force.

F.2. Natural Frequency of the Spring and its Derivation

Referring to a freebody diagram of an element length dx of the spring shown in Fig. F.1, the equilibrium conditions are

$$-\frac{\partial F}{\partial x} = m_1 \frac{\partial^2 y}{\partial t^2} \qquad : m_1 = \text{mass per unit length}$$

$$-\frac{\partial M}{\partial x} = I_1 \frac{\partial^2 \phi}{\partial t^2} \qquad : I_1 = \text{moment of mass per unit length} \qquad (F.2)$$

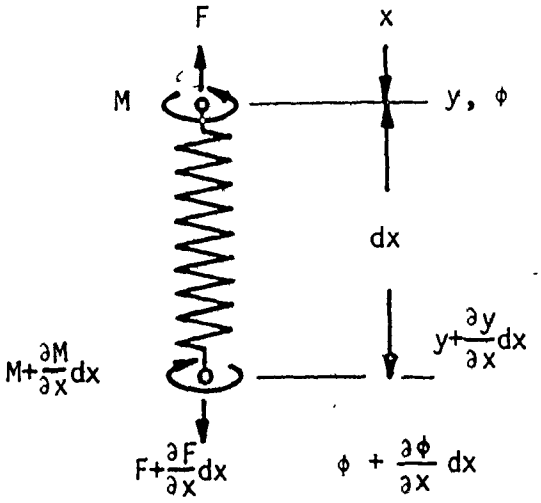

Fig. F.1. Freebody diagram of spring element dx.

Expressing the deformation of the element as a linear function of F and M, the deformation conditions become

$$
\begin{aligned}
-\frac{\partial \phi}{\partial x} &= a\,M + c\,F \\
-\frac{\partial y}{\partial x} &= c\,M + b\,F
\end{aligned}
\qquad (F.3)
$$

The coefficient c in the two equations is justified by the reciprocity of the displacements.

Eliminating M and F from Eqs. (F.2) and (F.3) gives

$$
\begin{aligned}
\frac{\partial^2 \phi}{\partial x^2} &= a\,I_1 \frac{\partial^2 \phi}{\partial t^2} + c\,m_1 \frac{\partial^2 y}{\partial t^2} \\
\frac{\partial^2 y}{\partial x^2} &= b\,m_1 \frac{\partial^2 y}{\partial t^2} + c\,I_1 \frac{\partial^2 \phi}{\partial t^2}
\end{aligned}
\qquad (F.4)
$$

For a steady state condition, assuming harmonic motion

$$
\phi = \Phi\, e^{i\omega t}, \qquad y = Y\, e^{i\omega t} \qquad (F.5)
$$

and substituting these into Eq. (F.4), we get

$$
\begin{aligned}
-\frac{d^2 \Phi}{dx^2} &= (a\,I_1\,\Phi + c\,m_1\,Y)\,\omega^2 \\
-\frac{d^2 Y}{dx^2} &= (c\,I_1\,\Phi + b\,m_1\,Y)\,\omega^2
\end{aligned}
\qquad (F.6)
$$

Eliminating Φ from Eq. (F.6) to get

$$\frac{1}{\omega^4} Y'''' + \frac{1}{\omega^2} \cdot Y'' \left(aI_1 + bm_1 \right) + Y \left(ab - c^2 \right) I_1 m_1 = 0 \qquad (F.7)$$

and substituting $Y = e^{i\lambda x}$ into Eq. (F.7), we get the roots of the resulted equation as

$$\left(\frac{\lambda}{\omega}\right) = \pm \sqrt{\frac{1}{2} \left[\left(a\Phi + bm_1 \right) \pm \sqrt{\left(a\Phi + bm_1 \right)^2 - 4 \left(ab - c^2 \right) \Phi m_1} \right]} \qquad (F.8)$$

and the general solution of Eq. (F.7) becomes

$$Y = A \sin \lambda_1 x + B \cos \lambda_1 x + C \sin \lambda_2 x + D \sin \lambda_2 x \qquad (F.9)$$

Considering boundary conditions i.e.

$$x = 0 \quad : \quad Y = 0, \qquad \Phi = 0$$

$$x = \ell \quad : \quad Y = y_o, \qquad \Phi = 0$$

we find

$$B = D = 0 \quad : \quad \lambda_1 \neq \lambda_2$$

and

$$A = \frac{y_o}{\Delta} \left(\lambda_2^2 - b m_1 \omega^2 \right) \sin \lambda_2 \ell$$

$$C = \frac{y_o}{\Delta} \left(\lambda_1^2 - b m_1 \omega^2 \right) \sin \lambda_1 \ell$$

where

$$\Delta = \left(\lambda_2^2 - \lambda_1^2 \right) \sin \lambda_1 \ell \sin \lambda_2 \ell \, .$$

The resonance conditions are thus,

$$\sin \lambda_1 \ell = 0, \qquad \sin \lambda_2 \ell = 0$$

i.e.

$$\lambda_1 = n_1 \frac{\pi}{\ell} \qquad (n_1 = 0, 1, 2, \ldots)$$

$$\lambda_2 = n_2 \frac{\pi}{\ell} \qquad (n_2 = 0, 1, 2, \ldots)$$

where

$$n_1 \neq n_2 \qquad \text{since} \quad \lambda_1 \neq \lambda_2 .$$

From Eq. (F.8), the natural frequency is found by :

$$\omega_n = \frac{n_{1,2}\, \pi}{\ell} \frac{\sqrt{2}}{\sqrt{(a\Phi + bm_1) \pm \sqrt{(a\Phi + bm_1)^2 - 4 (ab - c^2) \Phi m_1}}} \qquad (F.10)$$

To get the values of a, b, c, m_1 and I_1, let us consider the strain energy of the massless spring, i.e.

$$L = \frac{1}{2} \left(\frac{M_t}{GI_t} + \frac{M_b}{EI_b} \right) \ell \qquad (F.11)$$

where M_t = torsional moment of spring wire

G = shear modulus of spring material

I_t = torsional moment of inertia of spring wire $\frac{\pi}{32} d^4$

M_b = bending moment of spring wire

E = modulus of elasticity of spring material

I_b = bending moment of inertia of spring wire $I_b = \frac{I_t}{2}$

If an arbitrary cross-section normal to the helix has the pitch angle α,

$$M_b = -F r \sin\alpha + M \cos\alpha$$
$$M_t = R r \cos\alpha + M \sin\alpha \qquad (F.12)$$

where

$$\sin\alpha = \frac{h}{2\pi r} \quad ; \quad h = \text{pitch}, \quad r = \text{radius of helix cylinder}$$

and the length of wire ℓ is

$$\ell = 2\pi r k / \cos\alpha \quad ; \quad k = \text{number of winding} \qquad (F.13)$$

Then, substituting Eqs. (F.12) and (F.13) into Eq. (F.11) gives

$$L = \frac{1}{2}\left[\frac{1}{GI_t}(F r \cos\alpha + M \sin\alpha)^2 + \frac{1}{EI_t}(M \cos\alpha + F r \sin\alpha)^2\right] \ell$$

Since $y = \frac{\partial L}{\partial F}$ and $\phi = \frac{\partial L}{\partial M}$,

$$\frac{\phi}{\ell} = M\left(\frac{\sin^2\alpha}{GI_t} + \frac{\cos^2\alpha}{EI_b}\right) + F r \sin\alpha \cos\alpha \left(\frac{1}{GI_t} - \frac{1}{EI_b}\right)$$
$$\frac{y}{\ell} = F r^2 \left(\frac{\cos^2\alpha}{GI_t} + \frac{\sin^2\alpha}{EI_b}\right) + M r \sin\alpha \cos\alpha \left(\frac{1}{GI_t} - \frac{1}{EI_b}\right) \qquad (F.14)$$

A comparison of Eq. (F.14) and Eq. (F.3) gives that

$$a = \frac{\sin^2\alpha}{GI_t} + \frac{\cos^2\alpha}{EI_b}, \qquad b = \left(\frac{\cos^2\alpha}{GI_t} + \frac{\sin^2\alpha}{EI_b}\right) r^2$$
$$C = r \sin\alpha \cos\alpha \left(\frac{1}{GI_t} - \frac{1}{EI_b}\right) \qquad (F.15)$$

The total mass of the spring $m = m_1 \ell$, so that

$$m_1 = \frac{m}{\ell} = \rho \frac{\pi}{4} d^2 \qquad ; \rho = \text{specific mass of spring material}$$

and the moment of inertia of entire spring with respect to its axis

$$I = k \frac{2 \pi r^3 m_1}{\cos \alpha}$$

so that

$$I_\ell = \frac{I}{\ell} = r^2 m_1 \quad .$$

Substituting Eq. (F.15), m_1 and I_1 into Eq. (F.10) yields

$$(\omega_n)_{1,2} = \frac{n_{1,2} \pi}{\ell} \frac{\sqrt{2}}{\sqrt{\frac{r^2 m_1}{I_t} [\frac{1}{G} + \frac{2}{E} \pm (\frac{1}{G} - \frac{2}{E})]}} \qquad (F.16)$$

and thus,

$$(\omega_n)_1 = \frac{n_1 \pi}{\ell} \sqrt{\frac{G I_t}{r^2 m_1}} = n_1 \sqrt{\frac{G}{2\rho}} \frac{d}{D^2 k} \cos \alpha$$

$$(\omega_n)_2 = \frac{n_1 \pi}{\ell} \sqrt{\frac{E I_b}{r^2 m_1}} = n_2 \sqrt{\frac{E}{\rho}} \frac{d}{2D^2 k} \cos \alpha$$

APPENDIX G

SIMULATION OF BACKLASH AND CLEARANCE

Depending on which characteristics are desired, the backlash or clearance in a mechanism is generally handled by two approaches :

1. Dynamic simulation
2. Stochastic simulation

G.1 Dynamic Simulation

When the dynamic effect of backlash or clearance on a system is required, it is generally simulated through dynamics, and here a link coupling with clearance is presented as a representative model for general applications such as power transmission systems (gears, belts and couplings), face cam roller systems, 4-bar mechanisms, slider crank mechanisms etc.

The system model of a link coupling is shown in Fig. G.1 and its dynamic model (impact pair) in Fig. G.2.

From the dynamic model, the following equations of motion are derived.

1. Contact

If $| x_2 - x_1 | \geq e$, contact exists

$$\text{and,} \quad m_1 \ddot{x}_1 = g (x_2 - x_1) + f_1(t)$$

$$m_2 \ddot{x}_2 = - g (x_2 - x_1) + f_2(t)$$

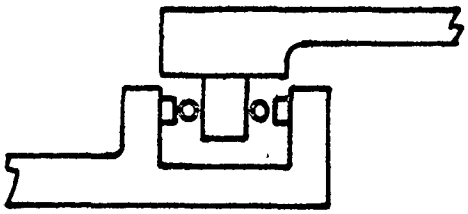

Fig.G.1 Link coupling with clearance

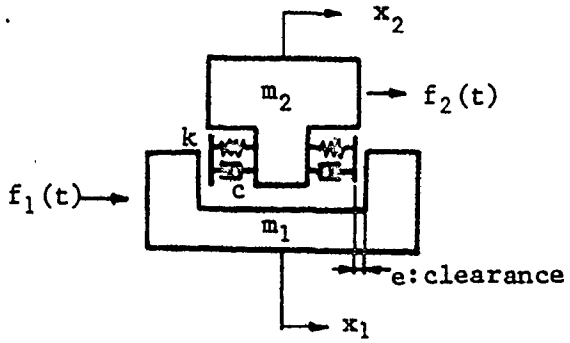

Fig.G.2 Dynamic model (impact pair)

2. No contact

If $| x_2 - x_1 | < e$, no contact

$$\text{and,} \quad m_1 \ddot{x}_1 = f_1(t)$$

$$m_2 \ddot{x}_2 = f_2(t)$$

The above differential equations may be nonlinear and non-homogeneous, depending on the functions $g(x)$, $f_1(t)$ and $f_2(t)$. The general force-displacement characteristic of the impact pair is shown in Fig. G.3.

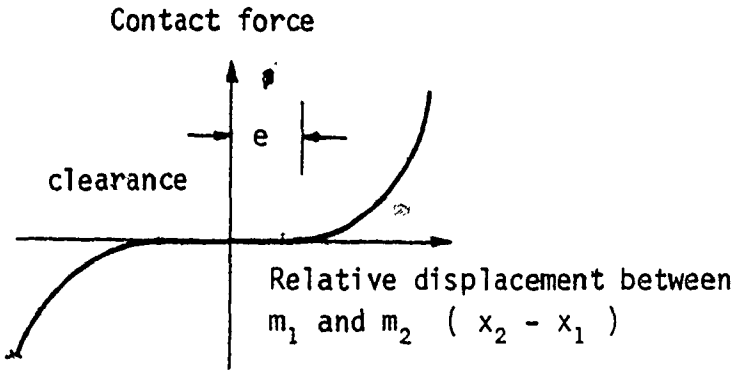

Fig. G.3 General Force-Displacement Characteristic of Impact Pair.

G.2 Stochastic Simulation

When stochastic information such as the mean value, standard deviation or variance of a system performance due to backlash or clearance is needed, especially in the error analysis of the system, the backlash or clearance is simulated through a stochastic model of the system consisting of a series of random variables.

For example, let an output (y) of a system be expressed in terms of n variables ($x_1, x_2, \ldots, x_n$) and an input (z) as

$$y = y (x_1, x_2, \ldots, x_n, z). \qquad (G.1)$$

When the independent variables are assumed to be random variables varying in the range of backlash, clearance or even tolerance, from Eq. (G.1) it is obvious that the output y is a function of random variables. Then, any given range of y may be associated with the corresponding probability if the probability densities, or at least

certain numerical characteristics, such as mean $M[x_i]$ and variance $V[x_i]$ of random variables x_i, are known.

To evaluate the numerical characteristics of y, the right-hand side of Eq. (G.1) is expanded in Taylor Series about the mean of the random variables, and the terms having order two and above are neglected. As a result, we get,

$$y \approx y (M[x_i], i = 1, 2, \ldots n) + \sum_{i=1}^{n} \frac{\partial y}{\partial x_i} (x_i, i = 1, 2, \ldots n) (x_i - M[x_i]) . \qquad (G.2)$$

When x_i, $i = 1, 2, \ldots n$ are independent, all the n random variables are uncorrelated, and hence

$$M[y] = y (z, M[x_i], i = 1, 2, \ldots , n)$$

and (G.3)

$$V[y] = \sum_{i=1}^{n} \left(\frac{\partial y}{\partial x_i} \right)^2_{M[x_i]} V[x_i] .$$

Once the variance of y has been found for a particular value of input z, use may be made of standard statistical tables to associate any given range of y (for the given value of z) with its probability of occurrence.

APPENDIX H

COMPUTER PROGRAM USER'S INFORMATION

**** This appendix is available from the author. ****